



2807709696

ROYAL FREE THESES 1998

INHIBITION OF PLATELET AGGREGATION
BY APOLIPOPROTEIN E

by

David Ramsey Riddell

A thesis submitted in partial fulfilment
of the requirements for the degree of

Doctor of Philosophy

Royal Free Hospital School of
Medicine University of London

1998

MEDICAL LIBRARY
ROYAL FREE HOSPITAL
HAMPSTEAD

09963

ProQuest Number: U641944

All rights reserved

INFORMATION TO ALL USERS

The quality of this reproduction is dependent upon the quality of the copy submitted.

In the unlikely event that the author did not send a complete manuscript and there are missing pages, these will be noted. Also, if material had to be removed, a note will indicate the deletion.



ProQuest U641944

Published by ProQuest LLC(2015). Copyright of the Dissertation is held by the Author.

All rights reserved.

This work is protected against unauthorized copying under Title 17, United States Code.
Microform Edition © ProQuest LLC.

ProQuest LLC
789 East Eisenhower Parkway
P.O. Box 1346
Ann Arbor, MI 48106-1346

Royal Free Hospital School of Medicine University of London

Abstract

INHIBITION OF PLATELET
AGGREGATION BY APOLIPOPROTEIN E

by David Ramsey Riddell

The aim of my PhD thesis was to characterise the mechanism by which apolipoprotein E (apoE) inhibits agonist-induced platelet aggregation. Although pure apoE was inactive, apoE/phospholipid (apoE:DMPC) complexes induced a potent dose-dependent inhibition of platelet aggregation. This inhibition was abolished when platelets were pre-incubated with nitric oxide (NO) synthase inhibitors, implying that apoE stimulated NO production. Additionally, apoE:DMPC vesicles induced a marked dose-dependent increase in cGMP, indicating a stimulation of guanylate cyclase, the physiological target for NO. Confirmation that apoE stimulates NO synthase was obtained by use of an enzymatic assay; platelets pre-treated with apoE:DMPC produced four times more citrulline (the by-product of NO synthesis) than controls. The initial activating step was an apoE-receptor interaction. Chemically-modifying the arginine residues of apoE blocked the rise in platelet cGMP and the anti-aggregatory effect, while receptor associated protein (RAP), a potent inhibitor of apoE-receptor interactions, also prevented apoE's anti-platelet action. Finally, studies using synthetic peptides identified the active domain within the apoE molecule as the "classical" LDL receptor-binding domain (residues 142-145). Homology cloning was used to identify the platelet receptor. Sets of degenerate primers were used in RT-PCR to amplify the conserved binding domain of the LDL receptor super family from HEL cells (a megakaryocytic cell line). One PCR product matched apoE receptor 2 (apoER2), a newly described receptor confined mainly to the brain. Using a specific anti-peptide antiserum, apoER2 protein was detected in platelet membranes. Intriguingly, sequence analysis of cytoplasmic apoER2 identified a number of peptide motifs involved in tyrosine kinase signalling, implying this as the mechanism by which activated apoER2 and NO synthase are coupled. Since apoE and NO are both implicated in the pathology of atherosclerosis and Alzheimer's disease, the elucidation of the molecular mechanism by which apoE binding to apoER2 can activate platelet NO synthase may have widespread ramifications.

MEDICAL LIBRARY

RESEARCH CENTRE

TABLE OF CONTENTS

DEDICATION.....	10
ACKNOWLEDGEMENTS.....	11
ABBREVIATIONS.....	12
CHAPTER 1. INTRODUCTION	14
1.1 BACKGROUND.....	15
1.2 PLATELETS.....	15
1.2.1 Preface.....	15
1.2.2 Platelet Production.....	15
1.2.3 Platelet Structure.....	16
1.2.4 Stages in the Haemostatic Process and Physiological Platelet Agonists.....	17
1.2.5 Effects of ADP on Platelet Biochemistry.....	21
1.2.6 The Biochemistry of Inhibition of Platelet Aggregation.....	25
1.3 APOLIPOPROTEIN E.....	30
1.3.1 Preface.....	30
1.3.2 Discovery and Initial Characterisation of ApoE.....	30
1.3.3 Gene Regulation and Biosynthesis of Human ApoE.....	31
1.3.4 Sites of Synthesis.....	32
1.3.5 ApoE Polymorphism.....	33
1.3.6 Structure of ApoE.....	34
1.3.7 ApoE Receptors.....	38
1.3.8 Physiological Roles of ApoE.....	43
1.4 APOE AND PLATELET AGGREGATION.....	48
1.5 AIMS OF THESIS.....	49
CHAPTER 2. GENERAL MATERIALS AND METHODS	50
2.1 MATERIALS.....	51
2.2 ISOLATION OF PLASMA LIPOPROTEINS.....	51
2.2.1 Background.....	51
2.2.2 Blood Sampling.....	52
2.2.3 Sequential Preparative Ultracentrifugation.....	53
2.3 GENERAL APOLIPOPROTEIN ANALYSES.....	56
2.3.1 Protein Measurement.....	56
2.3.2 SDS-Polyacrylamide Gel Electrophoresis.....	57
2.3.3 Immunoblotting.....	61

2.4	ISOLATION AND CHARACTERISATION OF APOE.....	63
2.4.1	<i>Apolipoprotein E Phenotyping: Isoelectric Focusing and Immunoblotting.....</i>	64
2.4.2	<i>Quantification of Apolipoprotein E Levels in Plasma: Rocket Immunoelectrophoresis.....</i>	66
2.4.3	<i>Isolation of Apolipoprotein E: Delipidation and Affinity Chromatography.....</i>	68
2.4.4	<i>Preparation of ApoE:DMPC Complexes.....</i>	70
2.4.5	<i>Characterisation of ApoE:DMPC Complexes.....</i>	70
2.5	PLATELETS: ISOLATION AND AGGREGATION.....	72
2.5.1	<i>Background.....</i>	72
2.5.2	<i>Buffers and Solutions.....</i>	73
2.5.3	<i>Blood Sampling.....</i>	73
2.5.4	<i>Preparation of Platelet-Rich Plasma.....</i>	73
2.5.5	<i>Preparation of Washed Platelets.....</i>	74
2.5.6	<i>Platelet Counting.....</i>	74
2.5.7	<i>Platelet aggregation.....</i>	75
2.6	USE OF RT-PCR TO IDENTIFY PLATELET APOE RECEPTORS.....	78
2.6.1	<i>PCR Technology.....</i>	78
2.6.2	<i>Total RNA Extraction.....</i>	81
2.6.3	<i>Reverse Transcription Protocol.....</i>	81
2.6.4	<i>General Protocol for PCR Amplification.....</i>	82
2.6.5	<i>Agarose Gel Electrophoresis.....</i>	83
2.6.6	<i>Extraction of DNA from Agarose Gels.....</i>	84
2.6.7	<i>Restriction Digestion of PCR Products.....</i>	84
2.6.8	<i>Cloning and Sequencing of PCR Products.....</i>	85
2.7	STATISTICS.....	87
CHAPTER 3. CHARACTERISATION OF THE ANTI-AGGREGATORY EFFECT OF		
“NATIVE” HDL-E PARTICLES AND PURIFIED APOLIPOPROTEIN E.....		
3.1	INTRODUCTION.....	89
3.2	SPECIALISED MATERIALS AND METHODS.....	90
3.2.1	<i>Materials.....</i>	90
3.2.2	<i>Preparation of Anti-ApoE Sepharose Affinity Matrix.....</i>	90
3.2.3	<i>HDL-E Isolation from Plasma.....</i>	91
3.2.4	<i>ApoE:DMPC Complexes.....</i>	92
3.2.5	<i>Preparation of Chemically Modified ApoE:DMPC Complexes.....</i>	92
3.2.6	<i>Platelet Aggregation.....</i>	92
3.2.7	<i>Electron microscopy.....</i>	92
3.3	RESULTS AND DISCUSSION.....	93
3.3.1	<i>Effects of Native Immunoaffinity-Isolated HDL-E Particles on Platelet Aggregation.....</i>	93
3.3.2	<i>Inhibition of Platelet Aggregation by ApoE:DMPC.....</i>	95
3.3.3	<i>ApoE:DMPC Inhibits Platelet Aggregation Induced by a Variety of Agonists.....</i>	95
3.3.4	<i>Effects of Free ApoE, DMPC Vesicles and ApoE:DMPC Complexes on ADP-Induced Platelet Aggregation.....</i>	95
3.3.5	<i>Effects of ApoE:DMPC on Platelet Morphology.....</i>	99
3.3.6	<i>Effects of Purified Human Plasma ApoE, Human Recombinant ApoE and Rabbit Plasma ApoE on ADP-Induced Platelet Aggregation.....</i>	99
3.3.7	<i>Effects of Chemically Modified ApoE:DMPC on ADP-Induced Platelet Aggregation.....</i>	102
3.4	CONCLUSIONS.....	102

CHAPTER 4. THE BIOCHEMICAL BASIS FOR INHIBITION OF PLATELET AGGREGATION BY APOLIPOPROTEIN E	104
4.1 INTRODUCTION.....	105
4.2 SPECIALISED MATERIALS AND METHODS.....	106
4.2.1 <i>Materials</i>	106
4.2.2 <i>ApoE:DMPC Complexes</i>	106
4.2.3 <i>Preparation of [³H]Cholesterol-Labelled Platelets</i>	106
4.2.4 <i>Cholesterol Removal Studies</i>	106
4.2.5 <i>Platelet Aggregation</i>	107
4.2.6 <i>Cyclic Nucleotide Assays</i>	107
4.2.7 <i>NO Synthase Assays</i>	107
4.3 RESULTS.....	112
4.3.1 <i>Ability of ApoE:DMPC to Remove Cholesterol From Platelet Membranes</i>	112
4.3.2 <i>Effects of ApoE:DMPC on Intraplatelet cGMP and cAMP Levels</i>	112
4.3.3 <i>Effects of IBMX on ApoE:DMPC Treated Platelets</i>	115
4.3.4 <i>Effects of the NO Donor, S-Nitroso-L-Glutathione, on ADP Induced Platelet Aggregation</i>	118
4.3.5 <i>Effects of Soluble Guanylate Cyclase inhibitors on ApoE:DMPC Treated Platelets</i>	119
4.3.6 <i>Effects of NOS Inhibitors on the Aggregation of ApoE:DMPC Treated Platelets</i>	119
4.3.7 <i>Stimulation of Platelet NOS Activity by ApoE:DMPC Vesicles</i>	121
4.4 DISCUSSION.....	127
4.4.1 <i>Cholesterol Removal Studies</i>	127
4.4.2 <i>ApoE:DMPC Stimulates Intraplatelet cGMP Production</i>	127
4.4.3 <i>Indirect Evidence for an ApoE:DMPC Stimulation of Platelet NOS</i>	128
4.4.4 <i>Direct Evidence for an ApoE:DMPC Stimulation of Platelet NOS</i>	128
4.4.5 <i>Conclusions</i>	132
 CHAPTER 5. MOLECULAR CHARACTERISATION OF A HUMAN PLATELET RECEPTOR THAT BINDS APOLIPOPROTEIN E	 134
5.1 INTRODUCTION.....	135
5.2 SPECIALISED MATERIALS AND METHODS.....	136
5.2.1 <i>Materials</i>	136
5.2.2 <i>ApoE:DMPC Complexes</i>	136
5.2.3 <i>Platelet Aggregation</i>	136
5.2.4 <i>Hepatocarcinoma Cell Culture</i>	136
5.2.5 <i>Megakaryoblastic Cell Culture</i>	137
5.2.6 <i>Preparation of Purified Cell Membranes</i>	137
5.2.7 <i>Western Blotting of the LRP</i>	137
5.2.8 <i>Preparation of Washed Platelets, Monocytes, Lymphocytes and Neutrophils for RNA Extraction</i>	138
5.2.9 <i>Assessment of RNA Integrity</i>	138
5.2.10 <i>Initial RT-PCR Amplification of LRSF Members from HEL Cell cDNA</i>	139
5.2.11 <i>Platelet, HEL and Meg-01 Cell RT-PCR Amplification</i>	140
5.2.12 <i>Long RT-PCR</i>	141
5.2.13 <i>Preparation of Anti-ApoER2 Antibodies</i>	141
5.2.14 <i>Immunoprecipitation of Platelet ApoER2</i>	142
5.2.15 <i>Isolation of Cytosolic Platelet Proteins Which Bind Cytoplasmic ApoER2</i>	142

5.3 RESULTS AND DISCUSSION.....	143
5.3.1 <i>Identification of the Anti-Platelet Domain Within the ApoE Molecule.....</i>	<i>143</i>
5.3.2 <i>Characteristics of the Platelet ApoE Receptor.....</i>	<i>147</i>
5.3.3 <i>Characteristics of the Platelet ApoE Receptor - Conclusions.....</i>	<i>151</i>
5.3.4 <i>Homology Cloning of the Platelet Receptor.....</i>	<i>151</i>
5.3.5 <i>Characterisation of Platelet ApoER2.....</i>	<i>155</i>
5.3.6 <i>Production of an Anti-Peptide Antiserum to ApoER2.....</i>	<i>160</i>
5.3.7 <i>Immunoprecipitation of Platelet ApoER2.....</i>	<i>160</i>
5.3.8 <i>The Role of ApoER2 Variants in Platelets and Megakaryocytes.....</i>	<i>162</i>
5.3.9 <i>Is ApoER2 a Signal Transductant?.....</i>	<i>164</i>
5.3.10 <i>Platelet ApoER2 and eNOS Activation.....</i>	<i>167</i>
CHAPTER 6. GENERAL DISSUSSION.....	169
6.1 THE APOE/APOER2/NO LINK: IMPLICATIONS FOR VASCULAR DISEASE.....	170
6.2 THE APOE/APOER2/NO LINK: IMPLICATIONS FOR NEUROLOGICAL DISEASES.....	171
6.3 CONCLUSIONS.....	172
BIBLIOGRAPHY.....	174
PUBLICATIONS.....	202

LIST OF FIGURES

<i>Number</i>	<i>Page</i>
CHAPTER 1	
FIGURE 1.2-1	ULTRASTRUCTURAL FEATURES OF PLATELETS..... 17
FIGURE 1.2-2	PLATELET ACTIVATION REACTIONS..... 18
FIGURE 1.2-3	PLATELET SHAPE CHANGE. 20
FIGURE 1.2-4	A SIMPLIFIED OVERVIEW OF ADP MEDIATED INTRA-PLATELET SIGNALLING. 24
FIGURE 1.2-5	THE PRIMARY STRUCTURE OF THE NOS ISOENZYMES. 27
FIGURE 1.3-1	THE COMPLETE AMINO ACID SEQUENCE OF HUMAN APOLIPOPROTEIN E3. 35
FIGURE 1.3-2	RIBBON MODEL OF THE STRUCTURE OF THE AMINO TERMINAL DOMAIN OF HUMAN APOE. 36
FIGURE 1.3-3	THE MAMMALIAN MEMBERS OF THE LDL-R SUPER FAMILY..... 39
FIGURE 1.3-4	THE ROLE OF APOE AND APOE RECEPTORS IN LIPOPROTEIN METABOLISM. 44
CHAPTER 2	
FIGURE 2.4-1	A SCHEMATIC REPRESENTATION OF APOE PHENOTYPE PATTERNS..... 66
FIGURE 2.4-2	A TYPICAL APOLIPOPROTEIN E ROCKET..... 67
FIGURE 2.4-3	ANALYSIS OF PURIFIED APOE ON A 15 % SDS-PAGE GEL..... 69
FIGURE 2.4-4	ANALYSIS OF APOE:DMPC COMPLEXES BY ELECTRON MICROSCOPY. 71
FIGURE 2.5-1	TYPICAL RESPONSES TO ADP..... 76
FIGURE 2.5-2	DETERMINATION OF THE DEGREE OF PLATELET AGGREGATION..... 77
FIGURE 2.6-1	SCHEMATIC DIAGRAM OF THE RT-PCR PROCESS..... 80
CHAPTER 3	
FIGURE 3.3-1	INHIBITION OF ADRENALINE-INDUCED PLATELET AGGREGATION BY HDL-E..... 94
FIGURE 3.3-2	INHIBITION OF ADP-INDUCED AGGREGATION BY APOE:DMPC AS A FUNCTION OF TIME. 96
FIGURE 3.3-3	INHIBITION OF AGONIST-INDUCED PLATELET AGGREGATION BY APOE:DMPC..... 97
FIGURE 3.3-4	INHIBITION OF ADP-INDUCED AGGREGATION BY APOE:DMPC. 98
FIGURE 3.3-5	SCANNING ELECTRON MICROGRAPHS OF PRP INCUBATED IN THE PRESENCE OR ABSENCE OF APOE:DMPC. 100
FIGURE 3.3-6	HUMAN PLASMA APOE-3, RECOMBINANT HUMAN APOE-3 AND RABBIT PLASMA APOE ALL INHIBIT ADP-INDUCED PLATELET AGGREGATION..... 101
FIGURE 3.3-7	FAILURE OF CHD-APOE:DMPC TO INHIBIT ADP-INDUCED PLATELET AGGREGATION. ... 103
CHAPTER 4	
FIGURE 4.3-1	RELEASE OF CHOLESTEROL FROM PLATELET MEMBRANES BY APOE:DMPC AS A FUNCTION OF TIME. 113

FIGURE 4.3-2	APOE:DMPC COMPLEXES INCREASE INTRAPLATELET cGMP AND cAMP LEVELS IN A DOSE-DEPENDENT MANNER BUT ONLY IN THE PRESENCE OF ADP.	114
FIGURE 4.3-3	APOE:DMPC INDUCED INCREASES OF INTRAPLATELET cGMP AND cAMP LEVELS CORRELATE WITH THE CONCOMITANT INHIBITION OF AGGREGATION.....	116
FIGURE 4.3-4	IN THE PRESENCE OF IBMX, APOE:DMPC VESICLES STILL ELICITED A DOSE-DEPENDENT RISE IN cGMP BUT NOT cAMP.	117
FIGURE 4.3-5	GSNO INHIBITS PLATELET AGGREGATION IN A DOSE DEPENDENT MANNER.	118
FIGURE 4.3-6	SGC INHIBITORS PREVENT THE ANTI-AGGREGATORY ACTION OF APOE:DMPC COMPLEXES.	120
FIGURE 4.3-7	SGC INHIBITORS PREVENT cGMP INCREASES INDUCED BY APOE:DMPC COMPLEXES.	121
FIGURE 4.3-8	NOS INHIBITORS PREVENT THE ANTI-AGGREGATORY ACTION OF APOE:DMPC COMPLEXES.	122
FIGURE 4.3-9	CONSUMPTION OF HbO ₂ BY PLATELETS.....	123
FIGURE 4.3-10	PRODUCTION OF NO ₂ /NO ₃ ⁻ BY PLATELETS.....	124
FIGURE 4.3-11	APOE:DMPC COMPLEXES INCREASE INTRAPLATELET NO SYNTHASE ACTIVITY IN LYSSED PLATELET PREPARATIONS.	126
FIGURE 4.4-1	PROPOSED MECHANISM FOR APOE-MEDIATED INHIBITION OF AGONIST-INDUCED PLATELET AGGREGATION.....	133

CHAPTER 5

FIGURE 5.3-1	THE INHIBITORY ACTIVITY OF APOE IS LOCATED IN ITS AMINO TERMINUS.....	143
FIGURE 5.3-2	LACTOFERRIN INHIBITS ADP-INDUCED PLATELET AGGREGATION.....	146
FIGURE 5.3-3	RAP BLOCKS THE ANTI-AGGREGATORY EFFECT OF APOE:DMPC.....	148
FIGURE 5.3-4	IMMUNOBLOT ANALYSIS OF LRP IN PLATELET MEMBRANES.....	149
FIGURE 5.3-5	APOE-2, APOE-3 AND APOE-4 ALL INHIBIT ADP-INDUCED PLATELET AGGREGATION.....	150
FIGURE 5.3-6	RT-PCR USING DEGENERATE PRIMERS DESIGNED AGAINST THE LRP AND GP330.....	153
FIGURE 5.3-7	RT-PCR USING DEGENERATE PRIMERS DESIGNED AGAINST THE LDL-R, VLDL-R AND APOER2.....	154
FIGURE 5.3-8	SPECIFIC PRIMERS DIRECTED TOWARDS APOER2 AMPLIFY A 604 BP PRODUCT IN PLATELETS.	156
FIGURE 5.3-9	RESTRICTION MAPPING OF THE PLATELET 604 BP PCR PRODUCT.....	157
FIGURE 5.3-10	EXPRESSION OF APOER2 Δ 4-6 IN HUMAN PLATELETS.	158
FIGURE 5.3-11	LONG PCR OF HEL CELL APOER2.	159
FIGURE 5.3-12	WESTERN BLOTTING OF APOER2 USING THE ANTI-PEPTIDE ANTISERUM α ER2INS.....	161
FIGURE 5.3-13	IMMUNOPRECIPITATION OF PLATELET APOER2.....	162
FIGURE 5.3-14	THE CYTOPLASMIC TAIL OF APOER2 CONTAINS PTB RECOGNITION MOTIFS, SH3 RECOGNITION MOTIFS AND cGMP/cAMP DEPENDENT PROTEIN KINASE PHOSPHORYLATION SITES.....	165
FIGURE 5.3-15	CYTOPLASMIC APOER2 BINDS A 40 kDA TYROSINE-PHOSPHORYLATED PROTEIN IN PLATELET CYTOSOL.	166
FIGURE 5.3-16	HYPOTHESIS - A NOVEL CELL SIGNALLING ROLE FOR APOER2 IN PLATELETS.....	168

LIST OF TABLES

<i>Number</i>		<i>Page</i>
CHAPTER 2		
TABLE 2.2-1	DENSITY CLASSES OF PLASMA LIPOPROTEINS.....	52
TABLE 2.2-2	PRESERVATIVE COCKTAIL FOR BLOOD COLLECTION.....	53
TABLE 2.2-3	PRESERVATIVE SOLUTIONS FOR LIPOPROTEINS.....	53
TABLE 2.2-4	PREPARATION OF STOCK DENSITY SOLUTIONS.....	54
TABLE 2.3-1	EFFECTIVE RANGE OF SEPARATION OF SDS-POLYACRYLAMIDE GELS.....	58
TABLE 2.3-2	SOLUTIONS FOR PREPARING GELS FOR SDS-POLYACRYLAMIDE GEL ELECTROPHORESIS.....	60
TABLE 2.6-1	SEPARATION RANGES FOR TYPICAL AGAROSE GEL CONCENTRATIONS.....	84
TABLE 2.6-2	RESTRICTION ENZYMES AND REACTION CONDITIONS.....	85
CHAPTER 4		
TABLE 4.3-1	CHD-APOE:DMPC, FREE APOE OR DMPC ALONE DO NOT INCREASE INTRAPLATELET cGMP LEVELS.....	115
TABLE 4.3-2	CONVERSION OF L-[³ H]ARGININE TO L-[³ H]CITRULLINE IN INTACT PLATELET PREPARATIONS.....	125
CHAPTER 5		
TABLE 5.3-1	AMINO ACID SEQUENCES OF APOE AND LACTOFERRIN PEPTIDES.....	144
TABLE 5.3-2	SYNTHETIC PEPTIDES INHIBIT ADP-INDUCED PLATELET AGGREGATION.....	145
TABLE 5.3-3	COMPARISON OF THE LIGAND SPECIFIES OF THE LDL-R, VLDL-R AND THE PLATELET APOE RECEPTOR.....	163

DEDICATION

I would like to dedicate this thesis to my parents, Wendy and David Riddell, for all their love, support and encouragement through the years.

ACKNOWLEDGEMENTS

I would like to express my gratitude to Dr. James S. Owen for his constant guidance, support, encouragement and friendship throughout this project and for his critical reviewing of this manuscript.

I am very grateful to all my friends and work colleagues at the Royal Free who have contributed directly or indirectly to this project. I would especially like to thank Dr. D. Chawla for “showing me the ropes” when I was a fresh-faced graduate and Dr A. Graham for many helpful discussions. I also wish to thank Drs D. Vinogradov, S. Schepelmann and N. Chadwick for their help and training in molecular biology techniques.

I would also like to acknowledge the financial support of the “British Heart Foundation”.

Last but not least, I would like to express my appreciation to Ms A. Stannard, not only for; assisting with this work, proof reading this manuscript and cooking a great lasagne, but for being there when it mattered. Thank you.

Dave Riddell, May 1998.

ABBREVIATIONS

AD	Alzheimer's disease
ADP	adenosine diphosphate
apoE	apolipoprotein E
apoER2	apolipoprotein E receptor 2
APP	amyloid precursor protein
APS	ammonium persulphate
A β	amyloid beta peptide
BCIP	bromochloroindolyl phosphate
bisacrylamide	N, N'-methylenebisacrylamide
BSA	bovine serum albumin
CAM	calmodulin
cAMP	cyclic adenosine 3', 5'-monophosphate
cGMP	cyclic guanosine 3', 5'-monophosphate
CHD	cyclohexanedione
CNS	central nervous system
CSF	cerebrospinal fluid
DAG	diacylglycerol
DEPC	diethylpyrocarbonate
DMPC	dimyristoylphosphatidylcholine
dNTPs	deoxynucleotide triphosphates
DPI	diphenyleneiodonium chloride
DTT	dithiothreitol
ECL	enhanced chemiluminescence
EDTA	ethylenediaminetetra-acetate
EGF	epidermal growth factor
Ethyl-ITU	2-Ethyl-isothiopseudourea
FAD	flavin adenine dinucleotide
FBS	foetal bovine serum
FMN	flavin mononucleotide
GP	glycoprotein
GSNO	S-nitroso-L-glutathione
HbO ₂	oxyhaemoglobin
HDL	high density lipoprotein
HEL	human erythroleukaemia
HL	hepatic lipase
HSA	human serum albumin
HSPG	heparin sulphate proteoglycan
IBMX	3-isobutyl-1-methyl-xanthine
IDL	intermediate density lipoprotein
IEF	isoelectric focusing
IP ₃	inositol 1,4,5-trisphosphate
LCAT	lecithin-cholesterol acyltransferase
LDL	low density lipoprotein

LDL-R	low density lipoprotein receptor
L-NAME	N ^G -nitro-L-arginine methyl ester
L-NMMA	N ^G -monomethyl-L-arginine
LPL	lipoprotein lipase
LRP	low density receptor-related protein
LRSF	low density lipoprotein receptor super family
metHb	methaemoglobin
MLC	myosin light chain
MLCK	myosin light chain kinase
NADPH	reduced nicotinamide adenine dinucleotide phosphate
NBT	nitro blue tetrazolium
NO	nitric oxide
NOS	nitric oxide synthase
ODQ	1H-[1,2,4]oxadiazolo[4,3-a]quinoxalin-1-one
PAF	platelet-activating factor
PAI-1	plasminogen activator inhibitor
PBS	phosphate buffered saline
PCR	polymerase chain reaction
PDE	phosphodiesterase
PGI ₂	prostacyclin
PK	protein kinase
PLA ₂	phospholipase A ₂
PLC	phospholipase C
PMSF	phenylmethylsulphonylfluoride
PPP	platelet poor plasma
PRP	platelet rich plasma
PTB	phosphotyrosine-binding domain
pY	phosphotyrosine
RAP	receptor associated protein
ROC	receptor operated channels
RT	reverse transcription
SDS-PAGE	sodium dodecyl sulphate polyacrylamide gel electrophoresis
SGC	soluble guanylate cyclase
SH2	src-homology 2
SH3	src-homology 3
SSC	saline sodium citrate
TBS	tris buffered saline
TEMED	N, N, N, N'-tetramethylethylenediamine
tPA	tissue-type plasminogen activator
TXA ₂	thromboxane A ₂
VLDL	very low density lipoprotein
VLDL-R	very low density lipoprotein receptor

Chapter 1

1. INTRODUCTION

1.1 Background.

Over the last decade, considerable interest has focused on the role of platelets and platelet inhibitor therapy in atherosclerotic diseases. The well established role of platelets in arterial thrombosis has provided the rationale for many drugs which inhibit platelet functions and the treatment of both cardiovascular and cerebral vascular diseases has been unquestionably transformed by the use of anti-platelet therapy. Fortunately, there has been remarkable growth in our understanding of the molecular mechanisms of platelet aggregation and several new anti-platelet agents have emerged in recent years (reviewed in [1, 2]). Interestingly, the reverse is also true. Elucidating the molecular mechanisms of agents that influence aggregation by unknown means has led to the characterisation of numerous important cell-signalling pathways. Indeed, platelets are used as a model system for the study of signal transduction mechanisms [3-5].

It has been recently shown that apolipoprotein E (apoE), a plasma protein that is increasingly implicated in the pathophysiology of vascular and neurological disorders [6], is a potent anti-platelet agent [7]. In this thesis, I have sought to further characterise the anti-platelet effect of apoE and to delineate the molecular basis of inhibition.

1.2 Platelets.

1.2.1 PREFACE.

Blood platelets are one of the most abundant, mobile cell types in the body. There are normally between 150 and 300 million platelets in every ml of blood, about 1000 billion (10^{12}) platelets within the human circulation [8]. This high number of circulating platelets reflects their fundamental role in normal haemostasis, namely, to plug holes in leaky blood vessels. Platelets circulate in blood as smooth biconvex discs of an average volume of 5 to 7.5 fl, 14 times smaller than that of erythrocytes. Each day an estimated $1.5 - 3.5 \times 10^7$ platelets per ml of blood are produced by their mother cells, megakaryocytes. Their normal life span within the circulation is 10 days [9].

1.2.2 PLATELET PRODUCTION.

Platelets are produced in the bone marrow by cytoplasmic fragmentation of megakaryocytes (reviewed in [9, 10, 11]). The precursor of the megakaryocyte – the megakaryoblast – arises by a process of differentiation from haemopoietic stem cells. The megakaryocyte undergoes a unique biological process known as “endomitotic synchronous

nuclear replication”, which is defined as repeated nuclear replication in the absence of cytoplasmic division. Thus, megakaryocytes possess 2^n polyploid nuclei, with 4 to 64 times the amount of haploid nuclear material. At a variable stage in development, most commonly at the eight-nucleus stage, further nuclear replication and cell growth ceases, the cytoplasm becomes granular and platelets are then liberated. Each megakaryocyte is responsible for the production of about 4000 platelets. The time interval from differentiation of the stem cell to the production of platelets averages about 10 days in man.

1.2.3 PLATELET STRUCTURE.

The function of platelets evolves from their unique structure (reviewed in [9, 10, 11]). Indeed, the platelet is an unusual cell; it does not have a nucleus and, therefore, is unable to synthesize proteins. Thus, the functional behaviour of the platelet is pre-regulated by the bone marrow derived megakaryocyte [12]. The ultrastructure of platelets is represented in Figure 1.2-1. The glycoproteins of the surface coat are particularly important in the platelet reactions of adhesion and aggregation, which are the initial events leading to platelet plug formation during haemostasis [13]. Specific glycoprotein receptors in the **plasma membrane** react with aggregating agents, inhibitors and coagulation factors. Adhesion to collagen is facilitated by glycoprotein (GP) Ia-IIa. GPIb (defective in Bernard-Soulier syndrome) and GPIIb-IIIa (defective in thrombasthenia) are important in the attachment of platelets to von Willebrand factor and hence to vascular subendothelium [13]. GPIIb-IIIa is also the receptor for fibrinogen, which is important in platelet-platelet aggregation [14]. The plasma membrane invaginates into the platelet interior to form an **open canalicular system**, which provides a large reactive surface to which the plasma coagulation proteins may be selectively absorbed. The membrane phospholipids (platelet factor 3) are of particular importance for initiating conversion of coagulation factor X to Xa and prothrombin to thrombin during the coagulation cascade. The contractile protein complex system comprises of microfilaments in the submembranous area and throughout the platelet cytoplasm. A circumferential skeleton of **microtubules** is responsible for the maintenance of the normal circulating discoid shape.

In the platelet interior: calcium, nucleotides (particularly ADP) and serotonin are contained in electron-**dense granules**. Specific **α -granules** contain a heparin antagonist (platelet factor 4), platelet-derived growth factor, β -thromboglobulin, fibrinogen, von Willebrand factor and other clotting factors. Other specific organelles include **lysosomes**,

which contain acid hydrolases and **peroxisomes**, which contain catalase. During the release reaction described below, the contents of the granules are discharged into the open canalicular system. Energy for platelet reactions is derived from oxidative phosphorylation in **mitochondria** and from anaerobic glycolysis utilising platelet **glycogen**. The **dense tubular system** of platelets which represents residual endoplasmic reticulum contains substantial quantities of calcium and may be the site of synthesis of prostaglandins and thromboxane A₂ [15].

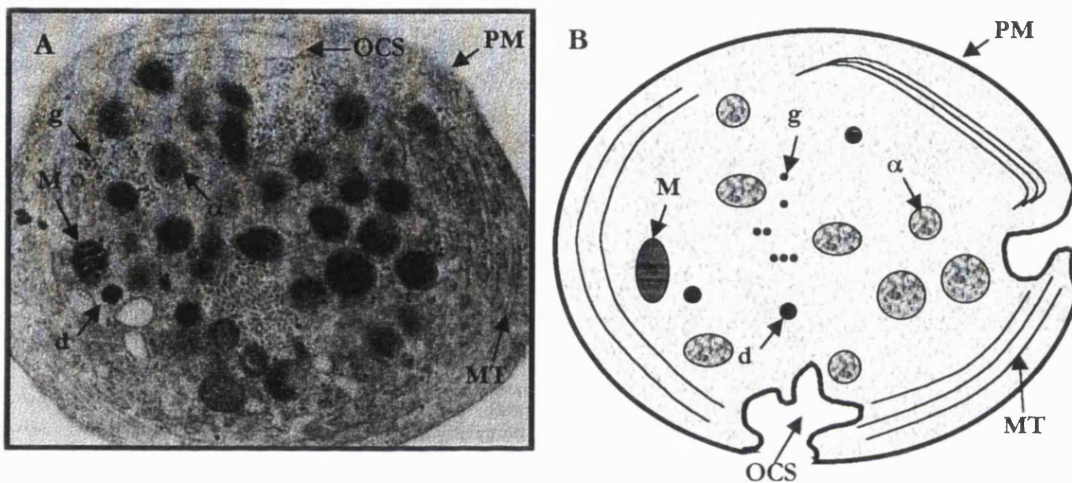


Figure 1.2-1 Ultrastructural Features of Platelets.

A transmission electron micrograph (panel A) and diagram (panel B) depicting the relevant ultrastructural features of platelets. These include plasma membrane (PM), microtubules (MT), α -granules (α), dense granules (d), mitochondria (M), glycogen crystals (g) and the open canalicular system (OCS).

1.2.4 STAGES IN THE HAEMOSTATIC PROCESS AND PHYSIOLOGICAL PLATELET AGONISTS.

The main function of platelets is to form mechanical plugs during the normal haemostatic response to vascular injury. When platelets are either removed from the circulation, contact extravascular tissue or are exposed to a physiological activator (platelet agonist), they undergo a variety of changes termed “platelet activation” (reviewed in [16]). Four general platelet responses resulting from activation have been identified: shape change, adhesion, aggregation and degranulation (Figure 1.2-2).

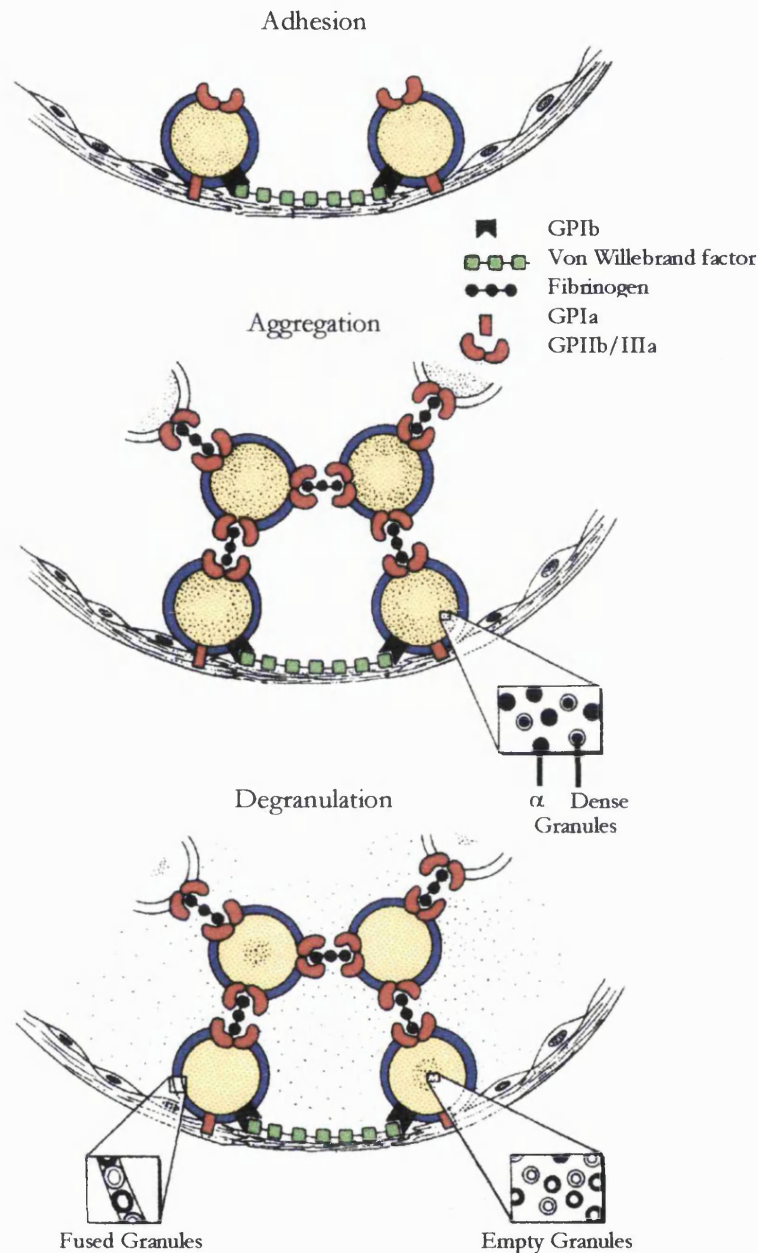


Figure 1.2-2 Platelet activation reactions.

Platelet adhesion is the process whereby platelets form a carpet-like monolayer on a blood vessel wall at the site of injury and exposed subendothelium. This is facilitated by an interaction between plasma membrane glycoproteins and constituents of the subendothelial matrix. The most important interactions are between the GPIb and von Willebrand factor and between the GPIa-IIa and collagen. Platelet aggregation results when platelet surface receptors for fibrinogen (GPIIb-IIIa complex) become activated, allowing platelet aggregation to occur. The platelet "release reaction" results from a series of intracellular signalling events that cause platelet granule membranes to fuse with invaginations in the plasma membrane, known as the open canalicular system, leading to discharge of the granule contents into the extracellular space. The increase in membrane surface allows the cell to swell, and antibodies to bind to proteins originally present in the membranes of the platelet's granules. Some of these proteins (such as P-selectin) allow platelets to interact with other cell types.

1.2.4.1 Platelet Agonists.

Platelet activation responds through discrete receptors to a number of physiological agonists and foreign surfaces. Some agonists are classified as “weak” (ADP, thromboxane A₂, platelet-activating factor [PAF] and serotonin) because they depend on autocrine stimulation (see below) to promote the full sequence of responses, while others are “strong” agonists (thrombin and collagen) that activate all responses directly without autocrine stimulation [16]. Interestingly, adrenaline is a platelet agonist that was long thought to be a true agonist, i.e. stimulating platelets by itself. However, recent investigations strongly suggest that adrenaline is only able to potentiate the action of other true platelet agonists such as ADP and thrombin [17]. Adrenaline does, however, aggregate platelets when added to platelet suspensions alone, since these suspensions always contain extracellular ADP that has leaked from platelets during cell preparation. Such synergistic interaction among agonists is very typical for platelet activation and most likely takes place *in vivo*.

1.2.4.2 Platelet Adhesion.

Following blood vessel injury, platelets adhere to the exposed subendothelial connective tissues. Subendothelial microfibrils bind the larger multimers of von Willebrand factor and through these react with platelet membrane GPIb [13, 18, 19]. A large number of adhesion proteins are involved in platelet-vessel wall and platelet-platelet interactions (for reviews see [18, 19, 20]). The GPIIb-IIIa receptor complex becomes exposed and forms a secondary binding site with von Willebrand factor further promoting adhesion [13]. Adhesion to collagen is facilitated by GPIa [20]. Platelet adhesion induces a series of metabolic reactions that initiate the shape change, aggregation and degranulation.

1.2.4.3 Shape Change.

The shape change is noted at a very early stage when platelets are activated by all platelet true agonists; as adrenaline is not a true agonist, it does not cause shape change [17]. Shape change occurs in the first few seconds after platelet activation, and is characterised, as the name suggests, by a change in platelet morphology from discs to spheres with pseudopodia [21] (Figure 1.2-3). The production of pseudopodia increases the membrane surface area thereby enhancing cellular interactions. Significant changes occur within the cytoplasm, where the granules are concentrated and enclosed in peripheral microtubules, and the microfilaments which accumulate at the centre of the cell [22].

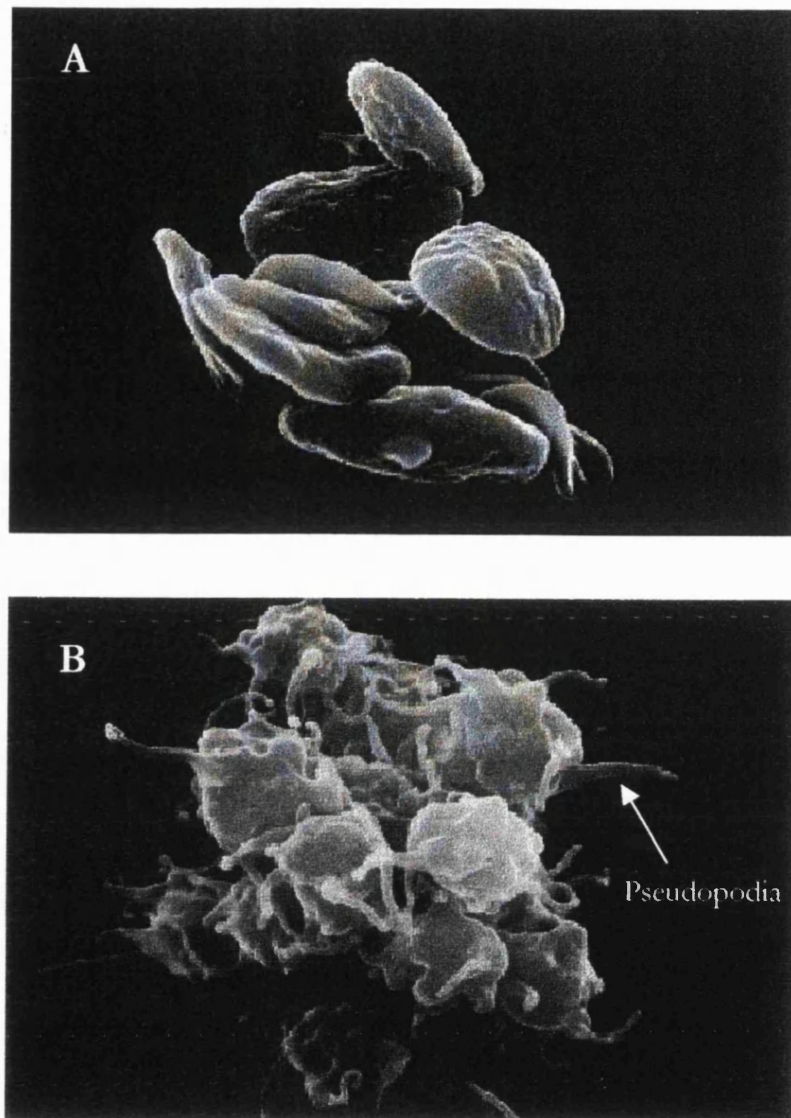


Figure 1.2-3 Platelet Shape Change.

Scanning electron micrographs of resting (panel A) and agonist stimulated (panel B) platelets. Note the appearance of many pseudopodia on activation/stimulation that increases the membrane area thereby enhancing cellular interactions.

1.2.4.4 Platelet Aggregation.

Platelets adhere to each other in response to a stimulus and form aggregates of various sizes. Aggregation is a complex phenomenon, resulting from numerous inter-linked reactions at the surface of the platelet membrane and in the cytoplasm [23, 24]. Platelets are activated by binding of agonists (ADP, serotonin, thrombin or collagen) to their respective cell surface receptors and aggregation then occurs within one minute [1]. Platelet-platelet interactions are facilitated by fibrinogen and thrombospondin, which link to adhesive proteins on the platelet membrane, i.e. the activated GPIIb-IIIa complex. Each molecule of fibrinogen can recognise two GPIIb-IIIa complexes, which allows

bridges to form between two adjacent platelets [14]. In platelet rich plasma (PRP), aggregation is characterised by a decrease in the optical density (see section 2.5.7). When minor stimulation occurs, the aggregated platelets dissociate from each other and become resuspended; this “primary aggregation” is therefore reversible. A strong stimulus results in “secondary aggregation”, which is irreversible due to the secretion of platelet granular constituents such as ADP. The release of ADP promotes further aggregation (autocrine stimulation) and leads to the formation of a plug over the damaged area [16].

1.2.4.5 Degranulation.

Concomitant with aggregation, the platelet discharges the contents of its granules [16, 18]. The ADP, calcium and serotonin released from the dense granules, as well as the fibrinogen and thrombospondin released from the α -granules, participate in platelet activation. As noted earlier, secreted ADP potentiates the effect of agents that stimulate secretion such as collagen and thrombin [25, 26]. Numerous other substances are also released during secretion: thromboxane A_2 , arachidonic acid derivatives, histamine, adrenaline, amino acids, platelet factor 4, fibronectin, von Willebrand factor, factor V, β -thromboglobulin, platelet-derived growth factor and tumour growth factor- β [1, 24, 27].

1.2.5 EFFECTS OF ADP ON PLATELET BIOCHEMISTRY.

ADP was the first platelet agonist to be discovered [28], but the mechanism of its effect on platelets has not yet been fully elucidated. The physiological importance of ADP in haemostasis and as a mediator of thrombosis has been demonstrated by means of ADP-depletion systems (apyrase) on human platelets [26] and in animal thrombosis models [25, 29] or by the use of Fawn-Hooded rats, a strain possessing platelets which are deficient in dense granules [30]. All of these model systems exhibit decreased platelet activation *in vitro* and *in vivo* and display bleeding tendencies. Since ADP was the agonist of choice for most of the studies outlined in this thesis, the remainder of this review will focus on the biochemical events induced in platelets by ADP activation.

1.2.5.1 Calcium Homeostasis.

Calcium signalling is central to the process of platelet activation (reviewed in [31]). Calcium levels in the cytoplasm and in the releasable store (the dense tubular system) are tightly controlled by a system of pumps, leaks and receptor operated channels (ROC). Both Ca^{2+} homeostasis at rest and the processes of Ca^{2+} influx and release during activation are modulated and controlled by other second messengers. These include cyclic adenosine 3', 5'-monophosphate (cAMP), cyclic guanosine 3', 5'-monophosphate (cGMP) and diacylglycerol (DAG) which stimulate their respective protein kinases (PKs): PKA,

PKG and PKC. These kinases, in turn, modulate the activity of the pumps, leaks, ROCs or other regulatory proteins by phosphorylation [32]. In addition, cytoplasmic Ca^{2+} has a modulatory influence on itself, mediated by its calmodulin complex (Ca-CAM), which activates numerous regulatory enzymes (e.g. nitric oxide synthase, see *section 1.2.6*).

1.2.5.2 Ca^{2+} Influx and Mobilization from Intracellular Stores.

Most aggregating agents act largely via G protein-coupled receptors to stimulate phospholipase C (PLC), with a resultant stimulation of PKC by DAG and mobilization of intracellular Ca^{2+} by inositol (1,4,5)-trisphosphate (IP_3) [1, 2, 16, 33]. Such aggregating agents also cause an influx of extracellular Ca^{2+} , which is thought to be triggered by the discharge of intracellular Ca^{2+} stores [32]. However, in the case of ADP, the signal transduction pathways are more complex and poorly understood [34]. Activation of platelets by ADP follows a defined sequence. The first event that occurs is shape change when discoid shaped resting cells are rapidly converted to spiculated spheres, followed by platelet aggregation and granule secretion, which releases more ADP [35]. Acting extracellularly, ADP causes a number of intracellular events including: mobilisation of intracellular calcium stores [36], a rapid calcium influx unrelated to intracellular Ca^{2+} mobilisation [37, 38] and inhibition of adenylate cyclase [39]. Although still controversial, recent research indicates that platelets contain three distinct ADP receptors that are linked to each separate event [40, 41] (see Figure 1.2-4). The intra-cellular signalling events associated with ADP stimulation have been reviewed in detail elsewhere [1, 2, 16, 32, 33]. However, a simplified overview of ADP-induced platelet activation, linking the newly described receptors with characterised signalling pathways, is outlined below:

1.2.5.3 Platelet ADP Receptors.

The three distinct ADP receptors on platelets are defined as: $\text{P}_2\text{T}_{\text{PLC}}$, which is a G protein-coupled receptor that stimulates PLC activity; P_2X_1 , an ADP sensitive ROC and $\text{P}_2\text{T}_{\text{AC}}$, a G protein-coupled receptor that inhibits adenylate cyclase [40].

The Role of $\text{P}_2\text{T}_{\text{PLC}}$.

Platelet activation via $\text{P}_2\text{T}_{\text{PLC}}$ induces the metabolism of inositol phosphates by stimulating PLC [41, 42]. PLC generates DAG and inositol mono-, di-, tri- or tetra-phosphates (IPs). DAG is a second messenger activator of PKC. The activation of PKC causes phosphorylation of numerous platelet proteins including pleckstrin and myosin light chain (see section 1.2.5.4), leading to shape change, fusion of the granules, secretion, and aggregation [1]. IPs are second messengers for the release of the intracellular calcium stored in the dense tubular system. IP_3 recognises a specific site on the membrane of the

dense tubular system, opening a calcium channel that is pH-sensitive. This leads to increases in free Ca^{2+} levels in the platelet cytoplasm [1, 2].

The Role of P_2X_1 .

Further rises in cytoplasmic Ca^{2+} are mediated by an ADP sensitive ROC (P_2X_1) [40]. This rapid influx of extracellular Ca^{2+} activates phospholipase A_2 (PLA_2). This enzyme releases arachidonic acid by acting on phospholipids such as phosphatidylcholine, which are cyclized to prostaglandin endoperoxides by cyclo-oxygenase [1, 2, 16]. These are then converted to thromboxane A_2 (TXA_2) by thromboxane synthetase. In a feedback mechanism, TXA_2 diffuses out of the membrane and binds to a specific platelet receptor, this in turn activates PLC and thus further potentiates the release of intracellular Ca^{2+} stores. TXA_2 may also further activate platelet Ca^{2+} ROCs [1, 2].

The Role of $\text{P}_2\text{T}_{\text{AC}}$.

In common with most other aggregating agents, ADP also inhibits adenylate cyclase. This effect is mediated by the G-protein linked ADP receptor ($\text{P}_2\text{T}_{\text{AC}}$), is distinct from Ca^{2+} mobilisation and is dependent on the inhibitory G protein, G_i [40, 1]. Although the inhibitory effects of agonists such as adenosine and prostacyclin on platelets are known to be mediated by stimulation of adenylate cyclase (see *section 1.2.6*), the inhibition of adenylate cyclase alone is not sufficient to cause platelet aggregation. However, suppression of adenylate cyclase activity may help offset the effects of inhibitory agonists encountered in the circulation or generated in the process of aggregation (e.g. prostacyclin [PGI_2]) [see *section 1.2.6*].

1.2.5.4 ADP Induced Modification of Platelet Proteins.

Phosphorylation of Proteins.

Platelet activation causes phosphorylation of several proteins, three of which have been intensively studied (reviewed in [1, 42]). Myosin light chain (MLC) of 20 kDa can be phosphorylated by MLC kinase (MLCK) in the presence of the Ca-CAM complex and PKC. The phosphorylation state of MLC is important for mediating the shape change reaction, since phosphorylation of MLC enables filaments of myosin to form, the ATPase of myosin to be activated by actin and the actin-myosin complex to contract. ADP activates phosphorylation of MLC, which occurs very quickly and transiently, just before the shape change [43]. Interestingly, $\text{P}_2\text{T}_{\text{PLC}}$ appears to be the only platelet ADP receptor linked to the shape change reaction [41]. Therefore, it is reasonable to assume that $\text{P}_2\text{T}_{\text{PLC}}$ mediated signalling events will lead to the phosphorylation of the MLC [41].

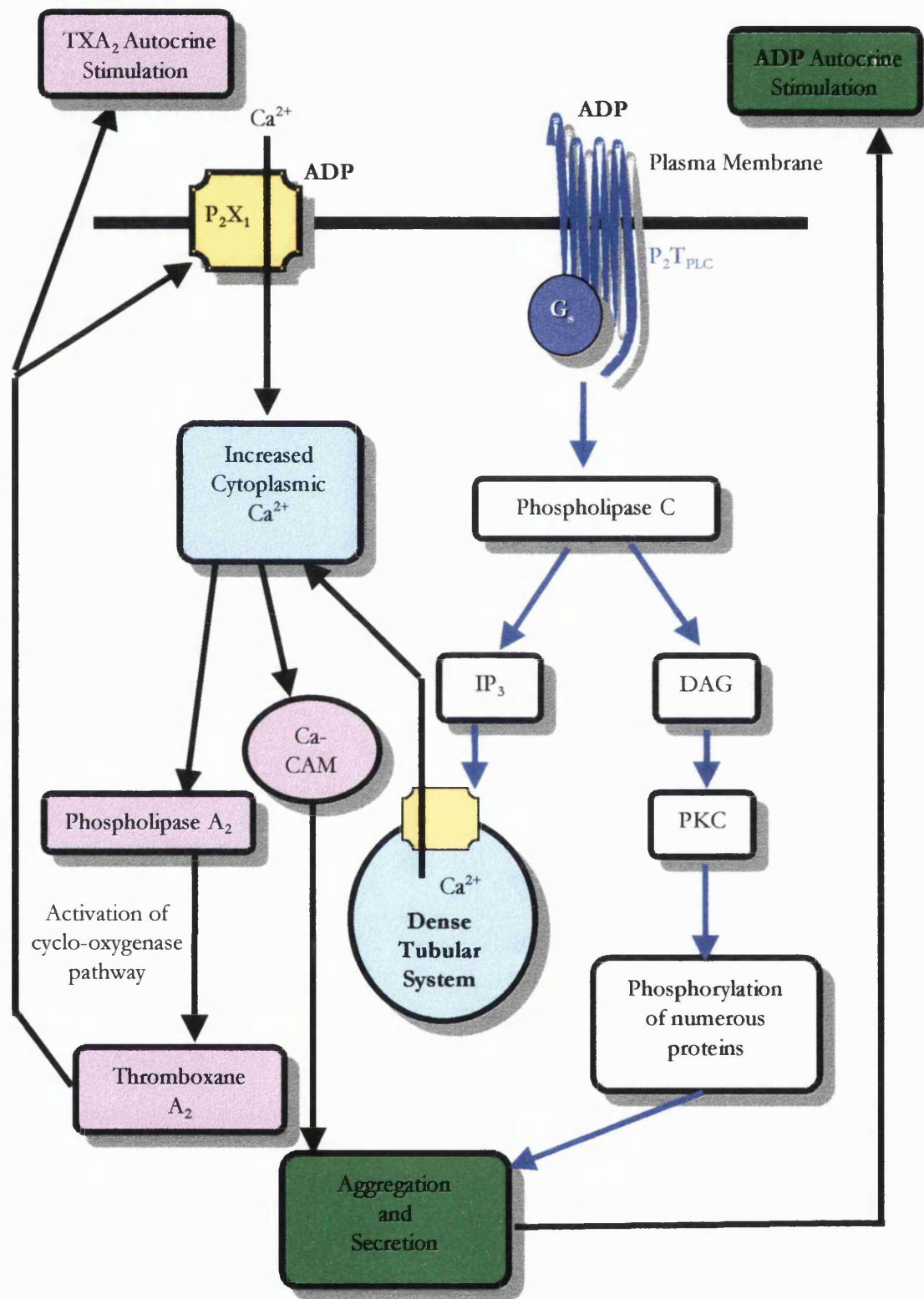


Figure 1.2-4 A simplified overview of ADP mediated intra-platelet signalling.

Together P_2T_{PLC} and P_2X_1 can mobilise a sudden influx of Ca^{2+} into the platelet cytoplasm [40, 41] and promote platelet shape change, aggregation and degranulation by activating and/or inhibiting a myriad of Ca^{2+} and phosphorylation sensitive signalling networks [32]. This activation is possibly enhanced by activation of P_2T_{AC} and inhibition of platelet adenylate cyclase (not shown).

Pleckstrin (p47) a protein of 47 kDa is phosphorylated by PKC [1, 42]. This explains why agonists, which activate PLC and thus produce DAG are strong activators of pleckstrin phosphorylation. The role of pleckstrin is at present unknown, but its phosphorylation is always associated with platelet secretion [44]. Moderate phosphorylation of pleckstrin can be achieved after activation with ADP [45].

Actin-binding protein is a 250 kDa protein that can be phosphorylated by PKC after ADP stimulation [1, 42]. It dissociates from its inactive complex with GPIb, and by associating with α -actinin, actin and tropomyosin, can form the cytoskeleton of pseudopodia.

A large number of platelet proteins can also be phosphorylated on tyrosine residues, and platelets are particularly rich in the Src family of tyrosine kinases [46]. However, in most cases it has been shown that platelet tyrosine phosphorylation events are mediated by the membrane glycoproteins. ADP stimulates phosphorylation of various proteins but only in the presence of fibrinogen which seems to suggest that this mechanism is due to activation of the GPIIb-IIIa complex rather than a direct effect of ADP.

Cytoskeletal Proteins.

The shape change, production of pseudopodia, movement of granules to the centre of the cytoplasm, secretion and aggregation are only possible in the presence of cytoskeletal proteins, in particular by the interactions between actin and myosin, and the combined effects of filamin, profilin, gelsolin, α -actinin, vinculin, and talin [47]. The polymerisation of actin has been investigated in several studies. The conversion of G-actin (globular) into F-actin (filamentous) can be measured during activation by thrombin [48], collagen [49] and ADP [50, 51]. With ADP, the polymerisation of actin occurs in two stages that coincide with the shape change and aggregation, respectively [51].

1.2.6 THE BIOCHEMISTRY OF INHIBITION OF PLATELET AGGREGATION.

The activation of human platelets is inhibited by a variety of agents that exert their effects through distinct mechanisms. Examples include inhibitors of thromboxane A_2 generation (e.g. aspirin) [52], inhibitors of thrombin (e.g. hirudin) [53], scavengers of ADP (e.g. apyrase) [54], and physiological and pharmacological cyclic nucleotide-elevating agents [32]. Vascular endothelial cells, under basal conditions and in response to numerous vasoactive agents, synthesize and release PGI₂ and the endothelium-derived relaxing factor, nitric oxide (NO), two of the most important physiological platelet inhibitors [55]. PGI₂ and NO increase the intracellular messenger molecules cAMP and cGMP, respectively, in

human platelets and other target cells [32]. The inhibition of platelet activation caused by PGI₂ and NO is mediated by cAMP- and cGMP-dependent protein kinases, PKA and PKG, respectively, which are present in very high levels in human platelets [56].

1.2.6.1 The PGI₂/cAMP Pathway.

Adenylate cyclase is localised on the internal surface of the platelet membrane. It produces cAMP from ATP [57]. A low intracellular cAMP concentration is maintained by numerous phosphodiesterases (see below), which convert it to adenosine. Platelet adenylate cyclase can be activated through G-protein linked receptor-dependent mechanisms by agents such as adenosine and PGI₂ [58, 59]. The following major effects of cAMP on platelets have been identified to date: **i)** it regulates the intra-cellular calcium concentration by inhibiting the exit of calcium from the dense tubular system and by stimulating its resequestration [60, 61], **ii)** it activates cAMP-dependent kinases (PKA) which phosphorylate MLC, actin-binding protein, a G protein of 21 kDa, tubulin and GPIb, all with inhibitory effects on aggregation [42, 49, 62-63] and **iii)** it also induces deactivation of the GPIIb-IIIa complex [64].

1.2.6.2 The NO/cGMP Pathway.

NO is an important physiological messenger with various biological properties (reviewed in detail in [65-70]). It serves as a neuronal messenger in the brain and in the non-adrenergic non-cholinergic nerve system. Macrophages contain an inducible NO synthase isoform that is activated during immunological responses. The continuous generation of NO by the vascular endothelium is crucial for the regulation of blood pressure and blood flow [65, 66, 68]. Also, endothelium-derived NO is important for the prevention of excessive platelet adhesion and aggregation [69].

NO Synthesis.

NO is generated via a five-electron oxidation of a terminal guanidinium nitrogen on the amino acid L-arginine [65-70]. This stereo-specific reaction is both oxygen and reduced nicotinamide adenine dinucleotide phosphate (NADPH) dependent and yields the co-product L-citrulline in addition to NO. This multistep electron oxidation is facilitated by a single enzyme, NO synthase (NOS) [70]. On the basis of several criteria including cellular location, regulation of activity and substrate/inhibitor profiles, the NOS enzyme can be divided into three distinct isoforms: firstly, a constitutive form, whose activity is regulated by Ca²⁺ and calmodulin (Ca-CAM) and which is found in vascular endothelial cells (NOS-III, eNOS [65, 68]); secondly, another Ca-CAM-requiring constitutive enzyme present in neural tissue, both centrally and peripherally (NOS-I or nNOS [65, 66, 70]); and

thirdly, a Ca^{2+} -independent isoform isolated from macrophages, vascular smooth muscle cells and hepatocytes following induction by specific cytokines (NOS-II or iNOS [65-67, 70]). Molecular cloning of the three NOS isoforms shows that the human eNOS, nNOS and iNOS isoenzymes have 1203, 1433 and 1153 amino acids (133, 161 and 131 kDa) respectively (Figure 1.2-5). Each exists as a homodimer of approximately 260 kDa (320 kDa for nNOS); only the dimeric forms exhibit catalytic activity [70]. They all have consensus sequences for binding of flavin adenine dinucleotide (FAD), flavin mononucleotide (FMN) and NADPH and a conserved sequence throughout NOS isoforms toward the amino terminal that is thought to function as heme-, tetrahydrobiopterin- and substrate-binding sites [65, 70]. Spanning these two regions termed “reductase” and “oxygenase” domains, respectively, is a calmodulin-binding site. This may represent an important site of regulation because binding of calmodulin permits the transfer of electrons from NADPH (via the flavins) to the heme catalytic site [65, 70]. The constitutive isoforms are dependent on Ca^{2+} , which is thought to interact with calmodulin to initiate binding to NOS [65-70]. The inducible isoform has calmodulin permanently bound, and its activity is therefore Ca^{2+} independent [65-70]. Additionally, all NOS isoforms have a consensus for PKA phosphorylation and eNOS has an amino-terminal consensus sequence for myristoylation [65].

During the last few years there has been accumulating evidence that platelets themselves exhibit an L-arginine-NO pathway that may act as a negative feedback mechanism to inhibit excessive activation and aggregation [69]. For a more detailed review of platelet NOS see *section 4.4*.

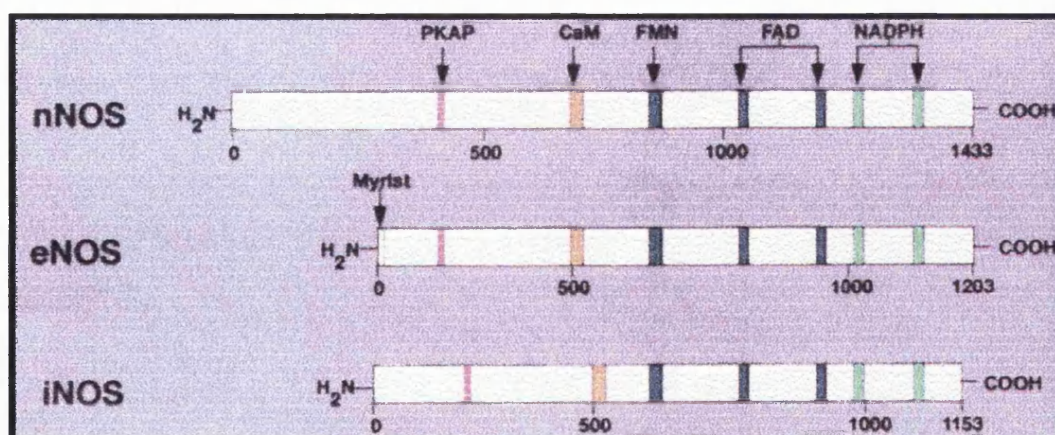


Figure 1.2-5 The primary structure of the NOS isoenzymes.

Consensus sequences for cofactors and calmodulin (CaM) binding, for PKA phosphorylation (PKAP) and for myristoylation (Myrist) are shown.

Actions of Nitric Oxide and Synthesis of cGMP.

The physiological and pathophysiological roles attributable to the actions of NO have grown exponentially since its identification as the endothelium-derived relaxing factor in 1987 [67]. Classically, molecules acting as inter- or intracellular messengers interact with specific receptor proteins on target cells to induce a necessary response. However, owing to its radical and lipophilic properties, NO does not adhere to this archetypal signalling process, but diffuses randomly away from its point of synthesis to interact with various intracellular molecules; as such, there is no specific “NO receptor” [65]. Importantly, however, these properties are imperative in mediating many of the biological effects attributed to NO. For instance, reaction of NO with metabolic enzymes or viral DNA or its reaction with superoxide anion (O_2^-) to yield peroxynitrite anion ($ONOO^-$), may be important in the cytostatic and cytotoxic effects of inflammatory cells in removing pathogens [66]. Nevertheless, the best characterised target site for NO is iron, bound within certain proteins as heme or iron-sulphur complexes [65]. Of primary physiological significance is the interaction of NO with the heme component of soluble guanylate cyclase, stimulating enzymatic conversion of GTP to cGMP; as such, guanylate cyclase is often termed the “NO receptor” [65, 67, 69]. This mechanism is responsible for the overwhelming majority of anti-platelet effects mediated by NO [69].

1.2.6.3 Guanylate Cyclase.

In contrast to adenylate cyclase, which is exclusively membrane-bound [57], guanylate cyclase exists in both the cytosolic and particulate fractions [71]. Extensive research in the past two decades has resulted in the identification of several isoforms of guanylate cyclase, which are classified by their cellular location [71, 72]. Particulate guanylate cyclase is found in the plasma membrane of various cells, and at least five distinct isoforms have been cloned and characterised. Although the precise physiological role(s) for particulate guanylate cyclases have yet to be fully elucidated, their primary function appears to be as receptor sites for the atrial natriuretic peptides and an endogenous intestinal peptide, guanylin [73]. However, with respect to the NO-cGMP signal transduction pathway, it is the soluble isoform of guanylate cyclase that plays a pivotal role [65, 71]. This heme-containing enzyme is found in the cytosolic fraction of nearly all mammalian cells. Platelets are particularly rich in soluble guanylate cyclase [71, 74].

1.2.6.4 Inhibition of Platelet Functions by NO and cGMP.

The activation of platelet soluble guanylate cyclase (SGC) and the increased formation of cGMP are the major mechanisms by which NO exerts its inhibitory actions on platelet function [65, 69], since the effects of NO can be mimicked by the addition of cGMP analogues [75]. Other mechanisms of NO action on platelets, such as ADP ribosylation, have also been described [76], but the relative functional importance of non-cGMP-mediated effects of NO has not been established thus far.

The effects of NO on platelet function differ significantly from those of other anti-platelet agents such as the cyclo-oxygenase inhibitor, acetylsalicylic acid (aspirin). Whereas acetylsalicylic acid induces an irreversible inhibition of platelet function usually during the second, irreversible phase of aggregation, NO inhibits platelet activation at an earlier stage and its effects are quickly and completely reversible [69, 71]. Thus, as well as inhibiting platelet adhesion to the vessel wall [77], NO can also interfere with the initial thrombus formation by inhibiting aggregation [69] and thus the autocrine stimulation of adjacent platelets.

As outlined above, the activation of SGC in platelets results in the conversion of GTP to cGMP. Cyclic GMP in turn, stimulates platelet cGMP-dependent protein kinase I [78]. The subsequent biochemical effects triggered by this kinase are less clear, although in platelets, inhibition of fibrinogen binding to the GPIIb-IIIa receptor, inhibition of phosphorylation of MLC and modulation of PLA₂ and PLC-mediated responses results (reviews in [79-81]). Stimulation of the 50 kDa vasodilator-stimulated phosphoprotein [81] and of the ras-related protein rap1B [82] also occurs. Intracellular Ca²⁺ is an important target for cGMP-controlled platelet responses and an increase in guanylate cyclase activity results in reduction of intracellular Ca²⁺ concentrations. Indeed, receptor-mediated Ca²⁺ influx and mobilisation are potently inhibited by cGMP production in platelets [32].

1.2.6.5 Platelet Cyclic Nucleotide Phosphodiesterases.

The intraplatelet concentrations of cAMP and cGMP are not only controlled by the synthesizing cyclase enzyme but also by degrading enzymes, cyclic nucleotide phosphodiesterases (PDEs). The purification of PDEs from the cytosolic fraction of human platelets by DEAE-cellulose chromatography yields three peaks of activity [83]. The first enzyme (PDE I) has a higher affinity for cGMP than for cAMP and hydrolyses mainly cGMP at low substrate levels. The second enzyme (PDE II) exhibits low affinity for both cyclic nucleotides [84]. The third enzyme (PDE III) has a higher affinity for cAMP and its activity is inhibited by low levels of cGMP [85, 86]. Thus, increases in cGMP can also significantly affect metabolism of cAMP in platelets.

1.3 Apolipoprotein E.

1.3.1 PREFACE.

Plasma apolipoproteins serve to regulate lipoprotein metabolism and to control the transport and redistribution of lipids among tissues and cells. Apolipoproteins achieve this by performing at least one of three major roles (reviewed in [87, 88]). Firstly, because of their ability to bind lipid, apolipoproteins stabilise the pseudomicellar structure of lipoprotein particles. Secondly, apolipoproteins can act as cofactors or activators of various enzymes or lipid transfer proteins that participate in the metabolism or “remodelling” of lipoproteins as they circulate in plasma. Finally, some specific apolipoproteins serve as ligands for cell surface lipoprotein receptors and can direct, therefore, the delivery and redistribution of lipids to cells.

Of the 14 plasma apolipoproteins that have been described, apolipoprotein E (apoE) is one of the best characterised in terms of its structural and functional properties (reviewed in [6, 89, 90]). In humans, apoE is a constituent of liver-synthesized very low density lipoprotein (VLDL), which functions primarily to transport triglyceride from the liver to peripheral tissues. It is also present in a subclass of high density lipoprotein (HDL) which participates in cholesterol redistribution among cells. In addition, apoE becomes a significant protein constituent of intestinally synthesized chylomicrons, which transport dietary triglyceride and cholesterol. The major physiological role for apoE in lipoprotein metabolism is its ability to mediate high-affinity binding of apoE-containing lipoproteins to the low density lipoprotein receptor (LDL-R). ApoE binding to the receptors initiates the cellular uptake and degradation of lipoproteins. This releases the lipoprotein cholesterol, which ultimately regulates intracellular cholesterol metabolism. ApoE shares this delivery function with apoB-100, the protein constituent of plasma low density lipoprotein (LDL). Furthermore, apoE mediates the binding of chylomicron remnants to a second hepatic receptor, the low density receptor related protein (LRP). The precise mechanisms involved in the interaction of apoE with lipoprotein receptors and in regulation of lipoprotein metabolism (and other apoE metabolic roles) will be discussed later.

1.3.2 DISCOVERY AND INITIAL CHARACTERISATION OF APOE.

The first detailed description of apoE was published in 1973 by Shore and Shore [91]. It was identified as a component of triglyceride-rich VLDL and was referred to as the “arginine-rich” protein (ARP), due to its relatively high content of arginine compared to the other apolipoproteins. In 1975, Utermann suggested the designation “apoE” for

this protein, consistent with the alphabetical nomenclature that was becoming commonly used in this field [92]. However, this designation was not universally adopted for several years. Consequently, during the late 1970s the protein was referred to as both ARP and apoE.

ApoE was initially characterised in several animal species after it was realised that dietary cholesterol altered its distribution in plasma. Thus, apoE becomes a major protein constituent of several cholesterol-enriched lipoproteins that accumulate in the plasma of rabbits, dogs, swine, rats and monkeys fed high levels of fat and cholesterol [90]. It is now known that these cholesterol-enriched, apoE-containing lipoproteins are chylomicron and VLDL remnants (referred to collectively as β -VLDL) and a subclass of HDL (referred to as either HDL₁, HDL_c, or simply HDL-E; for review see [93, 94]). As mentioned previously, apoE is also present in chylomicrons, VLDL and HDL in normolipidaemic humans and is approximately equally distributed between VLDL and HDL in plasma that is devoid of chylomicrons [95]. The normal human plasma concentration of this protein is between 3 - 7 mg/dl [89, 90].

1.3.3 GENE REGULATION AND BIOSYNTHESIS OF HUMAN APOE.

Human apoE is a 34.2 kDa protein consisting of a single 299 amino acid polypeptide chain. The primary structure was first determined by direct amino acid sequencing of the protein purified from human VLDL [96] and later confirmed by nucleic acid sequencing of a full-length cDNA [97]. ApoE is encoded by the 3.7 kilobase *APOE* gene located on chromosome 19, which contains four exons and three introns [98-100]. The *APOE* gene is linked to another apolipoprotein, apoC-I and an apoC-I pseudogene [101]. The LDL-R and apoC-II genes have also been mapped to this chromosome [102, 103], but apparently, they are not closely linked to each other or to *APOE*. The *APOE* promoter sequence TATAATT occurs approximately 30 base pairs (bp) upstream from the transcriptional initiation site. Other promoter and enhancer elements important in regulating apoE biosynthesis have also been identified [104]. The apoE mRNA is 1163 bp in length [97]. This mRNA encodes a precursor protein containing an 18 amino acid signal peptide that is removed co-translationally during the translocation of the protein through the endoplasmic reticulum [97]. In humans, apoE is secreted as an O-glycosylated protein due to a single glycosylation site at Thr₁₉₄ [105]. In plasma, 90 % of apoE is desialylated, although the relevance of this phenomenon for its function and metabolism is not understood at present [6]. Sialic acid variations of apoE often appear as multiple bands on polyacrylamide gels.

1.3.4 SITES OF SYNTHESIS.

ApoE is produced in most organs and significant quantities of apoE mRNA are detected in the liver, brain, spleen, lung, adrenal, ovary, kidney and muscle in several different species [89, 90].

1.3.4.1 Liver ApoE.

The largest quantity of apoE mRNA is present in the liver, which is the major source of apoE, accounting for the majority of plasma apoE. Hepatic parenchymal cells are largely responsible for apoE production within the liver [106] and secrete apoE as a component of VLDL. However, it is possible that liver-synthesized apoE is released independently of VLDL, as discoidal particles that contain mainly phospholipids [107].

1.3.4.2 Brain ApoE.

The second largest concentration of apoE mRNA is found in the brain (about one-third the amount in liver) [6, 90, 108]. In the brain, astrocytes are the cell type responsible for producing the majority of brain apoE [109, 110], although glial cells and neurones have been reported to produce apoE under certain conditions [110, 111]. It is noteworthy that apoE is also a major apolipoprotein of cerebrospinal fluid (CSF) in humans and dogs [6, 89, 112]. ApoE exists in the CSF as small spherical or discoidal lipoproteins that transport cholesterol and phospholipid. Unlike the plasma, in which apoB-100 containing LDL is the major cholesterol transporter, the CSF lacks both apoB-100 and LDL; presumably, apoE assumes the major role of lipid transport in CSF. The principal role of brain apoE may be the redistribution of lipids among cells to maintain cholesterol homeostasis in the cerebral environment. Another function proposed for apoE in the nervous system is a targeting protein for local redistribution of cholesterol within neural tissues undergoing repair or remodelling [90]. This proposal is based on observations made in rat sciatic nerve undergoing regeneration and remyelination [113, 114]. Because apoE has been localised in brain tumours, it has been postulated as a possible marker for glial neoplasms [115]. High concentrations of apoE in tumour cells is unsurprising; the proliferation of these cells is more rapid than of non-tumour cells, and therefore greater quantities of lipid are required for cellular membrane construction. The high rate of synthesis of apoE in tumour cells might be a response to an increased demand for cholesterol.

1.3.4.3 Macrophage ApoE.

Macrophages derived from the peritoneal cavity of mice or from human blood monocytes also produce large quantities of apoE (reviewed in [90, 116]). Indeed, apoE synthesis and secretion is induced to very high levels by cholesterol-loading macrophages

and can represent as much as 5 % to 10 % of all newly synthesized proteins. The apoE released from these cells express important differences compared to plasma apoE. The most obvious of these is that apoE is secreted in combination with phospholipid and occurs in the form of apoE/phospholipid disks. Another significant difference is the higher degree of sialylation in macrophage-derived apoE. It is possible that macrophages are also responsible for the apoE mRNA seen in the spleen and lung. However, the involvement of other cell types in apoE synthesis has not been excluded.

Clearly, human apoE has a wide tissue distribution with a role related generally to inter- or intra-organ cholesterol transport. This implies an important physiological role for apoE, which, at present, is incompletely understood. For example, little is known about the apoE content in different tissues, nor how these tissues release apoE into the extracellular fluid and other body fluids.

1.3.5 APOE POLYMORPHISM.

The polymorphic nature of apoE was established by Utermann and his associates [117], using isoelectric focusing (IEF), and further clarified by Zannis and Breslow [118], using two-dimensional electrophoresis. The three major isoforms of apoE, referred to as apoE-2, E-3 and E-4, are products of three alleles ($\epsilon 2$, $\epsilon 3$, $\epsilon 4$) at the *APOE* locus. Three homozygous phenotypes (apoE-2/2, E-3/3 and E-4/4) and three heterozygous phenotypes (apoE-3/2, E-4/3 and E-4/2) arise from expression of these alleles. The most common phenotype is apoE-3/3 and the most common allele is $\epsilon 3$, therefore, apoE-3 is considered the parent form of the protein, with apoE-4 and E-2 as variants [6, 89, 90]. ApoE-2 is associated with recessive forms of type III hyperlipoproteinaemia and is defective in receptor binding [6, 119]. ApoE-4 displays normal binding but produces a dominant hyperlipidaemia, is a risk factor for restenosis and is implicated in the pathogenesis of Alzheimer's disease (for review, see [6, 120, 121]). The molecular basis for apoE polymorphism was elucidated by analysis of the amino acid sequences of the three isoforms [122]. Amino acid substitutions account for the differences among apoE-4, E-3 and E-2. ApoE-3 contains a single cysteine at residue 112 and an arginine at position 158; apoE-2 contains cysteine residues at both positions 112 and 158; and apoE-4 contains arginine residues at both positions. The charge differences among the three isoforms detected by IEF are explained by the single amino acid substitutions. A secondary form of apoE polymorphism is explained by post-translational sialylation and is designated apoE-1 [118].

The three major isoforms differ from each other with respect to their association with lipoproteins, their binding affinity for the LDL-R, and their interaction with heparin [6, 89, 90, 123-125]. ApoE-3 displays a preference for HDL, as does apoE-2, whereas apoE-4 interacts with large lipoproteins such as VLDL [123]. Additionally, apoE-3 and apoE-4 bind equally well to the LDL-R, while apoE-2 displays only approximately 1 % of their binding activity [90, 124]. Besides a reduced affinity for the LDL-R, apoE-2 also shows reduced binding to heparin sulphate proteoglycan (HSPG) [125], unlike apoE-3 and apoE-4 which bind HSPG with a high affinity. This heparin binding property of apoE has been utilised for purifying apoE polypeptide or apoE-containing lipoproteins by affinity chromatography (see *sections 2.4.3 and 3.2.3*).

1.3.6 STRUCTURE OF APOE.

Many aspects of the structure-function relationships of apoE have recently been reviewed in some detail by Weisgraber [89]. Briefly, apoE differs from other apolipoproteins in its tertiary structure. From the Chou-Fasman algorithm, apoE is predicted to be highly helical and segregated into two fragments separated by a large section whose structure is predicted to be random [89, 126, 127]. Several lines of evidence suggest that apoE is folded into two independent structural domains, corresponding to two functional moieties of the protein. For example, curves for denaturation in the presence of guanidine hydrochloride, followed by circular dichroism or fluorescence spectroscopy, display two transitions that is indicative of two separate structural domains. Moreover, limited thrombolytic digestion of purified plasma apoE separates two fragments that have been protected against proteolysis [89, 126, 127]. One fragment corresponds to a 22 kDa amino terminal fragment (amino acids 1 to 191), the other to a 10 kDa carboxyl terminal fragment (amino acids 216 to 299). These two fragments have been used as models for the two structural domains of apoE (see Figure 1.3-1)

1.3.6.1 The Amino Terminal Domain.

The amino terminal moiety of apoE displays physicochemical properties similar to those of other globular proteins and remains monomeric in solution [127]. This domain includes both the receptor-binding and heparin-binding sites of apoE [89, 90]. The recent determination of the crystalline structure of this 22 kDa fragment showed its organisation into an anti-parallel four-helix bundle, which is a common folding motif of α -helical proteins (Figure 1.3-2) [128, 129]. The helices in the apoE-3 22 kDa fragment are amphipathic in nature. The hydrophobic side chains are sequestered in the interior of the bundle, and the packing of these hydrophobic residues probably contributes to the

stability of the tertiary structure. Most of the acidic and basic residues are involved in salt bridges, which contributes to the high stability of this bundle. Interestingly, the basic residues in the vicinity of amino acids 136 to 158 are not involved in salt bridges and are therefore, solvent exposed, resulting in a large area of positive charges over helix 4. This area of positive charge is thought to mediate the interaction between apoE and its receptors (see *section 1.3.6.3*).

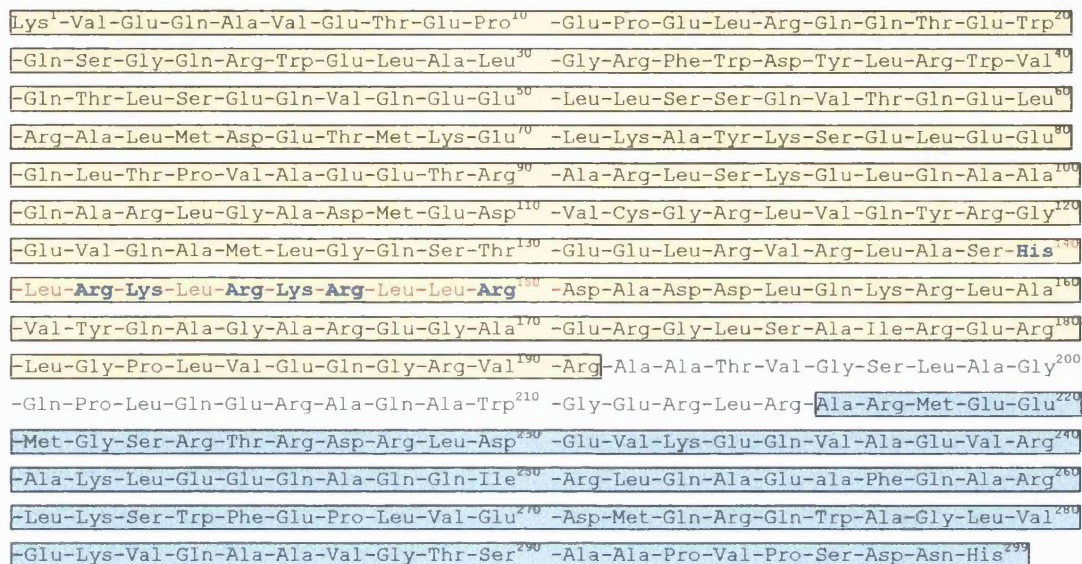


Figure 1.3-1 The complete amino acid sequence of human apolipoprotein E3.

Adapted from Rall et al. [96]. Thr₁₉₄ contains a variably sialylated carbohydrate moiety. Thrombin cleaves at the carboxyl terminal side of Arg₁₉₁ and Arg₂₁₅ [89]. The 22 kDa fragment is boxed in yellow, while the 10 kDa fragment is boxed in blue. The LDL-R binding domain is highlighted in red. The basic amino acids within the LDL-R binding domain that are important for LDL-R binding are printed blue bold.

1.3.6.2 The Carboxyl Terminal Domain.

Studies to determine the role of the carboxyl-terminal region of apoE were mainly performed with truncated variants and synthetic peptide fragments [89, 130, 131]. The carboxyl terminus beyond residue 191 contains three predicted helices, helix A (amino acids 203-223), helix B (225-266) and helix C (268-289). Interestingly, in the absence of lipids, apoE self-associates as a tetramer over a wide concentration range [128, 132]. In contrast, self-association does not occur in lipid surfaces, implying that self association and the lipid binding moieties of apoE are structurally related. Indeed, lipid association experiments with different lipoproteins or dimyristoylphosphatidylcholine (DMPC) vesicles suggest that helix C and the end of the helix B play major roles both in lipid binding and in the tetramerisation of apoE [130, 131]. More precisely, fragment 263-286

seems to be critical for lipid binding and association of apoE with VLDL [131]. However, the exact structural organisation of the carboxyl-terminal of apoE must await crystallisation of this domain or indeed the crystallisation of the entire apoE molecule.

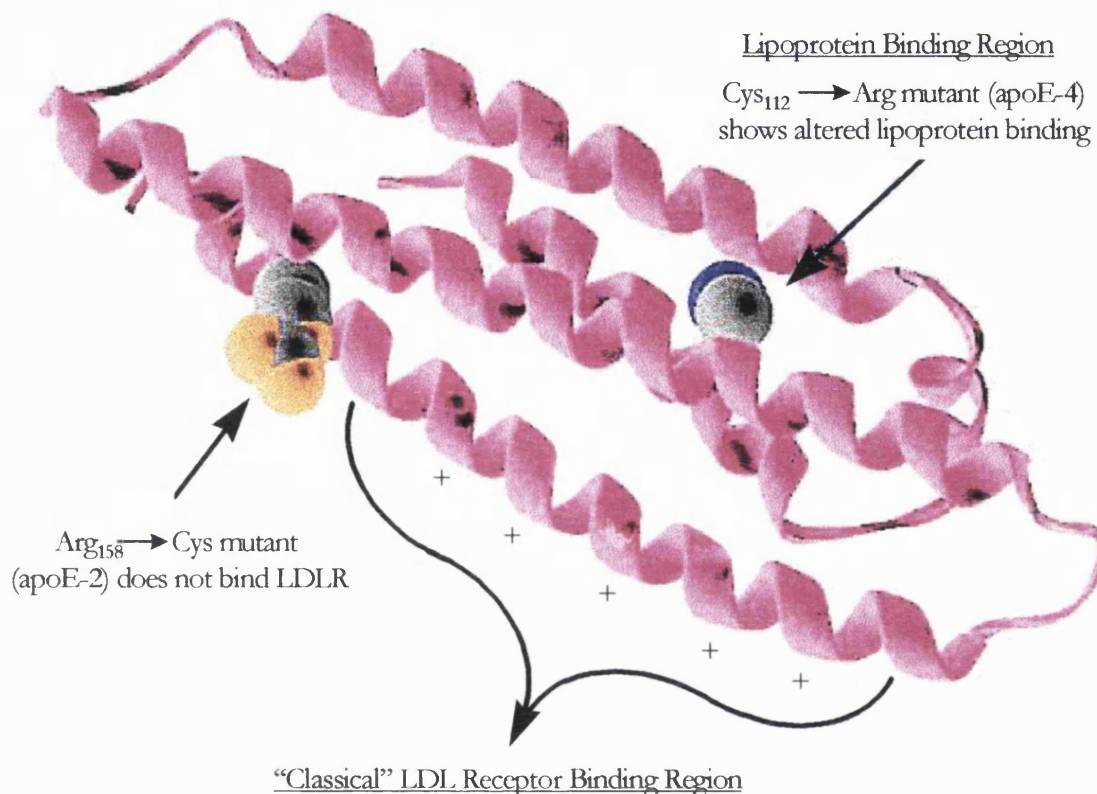


Figure 1.3-2 Ribbon model of the structure of the amino terminal domain of human apoE.

Four of the five helices of the amino terminal of apoE are arranged in an anti-parallel four-helix bundle. The “classical” positively charged LDL-R binding region of apoE (~ residues 130-150) is indicated on helix 4. The amino acid substitutions that constitute the apoE-2 and apoE-4 mutations are also indicated.

1.3.6.3 The Receptor Binding Domain of ApoE.

The receptor binding domain of apoE has been mapped in detail (for review, see [89, 90, 133]). Initially, it was established that a limited number of arginine and lysine residues within apoE were essential for binding to the LDL-R. Selective chemical modification of either arginine or lysine residues completely inhibited apoE binding to the LDL-R *in vitro* [134, 135]. Furthermore, modification of the arginine or lysine residues of apoE-containing lipoproteins markedly retarded their plasma clearance *in vivo*, further establishing the key role of these residues in mediating specific lipoprotein catabolism via

the LDL-R pathway [136]. The specific amino acid residues of apoE involved in mediating receptor binding have been identified by using four complementary experimental approaches: **i)** identifying and sequencing natural apoE mutants defective in receptor binding, **ii)** generating apoE fragments and testing their receptor binding activity, **iii)** epitope mapping of apoE monoclonal antibodies that block binding of apoE-containing lipoproteins, and **iv)** producing site-directed mutant forms of apoE. As noted, apoE variants associated with type III hyperlipoproteinaemia do not bind normally to the lipoprotein receptors [6, 89, 90, 124, 125]. The most common variant is apoE-2, in which cysteine replaces the normally occurring arginine at residue 158. However, several other rare apoE variants associated with this disorder also bind defectively [89, 90, 124]. Sequencing showed that single amino acid substitutions in the defective mutants are clustered near residues 130 to 160. In all of these natural mutants, neutral amino acids substitute for the basic arginine or lysine residues in this region of the molecule. These data focused attention on this region of apoE as being the putative receptor binding domain. In a second series of studies, apoE was cleaved into smaller fragments by two different procedures utilising thrombin and cyanogen bromide [137]. As outlined earlier, thrombin produced two major polypeptides, the 22 kDa amino-terminal fragment and the 10 kDa carboxyl-terminal fragment. The amino-terminal fragment possessed full receptor binding activity, whereas the carboxyl-terminal fragment had none. The only cyanogen bromide fragment with receptor binding activity encompassed residues 126 to 218 [137]. A third line of evidence also highlighted this same region of apoE. The epitope of a monoclonal antibody to apoE that blocked receptor binding (designated 1D7) was localized to residues 142 to 145 [138, 139]. The role of other specific amino acid residues in receptor binding has been elucidated by a fourth approach, site-directed mutagenesis. Recombinant techniques can be used to produce apoE-3 in *E. coli* that displays normal binding and plasma clearance [140]; this allows comparison with apoE mutated at specific sites in the receptor binding domain or at distant sites which might influence conformation. Basic amino acids converted to neutral residues reduced binding to approximately 10 % to 50 % of normal, comparable to the range seen with naturally occurring variants [89, 90, 140]. The remarkable consistency of all the foregoing data indicates that the basic amino acids arginine and lysine (and histidine) in the vicinity of residues 140 to 150 are important in mediating the binding of apoE to the LDL-R. Indeed, only here do the arginine and lysine residues occur in doublets and triplets. Thus, the basic amino acids in this region are important for normal receptor binding, but note that substitutions outside this immediate region (residues 130 – 140 and 150 - 160) can also have an effect by altering the conformation of the binding domain [89, 121].

1.3.7 APOE RECEPTORS.

ApoE is recognised by a family of related receptors, the LDL receptor super family (LRSF) [133, 141-144]. In mammals, the members of the LRSF include the LDL-R itself, the very low density lipoprotein receptor (VLDL-R), the multifunctional α_2 -macroglobulin receptor/LDL receptor-related protein (LRP), gp330/megalin and the newly characterised brain receptor, apolipoprotein E receptor 2 (apoER2) (see Figure 1.3.3).

The LRSF members are defined by common structural elements that show high degrees (50 - 100 %) of sequence identity, not only between each family member but also across a wide range of species [141-145]. Such sequence conservation is thought to have evolved by duplication and/or exon shuffling events from an ancestral gene [145]. Obligatory for membership of this gene family is the presence of extracellular LDL-R "class A" repeats, also known as LDL-R ligand binding repeats. Each class A repeat consists of approximately 40 amino acids, each containing six cysteine residues that are disulphide bonded in the pattern one to three, two to five and four to six. Reduction of these disulphide bridges destroys the structure and abolishes ligand binding [146, 147]. Additionally, each of these repeats forms a complex with a single Ca^{2+} ion, which also stabilises the ligand binding structure [147, 148]. The class A repeats are arranged in head to tail fashion and are preceded and/or followed by epidermal growth factor-precursor repeats (EGF), each also with six cysteines. Other common elements are the "YWTD-repeats", characterised by a length of approximately 50 residues containing a consensus tetrapeptide sequence F/YWXD. Typically, these are present in a group of five, flanked by EGF repeats. The LDL-R, VLDL-R and apoER2 contain a juxtamembrane O-linked sugar domain of approximately 60 amino acids that is enriched in clusters of serine and threonine [141]. There is a single membrane spanning stretch. The intracellular domain of all LRSF members identified so far contain one or more tyrosine containing hexapeptides (FxNPxY) that serve as an internalisation signal to direct the receptors to clathrin-coated pits.

1.3.7.1 The LDL Receptor.

The LDL-R was the first characterised member of this family. It contains one cluster of seven class A repeats and one cluster of three EGF repeats, the latter separated by a cysteine-poor spacer that contains five copies of the YWTD sequence. The LDL-R binds plasma lipoproteins that contain apoB-100 or apoE, and it is responsible for the removal of most intermediate density lipoproteins (IDL) and LDL from plasma. As such, it plays an essential role in cholesterol homeostasis. Both IDL and LDL accumulate in

plasma of patients with familial hypercholesterolemia, who have mutations in the LDL-R gene. The biochemistry and cell biology of the LDL-R has been reviewed in detail by Myant [133].

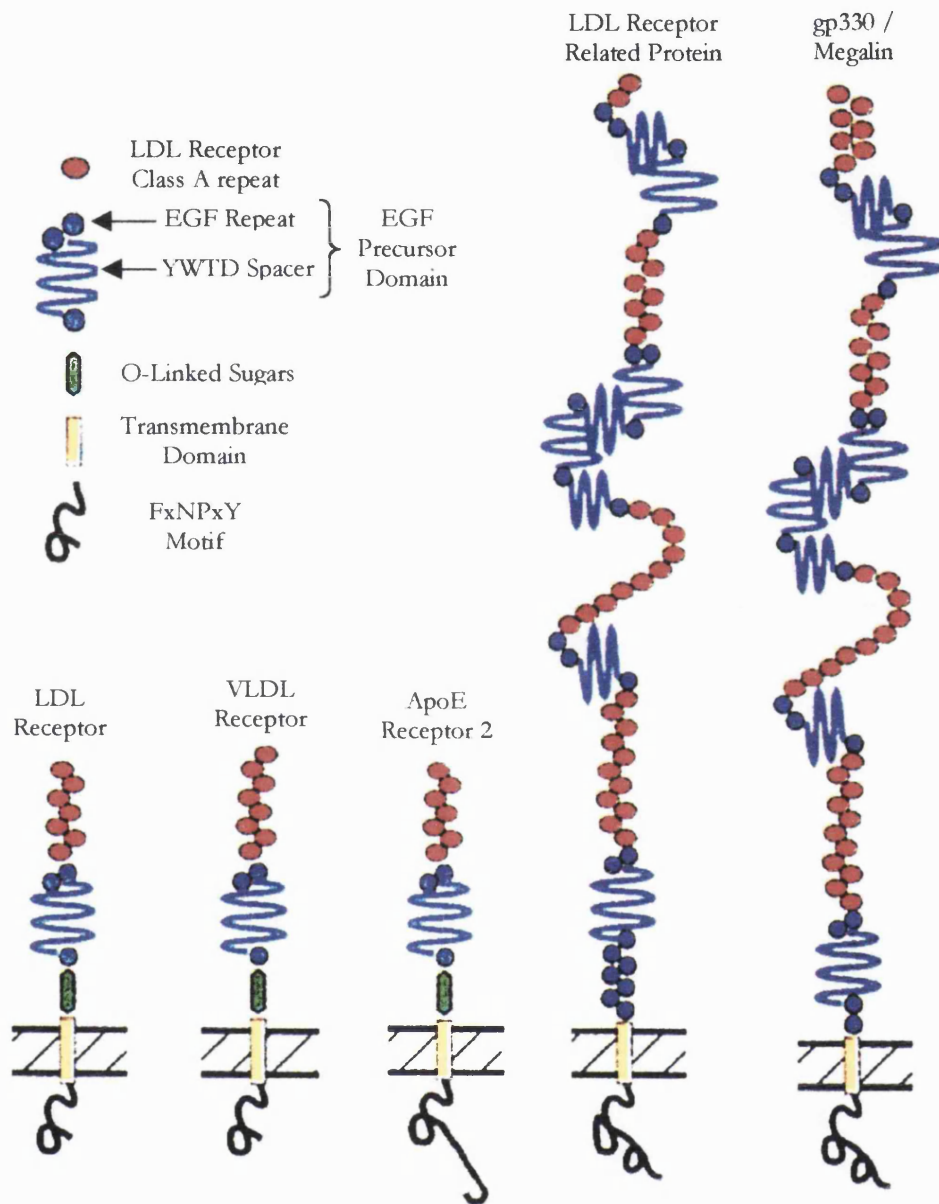


Figure 1.3-3 The mammalian members of the LDL-R super family.

1.3.7.2 The LDL Receptor-Related Protein.

The second member of the LDL-R gene family to be characterised was the LDL receptor-related protein (LRP), also designated the α_2 -macroglobulin receptor. This protein whose cDNA was cloned by homology with the complement repeat region of the LDL-R sequence [149] is much larger than the LDL-R (4525 versus 839 amino acids). It

contains 31 class A repeats and 22 EGF repeats that are separated by eight spacer regions, each containing multiple YWTD repeats [149, 150]. The juxtamembrane O-linked sugar domain is not present in the LRP. The carboxyl-terminal cytoplasmic domain is 100 amino acids long, twice the length of the LDL-R cytoplasmic domain, and contains two copies of the FxNPxP internalisation motif.

The 600 kDa LRP is synthesized as a single polypeptide chain precursor in the endoplasmic reticulum [150, 151]. During its passage through the secretory pathway, it is modified by N-linked glycosylation and by a proteolytic processing event that takes place in a late Golgi compartment. There, LRP is cleaved between amino acids 3924 and 3925. This tetrabasic cleavage site conforms to the consensus recognition sequence of furin, a resident protein precursor processing hydrolase in the secretory pathway. Proteolysis generates a large amino terminal subunit, LRP-515, which contains most the extracellular portion of the molecule and which remains tightly and non-covalently associated with the smaller transmembrane and cytoplasmic domain containing carboxyl terminal LRP-85 subunit. The significance of this cleavage for the function of LRP has not yet been elucidated. After cleavage, LRP is transported to the cell surface [150, 152].

LRP does not bind LDL, but it does bind β -migrating very low density lipoproteins (β -VLDL) that have been enriched *in vitro* with apoE [152-154]. β -VLDL is a mixture of cholesterol-rich remnant lipoproteins derived from intestinal chylomicrons and hepatic VLDL [155]. Although LRP is present on a variety of cell types and tissues, it is expressed predominantly in the liver [156, 157] where it has been proposed to act as a receptor for chylomicron remnants that become enriched with apoE during passage through hepatic sinusoids [149, 150, 157]. LRP also binds other ligands including lipoprotein lipase (LPL) [158], an enzyme that is normally bound to the surface of endothelial cells in adipose tissue and muscle, and lactoferrin, a 76 kDa glycoprotein with some sequence identity to apoE [159]. Kristensen et al. [160] found that the receptor for α_2 -macroglobulin-protease complexes was identical in its structure to that of LRP. α_2 -Macroglobulin is a plasma protease inhibitor that circulates in an inactive form. Upon binding a protease, the α_2 -macroglobulin is altered so that it binds to receptors on hepatocytes and is rapidly cleared from the circulation [161]. Another class of recently recognised ligands for LRP are complexes of plasminogen activators and their inhibitors [160]. By ligand blot analysis, LRP binds complexes of tissue-type plasminogen activator (tPA) and plasminogen activator inhibitor (PAI-1) [162]. LRP also binds complexes of urokinase-type plasminogen activator and PAI-1 [162, 163].

1.3.7.3 The gp330/Megalin.

The third member of the LRSF, called gp330 (or megalin), is less well characterised. This protein was originally identified as a target molecule in kidney for autoimmune antibodies in rats with Heymann's nephritis [164]. Gp330 is normally located in certain epithelial cells including those of the kidney (renal glomerulus and proximal tubule), yolk sac and epididymis, but not in liver [164, 165]. Antibodies against gp330 cause it to shed from the cell surface and to deposit in the basement membrane, causing nephritis. The deduced 4660 amino acid sequence, expected to constitute a mature unglycosylated protein of 520 kDa, consists of a probable amino-terminal signal peptide sequence (25 residues), an extracellular region (4400 amino acids), a single transmembrane domain (22 amino acids), and a carboxyl-terminal cytoplasmic tail (213 amino acids) [166]. The extracellular region contains 36 LDL-R class A repeats forming four clusters of putative ligand-binding domains and 16 EGF repeats separated by 8 YWTD spacer regions. The cytoplasmic tail contains two copies of the FxNPxY motif. The overall structure of gp330 is similar to that of the LRP and shows even greater similarity to the *Caenorhabditis elegans* protein, reported as a homologue of LRP. However, gp330 differs from these proteins in: **i)** the cysteine-rich repeat arrangements found in the extreme extracellular amino- and carboxyl-terminal regions, **ii)** the distribution pattern of cysteine residues in the YWTD spacer regions, **iii)** the location of the RX(K/R)R consensus recognition sequence of furin, a precursor processing endoprotease, and **iv)** the length and structure of the cytoplasmic tail. Gp330 binds similar ligands to LRP including apoE, lactoferrin and PAI-1 complexes [159]. The physiological and pathological role of gp330 is unknown at the present time.

1.3.7.4 The VLDL Receptor.

The VLDL receptor (VLDL-R) was first identified in rabbit heart [167] it is very similar in structure to the LDL-R, but contains eight rather than seven class A repeats in its ligand-binding domain and cannot bind LDL with high affinity (reviewed in [141, 168]). Unlike the LDL-R, the VLDL-R is not expressed in the liver but predominantly in heart, adipose tissue and brain [167-169], i.e. all tissues that metabolise fatty acids as an energy source. This fact, and the observation that the VLDL-R recognises apoE-containing lipoproteins, has led to the hypothesis that the VLDL-R may play an important role in the delivery of triglyceride-rich lipoproteins to peripheral tissues [170]. Such a proposal is supported by studies in the chicken, in which a very similar protein also with eight repeats in its binding domain, is essential for the accumulation of VLDL-derived lipid in developing eggs [141]. However, other evidence casts doubt on this interpretation. Mice lacking the VLDL-R showed no abnormalities in their lipoprotein profile [171].

Therefore, at present, the physiological role of the VLDL-R is uncertain. The ligand specificity of the VLDL-R is similar to the LRP in that it binds apoE, lactoferrin, LPL and complexes of urokinase-type plasminogen activator and PAI-1 (reviewed [141]).

1.3.7.5 The ApoE Receptor 2

Human apoE receptor 2 (apoER2) is a newly described receptor consisting of five domains that resemble those of the LDL-R and the VLDL-R [141, 144, 172, 173]. A key structural difference among the three receptors is the number of class A repeats in their ligand-binding domains; apoER2 and LDL-R contain a 7-fold repeat, whereas that of VLDL-R is 8-fold. Although apoER2 and LDL-R contain the same number of repeats, the ligand-binding domain structure of apoER2 is much more closely related to that of VLDL-R; apoER2 and VLDL-R contain a short linker sequence between repeats 5 and 6, whereas that of LDL-R is located between repeats 4 and 5. ApoER2 also contains a unique 59 amino acid insert within its otherwise LDL-R-/VLDL-R-like cytoplasmic tail [172, 174]. ApoER2 mRNA is detectable most intensely in brain and testis and, to a much lesser extent, in ovary, but is undetectable in other tissues in rabbit [172]. In human tissues, apoER2 mRNA is abundant in brain and placenta and undetectable in other tissues. This pattern of tissue expression of apoER2 mRNA suggests that the receptor plays a role in the uptake of apoE containing lipoproteins secreted in the central nervous system [141, 142, 172, 173].

Recently, Novak et al. identified a novel LDL-R homologue with an 8-fold cysteine-rich repeat predominantly expressed in chicken brain [174]. This chicken protein, designated LR7/8B consists of five domains resembling those of LDL-R, VLDL-R, and apoER2. Comparison of the amino acid sequence of LR7/8B with those of human LDL-R, VLDL-R and apoER2 reveals that it is a chicken homologue of apoER2; the two proteins have 77 % of their amino acids in common, and the identities extend throughout the proteins, excluding an extra cysteine-rich repeat present in LR7/8B and the cytoplasmic insertion sequence present in human apoER2 [173, 175].

Recent studies at the cDNA and genomic level have revealed that several splice variants of apoER2 are produced in brain [173, 175]. These include variants of apoER2 lacking repeats 4-6 (apoER2 Δ 4-6) or 4-7 (apoER2 Δ 4-7) in the ligand binding domain and apoER2 without the cytoplasmic insertion (Δ insert). The functional significance of alternative splicing and complete ligand specificity of apoER2 have yet to be determined. However, due to high similarity with the VLDL-R, apoER2 is predicted to have a similar ligand specificity as this receptor.

1.3.7.6 Receptor Associated Protein.

The receptor associated protein (RAP) is a 39 kDa protein (323 residues) that is a potent antagonist of members of the LRSF by preventing the interaction of ligands with these receptors. RAP is predominantly localised in intracellular compartments such as the endoplasmic reticulum, and copurifies with LRP during ligand affinity chromatography [176, 177]. In addition, RAP also interacts with high affinity to the VLDL-R [178], gp330 [179] and LR7/8B, the chicken homologue of apoER2 [174]. However, it binds with low affinity to the LDL-R [180]. Based on its biochemical properties, it has been proposed that the function of RAP is to assist in the folding and processing of the cysteine-rich class A repeats in LRSF members [176, 177, 181]. Disruption of the RAP gene in mice results in a 75 % reduction of functional LRP in the liver [181], supporting the role of RAP in the maturation and trafficking of LRP.

1.3.8 PHYSIOLOGICAL ROLES OF APOE.

1.3.8.1 Global Lipid Transport.

The major physiological role of apoE is to mediate the hepatic clearance of lipoproteins via two receptors, the LDL-R and LRP. A simplified scheme of lipoprotein metabolism is shown in Fig. 1.3-4. which highlights the role of apoE in major metabolic processes and the central importance of the liver in lipoprotein metabolism (for a general review of lipoprotein metabolism, see [182]).

Chylomicrons are synthesized in the intestine and transport dietary triglycerides and cholesterol. During their circulation, the core triglycerides of chylomicrons are hydrolyzed by LPL, to produce cholesterol-enriched remnant particles. On release by the intestine, chylomicrons contain no apoE, but as they circulate and are processed to remnants, the particles acquire apoE from HDL and are then rapidly removed from plasma by apoE-mediated mechanisms [89, 90]. However, the precise nature of this uptake process is ill defined. *In vivo* evidence suggests that LRP and HSPGs act together as the so-called “remnant receptor” [142]. In addition, the LDL-R also appears to play a role in uptake [183]. Thus, it appears that remnants may be cleared by two receptor systems.

VLDL is a triglyceride-rich lipoprotein containing apoE and apoB-100 that is synthesized by the liver. In a manner similar to that of chylomicrons, VLDL particles pass through a lipolytic cascade producing a spectrum of particles progressively decreasing in size [89, 184]. These include VLDL remnants and IDL. The cholesterol-rich LDL represents the final stage of this process [182, 184]. Although both VLDL and IDL

contain apoE and apoB-100, these particles are cleared through apoE interactions with the LDL-R and LRP [89], however, as indicated in Figure 1.3-4, not all IDL is cleared by the liver [89]. In healthy humans, nearly all of the IDL is converted to LDL, a process that involves a second lipase, hepatic lipase (HL). During LDL maturation the apoE is lost from the surface, leaving apoB-100 as the sole apolipoprotein. The clearance of the LDL is then via apoB-100 through the LDL-R [184]. In addition to mediating hepatic clearance of lipoproteins, it has been suggested that apoE is involved directly in the lipolytic cascade by serving as a modulator of HL, LPL and lecithin-cholesterol acyltransferase (LCAT) [185-188].

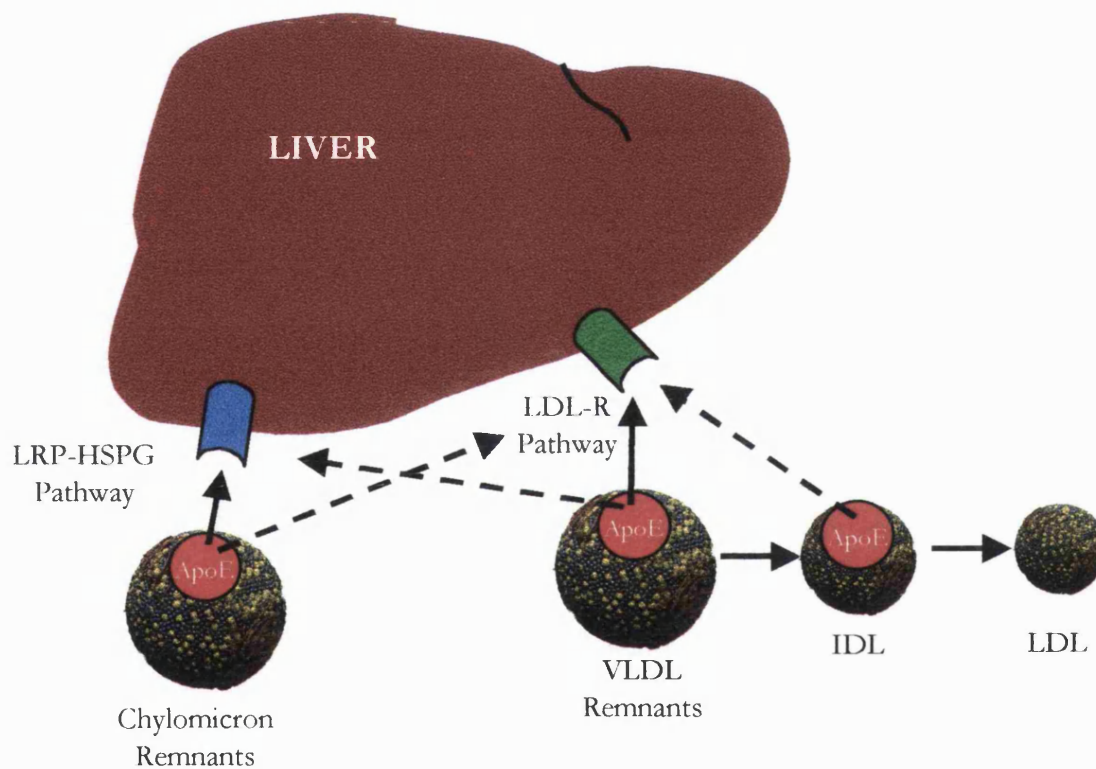


Figure 1.3-4 The role of apoE and apoE receptors in lipoprotein metabolism.

1.3.8.2 Local Lipid Transport.

As well as facilitating the hepatic clearance of lipoproteins, apoE also sequesters excess cell membrane cholesterol from the periphery. This local action of apoE is mediated by a minor subclass of HDL, γ -LpE, which constitutes a significant part of the normal cholesterol efflux capacity of plasma [107, 189, 190]. Macrophage produced apoE is the most probable source of γ -LpE in the periphery [107, 190].

1.3.8.3 The ApoE “Knockout” Mouse.

The importance of apoE in mediating hepatic clearance of lipoproteins and local cholesterol sequestration has been demonstrated in experiments with apoE-null (or “knockout”) mice [191]. These mice, either homozygous or heterozygous for *APOE* gene disruption, develop severe hyperlipidaemia, with plasma cholesterol levels raised five fold on a low fat diet and up to 15 fold on a high fat “western-type” diet [192]. Not surprisingly these animals have a greatly enhanced susceptibility for progressive atherosclerotic vascular disease both on low or high fat diets compared to genetically normal mice on the same diet (see section below).

1.3.8.4 ApoE and Atherosclerosis.

Atherosclerosis is an arterial disease that is recognised as a principal cause of death in the United States and Western Europe. In both humans and animal models, atherosclerosis culminates in a clinical event that is both catastrophic and revealing of a hitherto silent and occult process. These clinical manifestations include coronary heart disease with its myriad signs and symptoms: cerebral atherosclerosis, stroke and peripheral atherosclerosis affecting the extremities [193].

Even today, the cause and pathogenesis of atherosclerosis remain unresolved. However, intensive epidemiological, genetic and biochemical studies have provided key insights to the aetiology of the disease. Such studies have indicated that atherosclerosis is a multifactorial disorder to which hyperlipidaemia, increased oxidative stress, hypertension and increased platelet reactivity may contribute (reviewed in [194, 195]).

It has been known for many years that defective expression of apoE (either null expression or expression of variant forms) was associated with an increased risk for atherosclerotic vascular disease [90, 196, 197]. Until recently, this increased risk was largely ascribed to abnormalities in global lipoprotein transport and metabolism that attend defective expression. However, it has also been known for some time that apoE, in addition to being synthesized by hepatocytes and intestinal cells as components of lipoprotein particles, is also synthesized by a wide variety of peripheral cells including macrophages (*section 1.3.4.3*). Such production by extrahepatic cells has raised questions regarding potential physiological roles of apoE in peripheral tissues.

Abundant apoE is found in atherosclerotic vascular wall lesions and the macrophage is the major source of apoE in these lesions [198, 199]. Studies performed in genetically engineered mice provide the most convincing evidence for a prominent role of

macrophage-derived apoE in tissue and cellular cholesterol homeostasis. Indeed, utilising apoE-null mice as recipients, two groups have studied the effect of bone marrow transplantation from normal mice on lipoprotein profile and vessel wall disease [200, 201]. This supplies the apoE-null mouse with apoE derived from bone marrow macrophages. The transplanted mice express ~10 % of normal plasma levels of apoE, but even this promotes clearance of lipoproteins and significantly normalises cholesterol levels and the lipoprotein profile. Transplanted animals also resist diet-induced atherosclerosis compared with non-transplanted apoE-null animals. Although such protection of arteries could reflect an apoE effect on circulating lipoprotein levels, recent reports suggest that apoE directly protects the vessel wall from the atherosclerotic process [202, 203]. Thus, transgenic mice over-expressing apoE in the arterial wall do not differ in plasma cholesterol or lipoprotein profiles on a atherogenic diet compared with control mice, but their formation of atherosclerotic lesions is markedly inhibited [202]. This implies direct protective actions of apoE at the vessel wall, even in the presence of high levels of atherogenic lipoproteins.

It is reasonable to assume, therefore, that in addition to regulating cholesterol metabolism in the arterial wall, macrophage-derived apoE could impact vessel wall biology in other ways. Atherosclerotic lesions in humans have been shown to contain regional accumulations of T lymphocytes, which may participate in the atherosclerotic process [194, 204]. Since apoE has potent effects on lymphocyte function [205, 206], suppressing production of interleukin-2 and inhibiting lymphocyte proliferation, macrophage-derived apoE in the vessel wall could thereby modulate local lymphocyte function.

Another potentially important anti-atherogenic function of apoE, in the vicinity of the vascular wall, is the inhibition of platelet aggregation (see section 1.4).

1.3.8.5 ApoE and Alzheimer's Disease.

ApoE functions within the central nervous system (CNS) in a manner unrelated to lipid transport, perhaps to maintain synaptic integrity after injury and during ageing (reviewed in [90, 121]). ApoE is increased in several chronic neurodegenerative diseases. In addition, the $\epsilon 4$ allele has recently been linked with the development of late-onset familial and sporadic Alzheimer's disease (AD) and Lewy body dementia, which are neurodegenerative disorders associated with progressive dementia [207-210]. This indicates a central role for apoE in neuronal mechanisms.

AD is the fourth leading cause of death in developed countries [121]. The neuropathology of AD is characterised by the presence of both neuritic plaques and neurofibrillary tangles. Neuritic plaques represent extracellular amyloid deposits [121]. The amyloid beta ($A\beta$) peptide is the major component of these deposits and has been detected in both plasma and CSF of AD patients [211]. $A\beta$ originates from proteolytic cleavage of the larger amyloid precursor protein (APP). APP is present on a large variety of cells including neurones and platelets, however at the present time its function is unknown [212]. Before it was genetically linked to AD, apoE was detected immunochemically in amyloid deposits in neuritic plaques [208, 210]. Interestingly, apoE-4 forms a stable complex with $A\beta$ *in vitro*, while apoE-3 does not [213]. Thus, the presence of the ϵ 4 allele may help promote the formation of neuritic plaques. Note, however, that the role of neuritic plaques in the aetiology of AD remains controversial [121].

Neurofibrillary tangles, in contrast to neuritic plaques, appear to be intracellular in neurones. The tangles are characterised by structures referred to as paired helical filaments, whose major component is an extensively phosphorylated form of the tau protein [214]. Tau is a member of the microtubule-associated family of proteins that facilitate microtubule assembly and stability. Phosphorylation of tau reduces its binding affinity for microtubules, resulting in microtubule destabilisation [215]. ApoE also interacts with tau in an isoform specific manner [216]. In this case, apoE-3 forms a stable complex with tau whereas apoE-4 does not [121, 216]. It has been suggested that apoE-3 binding could stabilise microtubules and the cytoskeleton, and thus maintain the structure and function of neurones. The binding of apoE-3 to tau can also inhibit phosphorylation of tau and thus retards the paired helical filament formation that appears to be involved in the development of neurofibrillary tangles [216, 217]. These possibilities have led to the hypothesis that apoE-4 is associated with AD, not because it has direct pathological actions but lacks the protective effect of apoE-3 [216].

Clearly apoE plays an important role in the nervous system, and its impact on specific types of neurones has also been highlighted by studies of apoE-null mice, where a marked disruption in the synaptodendritic organisation and in the cytoskeletal apparatus of CNS neurones have been shown [218]. However, it should be noted that the multiple roles of apoE in the nervous system, and elsewhere, are far from clear at the present time.

1.4 ApoE and Platelet Aggregation.

Several studies suggest that plasma lipoproteins can influence the reactivity of blood platelets, including their aggregatory response to a variety of agonists (reviewed in [219, 220]). Platelet-rich plasma containing elevated levels of LDL has an enhanced sensitivity to certain aggregating agents, including the weak agonists, adrenaline and ADP [221, 222]. When platelets are freed from their plasma environment by gel filtration, they are rapidly sensitized by incubation with normal physiological amounts of LDL [219, 220, 223]. Interestingly, the oxidation state of LDL may also influence its pro-aggregatory potential [220, 224, 225]. The initial step in this sensitization process is thought to involve binding of LDL particles by saturable sites, distinct from the classical LDL-R of nucleated cells [226, 227], in the platelet surface [220, 228], possibly GPIIb-IIIa [229] or CD36 [230]. Subsequent events are uncertain although normal agonist-receptor coupling may be affected [219].

By contrast, there have been few studies on interactions between platelets and HDL particles, and the effects of HDL on platelet aggregability have been conflicting. In a large normal population, a weak negative correlation was found between the sensitivity of platelet-rich plasma to ADP and its HDL concentration [221] although addition of isolated HDL to platelet-rich plasma was reported not to affect ADP-induced aggregation [231]. Addition of physiological amounts of HDL to gel-filtered platelets either decreased [232] or had no effect on aggregability [223], whereas excess concentrations of HDL were considered to stimulate aggregation [223]. However, plasma HDL comprises a heterogeneous group of particles [233], most commonly separated by sequential, isopycnic ultracentrifugation into two major classes, HDL₂ and HDL₃ [see *section 2.2.3*]. A minor subclass, HDL-E, is also recognised; it floats within the HDL₂ density range by isopycnic ultracentrifugation but can be isolated either by rate-zonal ultracentrifugation [234] or, because it is rich in apoE, by heparin-Sepharose affinity column chromatography (*section 3.2.3.2*). When the influence of the different HDL subclasses were tested, Desai et al. found that HDL₂ and HDL₃ had opposite effects on agonist-induced aggregation of isolated platelet suspensions [7]. HDL₃ was pro-aggregatory, albeit at concentrations near or above the upper limit of the normal range, whereas HDL₂ was anti-aggregatory at physiological levels. Moreover, subfractionation of the particles floating within the HDL₂ density range, using heparin-Sepharose affinity chromatography, revealed that their inhibitory action resulted predominantly from the presence of HDL-E; inhibition of aggregation by the apoE-deficient fraction was moderate [7]. These findings suggested that the influence of whole HDL on platelet responsiveness might depend on the relative

concentrations of apoE present. Indeed, indirect evidence implicated apoE as the active constituent; chemically modifying apoE blocked binding and its anti-platelet action [7], while abnormal apoE-enriched HDL from patients with hepatic cirrhosis had a highly potent anti-aggregatory effect that correlated with apoE content ($r=0.70$, $P<0.001$) [235].

1.5 Aims of Thesis.

The aim of this thesis, therefore, was to extend the work of Desai et al. [7, 235], and to characterize the anti-platelet effects of apoE. This was achieved in three separate studies, each represented by a chapter in this thesis:

Aim 1: *To determine whether “native” immunoaffinity isolated HDL-E particles have anti-platelet activity and that isolated apoE preparations are active.*

Aim 2: *To establish the biochemical basis for inhibition of platelet aggregation by apoE.*

Aim 3: *To identify the apoE receptor in platelets and to probe the molecular basis by which it suppresses platelet reactivity.*

Chapter 2

2. GENERAL MATERIALS AND METHODS

2.1 Materials.

Methanol, ethanol, diethyl ether, isobutanol and glacial acetic acid, all of Analar grade, were purchased from BDH Laboratory Supplies (Poole, UK). Goat anti-mouse alkaline phosphatase conjugated IgG was purchased from Bio-Rad (Watford, UK) and polyclonal goat anti-apoE antibodies from Calbiochem Novabiochem Ltd. (Nottingham, UK). Two hybridoma cell lines (designated F5M1/C3 and F5M3/A10) which secreted monoclonal antibodies against human apoE were kindly donated by Dr. R. W. James (Hopital Cantonal, Geneva). All other reagents unless otherwise stated in the text were purchased from Sigma Chemical Co. (Poole, UK).

2.2 Isolation of Plasma Lipoproteins.

2.2.1 BACKGROUND.

Several procedures exist to separate lipoproteins into their various classes. The techniques most commonly used in clinical research laboratories are ultracentrifugation, precipitation, electrophoresis and gel filtration (reviewed in [236]). They may also be isolated on antibody affinity columns [237]. Although no procedure is perfect, ultracentrifugation is the preferred method for large-scale lipoprotein preparations. Precipitation by various combinations of agents followed by ultracentrifugation is the fastest and most economical method used for HDL separation. Both these techniques are considered in detail below.

2.2.1.1 Precipitation Methods.

Due to the specific interaction of apolipoprotein B (apoB) with a number of precipitating agents, lipoproteins containing apoB can be separated from non-apoB-containing lipoproteins. Thus, treating plasma will remove chylomicrons, VLDL, IDL and LDL leaving only HDL, which can be estimated by a cholesterol assay or isolated by a single ultracentrifugation step. A number of precipitation methods are available for use, the most popular being magnesium/phosphotungstic acid [236]. However, an unresolved problem with this method is that it gives lower values for HDL cholesterol, compared to other isolation techniques (often by around 10 %)[236]. This may be because it is particularly effective in precipitating the apoB-containing lipoprotein, Lp(a) [238], present

in the HDL-density range of many individuals, but it is also possible that it precipitates a variable amount of the apoA-I-containing lipoproteins. Nevertheless, the advantages of precipitation in terms of speed and cost usually outweigh this disadvantage.

2.2.1.2 Preparative Ultracentrifugation.

Lipoproteins have lower hydrated densities than the other plasma proteins, permitting their isolation from plasma by flotation ultracentrifugation [236, 239]. This method can be used to prepare bulk amounts of lipoproteins for large-scale investigations or small amounts for clinical studies. The density of plasma is increased by the addition of NaCl and/or NaBr and during ultracentrifugation, lipoproteins will float to the surface depending on their density and the prevailing small-solute density of the solution. The density range of plasma lipoproteins is given in Table 2.2-1. Individual lipoprotein classes can be isolated by sequentially increasing the plasma density. Ultracentrifugation times tend to be long and it has been shown that during the ultracentrifugation exchanges of lipid and apolipoprotein between lipoprotein classes occur [236]; this is the principal disadvantage of this technique. However, since most of our current definitions of the lipoprotein classes rely on their hydrated density, ultracentrifugation remains the method of choice for many investigations.

Lipoprotein Class	Density Range (g/ml)
Chylomicrons	< 0.940
VLDL	0.940 - 1.006
IDL	1.006 - 1.019
LDL	1.019 - 1.063
HDL ₂	1.063 - 1.125
HDL ₃	1.125 - 1.21

Table 2.2-1 Density classes of plasma lipoproteins

2.2.2 BLOOD SAMPLING.

Blood was withdrawn from the antecubital vein from healthy volunteers and patients with liver disease. In most instances 150 ml of blood per donor was collected into three polyethylene centrifuge tubes (50 ml) each containing a preservative cocktail that inhibits the multiple enzymatic degradations that can occur during and after withdrawal of blood

[240] (Table 2.2-2). The tubes were manually agitated during collection and then cooled on ice. Within 1 h, the blood was centrifuged for 20 min at 2000 *g* and 4 °C. The plasma was separated from the sedimented cells and benzamidine and phenylmethylsulphonylfluoride (PMSF) were added to give a final concentration of 1 mM (Table 2.2-3) and used immediately for lipoprotein preparation.

Stock Solution	Volume/50 ml Blood
0.2 M EDTA (Na Salt) pH 7.4	0.8 ml
0.3 M Sodium Chloride pH 7.4	1.4 ml
Sodium Azide 2.5 %	200 µl
Chloramphenicol 50 mg/ml in 50 % ethanol	80 µl
Gentamicin Sulphate 10 mg/ml	400 µl
Kallikrein Inactivator 20000 U/ml	25 µl

Table 2.2-2 Preservative cocktail for blood collection.

Stock Solution	Volume/50 ml Plasma
Benzamidine 1 M	50 µl
PMSF 0.2 M in anhydrous methanol (-20 °C)	250 µl

Table 2.2-3 Preservative solutions for lipoproteins.

2.2.3 SEQUENTIAL PREPARATIVE ULTRACENTRIFUGATION.

2.2.3.1 Preparation of Sodium Bromide Density Solutions.

Base density solution (1.006 g/ml).

57.0 g anhydrous NaCl,	➔	Make up to 5 litres.
0.5 g EDTA (Sodium salt),		Then add 15 ml distilled H ₂ O.
5 ml 1 M NaOH,		<i>This solution gives a refractive</i>
0.5 g Sodium azide.		<i>index value of 1.3345 at 20 °C</i>

All density solutions were prepared by adding a known weight of solid sodium bromide to the base density solution. For accurate density determination, the refractive index value for each solution was measured using a refractometer (Bellingham & Stanley Ltd.). Fine adjustment of densities were achieved by adding solutions, $d = 1.21$ or 1.478 g/ml (to ↑ density) and $d = 1.006$ g/ml (to ↓ density).

Density (g/ml)	Refractive Index Value	Solid NaBr Added (approx. g/ml)
1.006	1.3345	-
1.019	1.3368	-
1.045	1.3413	0.052
1.065	1.3448	0.075
1.10	1.3508	0.150
1.125	1.3547	0.165
1.157	1.3620	0.21
1.182	1.3643	0.25
1.21	1.3693	0.296
1.478	1.4160	0.79

NB. If turbid filter before final adjustment.

Table 2.2-4 Preparation of stock density solutions.

2.2.3.2 Ultracentrifugation.

Bulk lipoprotein fractions were prepared in a 12 x 38.5 ml rotor (Kontron TFT 50.38) either in a Kontron Centrikon T-2060 ultracentrifuge or a Sorvall OTD-65B ultracentrifuge.

2.2.3.3 Adjustment of Plasma Density.

The following equation was used to calculate the volume of density solution required to float lipoproteins:

$$V_1 \cdot d_1 + V_2 \cdot d_2 = (V_1 + V_2) \cdot d_3$$

Where: V_1 = Volume of plasma (or ultrafiltrate)

V_2 = Volume of density solution to be added

d_1 = Density of plasma (or ultrafiltrate)

d_2 = Density solution used for adjustment

d_3 = Density required

Sample Calculation:

Adjustment of density for chylomicron, VLDL and IDL isolation.

Thus, for a typical isolation in a 29 ml centrifuge tube: $V_1 = 19.333$ ml, $V_2 = 9.667$ ml, $d_1 = 1.006$ g/ml, $d_2 = \text{Unknown}$, and $d_3 = 1.019$ g/ml.

$$(19.333 \times 1.006) + 9.667 \times d_2 = 29 \times 1.019$$

$$19.448998 + 9.667d_2 = 29.551$$

$$9.667d_2 = 10.102002$$

$$d_2 = 1.045 \text{ g/ml}$$

2.2.3.4 Chylomicron, VLDL and IDL Preparation.

Thus, 19.333 ml of plasma was placed in a screw-capped polycarbonate centrifuge tube and its density adjusted to 1.019 g/ml by adding 9.667 ml of 1.045 g/ml density solution. The samples were centrifuged for 20 h at 37000 rpm (105000 g) and 16 °C. The lipoprotein fraction that floated to the top of the tube was collected in less than 4 ml, using a syringe and needle. The fraction was then either dialysed for immediate use or washed. The washing step involves refloating the lipoproteins at their density of isolation. Therefore, for this fraction, the lipoproteins were diluted to 29 ml with the stock 1.019 g/ml density solution and recentrifuged.

2.2.3.5 LDL Preparation.

The solution below the chylomicron, VLDL and IDL fraction was removed and discarded such that 19.333 ml remained in the centrifuge tube. Its density was adjusted to 1.065 g/ml by adding 9.667 ml of 1.157 g/ml density solution and mixed. The samples were again centrifuged for 20 h at 37000 rpm (105000 g) and 16 °C. The LDL fraction was collected and dialysed or washed (in 1.065 g/ml solution).

2.2.3.6 HDL Preparation.

After LDL isolation, HDL was prepared either as total HDL or HDL₂/HDL₃ sub-fractions. Alternatively, HDL can be prepared from plasma after precipitation of the apoB-containing lipoproteins followed by a single ultracentrifugation step.

Total HDL Preparation.

The solution below the LDL fraction was adjusted to 19.333 ml and its density was adjusted to 1.21 g/ml by adding 9.667 ml of 1.478 g/ml density solution and mixed. The samples were centrifuged for 40 h at 37000 rpm (105000 *g*) and 16 °C. The HDL fraction was collected and dialysed or washed (in 1.21 g/ml solution).

HDL₂ Preparation.

The solution below the LDL fraction was adjusted to 19.333 ml and its density was adjusted to 1.125 g/ml by adding 3.29 ml of 1.478 g/ml density solution and 6.38 ml of 1.125 g/ml solution. The isolation was performed as outlined for total HDL.

HDL₃ Preparation.

The solution below the HDL₂ fraction was removed and discarded such that 19.333 ml remained in the centrifuge tube. Its density was adjusted to 1.21 g/ml by adding 6.13 ml of 1.478 g/ml density solution and 3.54 ml of 1.21 g/ml solution. The isolation was performed as outlined for total HDL.

Preparation of HDL Following Magnesium/Phosphotungstic Acid Precipitation.

One hundred μ l of 0.5 M MgCl₂ and 100 μ l of 4 % (w/v) phosphotungstic acid (in 0.19 M NaOH) were added to every 1 ml of fresh plasma and mixed well. The plasma was then centrifuged immediately for 20 min at 2000 *g* and 20 °C. This step precipitated all apoB-containing lipoproteins, leaving plasma with HDL as the only lipoprotein. Total HDL (or HDL₂ and HDL₃) was isolated by altering the density of the plasma (still at 1.006 g/ml) and performing ultracentrifugation as before.

2.3 General Apolipoprotein Analyses.

2.3.1 PROTEIN MEASUREMENT.

Protein concentrations were measured using the Bio-Rad protein assay. This assay is based on the observation that the absorbance maximum for an acidic solution of Coomassie brilliant blue G-250 shifts from 465 nm to 595 nm when binding to proteins occurs. Bradford first demonstrated the usefulness of this principle [241], while Spector found that the extinction coefficient of a dye-albumin complex solution was constant over a 10-fold concentration range [242]. Thus, Beer's Law may be applied for accurate quantification of protein by selecting an appropriate ratio of dye volume to sample

concentration. Over a broader range of protein concentrations, the dye-binding method gives an accurate, but not entirely linear, response.

2.3.1.1 Procedure.

Several dilutions of an appropriate protein standard (usually bovine serum albumin or bovine gamma globulin) were prepared in distilled water to a final volume of 200 μl . A typical standard curve in the range of 0 - 20 μg protein/200 μl was freshly prepared each time the assay was performed. The triplicate unknown samples were diluted to 200 μl in distilled water. To each tube, 1 ml of freshly diluted dye reagent [20 % (v/v) solution of Bio-Rad concentrate] was added and the tubes vortexed. After an incubation of 10 min at room temperature, the OD₅₉₅ versus reagent blank was measured. The concentration of standards versus their OD₅₉₅ was plotted and the concentration of the test samples determined from the standard curve using Elsevier-Biosoft's Lowry analysis software (Cambridge, UK).

2.3.2 SDS-POLYACRYLAMIDE GEL ELECTROPHORESIS.

Fractionation of proteins in polyacrylamide gels is one of the primary means for their characterisation because of its speed and ease of use. Many methods to separate both native and denatured proteins exist in the literature [243]. However, the most widely used technique is sodium dodecyl sulphate polyacrylamide gel electrophoresis (SDS-PAGE).

The goal of SDS-PAGE is to separate polypeptides in a complex mixture solely on the basis of molecular size. Firstly, the polypeptide sample is denatured with heat in the presence of SDS and a reducing agent, usually β -mercaptoethanol. In the presence of excess SDS, about 1.4 g of the detergent binds to each gram of polypeptide, giving the polypeptide a constant negative charge per mass unit [244, 245]. SDS-polypeptide complexes will therefore all move towards the anode during electrophoresis, and owing to the molecular-sieving properties of the gel, their mobilities are inversely proportional to the log₁₀ of their molecular weights. If standard proteins of known molecular weight are also run, the molecular weights of the sample proteins can thus be determined.

Polyacrylamide gels are composed of chains of polymerised acrylamide that are cross linked by a bifunctional agent such as N, N'-methylenebisacrylamide (bisacrylamide). The effective range of separation of SDS-polyacrylamide gels depends on the concentration of polyacrylamide used to cast the gel and the amounts of cross-linking [244, 245]. Cross-links formed from bisacrylamide add rigidity and tensile strength to the gel and form pores

through which the SDS-polypeptide complexes must pass. The size of these pores decreases as the bisacrylamide:acrylamide ratio increases. However, most gels are cast with a molar ratio of 1:29, which has been shown to be capable of resolving polypeptides that differ in size by as little as 3 %. Table 2.3-1 shows the linear range of separation obtained with gels cast with concentrations of acrylamide that range from 3 to 15 % (w/v).

Sharp banding of the polypeptides is achieved by using a discontinuous gel system which has both stacking and resolving gel layers that differ in either salt concentration, pH, acrylamide concentration or a combination of these. After migrating through a stacking gel of high porosity [usually 4 % (w/v) acrylamide], the SDS-polypeptide complexes are deposited in a very thin zone (or stack) on the surface of the resolving gel. The ability of discontinuous buffer systems to concentrate all of the complexes in the sample into a very small volume greatly increases the resolution of SDS-polyacrylamide gels.

The primary uses for SDS-PAGE in this thesis were: the determination of the size of a protein, the estimation of protein purity in a solution and the fractionation of a complex protein mixture prior to immunoblotting (Western blotting).

Acrylamide Concentration % (w/v) <small>At a molar ratio of 1:29 bisacrylamide:acrylamide.</small>	Linear Range of Separation kDa
3	95 - 400
5	57 - 212
7.5	36 - 94
10	16 - 68
15	12 - 43

Table 2.3-1 Effective range of separation of SDS-polyacrylamide gels.

2.3.2.1 Buffers and Solutions.

Gel Components:

30 % Acrylamide mix: 29 % (w/v) acrylamide and 1 % (w/v) N, N'-methylenebisacrylamide.

Tris buffers: the stock buffer for the resolving gel is 1.5 M Tris.HCl (pH 8.8) and for the stacking gel is 1.0 M Tris.HCl (pH 6.8).

10 % (w/v) *Ammonium persulphate (APS)*: APS provides the free radicals that drive polymerisation of acrylamide and bisacrylamide.

TEMED (N, N, N, N'-tetramethylethylenediamine): TEMED accelerates the polymerisation of acrylamide and bisacrylamide by catalysing the formation of free radicals from APS.

10 % (w/v) *Sodium dodecyl sulphate (SDS) solution*.

Electrophoresis Buffers:

Running buffer: 25 mM Tris (pH 8.3), 192 mM glycine, 0.1 % (w/v) SDS.

2 × Sample buffer: 100 mM Tris.Cl (pH 6.8), 4 % (w/v) SDS, 0.1 % (w/v) bromophenol blue, 10 % (v/v) glycerol, 1 % (v/v) β-mercaptoethanol (optional)

Coomassie Stain:

Stain: 0.25 % (w/v) Coomassie brilliant blue R-250, 50 % (v/v) methanol and 10 % (v/v) acetic acid.

Destain: 30 % (v/v) methanol and 10 % (v/v) acetic acid.

Silver Stain:

0.25 % (w/v) *Sodium dithionite*.

0.2 % (w/v) *Silver nitrate in 1 mM formaldehyde*.

Developer: 6 % (w/v) sodium carbonate, 6 mM formaldehyde and 20 μM sodium dithionite.

2.3.2.2 Gel Preparation.

Mini gels usually 1.5 mm thick were cast in Bio-Rad MiniProtean II electrophoresis cassettes with a 10 or 15 well comb. The acrylamide solution for the resolving gel was prepared using the values given in Table 2.3-2. The solution was poured into the cassette, with its meniscus far enough below the top of the notched plate to allow for the length of the comb plus 0.5 cm. The acrylamide solution was then carefully overlaid with water-saturated isobutanol and placed in a vertical position at room temperature. After the gel had set (about 20 - 30 min), the isobutanol was poured off and the top of the resolving gel was washed several times with distilled water and drained. The acrylamide solution for the stacking gel was prepared (Table 2.3-2) and was poured directly onto the polymerised resolving gel. The appropriate comb was inserted and the stacking gel was then allowed to set (about 10 min).

Solution Components (enough for 1 x 10 ml gel) * Solutions added last to initiate polymerisation.	8 % resolving	12 % resolving	15 % resolving	4 % stacking
Water	4.6 ml	3.3 ml	2.3 ml	6.1 ml
30 % Acrylamide mix	2.7 ml	4.0 ml	5.0 ml	1.3 ml
Tris buffer	2.5 ml (pH 8.8)	2.5 ml (pH 8.8)	2.5 ml (pH 8.8)	2.5 ml (pH 6.8)
10 % SDS	100 µl	100 µl	100 µl	100 µl
*10 % APS	100 µl	100 µl	100 µl	100 µl
*TEMED	6 µl	4 µl	4 µl	10 µl

Table 2.3-2 Solutions for preparing gels for SDS-polyacrylamide gel electrophoresis.

2.3.2.3 Running the Gel.

The samples (including molecular weight markers) were added 1:1 with 2 x sample buffer and heated in a boiling water bath for 5 min. After the stacking gel had set, the comb was carefully removed and the wells were immediately washed with distilled water (to remove unpolymerized acrylamide) and the wells straightened. The cassette was inserted into the electrophoresis chamber, which was then filled with running buffer. The samples were loaded into the bottom of the wells using a micropipetter fitted with a long narrow tip. The electrophoresis was started at a constant current of 20 mA per gel. After the dye front had moved into the resolving gel, the current was increased to 30 mA. When the dye front reached the bottom of the gel, the power pack was switched off and the cassette removed. The glass plates containing the gel were carefully prized apart and the gel removed. The bottom left corner of the gel was cut to help lane identification.

At this stage, the gels were ready for staining, electrotransfer or autoradiography (if radiolabelled polypeptides were used).

2.3.2.4 Coomassie Blue Staining (sensitivity of 0.1 - 0.5 µg per band).

After electrophoresis the gel was transferred to a clean plastic container and about 100 ml of Coomassie brilliant blue stain was added. This was incubated for 1 - 2 h at room temperature with shaking. The stain was removed and saved (the staining solution can be used between 20 and 40 times before replacing). The gel was destained by successive incubations in destain solution at room temperature with shaking.

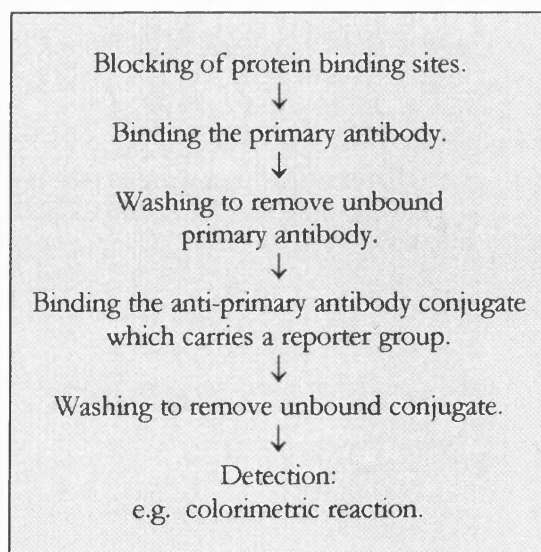
2.3.2.5 Silver Staining (sensitivity of 1 - 10 ng per band).

After Coomassie staining the gel was washed (2 x 20 min) in 50 ml of 30 % (v/v) ethanol with shaking. The ethanol solution was removed and the gel further washed (3 x 15 min) in 50 ml of distilled water. The gel was then incubated for 1 min in 50 ml of 0.25 % (w/v) sodium dithionite solution and washed (2 x 1 min) with distilled water. The water was removed and the gel was incubated with the silver nitrate solution for 30 min followed by a wash in distilled water for 1 min. The gels were then developed by adding 50 ml of developing solution. Bands usually appeared after about 10 - 15 min. Once the background began to darken, the reaction was stopped by adding 5 % (v/v) acetic acid.

Note: When silver staining, gloves were always worn, as fingerprints stain, and only scrupulously clean glassware was used to maintain the sensitivity of the reactions.

2.3.3 IMMUNOBLOTTING.

Antibodies are commonly used to detect antigens in complex mixtures. Some of the more common immunodetection methods include enzyme-linked immunosorbent assay (ELISA), radioimmunoassay (RIA), double immunodiffusion, immunoprecipitation and immunoblotting [245]. This section will focus mainly on the immunoblotting techniques, Western blots and dot blots. Western blots and dot blots require the immobilisation (transfer) of a sample onto a membrane. This is the step where the two procedures differ. With Western blots, proteins are transferred to a membrane after polyacrylamide gel electrophoresis; for dot blots, non-denatured antigen-containing samples are spotted directly onto a membrane. After the transfer step, both methods essentially follow the same basic steps to detect antigens. These steps are summarised below:



2.3.3.1 Buffers and Solutions.

Transfer buffer: 25 mM Tris (pH 8.3), 192 mM glycine, 20 % (v/v) methanol.

Washing buffers: TBS: 20 mM Tris.HCl (pH 7.5), 150 mM NaCl

TTBS: TBS supplemented with 0.05 % (v/v) Tween 20.

Blocking buffer: 3 % (w/v) gelatin or 5 % (w/v) bovine serum albumin (BSA) in TTBS.

Antibody buffer: polyclonal and monoclonal antibodies were prepared in either 1 % (w/v) gelatin or 2 % (w/v) BSA in TTBS. Monoclonal antibodies were prepared in either 3 % (w/v) gelatin or 5 % (w/v) BSA in TBS.

Alkaline phosphatase buffer: 100 mM Tris.HCl (pH 9.5), 100 mM NaCl, 5 mM MgCl₂.

Nitro blue tetrazolium (NBT): 5 % (w/v) NBT in 70 % (v/v) dimethylformamide.

Bromochloroindolyl phosphate (BCIP): 5 % (w/v) BCIP in 100 % dimethylformamide.

2.3.3.2 Sample Transfer.

Note: When handling nitrocellulose, gloves were always worn, as fingerprints stain.

Dot Blots.

A protein solution of at least 1 µg/ml was spotted onto a nitrocellulose sheet at 0.1 ml/cm². The protein was allowed to dry for 1 h at room temperature. If the amount of protein was not limiting, higher concentrations of proteins (up to 100 µg/cm² nitrocellulose) were used to increase the signal strength.

Semi-Dry Electrotransfer for Western Blots.

A Bio-RAD Trans-Blot SD (semi-dry) transfer cell was used to transfer proteins from polyacrylamide gels to nitrocellulose. This semi-dry electrotransfer method gives an even and rapid transfer and can be adapted to handle stacks of gel-membrane sandwiches [245]. The polyacrylamide gel used for transfer was run with pre-stained molecular weight markers, which transfer onto the nitrocellulose and act as internal markers of transfer. Four sheets of 3MM absorbent paper (Whatman, Maidstone, UK) and one sheet of nitrocellulose (BDH Laboratory Supplies) were cut to the size of the gel and soaked in transfer buffer for 2 min before transfer. The electrode plates of the cell were washed with distilled water and the transfer sandwich made up on the bottom plate as follows:

- bottom electrode
- 2 layers of absorbent paper soaked in transfer buffer
- 1 layer of nitrocellulose soaked in transfer buffer
- polyacrylamide gel slightly wetted in transfer buffer
- 2 layers of absorbent paper soaked in transfer buffer

Air bubbles were carefully removed by rolling a test tube over the sandwich and the upper electrode was placed on top of the stack. The electrodes were connected to the power pack and transfer allowed to proceed for 45 min with a constant current of 1.5 mA/cm² of gel. After transfer, the stack was removed and the bottom left corner of the nitrocellulose was cut to help lane identification.

2.3.3.3 Immunoblotting.

The nitrocellulose membrane was removed and incubated for 45 min in blocking buffer, followed by a 5 min wash in TBS. The membrane was then incubated for 1 h in primary antibody (diluted optimally in antibody buffer) and washed for 3 x 5 min with TTBS. After a further 1 h incubation with diluted secondary antibody (anti-IgG-alkaline phosphate conjugate), the membrane was again washed (3 x 5 min) in TTBS. Finally, the membrane was stained using the freshly prepared alkaline phosphatase substrate (66 µl NBT and 33 µl BCIP in 10 ml alkaline phosphatase buffer). Purple bands usually appeared after 10 - 30 min. Washing the blot in copious amounts of distilled water stopped the development reaction. The blot was then dried and stored in the dark.

2.4 Isolation and Characterisation of ApoE.

The isolation and purification of plasma apoE is difficult due to two main factors. Firstly, apoE has extensive polymorphism in humans, both genetically determined and polymorphism derived from post-translational glycosylation (sialylation) of the apoE polypeptide [118]. Depending on the purpose for which the apoE is intended, the choice of individuals and knowledge of their apoE phenotype may be critical to the investigation. Therefore, phenotyping of potential donors should always be carried out before preparative isolation is attempted. Secondly, in normal healthy individuals, plasma levels of apoE are not particularly high, usually about 3 - 7 mg/dl [89, 90]. To obtain sufficient apoE for some purposes, several units of blood may be required. Due to the low levels found in normolipidaemic subjects, a better source of apoE is from subjects with certain types of hyperlipidaemia (type IV or V for apoE-3/3, type III for E-2/2). Alternatively plasma from subjects with certain forms of liver disease, where apoE levels are greatly increased, can be used [235, 246]. Another potentially important source of apoE is from cholesterol-fed rabbit plasma. Such apoE has 80 % homology to human apoE-3, with up to 10 mg of pure polypeptide obtained per rabbit [247, 248].

2.4.1 APOLIPOPROTEIN E PHENOTYPING: ISOELECTRIC FOCUSING AND IMMUNOBLOTTING.

The three common variants of apoE differ in their amino acid sequence at positions 112 and 158 (E-2=Cys 112, Cys 158; E-3=Cys 112, Arg 158; E-4=Arg 112, Arg 158) [89]. Because arginine is positively charged, these amino acid substitutions enable separation of these isoforms by isoelectric focusing (IEF).

The technique of IEF is a widely used high-resolution technique for separating proteins and peptides according to their isoelectric point (pI). Resolution as high as 0.01 - 0.02 pH units can be obtained [249]. Briefly, a polyacrylamide or agarose gel is prepared to include carrier ampholytes, special mixtures of small amphoteric molecules of a known pH range. When a current is applied to the gel, the ampholytes form a linear pH gradient. The charged polypeptides move through the pH gradient and lose their charge completely where the pH of the gradient is equal to the pI of the polypeptide. At this point, movement stops and each polypeptide is concentrated into a narrow zone.

The apparent pI values are: E-2=5.57, E-3=5.8, E-4=6.03. However, post-translational modifications result in sialylated versions of the apoE isoforms; these bear additional negative charge and focus at positions anodal to the parent protein [89]. Thus for clear identification of the parent apoE isoform, plasma is initially treated with neuraminidase which desialylates the apoE.

In the method described herein, plasma samples are delipidated and the apolipoproteins separated by IEF on agarose gels. The proteins are then blotted on to nitrocellulose membranes and immunofixed using mouse monoclonal antibodies to human apoE. ApoE bands are visualised using goat anti-mouse IgG-alkaline phosphatase conjugate as the secondary antibody and NBT/BCIP as a substrate.

2.4.1.1 Sample Preparation.

Samples were collected into EDTA tubes and centrifuged at 2500 *g* for 15 min. The plasma was collected and either processed immediately or stored in 300 μ l aliquots at -70 °C for up to one year. Freshly prepared neuraminidase solution (15 μ l, 5 kU/l in 0.1 M acetate buffer, pH 4.5) was added to an equal volume of test plasma or control plasma (of known phenotype) and incubated at 37 °C for 2 h. One ml of methanol:ether (3:1, v/v) was added and the samples were mixed for 30 min on a rocking platform. Each sample was then centrifuged at 12000 *g* for 7 min and the supernatant discarded. The precipitate was resuspended in 1 ml diethyl ether, mixed for 30 min and recentrifuged as above. The

delipidated pellet was dried under nitrogen. At this stage the dried pellet was either stored under nitrogen at -20 °C or processed for IEF.

2.4.1.2 Gel Preparation.

IEF agarose (1.2 g) and sorbitol (7.2 g) were dissolved in 50 ml distilled water and heated in a microwave oven for 90 s at medium heat. The gel mixture was cooled to 65 °C before addition of 3.8 ml ampholines, pH 4 - 6.5 (Pharmacia Biotech, St. Albans, UK) and 22 g urea, both pre-warmed to 65 °C. The mixture was placed in a 65 °C oven for a further 5 min. An electrophoresis cassette was assembled by pipetting about 1 ml of distilled water onto a flat glass plate (20 x 26 cm). Gel-Bond film (Pharmacia) was placed with the hydrophobic side downward on top of the plate. A 1.5 mm U-frame glass plate was then placed on top and the cassette clamped together using bulldog clips. The assembled cassette was placed in a 65 °C oven for 5 min. The gel was poured into the pre-warmed cassette and was allowed to set at room temperature overnight. Just before use, the gel was removed from the cassette.

2.4.1.3 Isoelectric Focusing.

On the evening before IEF, 100 µl of buffer (50 mM Tris, pH 8.2, 350 µM SDS, 60 mM urea, 25 mM dithiothreitol [DTT]) was added to the sample pellet and was left to dissolve overnight at 4 °C. The dissolved pellet was gently mixed immediately before IEF, which was performed using a Pharmacia Multiphor II electrophoresis chamber. A circulating water bath, set at 8 °C, was connected to the electrophoresis cooling plate. The plate was then smeared with glycerol and the gel was placed on top avoiding air bubbles. Buffer strips were cut to 24.5 cm and soaked with 50 mM sulphuric acid (anode strip) or 1 M sodium hydroxide (cathode strip). Excess electrolyte was removed and the strips were placed on top of the gel. The electrode plate was placed on top with the anode and cathode aligned with their respective wicks. The electrophoresis chamber was plugged into the power pack and the gel pre-focused for 30 min (constant power of 4 W, maximum voltage at 1000 V and current at 15 mA).

After pre-focusing, the anode and cathode strips were renewed. Five µl of each sample and control were applied just above the cathode strip using the sample applicator. The samples were focused for 3 h at constant power of 8 W, setting the maximum voltage at 2000 V and current at 30 mA.

2.4.1.4 Immunoblotting.

A nitrocellulose sheet and 2 sheets of Whatman number 1 filter paper were cut to size and pre-soaked in TBS. The membrane was placed onto the surface of the gel, avoiding trapped air bubbles, followed by 2 sheets of wet filter paper and 4 sheets of dry number 3 filter paper. Finally, the blot was covered with a glass plate and pressed for 45 min using a 1 kg weight. After transfer, the membrane was removed and immunoblotted as outlined in *section 2.3.3* using 1 mg/l mouse monoclonal anti-apoE (F5M3/A10) as the primary antibody and 1/1000 goat anti-mouse IgG-alkaline phosphatase conjugate (Bio-Rad) as the secondary antibody. Finally, the membrane was stained using the freshly prepared alkaline phosphatase substrate (NBT/BCIP). The apoE phenotype was determined by comparing the band positions of known control samples with the unknown samples (Figure 2.4-1).

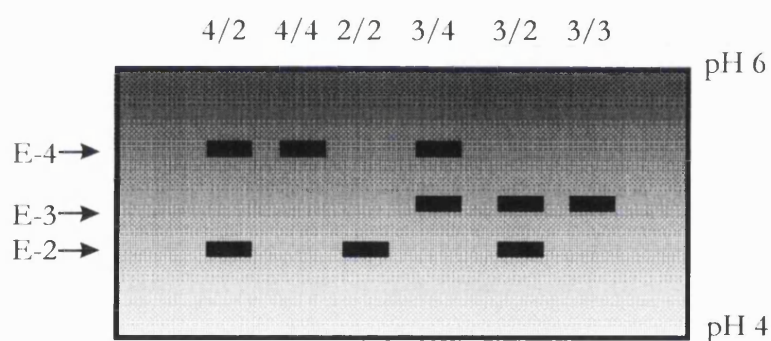


Figure 2.4-1 A schematic representation of apoE phenotype patterns.

2.4.2 QUANTIFICATION OF APOLIPOPROTEIN E LEVELS IN PLASMA: ROCKET IMMUNOELECTROPHORESIS.

ApoE levels in plasma can be quantified by using the Hydragel LpE Particles Kit (Sebia, Issy-les-Moulineaux, France). This kit utilises the technique of Laurell's rocket immunoelectrophoresis. Briefly, plasma samples are placed in wells cut in agarose containing monoclonal antibodies to apoE. On applying a direct electric current, apoE migrates towards the anode and the antibodies migrate towards the cathode. Initially, soluble apoE-antibody complexes are formed in apoE excess. When all of the apoE has migrated into the gel, equivalence is reached and apoE-antibody complexes precipitate in the shape of a rocket (Figure 2.4-2). The area under the rocket is directly proportional to the apoE concentration. When the precipitation arcs have become stationary (about 2 h),

a plot of rocket height against concentration will be linear. Thus, by the use of standards and the preparation of a standard curve, the concentration of apoE may be determined.

Quantification of LpB/E particles is determined by differential quantification. Firstly, on whole plasma, total apoE concentration is determined and secondly, the same plasma is treated with an anti-apoB antibody, which precipitates out all apoB-containing lipoproteins, thus leaving HDL-E levels to be quantified. The amount of LpB/E is obtained by subtracting the difference between the two rockets corresponding to the whole plasma and the treated plasma.

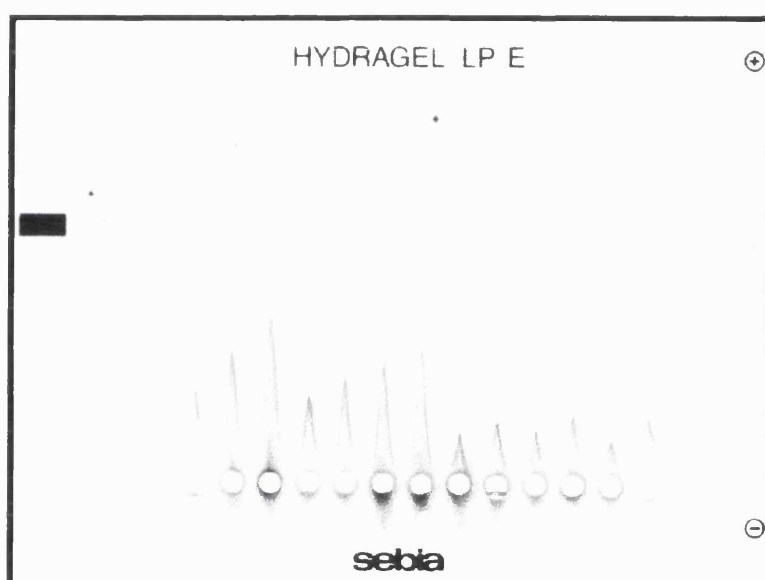


Figure 2.4-2 A typical apolipoprotein E rocket.

2.4.2.1 Reagents.

The Hydragel kit contained all the reagents required for apoE quantification, including the pre-made gels and standards.

2.4.2.2 Sample Preparation.

Either fresh plasma or singly frozen plasma was used for analysis. Samples for total apoE quantification were diluted 1:6 with diluent. Samples for HDL-E quantification were mixed 1 : 1 : 5 (plasma : anti-apoB : diluent) and incubated for 5 min at room temperature. The anti-apoB precipitate was sedimented with a 3000 g spin for 10 min at 4 °C. The supernatant was then analysed. A concentration curve was set up using the standard serum supplied with the kit.

2.4.2.3 Running the Gel

Five μl of the diluted samples and standards were applied to the wells and allowed to diffuse into the gel for 20 min before migration. The gels were placed in the electrophoresis tank (Sebia K20) containing 300 ml running buffer. The gels were positioned such that the wells were on the cathodic side. Electrophoresis was allowed to proceed for 2 h at a constant current of 15 mA/gel. After migration the gel was removed from the tank and placed on a flat surface. One thin filter paper soaked in saline and two dry thick filter papers were applied to the gel surface under a pressure of 1 kg for 20 min. The gel was then washed vertically in saline for 60 min. The gel was again pressed, with filter papers, for a further 10 min. After drying in an 80 °C oven the gel was immersed in staining solution for 5 min followed by successive washes in destaining solution until the background was completely clear. Rocket heights were measured from the leading edge of the well to the tip of the rocket. Distance migrated versus concentration of standards was plotted and the unknown sample concentrations determined from the standard curve.

2.4.3 ISOLATION OF APOLIPOPROTEIN E: DELIPIDATION AND AFFINITY CHROMATOGRAPHY.

The first step in the purification of apoE is the isolation of apoE-containing lipoproteins. The most convenient method for isolation is ultracentrifugation floatation of $d < 1.019$ g/ml lipoproteins (chylomicrons, VLDL and IDL). The lipoproteins are lyophilized in 200 ml conical glass tubes and then delipidated with organic solvents [250]. The apolipoproteins are then resolubilised in a guanidium-containing buffer, except for insoluble apoB. ApoE is then purified from this apolipoprotein solution by heparin-Sepharose affinity chromatography [251].

2.4.3.1 Lipoprotein Isolation.

ApoE containing lipoproteins were prepared from 150 ml - 200 ml fresh plasma. The $d < 1.019$ g/ml lipoprotein fractions were isolated as outlined in *section 2.2.3.4*. This lipoprotein preparation was then separated into 4 x 200 ml conical glass tubes, snap frozen in liquid nitrogen and freeze-dried until only 1 - 2 ml remained. At this stage the frozen lipoproteins were either stored at -70 °C or immediately delipidated.

2.4.3.2 Delipidation.

The lipoprotein preparations were defrosted and vigorously stirred magnetically. To each tube of stirring lipoprotein, 60 ml of ice cold methanol was added, followed by 140 ml of diethyl ether. The tubes containing precipitated apolipoprotein were allowed to settle on ice. The solvent was removed by aspiration and the precipitate washed in 120 ml

diethyl ether and allowed to settle again. This wash was repeated twice. The final pellet was allowed to dry until it was moist. Each pellet was then dissolved in about 25 ml of 0.2 M Tris.HCl, pH 8 containing 2 M guanidium HCl. The solubilized apolipoproteins were pooled and transferred into two 50 ml centrifuge tubes and centrifuged at 2000 g for 15 min to remove the insoluble apoB. The supernatant was removed and passed through a 0.8 μm /0.2 μm filter. The apolipoproteins were transferred to dialysis tubing and dialysed versus 2 x 4 litre changes of 25 mM ammonium bicarbonate.

2.4.3.3 Heparin-Sepharose Affinity Chromatography.

Heparin-Sepharose affinity chromatography takes advantage of the heparin binding property of apoE to separate it from contaminating proteins. The dialysed apolipoprotein solution in 25 mM ammonium bicarbonate (supplemented with 0.1 % mercaptoethanol) was bound to a 1 ml Hi-trap heparin-Sepharose column (Pharmacia) pre-equilibrated in the same buffer. The column was washed with 25 ml equilibration buffer, and then the apoE was eluted with 0.75 M ammonium bicarbonate. The apoE-containing fractions were pooled and assayed for protein content using the Bradford assay (*section 2.3.1*). Purity was assessed by performing SDS-PAGE on a 15 % gel. This procedure typically produced apoE of > 95 % purity with albumin being the major contaminant (Figure 2.4-3). The pure apoE was separated into 0.5 mg aliquots and stored at -70 °C for up to 1 year.

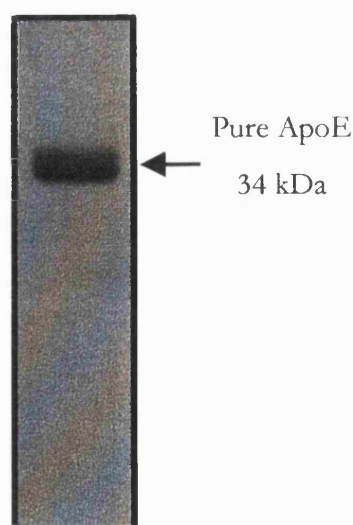


Figure 2.4-3. Analysis of purified apoE on a 15 % SDS-PAGE gel.

SDS-PAGE was performed on 1 μg of purified apoE as described in section 2.3.2. Note, the apoE doublet, which is due to differences in glycosylation of the mature polypeptide (see section 1.3.3).

2.4.4 PREPARATION OF APOE:DMPC COMPLEXES.

Although apoE-containing lipoproteins bind to apoE receptors, purified apoE devoid of lipids does not [252]. The apoE must be recombined with phospholipid to restore its receptor binding activity. The procedure described below recombines the apoE with the phospholipid, dimyristoylphosphatidylcholine (DMPC), to produce apoE:DMPC complexes that have been shown to bind with high affinity to the apoE receptors [252].

2.4.4.1 Production of DMPC Vesicles

Forty mg of DMPC was weighed into a 50 ml glass beaker, to which 10 ml of PBS was added. The DMPC was allowed to hydrate for 10 min at 20 °C and then sonicated (Sanyo Soniprep 150, small probe, setting an amplitude of 8 microns) for 30 min or until the solution was slightly translucent. The DMPC liposomes were then micro-centrifuged at 10000 rpm for 5 min to remove the titanium released from the sonication probe. This solution of DMPC vesicles was stored at room temperature.

2.4.4.2 Production of ApoE:DMPC

An aliquot of apoE, isolated as described in *section 2.4.3*, was reduced by the addition of β -mercaptoethanol (0.5 μ l / 100 μ g of apoE) for 30 min at room temperature. This is essential as both apoE-3 and apoE-2 form intramolecular disulphide bonds, which hamper apoE-lipid interactions. The DMPC vesicles were added to the protein (3.75 mg of vesicles per 1 mg of apoE), and the mixture was incubated on a rocking platform for 3 h at room temperature. After the apoE:DMPC has been dialysed against a buffer of choice, it can be used for receptor studies. However, for quantitative results the apoE:DMPC complexes should be separated from uncomplexed protein by flotation ultracentrifugation [252]. Thus, the apoE:DMPC complexes were adjusted to $d = 1.21$ g/ml, centrifuged at 105000 g for 20 h and the translucent apoE:DMPC collected from the top of the tube. After dialysis, the apoE:DMPC complexes could be stored at 4 °C for one month before loss of apoE activity (as judged by the platelet assay [see *section 2.5*]). At 4 °C the apoE:DMPC becomes cloudy but clarifies on warming to room temperature.

2.4.5 CHARACTERISATION OF APOE:DMPC COMPLEXES.

The morphology of the DMPC liposomes and apoE:DMPC complexes was examined using transmission electron microscopy [253]. Briefly, 1 μ g of apoE:DMPC protein was placed on a Formvar-coated grid for 5 min at 23 °C. The excess fluid was dried with filter paper, after which 10 μ l of 1 % uranyl acetate (pH 2.5) was placed on the grid and immediately dried. The grids were subsequently viewed with a Philips 501 electron microscope. DMPC vesicles were large spherical structures with a diameter of

35.9 ± 3.6 nm and formed aggregates in solution (Figure 2.4-4 *panel A*). The apoE:DMPC complexes appeared as disc-like structures that measured 18.8 ± 1.5 nm in diameter and 3.5 ± 0.4 nm in width. These discs were observed either in stacks of 5 to 10 discs (Figure 2.4-4 *panel B I*) or more commonly as single discs (Figure 2.4-4 *panel B II*). Some aggregates of multiple discs were seen (Figure 2.4-4 *panel B III*). The appearance of these particles is similar to that reported for macrophage secreted apoE/phospholipid discs and “nascent” HDL [253, 254].

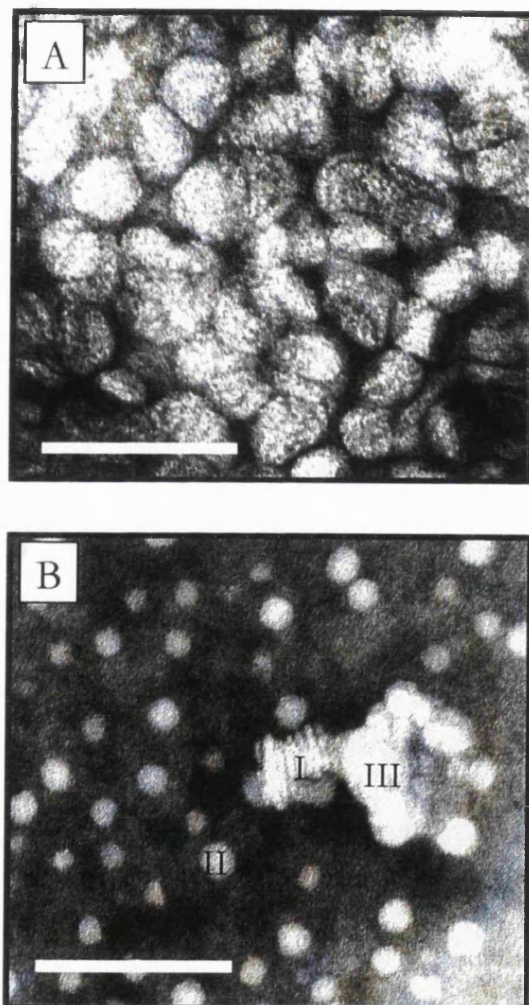


Figure 2.4-4 Analysis of apoE:DMPC complexes by electron microscopy.

Suspensions of DMPC liposomes alone (panel A) or apoE:DMPC complexes (panel B) were subjected to transmission electron microscopy as outlined in section 2.4.5. The white bar represents 100 nm.

2.5 Platelets: Isolation and Aggregation.

2.5.1 BACKGROUND.

Aggregation of platelets into a mass fulfils their main physiological function, that is, the formation of a haemostatic plug sealing off the break in an injured blood vessel. Whereas formation of platelet aggregates (thrombi) *in vivo* is difficult to measure, the process of platelet aggregation *in vitro* has been quantitatively analysed and employed in many studies of platelet function [16, 255].

Platelets are not “sticky” until they are stimulated by an agonist. Agonists are diverse consisting of: small molecular weight compounds such as ADP, serotonin and adrenaline; enzymes such as thrombin and trypsin; particulate material such as collagen and antigen-antibody complexes; lipids such as platelet-activating factor; and ionophores such as A23187. These agonists induce changes in the membrane of platelets, evoking their aggregation under appropriate conditions.

For aggregation to occur, the platelets must come into contact with one another, which is usually achieved by stirring the suspension. Aggregation in a suspension of platelets is detected on a macroscopic level by the development of visible clumps and clearing of the suspension. More sensitive measurements can be made in a platelet aggregometer, which is simply a photometer that records the clearing of a stirred suspension of platelets [28, 255, 256].

Aggregation of platelets *in vitro* constitutes a multi-step process that can be analysed by recording the tracing of changes in light transmission. Following the addition of certain agonists there is a decrease in light transmission due to a change in the shape of platelets from discoidal to spherical. This is followed by a gradual increase in transmission as the platelets aggregate and allow light to be transmitted through the platelet suspension. The initial phase of platelet aggregation (also termed the “primary phase”) is reversible unless it is followed by secretion of “pro-aggregatory” factors from the dense granules (e.g. ADP and serotonin) and α -granules (adhesive proteins such as fibrinogen, von Willebrand factor, thrombospondin and fibronectin). This “secondary phase” of platelet aggregation is irreversible and reaches a plateau that reflects the maximal level of light transmission [255, 256].

Platelet “stickiness” develops when the platelet membrane acquires the ability to bind fibrinogen. This dimeric molecule acts as a molecular “glue”, bridging the gap between platelets [14]. With stimuli that can induce secretion without prior aggregation,

e.g. thrombin or collagen, the fibrinogen can be secreted from the platelet α -granules, whereas with stimuli that require aggregation before secretion occurs, e.g. ADP and adrenaline, fluid-phase fibrinogen must be present. It is important to note that certain responses, e.g. secretion induced by ADP and the association of GPIIb-IIIa with the cytoskeleton, only occur when platelets have actually aggregated, not when they have been simply stimulated or even when they have bound fibrinogen [255].

2.5.2 BUFFERS AND SOLUTIONS.

Tri-sodium citrate (0.106 M)

Acid citrate dextrose (ACD) anticoagulant: 111 mM glucose, 85 mM trisodium citrate and 71 mM citric acid, pH 6.4.

Modified Tyrode's buffer: 150 mM NaCl, 7 mM NaHCO₃, 0.55 mM NaH₂PO₄·2H₂O, 2.7 mM KCl, 5.6 mM glucose, 5 mM MgCl₂ and 5 mM HEPES, pH 7.4.

Human fibrinogen: in modified Tyrode's buffer (4 mg/ml).

Human serum albumin (HSA): in modified Tyrode's buffer (3 mg/ml).

Prostacyclin: 15 mM solution stored in methanol at -70 °C then just before use diluted to 1.5 mM in 1 M Tris.HCl, pH 9.95

Agonists: ADP, adrenaline, collagen and thrombin were supplied as stock solutions Alpha Laboratories (Eastleigh, UK).

2.5.3 BLOOD SAMPLING.

Blood was withdrawn from the antecubital vein from healthy volunteers who had not taken any medication for ten days prior to donation. Disposable plastic syringes and tubes were used with a 21 G butterfly needle. It was important to execute a clean venipuncture with no difficulty drawing blood. The first few mls of blood were discarded to minimise the initial platelet activation present at the site of puncture. The blood was gently mixed with 0.106 M trisodium citrate (9 vol. blood to 1 vol. citrate) or ACD (4 vol. blood to 1 vol. anticoagulant) for studies involving platelet-rich plasma (PRP) or washed platelets, respectively.

2.5.4 PREPARATION OF PLATELET-RICH PLASMA.

Anticoagulated blood samples (10 ml or 20 ml) were centrifuged at 200 g for 15 min at 22 °C in a Mistral 2000R centrifuge to sediment red blood cells. The PRP was removed using a wide bore, plastic Pasteur pipette. The remaining blood was recentrifuged at 1000 g for 10 min to prepare platelet-poor plasma (PPP). The PRP samples were left at room temperature, in a sealed tube, for 15 - 30 min to recover from the centrifugation step. PRP kept at room temperature shows a "swirl" when agitated. This is characteristic of the

presence of asymmetric particles, in this case discoidal platelets. When agents such as ADP or chilling cause platelets to change their shape and become symmetrical spheres, the swirl disappears.

2.5.5 PREPARATION OF WASHED PLATELETS.

The presence of plasma proteins or other components may interfere with some studies on platelet aggregation. In this case, washed platelets must be used. Preparation of washed platelets is detailed below, while important aspects are noted here. Platelets sedimented by centrifugation from citrated PRP are almost impossible to resuspend due to platelet activation. To avoid this prostacyclin (PGI₂) is added, which temporarily inhibits platelet aggregation and permits the isolation of platelets that have a similar sensitivity to those in plasma [223]. Once isolated, albumin is usually added to platelet suspension media at 0.3 mg/ml, i.e. less than 1/10 of the plasma concentration. Albumin helps to prevent interaction of the platelets with foreign surfaces, be they plastic or siliconised-glass, it also traps small amounts of arachidonic acid or its products that may be liberated from the isolated platelets [255]. Fibrinogen must also be added if ADP or adrenaline is used as the stimulus.

2.5.5.1 Procedure.

ACD anticoagulated blood (40 - 80 ml) was centrifuged at 750 *g* for 5 min at 20 °C. The PRP was transferred into 2 x 15 ml polystyrene, conical base centrifuge tubes and was recentrifuged at 120 *g* for 10 min to sediment any contaminating red cells. PGI₂ was added to the PRP to a final concentration of 300 nM (1 µl of 1.5 mM stock/5 ml PRP), mixed gently and then recentrifuged at 750 *g* for 20 min to sediment the temporarily inactivated platelets. The PPP was removed and the platelet pellet was resuspended in modified Tyrode's buffer (0.25 ml per tube) by gently sucking and blowing with a 1 ml pipette. Platelets from the same subject were pooled, the count determined (*section 2.5.6*) and fibrinogen and HSA were added to give final concentrations of 0.4 mg/ml and 0.3 mg/ml, respectively. Finally, the volume of the platelet suspension was adjusted to give 6 x 10⁸ platelets/ml. The washed platelets were left at room temperature, in a sealed tube, for up to 1 h to recover from the effects of PGI₂.

2.5.6 PLATELET COUNTING.

Ten µl of PRP or 2 µl of washed platelets were diluted into 10 ml Isotron II (Coulter Electronics, Harpenden, UK.). The platelets were counted in a Coulter counter (Coulter Electronics) fitted with a 70 µm aperture probe. The settings were gain 1, aperture current

0.25 mA, lower threshold 3 and a volume of 0.1 ml counted. A mean of three separate dilutions was calculated using coincidence correction.

2.5.7 PLATELET AGGREGATION.

2.5.7.1 Recording Aggregation.

Aggregation was measured using the method established by Born [28]. This technique uses a platelet aggregometer to measure the change in percentage light transmission after addition of an agonist to a continually stirred platelet suspension. As the platelets aggregate, the amount of light transmitted through the cuvette increases and is detected by a photocell and recorded as a trace on a chart recorder.

Figure 2.5-1 shows typical tracings of ADP-induced aggregation in citrated platelet-rich plasma at 37 °C. In most aggregometers, the tracing shows considerable oscillation before the aggregating agent is added. This is due to the passage of the discoidal platelets across the light path (the “swirl”). Addition of the reagent causes brief obstruction of the light when the pipette or Hamilton syringe is inserted into the suspension. If a large volume of reagent is added, light transmission increases abruptly due to dilution. Next, light transmission decreases and the oscillations disappear due to the change in platelet shape from discs to spheres. These changes may not be very noticeable because they are superseded by the increase in light transmission due to aggregation.

Light transmission increases progressively as aggregation begins, and reaches a plateau when aggregation is maximal. Even with maximal aggregation, light transmission never reaches the value recorded by PPP. When large aggregates pass the beam, light transmission and hence the recording undergoes large oscillations. If a reagent lyses the platelets, light transmission increases and the oscillations disappear. If the concentration of ADP is too low, secretion of pro-aggregatory factors is not achieved and aggregation reverses because plasma enzymes break down ADP. This is termed the reversible “primary phase” of aggregation (Figure 2.5-1, *trace a*). At a critical concentration of ADP, usually 1 to 2 μM , two-phased aggregation is seen (Figure 2.5-1, *trace b*). This amount of ADP is termed the “threshold” concentration. The “secondary phase” is associated with secretion from the platelet dense granules. Both second phase aggregation and secretion depend upon the formation of endoperoxides and thromboxane A_2 from liberated arachidonic acid, and secretion of ADP from the dense granules. With higher concentrations of ADP the 2 phases merge (Figure 2.5-1, *trace c*). ADP-induced secretion and hence two-phased aggregation fails to occur at room temperature and requires close platelet contacts as well as a low concentration of divalent cations. Thus, if high

concentrations of ADP are added to PRP without stirring, neither aggregation nor secretion takes place.

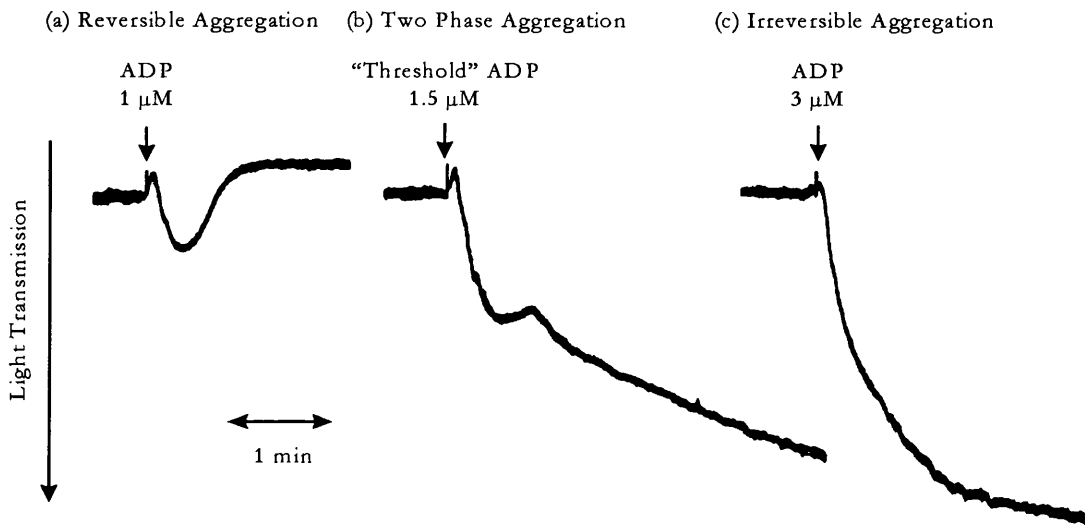


Figure 2.5-1 Typical responses to ADP.

2.5.7.2 Procedure.

All tests outlined in this thesis were conducted in a Payton dual channel aggregometer (Model No. 300 BD-5, Payton Associates Ltd, Hamilton, Canada) fitted with either 0.5 ml or 0.1 ml cuvette holders and linked to a Rikadenki dual channel recorder (Series R-00X, Rikadenki Mitsui Electronics Ltd, Surrey). The aggregometer stirrer speed was set at 900 rpm and the temperature of cuvettes was maintained at 37 °C. The chart recorder was set with a deflection of 10 mV and chart speed of 1 cm/min. The deflection limits of the recorder pen were set up so that a platelet-free solution, such as PPP or buffer, gave a deflection of 100 % and a platelet-rich solution, such as PRP or washed platelets, gave a deflection of 0 %.

Platelet suspensions (final concentration of 3×10^8 cells/ml for washed platelets and $1 - 2 \times 10^8$ cells/ml for PRP) were pre-incubated with modified Tyrode's buffer for a specified time, after which aggregation was initiated by addition of increasing concentrations of ADP, adrenaline, collagen or thrombin. The minimum amount of each agonist required to induce maximal aggregation within three minutes was determined; this "threshold" concentration of agonist was used in subsequent experiments in which Tyrode's buffer was replaced by increasing concentrations of the test samples. The aggregation of platelet/buffer mixtures, interspersed between platelet/test samples, was measured to ensure that the "threshold" concentration of agonist remained unchanged during the course of the study; if the extent of aggregation with the "threshold" concentration varied by more than 5 %, the experiment was abandoned.

2.5.7.3 Measuring Aggregation.

The magnitude of aggregation, as detected in an aggregometer can, be assessed by measuring the maximum change in light transmission (ΔT) at a specified time interval (usually 3 min). Alternatively, the maximum rate of aggregation (i.e. the tangent to the curve measured in millimetres or other units per unit time, termed also "slope value") can be used. Under most normal circumstances these two measurements correlate well [255], therefore, in this thesis, all aggregation was assessed by measuring ΔT values. A typical calculation is outlined below.

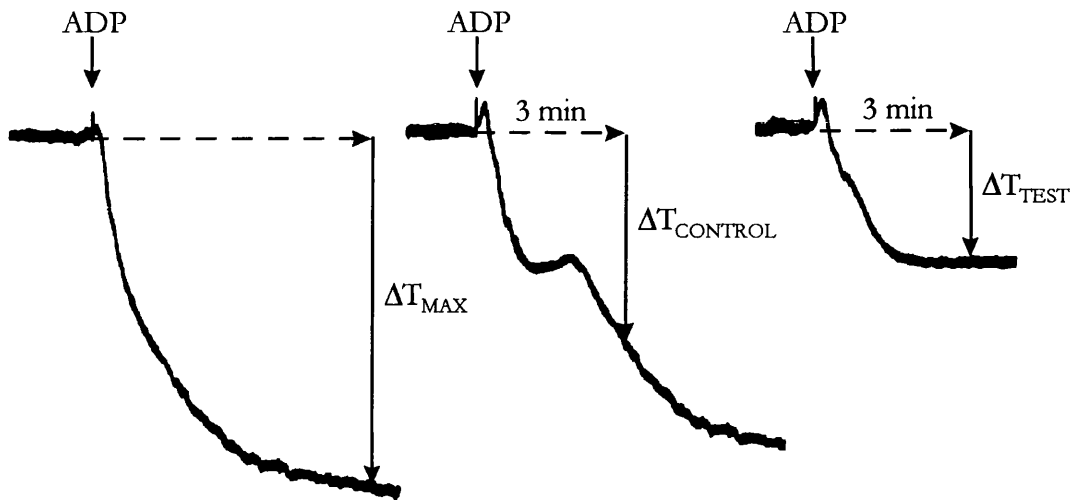


Figure 2.5-2 Determination of the degree of platelet aggregation.

For each platelet preparation the maximum amount of aggregation (ΔT_{MAX}), the threshold level of aggregation ($\Delta T_{CONTROL}$) and the test levels of aggregation (ΔT_{TEST}) were measured (Figure 2.5-2). The ΔT_{MAX} value was regarded as 100 % aggregation. Thus, the % aggregation of the control (% $A_{CONTROL}$) and test (% A_{TEST}) samples can be calculated as follows:

$$\% A_{CONTROL} = (\Delta T_{CONTROL} / \Delta T_{MAX}) \times 100$$

$$\% A_{TEST} = (\Delta T_{TEST} / \Delta T_{MAX}) \times 100$$

The % inhibition (% I_{TEST}) and the % stimulation (% S_{TEST}) of test *versus* control samples can also be calculated:

$$\% I_{TEST} = [1 - (\% A_{TEST} / \% A_{CONTROL})] \times 100$$

$$\% S_{TEST} = [(\% A_{TEST} / \% A_{CONTROL}) - 1] \times 100$$

2.6 Use of RT-PCR to Identify Platelet ApoE Receptors.

Evidence that high quality RNA can be isolated from platelets has allowed molecular biology techniques to be adapted to the study of platelet receptor expression [257]. Polymerase chain reaction (PCR) technology has been extensively used for the molecular characterisation of mutations in patients with genetic disorders such as Glanzmann thrombasthenia or Bernard-Soulier syndrome [257]. These studies have provided a substantial amount of information about platelet function. Therefore, using this technology it may be feasible to identify unknown platelet apoE receptors. As well as using the residual RNA present in platelets, RNA isolated from the megakaryoblastic cell lines, human erythroleukaemia (HEL) and Meg-01 can also be used as an indication of platelet receptor expression [258-260].

2.6.1 PCR TECHNOLOGY.

Molecular biology relies on techniques that enable the detection or capture of minute quantities of nucleic acids. The use of radioisotopes and, more recently, non-radioactive alternatives provides methods to detect and track nucleic acids. The cloning of nucleic acids into high copy number vectors allows amplification of DNA sequences in living cells, providing a nearly unlimited source of these DNA molecules for further manipulation. With the introduction of PCR [261], more sensitive levels of detection and higher levels of amplification of specific sequences are achieved, and in less time compared to previously used methods.

PCR is a relatively simple technique by which a DNA or cDNA template is amplified many thousand- or a million-fold quickly and reliably. By amplifying just a small portion of a nucleic acid target, that portion is effectively isolated from the rest of the nucleic acid in the sample and generates sufficient material for subsequent experimental analyses. The PCR process is exquisitely sensitive. While most biochemical analyses, including nucleic acid detection with radioisotopes, require the input of significant amounts of biological material, PCR requires very little. This feature makes the technique extremely useful in detecting low copy number transcripts from the residual RNA/cDNA that is isolated from platelets.

2.6.1.1 Basic PCR Methodology.

As originally developed, the PCR process amplified short (approximately 100 – 500 bp) segments of a longer DNA molecule [261]. A typical amplification reaction includes the sample of target DNA, a thermostable DNA polymerase, two oligonucleotide primers, deoxynucleotide triphosphates (dNTPs), reaction buffer and magnesium. The

components of the reaction are mixed and the reaction is placed in a thermal cycler, which is an automated instrument that takes the reaction through a series of different temperatures for varying amounts of time. This series of temperature and time adjustments is referred to as one cycle of amplification. Each PCR cycle theoretically doubles the amount of targeted template sequence (amplicon) in the reaction. Ten cycles theoretically multiply the amplicon by a factor of about one thousand and 20 cycles by a factor of more than a million in a matter of hours (Figure 2.6-1).

Each cycle of PCR amplification consists of three steps: production of single-stranded DNA templates, annealing the two oligonucleotide primers and synthesis of a copy from each strand of template. These steps should be optimised for each template and primer pair combination. The initial step is heating the target DNA to 95 °C or higher for 15 s to 2 min. In this denaturation process, the two intertwined strands of DNA separate from one another, producing the necessary single-stranded DNA template for the thermostable polymerase. The next step of a cycle reduces the temperature to approximately 40 - 70 °C, allowing the oligonucleotide primers to form stable associations (anneal) with the separated target DNA strands and hence serve as primers for DNA synthesis. This step usually lasts 30 - 60 s. Finally, the synthesis of new DNA begins when the reaction temperature is raised to the optimum for the DNA polymerase; this temperature is usually 72 °C. Extension of the primer by the polymerase lasts approximately 1 - 2 min. This step completes one cycle, and the next cycle begins with a return to 95 °C for denaturation. After 20 - 40 cycles, the amplified nucleic acid may then be analysed for size, quantity, sequence etc., or used in further experimental procedures, e.g. cloning.

2.6.1.2 RT-PCR.

The thermostable polymerases used in the basic PCR process require a DNA template and, as such, the technique is limited to the analysis of DNA samples. Yet, numerous instances exist in which the amplification of RNA from an organism would be preferred. This is particularly true in analyses involving the cloning of cDNAs from rare messages. In order to apply PCR methodology to the study of RNA, the RNA sample must first be reverse transcribed to cDNA to provide the necessary DNA template for the thermostable polymerase. This process is called “reverse transcription” (RT), hence the name RT-PCR. Avian myeloblastosis virus (AMV) or Moloney murine leukaemia virus (M-MLV or MuLV) reverse transcriptases are generally used to produce a DNA copy of the RNA template, using either random primers, an oligo(dT) primer or a sequence-specific primer [261]. After this initial reverse transcription step, the procedure follows the

temperature cycling steps of the basic PCR reaction, amplifying the target sequence as a DNA molecule (Figure 2.6-1).

The quality and purity of the starting RNA template is crucial to the success of RT-PCR. Either total RNA or mRNA can be used as the starting template, but both must be intact and free of contaminating genomic DNA. The efficiency of the first strand synthesis reaction, which can be related to the quality of the RNA template, will also significantly influence the success of the subsequent amplification.

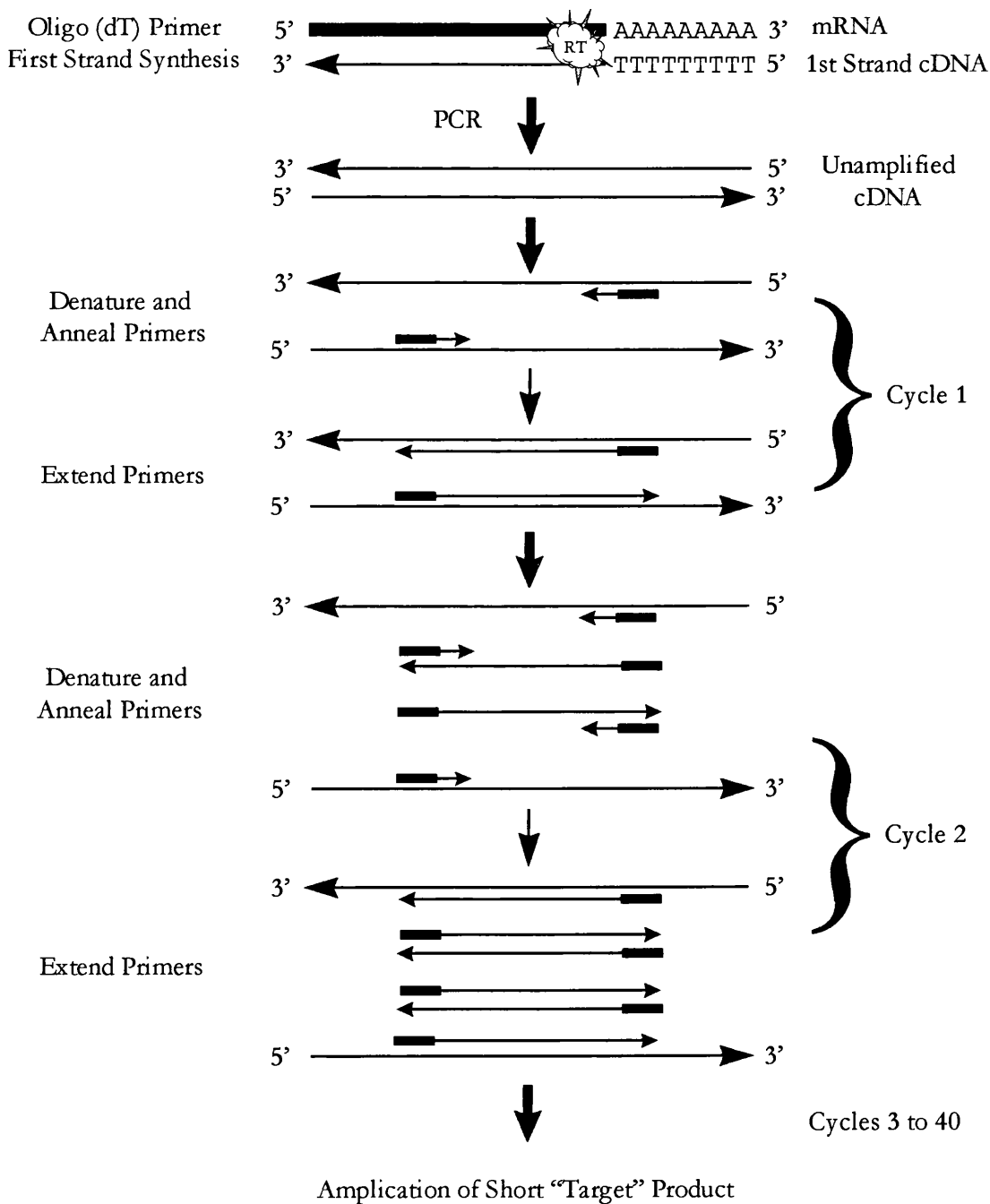


Figure 2.6-1 Schematic diagram of the RT-PCR process

2.6.2 TOTAL RNA EXTRACTION.

The guanidine isothiocyanate/phenol/chloroform technique for the isolation of total RNA originally published by Chomczynski and Sacchi [262] has been adapted for the extraction of total platelet RNA. RNA is extremely sensitive to RNases and extreme care must be taken to prevent contamination. Therefore, gloves were worn for all manipulations and disposable Rnase-free plastic-ware was used in preference to glassware. All solutions were treated with diethylpyrocarbonate (DEPC) and autoclaved.

Total RNA was extracted from washed cells and tissue using the guanidine isothiocyanate/phenol/chloroform total RNA isolation reagent (Advanced Biotechnologies Ltd, Surrey, UK). The washed cells/tissue were homogenised in the RNA reagent (1 ml per $0.5 - 1 \times 10^7$ cells) by repetitive pipetting and were incubated for 5 min at 4 °C to permit the complete dissociation of nucleoprotein complexes. Next, 0.2 ml of chloroform was added per 1 ml of RNA reagent, the samples were covered tightly and shaken vigorously for 15 s. The samples were placed on ice at 4 °C for 5 min after which the homogenate was centrifuged at 12000 g (4 °C) for 15 min. After the addition of chloroform and centrifugation, the homogenate formed two phases; an organic lower phase and an aqueous upper phase. The aqueous phase was transferred to a fresh tube, without disturbing the interface. An equal volume of isopropanol was added and the samples were incubated for 20 min on ice, followed by a centrifugation step of 12000 g (4 °C) for 20 min. The supernatant was removed and the RNA pellet washed twice with 75 % ethanol by vortexing and centrifugation for 5 min at 7500 g (4 °C). The RNA pellet was dissolved in 20 µl of DEPC-treated water by vortexing for 1 minute.

To ensure complete removal of genomic DNA contamination, RNA samples were treated with DNase I (30 U per 20 µl RNA in 40 mM Tris.HCl, 6 mM MgCl₂, pH 7.5) for 1 h at 37 °C. The samples were then made up to 200 µl with DEPC-treated water and extracted using phenol/chloroform/isoamyl alcohol [262]. The amount of RNA isolated was measured in a spectrophotometer and calculated using the following equation:

$$\text{RNA isolated } (\mu\text{g/ml}) = A_{260} \times \text{dilution factor} \times 40 \mu\text{g/ml.}$$

2.6.3 REVERSE TRANSCRIPTION PROTOCOL.

One µg or ¼ of the total amount of RNA isolated from each cell type was converted to cDNA with MuLV reverse transcriptase using the GeneAmp RNA PCR Kit (Perkin Elmer Applied Biosystems, Warrington, UK).

A master mix for reverse transcription was prepared by adding the reagents in the order and proportions shown below to 0.2 ml thin-walled PCR tubes:

Component	Volume	Final Concentration
25 mM MgCl ₂ Solution	4 µl	5 mM
10 x PCR Buffer II	2 µl	1x
DEPC Water	5.2 µl	--
dATP (100 mM stock)	0.2 µl	1 mM
dGTP (100 mM stock)	0.2 µl	1 mM
dTTP (100 mM stock)	0.2 µl	1 mM
dCTP (100 mM stock)	0.2 µl	1 mM
RNase Inhibitor	1 µl	1 U/µl
MuLV Reverse Transcriptase	1 µl	2.5 U/µl
Oligo d(T)16	1 µl	2.5 pM
Total RNA extracted from cells or DEPC water control.	5 µl	≤ 1 µg total RNA
Total volume, including sample.	20 µl	

Tube contents were covered with 20 µl light mineral oil and incubated in a Perkin Elmer GeneAmp PCR System 9600 as follows:

Annealing	Reverse Transcription	Denaturation of Enzyme	Cooling
25 °C for 10 min	42 °C for 20 min	95 °C for 5 min	4 °C for 5 min

2.6.4 GENERAL PROTOCOL FOR PCR AMPLIFICATION.

One-quarter of the total amount of cDNA (5 µl) from each cell type was amplified with the GeneAmp AmpliTaq Gold PCR DNA polymerase system (Perkin Elmer Applied Biosystems) using the following protocol.

A master mix for amplification was prepared by adding the reagents in the order and proportions shown below to 0.2 ml thin-walled PCR tubes:

Component	Volume	Final Concentration
GeneAmp 10 x PCR Buffer (containing 15 mM MgCl ₂)	5 µl	1x
DEPC Water	25.5 µl	--
dATP (10 mM stock)	1 µl	100 µM
dGTP (10 mM stock)	1 µl	100 µM
dTTP (10 mM stock)	1 µl	100 µM
dCTP (10 mM stock)	1 µl	100 µM
3' Primer	5 µl	1 - 10 µM
5' Primer	5 µl	1 - 10 µM
cDNA from reverse transcription	5 µl	< 1 µg total cDNA
AmpliTaq Gold	0.5 µl / with an additional 0.5 µl added every 20 cycles	2.5 U / 20 cycles
Total volume, including sample.	50 µl	

Tube contents were covered with 20 µl light mineral oil and incubated in a Perkin Elmer GeneAmp PCR System 9600. The incubation steps were optimised for each template and primer pair combination.

2.6.5 AGAROSE GEL ELECTROPHORESIS.

The results of a PCR reaction may be conveniently analysed using agarose gel electrophoresis, followed by staining the DNA with ethidium bromide and visualisation by ultraviolet (UV) irradiation of the gel [263]. The following protocol describes a typical minigel analysis. The minigel apparatus (Horizon minigel apparatus: Life Technologies, Paisley, UK) was set up as recommended by the manufacturer. The required weight of agarose (AquaPor LE GTAC agarose; National Diagnostics, Hull, UK) was added to the appropriate amount of 1 x Tris borate EDTA (TBE) buffer (from a 10 x stock; National Diagnostics). Table 2.6-1 outlines the separation ranges for typical gel concentrations. The mixture was heated in a microwave oven until the agarose just dissolved (usually 2 min) with mixing at regular intervals. The solution was cooled to 50 – 60 °C and, after adding ethidium bromide (0.5 µg/ml), was poured into the cast. The gel was allowed to set for ~30 min at room temperature. The comb and blocks were removed and a sufficient volume of 1 x TBE buffer containing ethidium bromide (0.5 µg/ml) was added to just cover the surface of the gel. The PCR products were mixed 9:1 with 10 x loading buffer (10 mM Tris.HCl, pH 7.5 containing 50 mM EDTA, 10 % Ficoll 400, 0.25 % bromophenol blue and 0.25 % xylene cyanol FF) and loaded (10 - 20 µl) into the wells.

The gel was run at a constant voltage of 150 V for ~30 min or until the dye front had migrated 2 cm from the bottom of the gel. After electrophoresis, the gel was removed, visualised and photographed on an UV lightbox.

DNA Size (bp)	Gel Concentration
100 - 3000	2.00 %
150 - 4000	1.75 %
200 - 5000	1.50 %
300 - 8000	1.25 %
400 - 12000	1.00 %
1000 - 23000	0.75 %

Table 2.6-1 Separation ranges for typical agarose gel concentrations.

2.6.6 EXTRACTION OF DNA FROM AGAROSE GELS.

DNA bands of interest were extracted from the agarose gel using the QIAquick gel extraction kit (Qiagen, Crawley, UK). Briefly, the DNA fragment was excised from the agarose gel with a clean, sharp scalpel, weighed and 3 vol. of buffer QX1 was added to 1 vol. of gel slice (100 mg = 100 μ l). For > 2 % agarose gels, 6 vol. of buffer QX1 was added. The gel mixture was solubilized at 50 °C for 10 min (20 min > 2 % agarose gels), mixed with 1 gel vol. of isopropanol, followed by 10 μ l 3 M sodium acetate, pH 5.0. The sample was centrifuged in a QIAquick spin column and for 1 min at 12000 g . The flow-through was discarded and the column was washed with 0.75 ml of buffer PE and recentrifuged. The dry column was placed in a clean 1.5 ml microfuge tube and eluted by adding 30 μ l TE buffer (10 mM Tris.HCl, 1 mM EDTA, pH 8.0), letting this stand for 1 min and then centrifuging for 1 min. The purified DNA fragment was either used immediately or stored at -20 °C.

2.6.7 RESTRICTION DIGESTION OF PCR PRODUCTS.

Restriction enzymes, also known as restriction endonucleases, recognise and cut specific DNA motifs of different lengths and base composition [264]. The typical restriction enzyme site is an exact palindrome of 4, 5, 6, 7 or 8 bp with an axis of rotational symmetry (e.g. the *EcoRI* recognition site is GAATTC). Six base cutters are used for cloning into specific regions of plasmids in which a series of unique sites known as polylinkers have been engineered. Most enzymes will not cut DNA methylated on one or both strands of their recognition site.

Ten μl of the PCR product was restriction digested using the following protocol. A master mix for digestion was prepared by adding the reagents in the order and proportions shown below to 0.2 ml thin-walled PCR tubes:

Component	Volume
Nuclease-free water	5 μl
Appropriate restriction enzyme 10 x buffer	2 μl
Acetylated BSA (1 mg/ml)	2 μl
DNA sample (in TE buffer)	10 μl
Restriction enzyme, 2 U	1 μl
Final volume	20 μl

All enzymes with their appropriate buffers were supplied by Life Technologies. The contents were mixed gently by pipetting and sedimented by brief centrifugation at 12000 *g*. The tubes were then incubated at the optimum temperature for 1 h. Table 2.6-2 outlines the reaction conditions for the enzymes used in this thesis. Next, 2 μl of 10 x gel loading buffer was added and the samples were run on agarose gels as before (*section 2.6.5*).

Enzyme	Cleavage Site	Reaction Conditions
BamHI	GGATCC	<i>REact3</i> buffer at 37 °C
EcoRI	GAATTC	<i>REact2</i> buffer at 37 °C
SmaI	CCCGGG	<i>REact4</i> buffer at 30 °C
PstI	CTGCAG	<i>REact2</i> buffer at 37 °C

Table 2.6-1 Restriction enzymes and reaction conditions

2.6.8 CLONING AND SEQUENCING OF PCR PRODUCTS.

To prepare DNA for sequencing, the PCR products must be cloned into a suitable plasmid vector and amplified using a suitable cell type (usually *E. Coli*), where they are replicated by the DNA synthesizing machinery of the host [265].

The ease with which a DNA fragment is cloned into a plasmid vector depends on several factors. Cloning is considerably more successful when only one DNA fragment is to be ligated into a vector. The compatibility of the ends of the vector and fragment is also important. Efficient cloning occurs when the vector and insert DNA contain complementary, overhanging ends; cloning is less efficient when both DNA fragments

possess blunt ends. The highest cloning efficiency is generally achieved with DNA cleaved by two different restriction enzymes that produce non-complementary overhangs. Since the insert DNA can only be ligated into the vector in one orientation, this is referred to as “directional cloning”.

Many different plasmid vectors are commercially available. These include general purpose cloning vectors as well as vectors designed for specialised applications, such as mutagenesis, protein expression and reporter gene studies. However, in most cases a standard sequencing vector, pUC18 (Stratagene, Cambridge, UK), was used to transfect *E. Coli*.

2.6.8.1 Preparation of Vector and PCR Products for Ligation.

The 5' end of each PCR primer was designed with a restriction site to facilitate cloning. The 5' primer contained a BamHI site and the 3' primer contained an EcoRI site. The whole PCR reaction mixture was electrophoresed on a 2 % agarose gel to identify products. Unique bands were excised from the gel and cut with EcoRI and BamHI. This mixture was again separated on a 2 % agarose gel and excised from the gel. Pre-digested EcoRI and BamHI cut pUC18 vector was supplied by Dr. D. Vinogradov (RFHSM, London, UK).

2.6.8.2 Ligation Reaction.

The following ligation reaction was set-up and incubated at 4 °C for 16 h:

Component	Volume
pUC18 DNA	1 µl (100 ng)
Cut PCR product	16 µl or 50 ng
T4 DNA ligase (Boehringer Mannheim, Lewes, UK)	1 µl
10 x ligase buffer (Boehringer Mannheim)	2 µl
Nuclease-Free Water to a final volume	20 µl

Following ligation, the vector was transformed in competent *E. Coli*.

2.6.8.3 Transformation of Plasmid DNA in Competent *E. Coli*.

When bacteria are treated with ice-cold solutions of CaCl_2 and then briefly heated, a transient state of “competence” is induced during which the bacteria are able to take up DNA derived from a variety of sources including recombinant vectors.

Procedure.

A 50 μl aliquot of competent cells (strain DH5 α ; supplied by Dr. D. Vinogradov) was thawed on ice and mixed with 10 ng of DNA (approximately 2 μl of the ligation reaction) by gently swirling the pipette tip. The cells were incubated on ice for 30 min, then 42 °C for exactly 90 s and again on ice for 2 min. Next, 125 μl of LB medium was added and the tubes incubated for 45 min at 37 °C with shaking at ~150 rpm. To select the transformants, the contents of each tube were spread onto LB agar plates containing 100 $\mu\text{g}/\text{ml}$ ampicillin, incubated at room temperature for 1 h and then incubated in a dry 37 °C incubator overnight. Since the pUC18 plasmid contains an ampicillin resistance gene, only transformed cells will grow. Positive colonies were picked up and grown overnight in a 50 ml tube containing 6 ml of LB broth containing 100 $\mu\text{g}/\text{ml}$ ampicillin with constant shaking (200 rpm) at 37 °C.

2.6.8.4 Analysis of Transformants and DNA Sequencing.

Recombinants obtained from cloning experiments were screened to identify clones containing the PCR products of interest. Promega's *Wizard Plus* Minipreps DNA purification columns were used to isolate pure plasmid from 3 ml of cells as outlined by the manufacturer (Promega, Southampton, UK). Plasmid DNA was eluted in 50 μl of pre-heated nuclease-free water (80 °C). The desired clones were identified by restriction digestion and agarose gel analysis.

Clones containing the desired PCR products were prepared for automated fluorescent sequencing by mixing 500 ng plasmid DNA with 32 pmol of either “-40 universal” or “M13 reverse” sequencing primers and made up to a final volume of 10 μl . Sequencing was carried out commercially by Oswel DNA sequencing services (Southampton, UK).

2.6.9 STATISTICS.

Values in text, tables and figures were expressed as the mean \pm S.E.M. Statistical differences between means were determined by Student's *t*-test and considered significant if $P < 0.05$. All analyses were performed using SigmaPlot for Windows (Jandel Scientific, Erkrath, Germany).

Chapter 3

3. CHARACTERISATION OF THE ANTI-AGGREGATORY EFFECT OF “NATIVE” HDL-E PARTICLES AND PURIFIED APOLIPOPROTEIN E.

3.1 Introduction.

As outlined in *Chapter 1 (section 1.4)*, Desai et al. have previously demonstrated that HDL particles enriched in apoE (HDL-E) are potent inhibitors of platelet aggregation [7, 235]. Chemically modifying the apolipoprotein constituents of HDL-E blocked its inhibitory effect implying that the active agent was the apoE polypeptide itself [7]. Further evidence implicating apoE was obtained by studying the anti-platelet effects of abnormal HDL isolated from a group of cirrhotic patients. Such HDL is known to contain high numbers of apoE molecules [235, 246]. Cirrhotic HDL was found to have a powerful anti-aggregatory effect which correlated closely with its apoE content ($r=0.70$, $P<0.001$) but not with its apoA-I ($r=-0.17$) or apoA-II ($r=0.23$) contents [235]. Although these data provide strong evidence for an anti-platelet role for HDL-E, there is an inherent methodological problem with these studies. The authors isolated HDL-E by a standard procedure involving an initial ultracentrifugation step to float the total HDL and then heparin-Sepharose chromatography. Unfortunately, although highly purified HDL is obtained by ultracentrifugation, the composition and integrity of the particles is known to be affected by this procedure. Indeed, some of the apolipoprotein molecules, particularly apoE, dissociate from the surface [266-268]. It is reasonable to assume therefore, that the HDL-E used in these studies may not be representative of the “native” HDL present in the circulation. In order to circumvent such apolipoprotein loss, immunoaffinity chromatography, employing antibodies specific for individual apolipoproteins, has previously been used to prepare lipoproteins directly from plasma [269, 270]. This procedure is considered to produce particles representative of “native” circulating lipoproteins. Accordingly, in the first part of this chapter, I have isolated HDL-E particles by chromatography on anti-apoE immunosorbent gels and analysed the anti-platelet activity of this more physiologically relevant lipoprotein preparation.

In addition to being an integral component of HDL-E, apoE is also present as the sole apolipoprotein on lipoprotein particles synthesized and released by macrophages [116]. These phospholipid-containing particles appear important for facilitating local cholesterol redistribution and reverse cholesterol transport. Macrophage-derived apoE

may also restrict development of atherosclerotic lesions by paracrine actions [116], one of which may reflect its ability to inhibit platelet aggregation at the locality of the lesion. Indeed, Higashihara and colleagues in Tokyo have shown that synthetically produced apoE/phospholipid complexes (apoE:DMPC) are potent inhibitors of platelet aggregation *in vitro* [271]. However, many basic aspects of the apoE-induced inhibition of platelet aggregation were not addressed in this report. Therefore, in the second part of this chapter, my aim was not only to confirm the anti-platelet action of purified apoE:DMPC preparations but also to further characterise the underlying mechanism.

3.2 Specialised Materials and Methods.

3.2.1 MATERIALS.

Monoclonal anti-apoE antibodies were purified from hybridoma cells provided as a kind gift from Dr. R. W. James (Geneva, Switzerland). Human apoE-3 was purified from the plasma of normal volunteers or from patients with primary biliary cirrhosis (PBC) whose plasma apoE levels were determined to be > 10 mg/dl. Rabbit apoE was purified from the plasma of cholesterol-fed animals. Recombinant apoE-3 was provided as a kind gift from Dr. T. Vogel (Jerusalem, Israel). All other chemicals unless otherwise stated were supplied by Sigma Chemical Co.

3.2.2 PREPARATION OF ANTI-APOE SEPHAROSE AFFINITY MATRIX.

CNBr-Sepharose 4B (1.7 g) was added to 50 ml of 1 mM HCl and agitated on an orbital shaker for 15 min at room temperature to remove stabilisers and to swell the gel to ~5 ml. The gel was transferred to a sintered glass funnel and washed with 500 ml 1 mM HCl. Ten mg of purified anti-apoE IgG (clone F5M1/C3) in coupling buffer (0.1 M NaHCO₃, 0.5 M NaCl, pH 8.3) was added (2 vol. antibody/1 vol. gel) and the mixture incubated overnight at 4 °C on an orbital mixer. The supernatant was analysed for protein (by measuring A₂₈₀) to confirm that the antibody had coupled to the matrix and then the gel was washed with 500 ml of coupling buffer. Ethanamine (1 M) was added to block reactive sites left on the gel by incubation on an orbital mixer for 2 h at room temperature. The matrix was washed again with 500 ml of coupling buffer and then washed alternately with 4 x 250 ml of coupling buffer and 4 x 250 ml of 0.1 M glycine, 0.5 M NaCl, pH 3.0. The anti-apoE immunoaffinity matrix was then stored in coupling buffer containing 0.25 % sodium azide at 4 °C.

3.2.3 HDL-E ISOLATION FROM PLASMA.

Blood was collected from either normal volunteers or patients with primary biliary cirrhosis (PBC) as outlined in *section 2.2.2*. The plasma obtained from each sample was divided into equal parts, one being processed by immunoaffinity isolation of HDL-E and the other by conventional heparin-Sepharose methodology. In each case, the maximum amount of HDL-E was isolated from each sample and was expressed as mg HDL-E protein/ml of plasma. The apoE content of each sample was assessed qualitatively by dot blot analysis of 10 µg HDL-E (*section 2.3.3*).

3.2.3.1 Affinity Chromatography on Anti-ApoE-Sepharose.

One ml of plasma from either PBC patients or normal subjects was pre-treated to remove apoB-containing lipoproteins (*section 2.2.3.6*) and incubated with the immunoaffinity matrix overnight at 4 °C with gentle rotation. Following incubation, the matrix was poured into a 10 x 1.5 cm glass column, which was subsequently connected to a Multirac fraction collector, model 2111, linked to a single channel chart recorder, model 2210 (LKB Instrumentation, Surrey, UK). The absorbance range of the UV recorder was set at 0.1, the chart speed set at 1 mm/min and the fraction collector at a 30 drop collection per tube (1.5 ml fractions). The affinity matrix was then extensively washed with equilibration buffer (PBS, pH 7.4), until the A_{280} returned to the baseline. The bound fraction (HDL-E) was eluted with 0.1 M glycine, pH 3.0, into 50 µl of 1 M Tris, pH 9.0 which adjusts the pH to 7.0. The elute was then concentrated in a Centriflo CF25 membrane cone (7 ml, 25000 MW retention; Amicon, UK). Analysis of the elute by SDS-PAGE confirmed that the apolipoprotein profile resembled that of HDL-E (results not shown).

3.2.3.2 Heparin-Sepharose Purification of HDL-E.

Total HDL was also isolated from 1 ml of plasma by ultracentrifugation (*section 2.2.3*) and then subfractionated by heparin-Sepharose affinity chromatography at 4 °C in a 10 x 1.5 cm glass column with 10 ml bed volume (Pharmacia). The heparin-Sepharose was equilibrated with buffer 1 (50 mM NaCl, 5 mM Tris.HCl, 25 mM MnCl₂, pH 7.4). Solid MnCl₂ was added to the total HDL to give a final Mn²⁺ concentration of 25 mM and this mixture was then applied to the column via a peristaltic pump at a rate of 0.5 ml/min. The unbound fraction (apoA rich HDL) was washed away with buffer 1 until the A_{280} returned to the baseline. The bound fraction (apoE rich HDL) was eluted with buffer 2 (95 mM NaCl, 5 mM Tris.HCl, pH 7.4) and the column was regenerated by sequential washes of buffer 3 (600 mM NaCl, 5 mM Tris HCl, pH 7.4) to remove additional material (traces of Lp(a) or LDL) and then buffer 1 containing 0.02 % sodium azide but excluding

MnCl₂. The collected fractions were concentrated in Centriflo CF25 membrane cones as before and stored at 4 °C.

3.2.4 APOE:DMPC COMPLEXES.

Pure apoE was incorporated into small, unilamellar vesicles of DMPC as outlined in *section 2.4.4*. The apoE-liposome complexes were extensively dialysed against Tyrode's buffer before use.

3.2.5 PREPARATION OF CHEMICALLY MODIFIED APOE:DMPC COMPLEXES.

Modification of the arginine residues of apoE was accomplished by established procedures using cyclohexanedione [252]. Briefly, apoE:DMPC vesicles (1 mg protein in 1 ml saline) were mixed with 1 ml of 0.3 M 1,2-cyclohexanedione (CHD) in 0.1 M sodium borate buffer (pH 8.1) and incubated at 37 °C for 2 h. The sample was then extensively dialysed against Tyrode's buffer at 4 °C. The modified apoE:DMPC vesicles (CHD-apoE:DMPC) were then filtered through a 0.45 µm Millipore filter and used directly in the subsequent aggregation experiments.

3.2.6 PLATELET AGGREGATION.

PRP (1 - 2 x 10⁸ cells/ml) or washed platelet preparations (3 x 10⁸ cells/ml) were pre-incubated with Tyrode's buffer for the stated times and aggregation was initiated by addition of increasing concentrations of ADP, adrenaline, collagen or thrombin at 37 °C in a Payton dual-channel aggregometer fitted with 0.1 ml cuvettes. The minimum amount of each agonist required to induce secondary aggregation within 3 min was determined; this "threshold concentration" of agonist was used in subsequent experiments in which Tyrode's buffer was replaced by increasing concentrations of the test samples (HDL-E, apoE:DMPC, CHD-apoE:DMPC, free apoE or DMPC liposomes alone). Some variation in the anti-aggregatory effects of apoE:DMPC was evident, presumably reflecting differences in the particular platelets used or in the individual apoE:DMPC preparations, but all experiments were repeated two or more times and were qualitatively reproducible.

3.2.7 ELECTRON MICROSCOPY.

Platelet samples were fixed in 3 % (v/v) glutaraldehyde in 0.1 M sodium cacodylate buffer, pH 7.4, containing 0.1 M sucrose. These samples were processed and analysed by the electron microscopy unit at the Royal Free Hospital School of Medicine. Briefly, the samples were dehydrated in a graded series of ethanol mixtures and critical point dried before being coated in carbon and gold in an Ion Tech saddle field using an ion source

sputter coater (Ion Tech, Teddington, UK). The platelets were then viewed in a Phillips 501 scanning electron microscope (Pye-Unicam, Cambridge, UK).

3.3 Results and Discussion.

3.3.1 EFFECTS OF NATIVE IMMUNOAFFINITY-ISOLATED HDL-E PARTICLES ON PLATELET AGGREGATION.

HDL-E was isolated from normal plasma both by a conventional ultracentrifugational method and by immunoaffinity chromatography. Subsequently, the ability of each HDL-E preparation to inhibit platelet aggregation was assessed. Although immunoaffinity chromatography removed significantly more HDL-E protein from normal plasma than the conventional procedure (39 & 77 *versus* 8 & 12 $\mu\text{g}/\text{ml}$ plasma, $n=2$), dot blotting revealed that there was no difference in apoE content (mg/mg total protein) between the two preparations (Figure 3.3-1 *panel B*). Consistent with this finding, both populations of HDL-E particles had a similar ability to inhibit adrenaline-induced platelet aggregation (Figure 3.3-1, *panel A*). Thus, this study confirms the findings of Desai et al. [7, 235] and also demonstrates that “native” HDL-E particles, isolated by immunoaffinity chromatography, are potent inhibitors of agonist-induced platelet aggregation.

Since important support for the anti-platelet effect of apoE was obtained from a study using “abnormal” HDL-E isolated from patients with hepatic cirrhosis, I repeated the above study with plasma obtained from jaundiced patients. In contrast to the studies using normal HDL-E, cirrhotic HDL-E isolated by immunoaffinity chromatography contained more apoE than that isolated conventionally (Figure 3.3-1, *panel D*). However, both techniques removed similar quantities of HDL-E protein from plasma (22 & 36 *versus* 18 & 25 $\mu\text{g}/\text{ml}$ plasma, $n=2$). This may be because some particles had more than one apoE molecule or because the grossly abnormal apolipoprotein and lipid composition of cirrhotic HDL [272-274] permits readier loss of apoE by ultracentrifugation. Accordingly, the “native” HDL-E was a much more effective anti-platelet agent (Figure 3.3-1, *panel C*) implying that isolation of cirrhotic HDL by ultracentrifugation may have underestimated its biological potency. This suggests that the importance of plasma HDL-E as an attenuator of platelet responsiveness in chronic liver disease [235], and hence its possible contribution to the aetiology of variceal bleeding [235] should be reassessed. Such studies are however, outside the scope of this thesis.

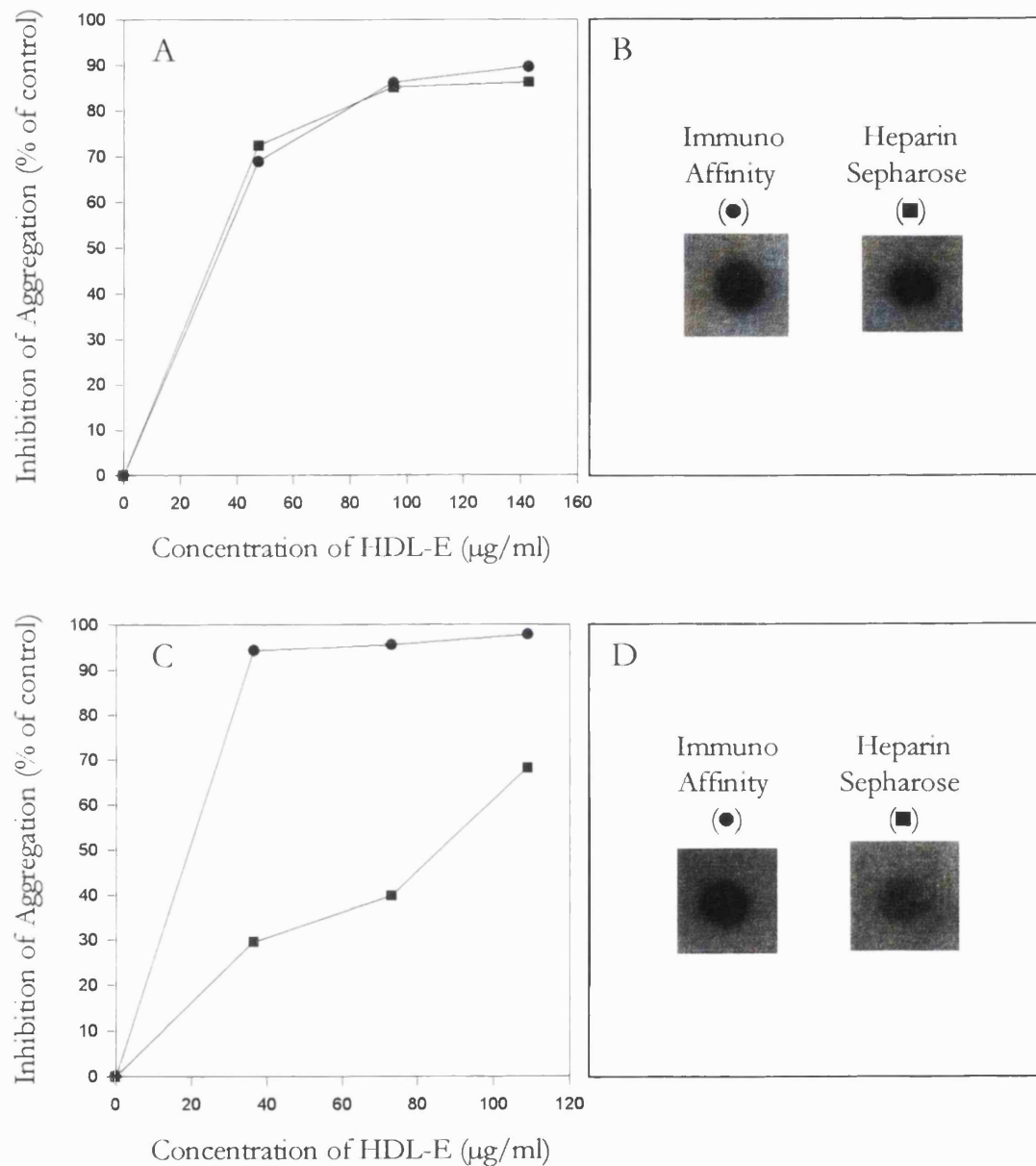


Figure 3.3-1 Inhibition of adrenaline-induced platelet aggregation by HDL-E.

*Panels A & C, washed platelets (3×10^8 / ml) were pre-incubated with various concentrations of immunoaffinity (●) or ultracentrifugation/heparin-Sepharose isolated HDL-E (■) for 30 s at 37 °C. The extent of aggregation was measured 3 min after addition of a pre-determined threshold concentration of adrenaline (5 µM). **Panels B & D, dot blot analysis of the HDL-E isolated by the two methods. Briefly, 10 µg of HDL-E was spotted onto nitrocellulose, which was in turn blocked and incubated with 1/1000 dilution of polyclonal anti-apoE for 1 h. The blots were developed as outlined in section 2.3.3.3. Panels A & B represent HDL-E isolated from normal plasma, while panels C & D are HDL-E from cirrhotic plasma.***

3.3.2 INHIBITION OF PLATELET AGGREGATION BY APOE:DMPC.

Recently, Higashihara and colleagues reported that apoE:DMPC complexes were potent inhibitors of collagen- and thrombin-induced aggregation in washed platelets [271]. However, their incubation times with apoE:DMPC seemed prolonged (30 min) since Desai et al. have shown that HDL-E potently inhibits ADP-, adrenaline- or collagen-induced aggregation with only a 2 min pre-incubation [7]. Additionally, Higashihara et al. failed to examine the effects of apoE:DMPC vesicles on aggregation induced by the so-called “weak” agonists, ADP and adrenaline (see *section 1.2.4.1*). To clarify these methodological discrepancies, I re-examined the time course for apoE-induced inhibition of aggregation and applied the appropriate time scale to my experiments using a variety of agonists. ApoE:DMPC was found to be a rapid and potent inhibitor of ADP-induced aggregation in both PRP and washed platelets (Figure 3.3-2 and Figure 3.3-3, *panel A*). However, there were clear differences between the two platelet preparations. Fifty μg protein/ml of apoE:DMPC inhibited aggregation in washed platelets after only a short incubation period (73.9 ± 1.8 % inhibition with a 30 s pre-incubation), while maximal inhibition (88.9 ± 2.2 %) required a 2 min pre-incubation. In contrast, apoE:DMPC inhibited PRP more slowly. Very little inhibition was observed with a 30 s pre-incubation (9.3 ± 2.2 % inhibition), but this rose to 62.5 ± 2.9 % with a 10 min pre-incubation. Based on these results, subsequent experiments with apoE:DMPC used 30 s and 10 min pre-incubation periods for washed platelets and PRP, respectively.

3.3.3 APOE:DMPC INHIBITS PLATELET AGGREGATION INDUCED BY A VARIETY OF AGONISTS.

When I pre-incubated washed platelets with apoE:DMPC for 30 s, I was able to confirm the observation of Higashihara et al. that apoE:DMPC inhibited collagen-induced platelet aggregation (Figure 3.3-3, *panel C*); similar findings were seen with adrenaline as an agonist (Figure 3.3-3, *panel B*). However, in contrast to the findings of Higashihara et al., no inhibition was observed when thrombin was used as the agonist (Figure 3.3-3, *panel D*), unless either very high amounts of apoE were added (> 200 μg protein/ml) or the incubations were prolonged (results not shown). A possible explanation of these discrepant results is discussed in *Chapter 4 - The Biochemical Basis for Inhibition of Platelet Aggregation by Apolipoprotein E*.

3.3.4 EFFECTS OF FREE APOE, DMPC VESICLES AND APOE:DMPC COMPLEXES ON ADP-INDUCED PLATELET AGGREGATION.

The biological activity of apoE is sensitive to its lipid environment; aqueous solutions of apoE are unable to interact with the LDL-R [275]. Moreover, the

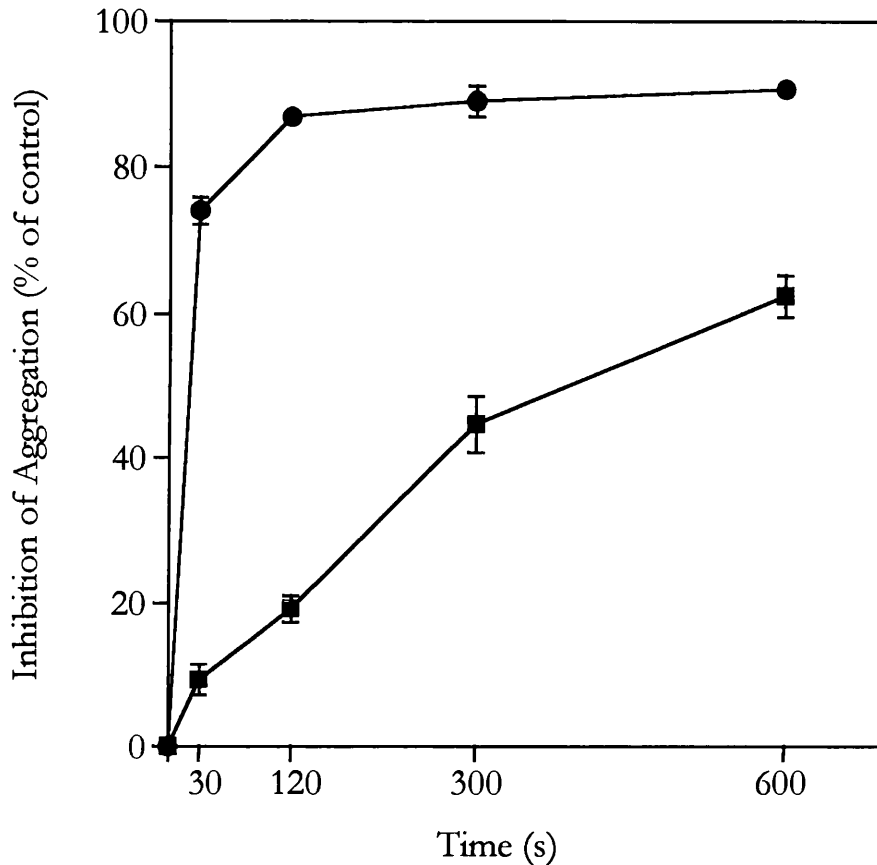


Figure 3.3-2 Inhibition of ADP-induced aggregation by apoE:DMPC as a function of time.

Washed platelet (●) or PRP (■) preparations were pre-incubated with 50 µg protein/ml apoE:DMPC complexes at 37 °C for various times. The extent of aggregation was measured 3 min after addition of a pre-determined threshold concentration of ADP (5-7 µM) and expressed as a percentage of controls with buffer alone. Points are the mean percentage inhibition of aggregation (± SEM) for three different experiments.

apoE in the surfaces of VLDL and chylomicrons is inactive unless these lipoproteins are from hypertriglyceridaemic subjects [276] or have undergone substantial lipolysis to form remnant particles [277]. Similarly, free apoE in solution had no effect on ADP-induced aggregation in both PRP and washed platelet preparations, although as before, it was a potent anti-platelet agent when complexed with phospholipid (DMPC) vesicles (Figure 3.3-4). Indeed, ADP-induced aggregation was inhibited in a dose-dependent manner by a physiological range (10 - 50 µg protein/ml) of apoE:DMPC (79.3 ± 5.1 % inhibition at 50 µg protein/ml apoE:DMPC, $n=3$, $P<0.001$ in washed platelets, [Figure 3.3-4, panel A] and 57.6 ± 5.5 % inhibition at 50 µg protein/ml apoE:DMPC, $n=3$, $P<0.001$ in PRP, [Figure 3.3-4, panel B]). DMPC vesicles alone had no effect on aggregation. Presumably, complexing the apoE polypeptide with DMPC allowed it to assume an appropriate

orientation and conformation for biological activity [275]. Again, however, apoE:DMPC was a less effective inhibitor of PRP preparations than washed platelets. This may be due to a number of factors. Conceivably, the anti-platelet effect of apoE may have been partially neutralised by components present in the citrated plasma. Alternatively, treatment of platelets with prostacyclin may have sensitized washed platelets to apoE-induced effects, resulting in a higher degree of inhibition.

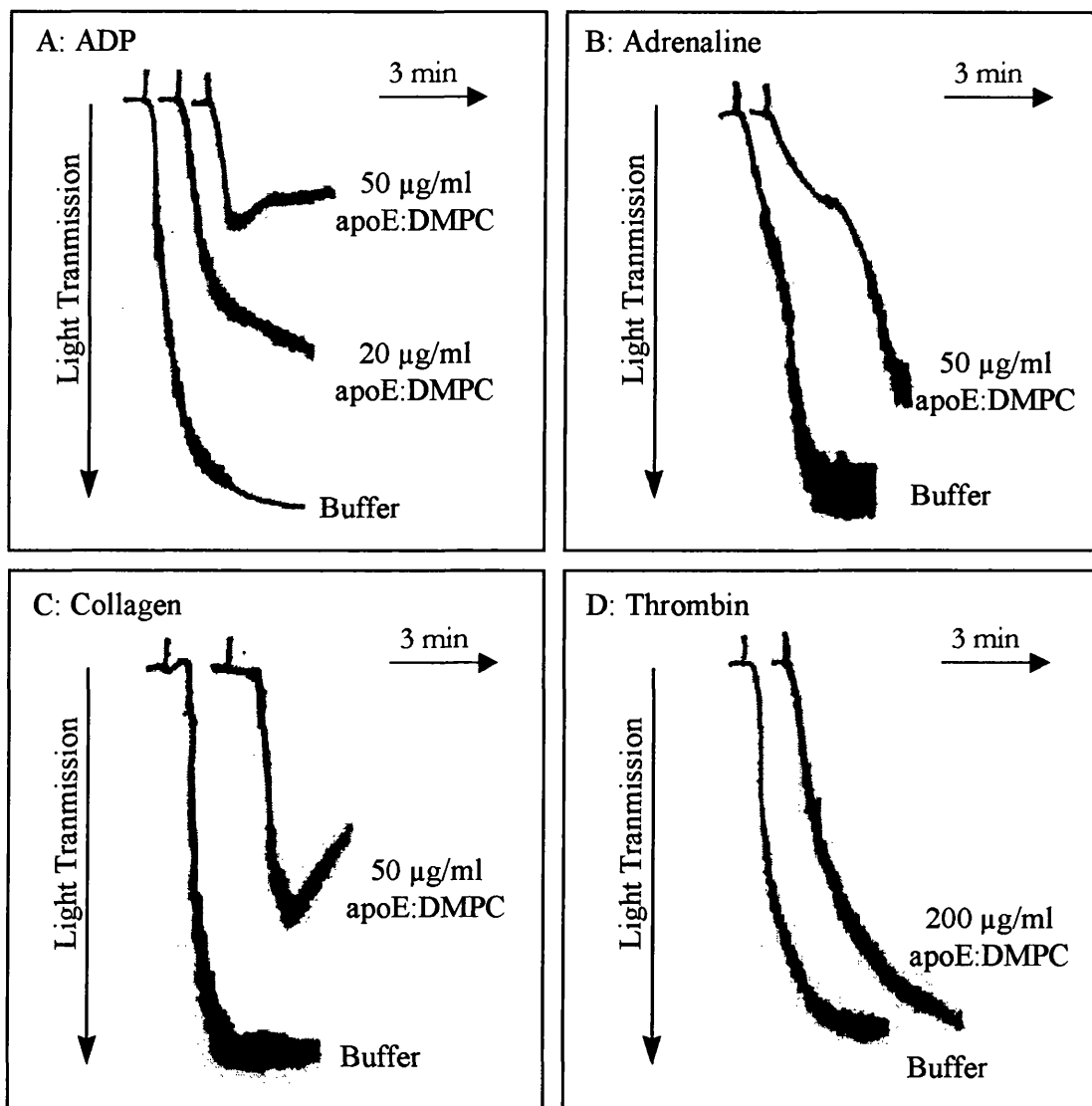


Figure 3.3-3 Inhibition of agonist-induced platelet aggregation by apoE:DMPC

Washed platelets ($3 \times 10^8 / ml$) were pre-incubated with various concentrations of apoE:DMPC for 30 s at 37 °C. The extent of aggregation was measured 3 min after addition of a pre-determined threshold concentration of ADP (5 μM) (**panel A**), adrenaline (5 μM) (**panel B**), collagen (2 $\mu g / ml$) (**panel C**) or thrombin (0.1 U/ml) (**panel D**). All experiments were repeated two or more times and were qualitatively reproducible. However, only single representative experiments are presented here.

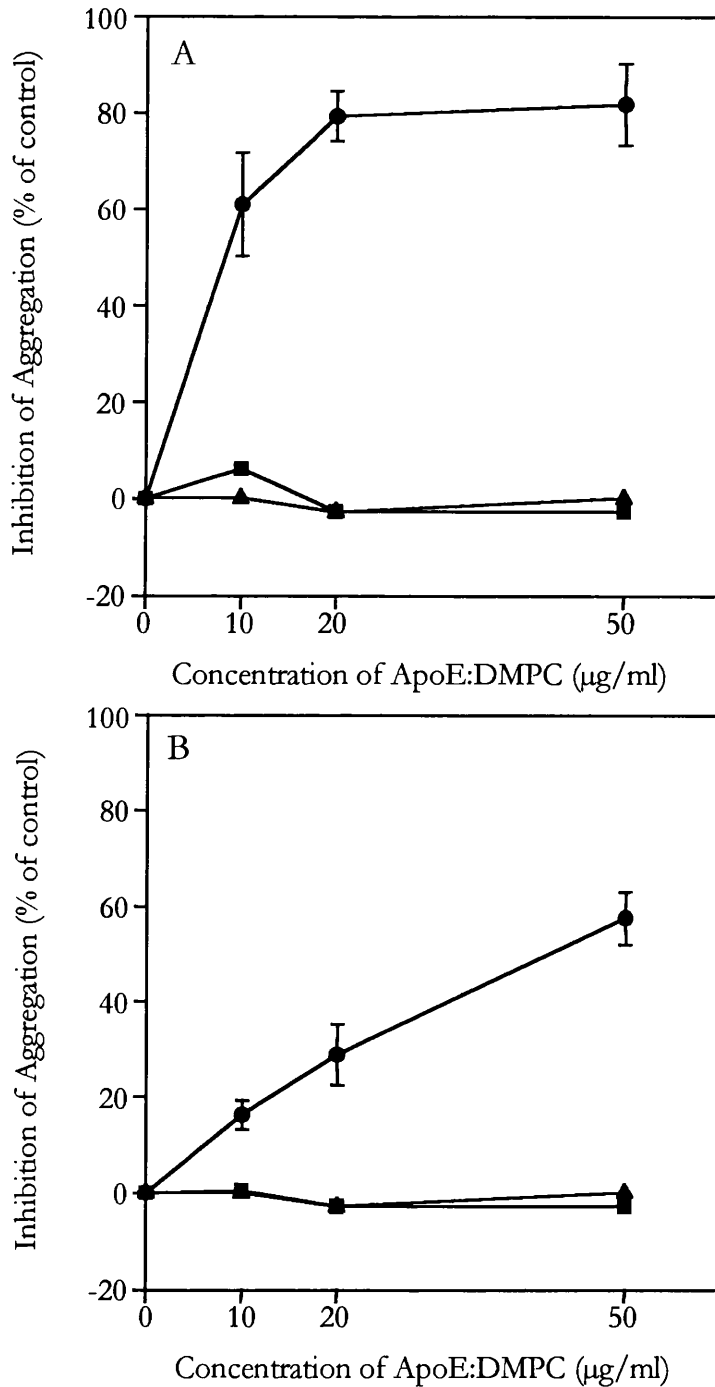


Figure 3.3-4 Inhibition of ADP-induced platelet aggregation by apoE:DMPC

Washed platelet (**Panel A**) or PRP (**Panel B**) preparations were pre-incubated with apoE:DMPC (●), free apoE (■) or DMPC vesicles alone (▲) for 30 s (washed platelets) or 10 min (PRP) at 37 °C. The extent of aggregation was measured 3 min after addition of a pre-determined threshold concentration of ADP (5-7 µM for washed platelets and 1-2 µM for PRP) and expressed as a percentage of controls with buffer alone. Points for apoE:DMPC are the mean percentage inhibition of aggregation (\pm SEM) for three different preparations tested on three separate platelet suspensions; other points represent at least two independent measurements.

3.3.5 EFFECTS OF APOE:DMPC ON PLATELET MORPHOLOGY.

To study the effects of apoE:DMPC on platelet morphology, PRP preparations in the presence or absence of apoE:DMPC were examined under the scanning electron microscope. The appearance of platelets without addition of agonist showed most of the cells in an inactivated state. The platelets were in single cell suspension and displayed the typical disc shape morphology (Figure 3.3-5, *panel A*). Addition of a threshold quantity of ADP induced a shape change from discs to spheres with the formation of many pseudopodia (Figure 3.3-5, *panel B*). Large clumps of aggregated platelets appeared, with many cells displaying a loss of single cell identity, indicative of irreversible aggregation. However, when PRP was pre-incubated with 50 µg protein/ml apoE:DMPC and then stimulated with ADP, only small clumps of aggregated platelets were observed. Indeed, many cells were not activated by the ADP and displayed a quiescent disc shape morphology (Figure 3.3-5, *panel C*). These data confirm the results obtained from the Born aggregometer and provide convincing evidence that apoE:DMPC is indeed a potent inhibitor of platelet activation.

3.3.6 EFFECTS OF PURIFIED HUMAN PLASMA APOE, HUMAN RECOMBINANT APOE AND RABBIT PLASMA APOE ON ADP-INDUCED PLATELET AGGREGATION.

The plasma concentration of human apoE is relatively low (30 - 60 mg/l), and represents about 1 - 2 % of total apolipoproteins [89, 90, 278], and almost half of this can be lost to the infranatant during conventional isolation of lipoproteins by ultracentrifugation [268]. This hampers the ready purification of large amounts of human apoE from plasma. Commercially available recombinant sources of human apoE-3 have helped alleviate this problem to certain degree. Unfortunately, this material is expensive, thus prohibiting its use in large quantities. An alternative source of apoE is from cholesterol-fed rabbits. Levels of apoE in cholesterol-fed animals can increase 10-fold [247], potentially allowing readier isolation of large amounts of the pure polypeptide. The primary structure of apoE has been determined in 10 species [89] and a high degree of sequence conservation exists, particularly in the receptor-binding region. Rabbit apoE is most homologous (~80 %) with human apoE-3 [89, 248], and it is suggested that the physical and physiological properties of this polypeptide may be similar to the human protein [248]. To determine whether these additional sources of apoE could be utilised to help define the molecular basis of platelet-apoE interactions, the anti-aggregatory effect of recombinant human apoE-3:DMPC and rabbit apoE:DMPC were compared with that of plasma purified human apoE-3:DMPC complexes.

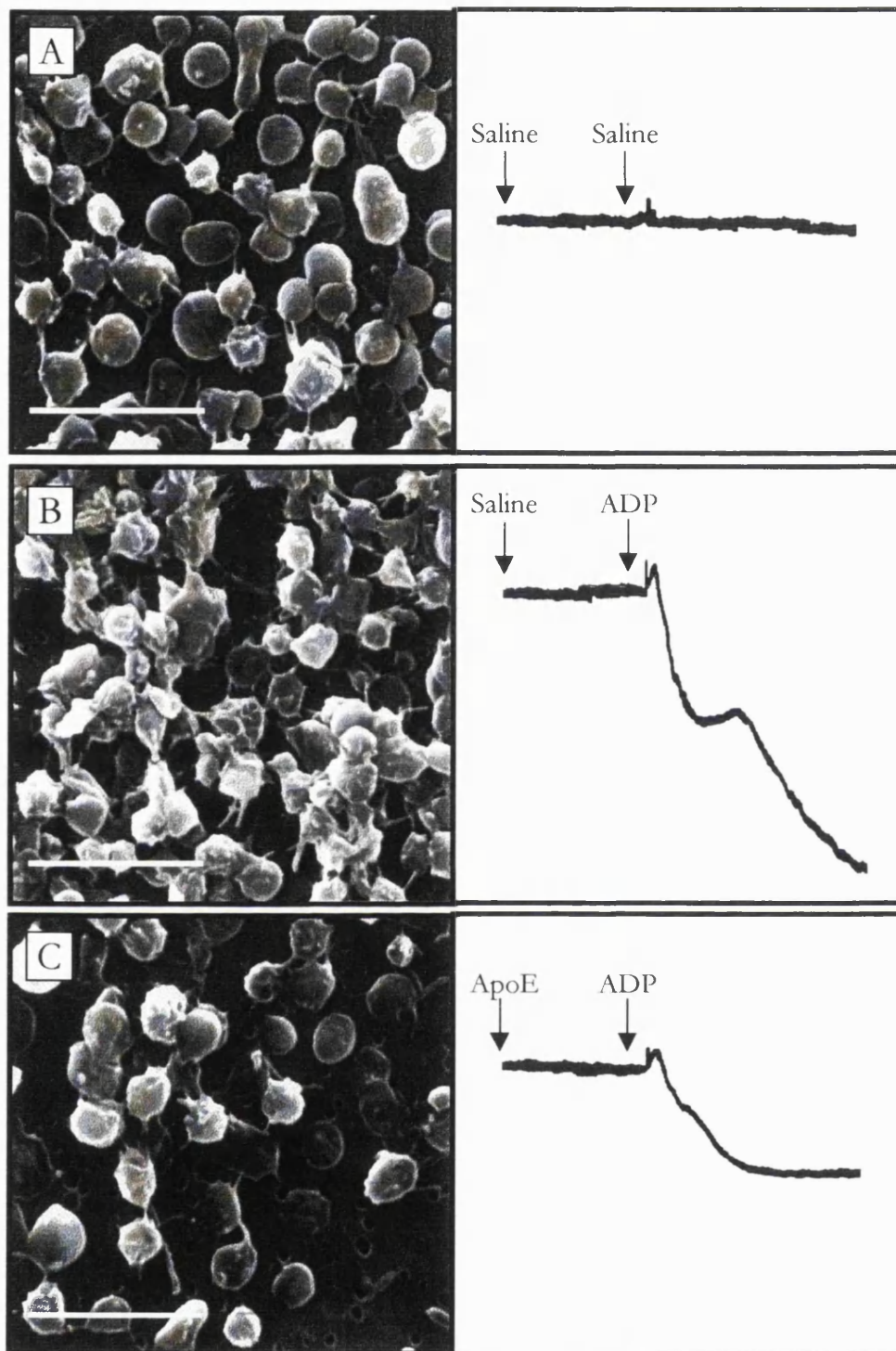


Figure 3.3-5 Scanning electron micrographs of PRP incubated in the presence or absence of apoE:DMPC.

Suspensions of PRP were incubated with buffer alone (panels A & B) or with 50 µg protein/ml apoE:DMPC (panel C) for 10 min at 37 °C. Three min after addition of either a saline control or a pre-determined threshold concentration of ADP (1-2 µM), the platelets were fixed in 3 % glutaraldehyde and prepared for scanning electron microscopy. The final magnification is $\times 5412$. The white bar represents 10 µm. The aggregation traces depict typical responses to the various treatments.

As expected, all the apoE:DMPC preparations inhibited platelet aggregation to a similar degree (plasma purified apoE-3; 69.8 ± 3.9 % versus human recombinant apoE-3; 72.5 ± 3.9 % versus rabbit apoE; 73.5 ± 0.8 % inhibition at $50 \mu\text{g}$ protein/ml apoE:DMPC, $P > 0.05$, $n = 3$, Figure 3.3-6). These results are consistent with the proposal that human and rabbit apoE have similar biological activities.

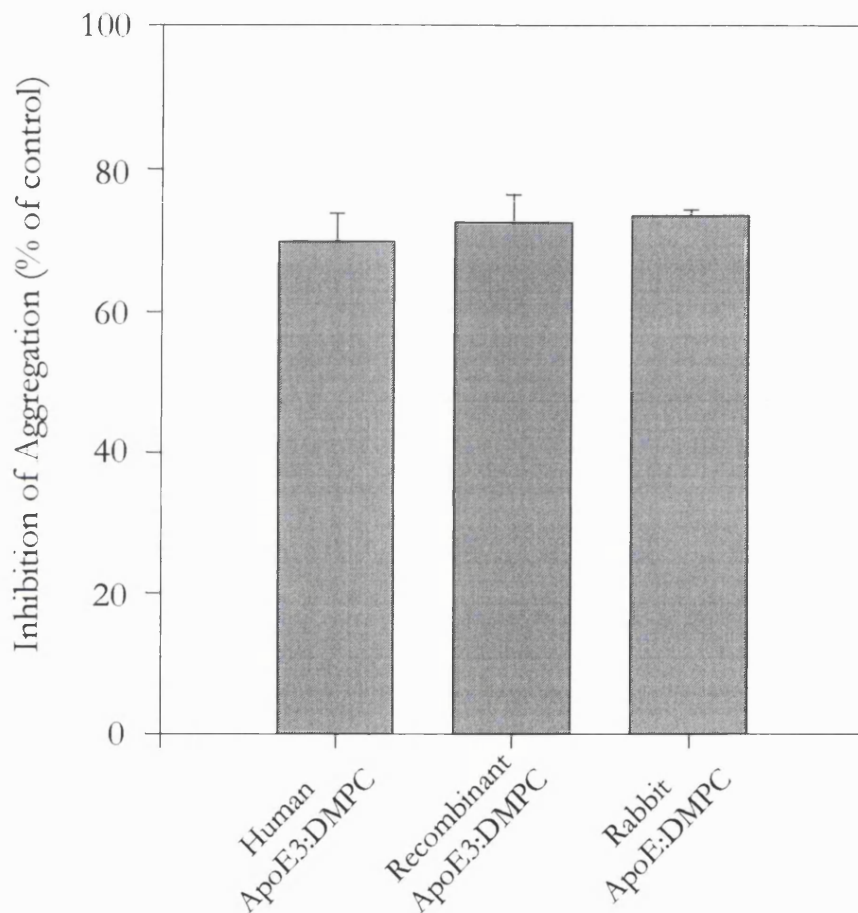


Figure 3.3-6 Human plasma apoE-3, recombinant human apoE-3 and rabbit plasma apoE all inhibit ADP-induced platelet aggregation.

Washed platelets (3×10^8 / ml) were pre-incubated with $50 \mu\text{g}$ protein/ml of either purified human plasma apoE-3, recombinant human apoE-3 or rabbit apoE complexed with DMPC for 30 s at 37°C and then threshold concentrations of ADP added ($5-7 \mu\text{M}$). Aggregation measurements were carried out in triplicate as described in section 2.5.7.

3.3.7 EFFECTS OF CHEMICALLY MODIFIED APOE:DMPC ON ADP-INDUCED PLATELET AGGREGATION.

Selective chemical modification of the arginine residues of apoE by cyclohexanedione (CHD) abolishes the ability of apoE to bind to its receptors [89, 252]. Recently, Desai et al. demonstrated that CHD-modified HDL-E was incapable of inhibiting platelet aggregation. They also showed that CHD-modified HDL-E could not bind to the platelet surface membrane [7]. In order to determine whether this effect was mediated via apoE, I treated apoE:DMPC vesicles with CHD and assessed the anti-platelet activity of these modified particles. In agreement with the results of Desai et al., CHD-apoE:DMPC was an ineffective inhibitor of ADP-platelet aggregation compared to its unmodified control ($-2 \pm 5\%$ versus $63 \pm 4\%$ inhibition, respectively; $P < 0.001$, Figure 3.3-7). These data imply that both HDL-E and apoE:DMPC particles are bound by the same specific receptor in the platelet membrane and that this receptor interacts with arginine residues of apoE. Additionally, the benign nature of CHD-apoE:DMPC suggests that it will be a good control in studies to characterise the molecular mechanisms for the apoE-induced inhibition of aggregation. An in-depth analysis of these results can be found in *Chapter 5 – Molecular Characterisation of a Human Platelet Receptor that Binds Apolipoprotein E*.

3.4 Conclusions.

The present study substantiates and expands on previous work implicating apoE as the active anti-platelet constituent of HDL-E. Indeed, this study has provided clear evidence that apoE, when complexed to phospholipid, is a potent inhibitor of agonist induced-platelet aggregation. It has been reported that platelet activation increases the prevalence [279] and incidence [280] of coronary heart disease and that macrophage produced apoE/phospholipid vesicles are potent anti-atherogenic particles [116, 199, 200, 203]. The intriguing possibility arises therefore, that inhibition of platelet activation by apoE may be an important regulatory process in the progression of atherosclerosis. Obviously, delineating the molecular basis for the anti-platelet effect of apoE is of fundamental importance in understanding this unique role for apoE. To that end, the preliminary observations outlined in this chapter have provided much of the experimental methodology required for defining the underlying inhibitory mechanism. Thus, the incubation times and doses of apoE:DMPC required for inhibition have been defined for both PRP and washed platelet preparations; abundant sources of biologically active apoE have been characterised; and a useful and benign control particle has been identified (CHD-apoE:DMPC). In the following chapter, these molecular tools have been utilised to further probe the anti-platelet effect of apoE.

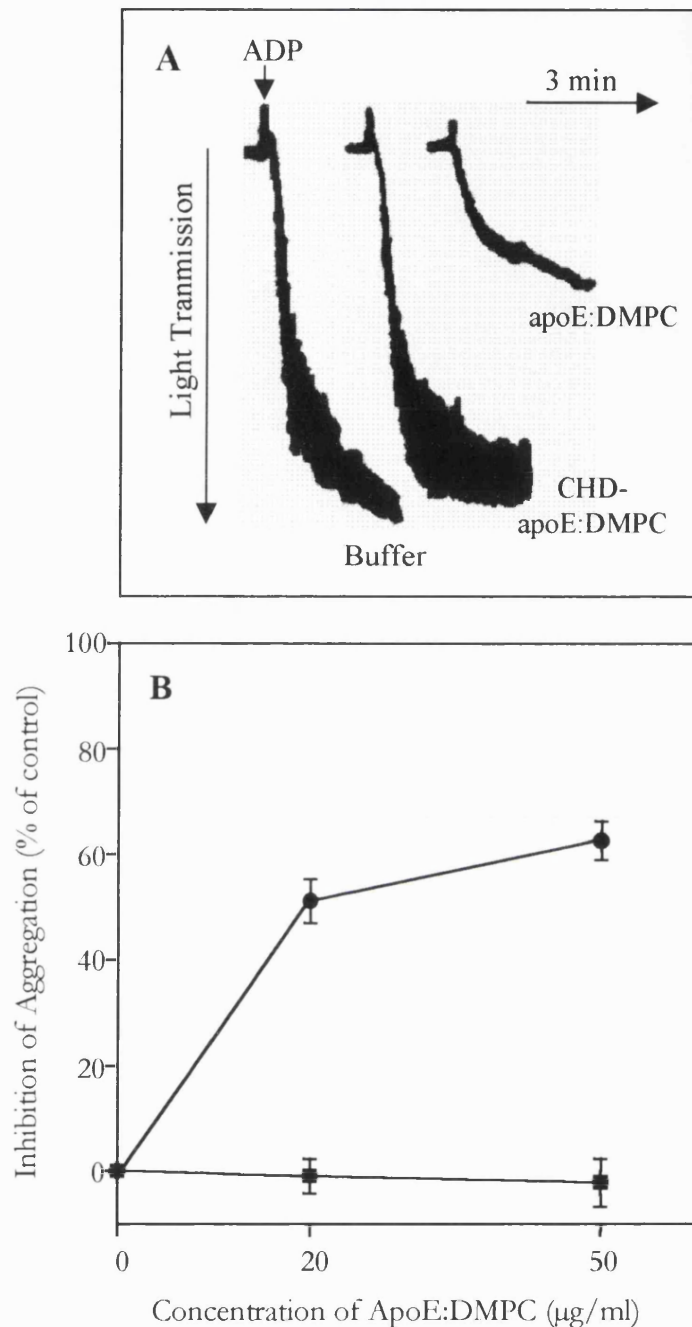


Figure 3.3-7 Failure of CHD-apoE:DMPC to inhibit ADP-induced platelet aggregation.

Panel A, washed platelets (3×10^8 cells/ml) were pre-incubated with CHD-apoE:DMPC or apoE:DMPC (both $50 \mu\text{g protein/ml}$) for 30 s and then threshold concentrations of ADP added ($5-7 \mu\text{M}$). The aggregation traces shown are from one representative experiment but were reproduced in two independent assays. **Panel B**, washed platelets were pre-incubated with apoE:DMPC (●) or CHD-apoE:DMPC (■) for 30 s at 37°C . The extent of aggregation was measured 3 min after addition of a pre-determined threshold concentration of ADP ($5-7 \mu\text{M}$) and expressed as a percentage of controls with buffer alone. Points are the mean percentage inhibition of aggregation (\pm SEM) for three different experiments.

Chapter 4

4. THE BIOCHEMICAL BASIS FOR INHIBITION OF PLATELET AGGREGATION BY APOLIPOPROTEIN E

4.1 Introduction.

The experiments outlined in *Chapter 3* gave convincing evidence that apoE:DMPC complexes are potent inhibitors of ADP-induced platelet aggregation. However, very little information was obtained concerning the molecular mechanism involved. In the initial report by Higashihara and colleagues, the anti-platelet activity of apoE:DMPC on collagen- and thrombin-induced aggregation was attributed to sequestration of cholesterol from the platelet plasma membrane [271]. On first inspection, this proposal is attractive. Cholesterol-deficient platelets are known to respond poorly to agonists [281]. Moreover, lipoprotein particles containing only apoE (γ -LpE) have recently been identified *in vivo* [107]. These particles have been characterised as major contributors of the reverse cholesterol pathway, mainly because they possess a strong capacity for removing cholesterol from the plasma membrane of cells [107, 189, 190, 282]. However, this effect seems an unlikely explanation for the inhibitory effect of apoE:DMPC on ADP-mediated aggregation since the platelet responsiveness to this agonist is relatively unaffected by cholesterol depletion [281].

An alternative explanation is that the anti-platelet action of apoE is mediated through a receptor-linked stimulation of platelet second messengers. Two important control elements involved in the suppression of platelet activation are the cyclic nucleotides, cAMP and cGMP, and agents that increase their intraplatelet levels, exert anti-aggregatory effects both *in vitro* and *in vivo*. For example, PGI₂ and adenosine limit platelet activation by raising cAMP [58, 59], while NO and several other nitroso compounds have a similar restrictive effect by increasing cGMP [283, 284]. In this chapter, I investigated whether the inhibitory action of apoE:DMPC might reflect its ability to sequester cholesterol from the platelet membrane, as well as its ability to stimulate cyclic nucleotide signalling within the platelet.

4.2 Specialised Materials and Methods.

4.2.1 MATERIALS.

N^G -nitro-L-arginine methyl ester (L-NAME), N^G -monomethyl-L-arginine (L-NMMA), D-NMMA, S-nitroso-L-glutathione (GSNO) and 1*H*-[1,2,4]oxadiazolo[4,3-*a*]quinoxalin-1-one (ODQ) were supplied by Alexis Corporation Ltd (Nottingham, UK). 3-isobutyl-1-methyl-xanthine (IBMX), diphenyleneiodonium chloride (DPI) and 2-ethylisothiopseudourea (Ethyl-ITU) were obtained from Calbiochem-Novabiochem Ltd. (Nottingham, UK). All other chemicals unless otherwise stated were supplied by Sigma Chemical Co.

4.2.2 APOE:DMPC COMPLEXES.

ApoE:DMPC and CHD-apoE:DMPC were prepared as outlined in *Chapter 3* and were extensively dialysed against Tyrode's buffer before use.

4.2.3 PREPARATION OF [3 H]CHOLESTEROL-LABELLED PLATELETS.

A [3 H]cholesterol-albumin emulsion was prepared as follows: a solution of 5 % HSA (w/v) in phosphate buffered saline (PBS, pH 7.4) was heated at 56 °C for 30 min. The solution was centrifuged (500 *g* for 15 min), 1 ml of supernatant was transferred into a clean glass tube and its contents were weighed. Five μ Ci of [3 H]cholesterol was transferred into a clean tube and the storage solvent evaporated under nitrogen. The [3 H]cholesterol was redissolved in 100 μ l acetone and added drop-wise into the vortexing HSA solution. The tube was placed in a 20 °C water bath and the acetone evaporated under a stream of nitrogen. The tube was vortexed after 10 min and 20 min. After 30 min the tube and contents were reweighed and the amount of water lost was added back drop-wise whilst vortexing. The [3 H]cholesterol-albumin emulsion was now ready to use. Platelets were pelleted from PGI₂-stabilised PRP, resuspended in the [3 H]cholesterol-albumin emulsion for 1 h and treated again with PGI₂ (300 nM). The mixture was then diluted 50-fold with Tyrode's buffer, centrifuged at 750 *g* for 20 min and the platelet pellet resuspended in buffer. The platelets were left to recover from the effects of PGI₂ and were used immediately for cholesterol-depletion studies.

4.2.4 CHOLESTEROL REMOVAL STUDIES.

Aliquots of [3 H]cholesterol-labelled platelet suspensions (600 μ l, 3×10^8 cells/ml) were incubated in the aggregometer with buffer, apoE:DMPC or CHD-apoE:DMPC at 37 °C. At defined time intervals up to 10 min, a portion (100 μ l) was removed, rapidly

centrifuged (12000 *g* for 30 s) and the [³H]cholesterol released into the supernatant (80 μ l) was measured by liquid scintillation counting. In addition, at zero-time an aliquot of the total platelet suspension (100 μ l) was dissolved in 1 M NaOH, neutralised and counted similarly. The percentage cholesterol released into the supernatant was determined by the following equation:

$$(\text{dpm released into the supernatant/dpm in the total platelet suspension}) \times 100$$

4.2.5 PLATELET AGGREGATION.

PRP or washed platelets (80 μ l) were pre-incubated with Tyrode's buffer (20 μ l) for 10 min or 30 s, respectively. Aggregation was initiated by addition of increasing concentrations of ADP at 37 °C in a Payton dual-channel aggregometer fitted with 0.1 ml cuvettes. The "threshold" concentration of ADP was determined (usually 3 – 7 μ M) and was used in subsequent experiments in which the Tyrode's buffer was replaced by free apoE, apoE:DMPC, CHD-apoE:DMPC, DMPC liposomes alone or GSNO at increasing concentrations. In experiments using NOS inhibitors, PRP was pre-incubated for 10 min at 20 °C with 300 μ M of the chemical analogues of L-arginine, L-NMMA or L-NAME or with 100 nM of haemoglobin. In the other inhibitory experiments, PRP was pre-incubated with 100 nM DPI, 3 μ M Ethyl-ITU or 10 μ M methylene blue for 1 min at 37 °C before addition of ADP. To examine effects of the SGC inhibitor, ODQ, washed platelets (3×10^8 /ml) were pre-incubated at 20 °C with 100 nM ODQ for 30 min before addition of either 200 nM GSNO or 50 μ g protein/ml apoE:DMPC.

4.2.6 CYCLIC NUCLEOTIDE ASSAYS.

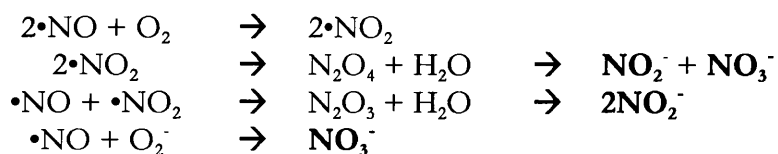
Intraplatelet cGMP and cAMP concentrations were measured in PRP with and without a 10 min pre-incubation at 20 °C with the PDE inhibitor, IBMX (1 mM). Aggregation was terminated after 3 min by addition of 40 μ l of 20 % (v/v) HClO₄. The samples were then neutralised with 1.08 M K₃PO₄ (80 μ l), centrifuged (2000 *g* for 15 min at 4 °C) and after acetylation were assayed for cGMP and cAMP contents by commercial radioimmunoassay kits (Amersham International plc, Buckinghamshire, UK). All samples were corrected for the cGMP and cAMP content of PPP.

4.2.7 NO SYNTHASE ASSAYS.

A comprehensive review of all the methods outlined in this section can be found in "*Nitric Oxide in Health and Disease*" [65].

4.2.7.1 Nitrite/Nitrate Assay.

NO undergoes a series of reactions with several molecules present in biological fluids. These include:



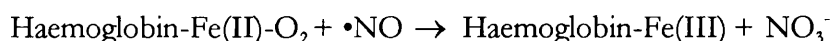
The final products of NO degradation *in vivo* are nitrite (NO_2^-) and nitrate (NO_3^-). The relative proportion of NO_2^- and NO_3^- is variable and cannot be predicted with certainty. Thus, the best index of total NO production is the sum of both NO_2^- and NO_3^- . These stable products can be detected using a discontinuous spectrophotometric assay. In the first instance, NO_3^- must be reduced to NO_2^- using nitrate reductase (*Aspergillus* species). Total NO_2^- can then be directly detected by observing the magenta-coloured azo dye that is formed from NO_2^- and the Griess reagent.

Procedure.

$\text{NO}_2^-/\text{NO}_3^-$ produced by the platelet was measured in PRP \pm 10 min pre-incubation with apoE:DMPC (20 μg - 200 $\mu\text{g}/\text{ml}$, 20 $^\circ\text{C}$). Aggregation was initiated with “threshold” quantities of ADP. After 3 min, aggregation was terminated by a rapid centrifugation (12000 g for 10 s). Eighty μl of the platelet supernatant was removed and total nitrate and nitrite levels were measured using a commercial $\text{NO}_2^-/\text{NO}_3^-$ assay kit (Alexis Corporation Ltd, Nottingham, UK). Briefly, several dilutions of a NO_3^- standard (NaNO_3) were prepared in 96-well plate. A typical standard curve in the range of 0 - 20 μM NO_3^- , in a final volume of 80 μl , was freshly prepared each time the assay was performed. The triplicate unknown samples were transferred to a 96-well plate. To each well, 10 μl of the supplied enzyme co-factor mixture was added, followed by 10 μl of the nitrate reductase mixture. The plate was covered and incubated for 3 h, at room temperature. Fifty μl of Griess reagent 1 (sulphanilamide) was then added, followed immediately by 50 μl of Griess reagent 2 (N-(1-Naphthyl)ethylenediamine). The colour was allowed to develop for 10 min at room temperature. The OD_{540} was measured using a Titertek Multiskan MCC/340 plate reader. OD_{540} versus concentration of standards was plotted and the unknown samples determined from the standard curve. All samples were corrected for the $\text{NO}_2^-/\text{NO}_3^-$ content of PPP.

4.2.7.2 Haemoglobin Assay.

The haemoglobin assay is a simple, continuous assay based on the direct reaction of NO and the oxygenated, ferrous form of haemoglobin (HbO₂), which yields the ferric form, methaemoglobin (metHb) and NO₃⁻. The reaction scheme is illustrated below:



The oxidation of HbO₂ is stoichiometric with NO and occurs at a rate that is faster than the reaction between molecular oxygen and NO. Consequently, the formation of NO can be reported as the consumption of HbO₂. The concentration of HbO₂ in a given solution is calculated using the following equation:

$$[\text{HbO}_2] \text{ (}\mu\text{M)} = [1.013 (\text{OD}_{576}) - 0.3269 (\text{OD}_{630}) - 0.7353(\text{OD}_{560})] \times 10^2$$

Procedure.

NO secreted into the supernatant was measured in washed platelets (final concentration of 3×10^8 cells/ml), since plasma absorbs strongly in the 550 nm - 650 nm range. Human A₀ ferrous HbO₂ was prepared in 100 mM HEPES (pH 7.5) as an 8 mg/ml solution (~180 μM) and quickly frozen at -80 °C in small aliquots. The following assay tubes were prepared:

Stock washed platelets (final concentration 3×10^9 /ml)	125 μl
Stock HbO ₂ solution (final concentration 3.6 μM)	5 μl
Tyrode's buffer	} 100 μl
or apoE:DMPC (final concentration 50 μg/ml)	
or GSNO (final concentration 2.5 μM)	

A control tube containing only buffer and HbO₂ was also prepared.

Following a 10 min incubation, at room temperature, Tyrode's buffer ± "threshold" ADP were added to give a final volume of 250 μl. After 3 min, aggregation was terminated by a rapid centrifugation (12000 g for 10 s). The platelet supernatant was then removed and diluted to 1 ml in Tyrode's buffer. The absorbance of each sample was measured at 560 nm, 576 nm and 630 nm and the concentration of HbO₂ consumed (relative to control) was calculated.

4.2.7.3 The Citrulline Assay.

Measuring NOS activity by monitoring the stoichiometric conversion of L-arginine to L-citrulline (and NO) is currently the standard assay for NOS activity in both crude and purified enzyme preparations. The use of a radioactive substrate (L-[³H]arginine), allows detection of pmol levels of conversion. The citrulline assay is a discontinuous assay that uses a small cation-exchange resin to separate radiolabelled citrulline from arginine. Before initiating the enzyme assay, it is essential to verify if the equilibrated resin effectively retains the radioactive L-arginine substrate, otherwise a high blank value for the liquid scintillation counting will greatly reduce the sensitivity of the assay. Greater than 95 % of the applied radioactivity should be retained by the resin. This represents a relatively low blank value. If more than 5 % of the radioactivity flows through the resin, the L-arginine must be purified before conducting the assay. Also, [³H]arginine is prone to radiolytic decay and must be purified every 2 months.

Purification of L-[³H]Arginine.

A disposable spin column was packed with 0.5 ml of Dowex AG 50W-X8 (Na⁺ form) cation exchange resin which had been equilibrated in 50 mM HEPES, pH 5.5 containing 5 mM EDTA. One hundred μ Ci of L-[³H]arginine was applied to this resin and the resin washed with 5 ml of distilled water. The pure L-[³H]arginine was eluted with two 2 ml washes of 0.5 M ammonium chloride and then lyophilised. The L-[³H]arginine was resuspended in 2 % (v/v) ethanol.

Intact Platelet Preparation.

Washed platelets were pelleted from PGI₂-stabilised PRP, resuspended in 1 ml Tyrode's buffer containing L-[³H]arginine (7.25 nM; 0.1 μ Ci) for 1 h and treated again with PGI₂ (300 nM). The mixture was then diluted 50-fold with Tyrode's buffer, centrifuged at 750 g for 20 min and the platelet pellet resuspended in buffer. The platelets were left to recover from the effects of PGI₂ and were used immediately for NOS measurements. The platelets (3 x 10⁸ cells/ml) were incubated for 10 min \pm apoE:DMPC liposomes (50 μ g protein/ml) in a final volume of 200 μ l. They were then stimulated with a "threshold" quantity of ADP for 3 min. The reaction was stopped with 1 ml of ice-cold NOS stop buffer (50 mM HEPES, pH 5.5 containing 5 mM EDTA and 5 mM L-NAME) and then centrifuged at 12000 rpm for 10 s. The supernatant was discarded and the pellet disrupted by adding 800 μ l of 20 % (v/v) HClO₄; the samples were then neutralised with 3 M K₃PO₄ (500 μ l) and centrifuged (2000 g for 15 min at 4 °C). The supernatant was either directly counted for total [³H] measurements or applied to a 2 ml column of Dowex AG 50W-X8

(Na⁺ form). The column was eluted with 2 x 3 ml water washes. The L-[³H]citrulline in the eluate was measured by liquid scintillation counting. Non-enzymatic formation of L-[³H]citrulline was controlled for by addition of the specific NOS inhibitor, L-NAME (1 mM), to a parallel set of tubes. The percentage conversion of L-[³H]arginine to L-[³H]citrulline was calculated as follows:

$$(\text{dpm eluted from resin}/\text{dpm in the total platelet suspension}) \times 100$$

Lysed Platelet Preparations.

Washed platelets (10^9 cells) were incubated with or without apoE:DMPC (50 µg protein/ 3×10^8 cells) for 10 min at 37 °C in a final volume of 1 ml. The reaction was stopped by addition of 100 µl of 10x homogenisation buffer (250 mM Tris.HCl, pH 7.4 containing 10 mM EDTA and 10 mM EGTA). The cells were pelleted in a microfuge for 30 s, resuspended in 75 µl of 1 x homogenisation buffer and lysed by two cycles of freezing in liquid nitrogen and thawing on ice. NOS activity was measured by the conversion of L-[³H]arginine to L-[³H]citrulline using the NOSdetect assay kit (Alexis) and expressed as pmol/h/ 10^9 platelets. Briefly, 50 µl of platelet extract was incubated with 50 µl of substrate buffer (50 mM Tris.HCl, pH 7.4 containing 1 mM NADPH, 6 µM tetrahydrobiopterin, 2 µM FAD, 2 µM FMN, 0.2 µM calmodulin, 1.2 mM CaCl₂ and 0.1 µCi L-[³H]arginine) for 1 h at 37 °C. The reaction was terminated by addition of 400 µl stop buffer (50 mM HEPES, pH 5.5 containing 5 mM EDTA) and 100 µl of cationic resin (Dowex AF 50W-X8). The Ca²⁺ dependency of platelet NOS was determined in a parallel set of experiments in which the CaCl₂ was omitted. The mixture was transferred to a spin filter, micro-centrifuged for 30 s and the L-[³H]citrulline in the eluate was measured by liquid scintillation counting. Non-enzymatic formation of L-[³H]citrulline was controlled for by addition of 1 mM L-NAME to a parallel set of tubes.

4.3 Results.

4.3.1 ABILITY OF APOE:DMPC TO REMOVE CHOLESTEROL FROM PLATELET MEMBRANES.

Incubation of washed [^3H]cholesterol-labelled platelets with apoE:DMPC (50 μg protein/ml) or CHD-apoE:DMPC (50 μg protein/ml) released similar amounts of cholesterol as a function of time. This corresponded to less than 1 % after my standard 30 s pre-incubation period and only about 2 % after a further 3 min when aggregation studies would be completed (Figure 4.3-1, *panel A*). ADP-induced aggregation was initiated in parallel incubations to monitor anti-platelet effects of apoE:DMPC (for the experiment, the inhibition of aggregation was between 60 - 70 %). However, in agreement with *Chapter 3*, CHD-apoE:DMPC was an ineffective inhibitor of platelet aggregation (-2 to 3 % inhibition) compared to its unmodified control. Neither free apoE (100 μg protein/ml) nor DMPC (375 μg phospholipid/ml) removed significant amounts of cholesterol from the platelets compared to the apoE:DMPC complex (Figure 4.3-1, *panel B*). The above data implies that an alternative mechanism to cholesterol sequestration exists.

4.3.2 EFFECTS OF APOE:DMPC ON INTRAPLATELET cGMP AND cAMP LEVELS.

Because attenuation of platelet responsiveness is frequently accomplished by changes in intraplatelet cGMP or cAMP levels [32], I measured the influence of apoE on these cyclic nucleotides during ADP-induced aggregation of PRP. The basal levels of platelet cGMP and cAMP (3.7 ± 1.1 and 11.7 ± 1.9 pmol/ 10^9 platelets, respectively, Figure 4.3-2; *panels A & C*) were not significantly altered by incubation with 50 μg protein/ml of apoE:DMPC vesicles (1.9 ± 0.7 and 9.5 ± 1.5 pmol/ 10^9 platelets, respectively; Figure 4.3-2, *panels A & C*). However, in the presence of threshold concentrations of ADP, the same apoE:DMPC complexes produced marked dose-dependent increases in both cGMP (33.9 ± 3.2 versus 13.6 ± 1.5 pmol/ 10^9 platelets at 50 μg protein/ml apoE:DMPC; $P < 0.001$, $n = 3$; Figure 4.3-2, *panel B*) and cAMP (23.5 ± 3.3 versus 7.4 ± 1.1 pmol/ 10^9 platelets at 50 μg protein/ml apoE:DMPC, $P < 0.001$, $n = 3$; Figure 4.3-2, *panel D*). These correlated with the observed concomitant inhibition of aggregation after 3 min ($r = 0.85$ for cGMP; Figure 4.3-3, *panel A*, and 0.81 for cAMP; Figure 4.3-3, *panel B*; both $P < 0.01$, $n = 10$). No significant changes in cGMP levels were noted with CHD-apoE:DMPC, free apoE or DMPC alone (Table 4.3-1).

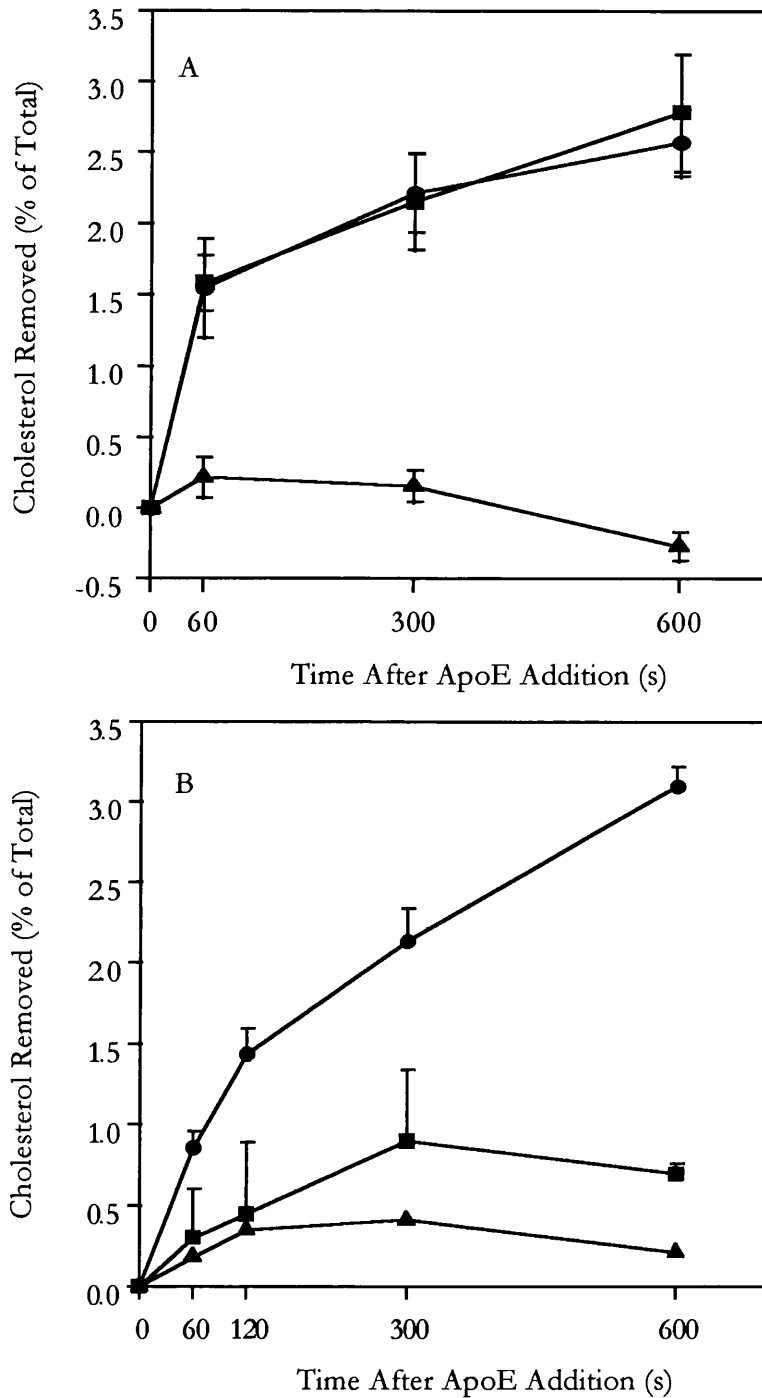


Figure 4.3-1 Release of cholesterol from platelet membranes by apoE:DMPC as a function of time.

Panel A, [^3H]cholesterol-labelled platelet suspensions were incubated with 50 μg protein/ml of apoE:DMPC (●), CHD-apoE:DMPC (■) or with buffer alone (▲). **Panel B**, [^3H]cholesterol-labelled platelet suspensions were incubated with 100 μg protein/ml apoE:DMPC (●), 375 μg phospholipid/ml DMPC liposomes (■) or 100 μg protein/ml free apoE (▲). Results (mean \pm SEM of three separate experiments) are expressed as a percentage of the initial cell [^3H]cholesterol which was released to the test acceptors in the media.

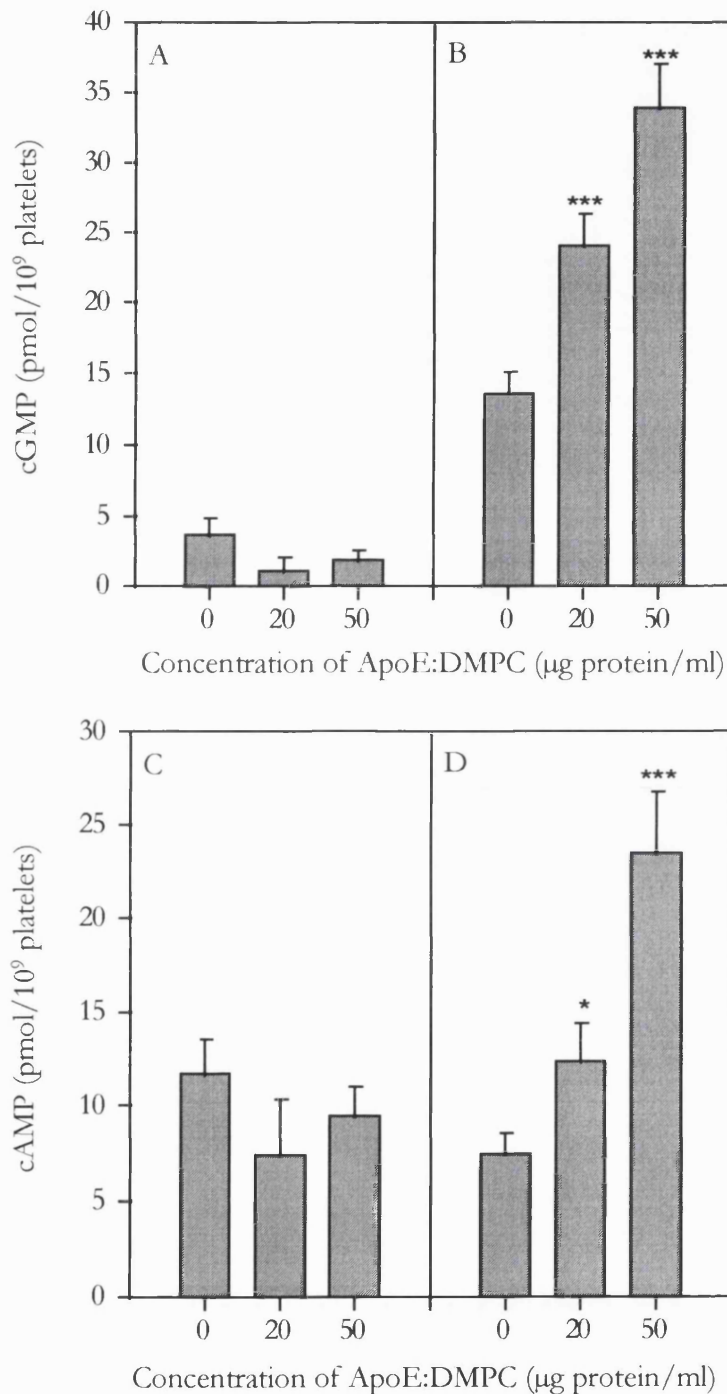


Figure 4.3-2 ApoE:DMPC complexes increase intraplatelet cGMP and cAMP levels in a dose-dependent manner but only in the presence of ADP.

PRP ($2-3 \times 10^8$ cells/ml) was pre-incubated with 20 or 50 µg protein/ml of apoE:DMPC for 10 min at 20 °C. The samples were transferred to an aggregometer (37 °C, 900 rpm). Buffer (**panels A & C**) or "threshold" quantities of ADP (1-2 µM) (**panels B & D**) were added and after a further 3 min incubation the platelets were immediately processed for cGMP and cAMP measurements. Results are expressed as mean \pm SEM of three separate experiments. The difference between the means (\pm apoE) was assessed by Student's *t*-test. * $P < 0.05$, *** $P < 0.001$.

Sample	0 µg/ml	20 µg/ml	50 µg/ml
apoE:DMPC	13.6 ± 1.54	24.0 ± 2.3***	33.9 ± 3.1***
CHD-apoE:DMPC	“	16.3 ± 4.0	14.4 ± 2.6
free apoE	“	19.7 ± 4.8	18.3 ± 5.3
DMPC alone	“	16.6 ± 3.0	14.7 ± 3.3

Table 4.3-1 CHD-apoE:DMPC, free apoE or DMPC alone do not increase intraplatelet cGMP levels.

PRP ($2-3 \times 10^8$ cells/ml) was pre-incubated with 0, 20 or 50 µg protein/ml of apoE:DMPC, CHD-apoE:DMPC and free apoE or with DMPC vesicles (0, 75 or 187.5 µg phospholipid/ml) for 10 min at 20 °C. The samples were transferred to an aggregometer (37 °C, 900 rpm), “threshold” quantities of ADP (1-2 µM) added and after a further 3 min incubation the platelets were immediately processed for cGMP content. The results given as pmol cGMP/ 10^9 platelets (\pm SEM) with the difference between the means (\pm apoE) assessed by Student's *t*-test. *** $P < 0.001$.

4.3.3 EFFECTS OF IBMX ON APOE:DMPC TREATED PLATELETS.

Levels of cGMP and cAMP are controlled directly by the activities of their synthesising enzymes, guanylate cyclase and adenylyate cyclase, respectively, and catabolising enzymes, cGMP and cAMP PDEs [52, 285]. When platelets were pre-incubated with the general PDE inhibitor, IBMX (1 mM) [286], cAMP levels in the presence of ADP were increased two-fold (14.8 ± 3.0 versus 7.4 ± 1.1 pmol/ 10^9 platelets; Figure 4.3-4, panel B) because of inhibition of platelet cAMP phosphodiesterase. Paradoxically, control levels of cGMP in the presence of ADP were diminished (2.6 ± 1.1 versus 13.6 ± 1.5 pmol/ 10^9 platelets; Figure 4.3-4, panel A). Importantly, however, apoE:DMPC vesicles (50 µg protein/ml) still elicited a dose-dependent rise in cGMP levels in the presence of IBMX (10.8 ± 0.8 versus 2.6 ± 1.1 pmol/ 10^9 platelets at 50 µg protein/ml apoE:DMPC; Figure 4.3-4, panel A). This indicated an apoE-induced increase in synthesis of this cyclic nucleotide rather than a decrease in its catabolism. By contrast, IBMX abolished the rise in cAMP (14.7 ± 3.4 versus 14.8 ± 3.0 pmol/ 10^9 platelets at 50 µg protein/ml apoE:DMPC; Figure 4.3-4, panel B).

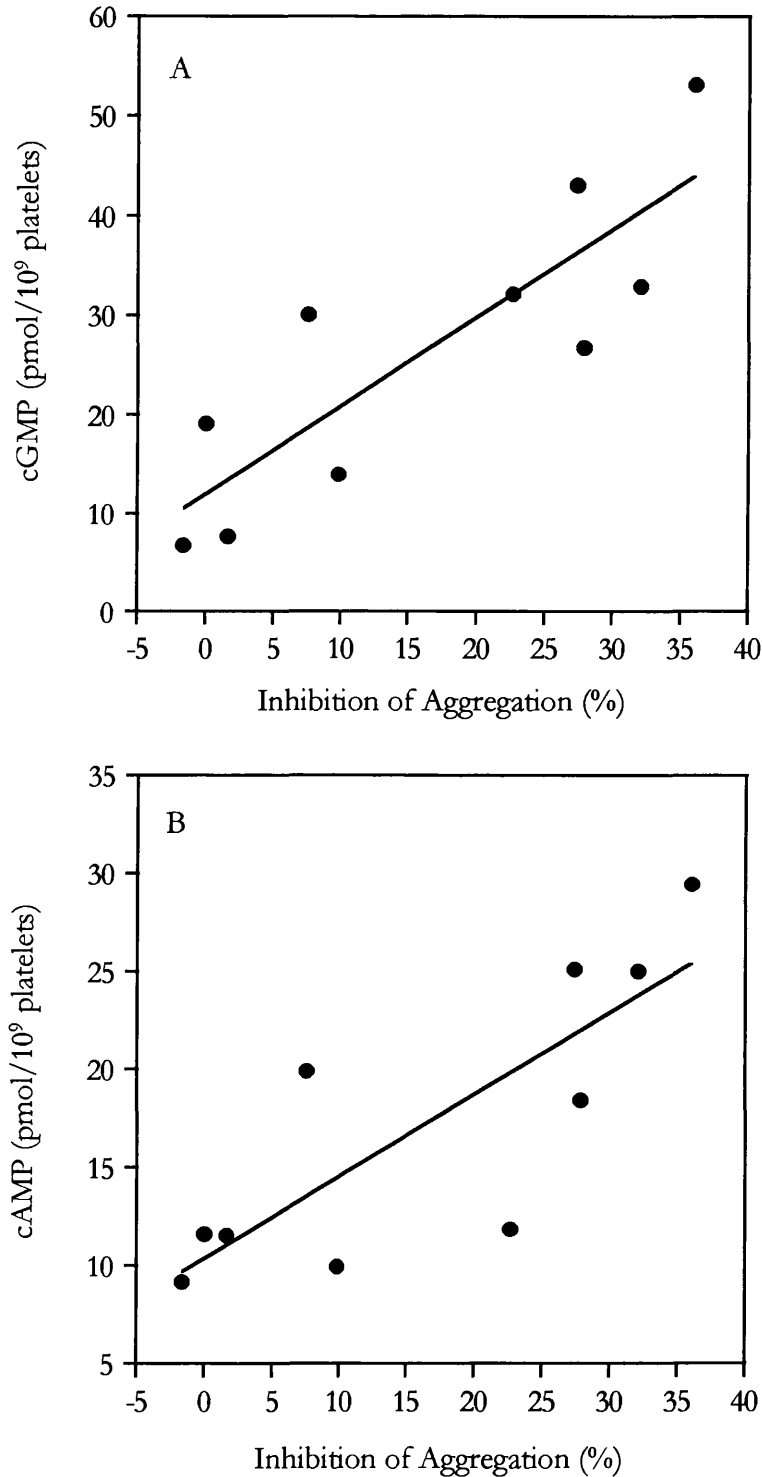


Figure 4.3-3 ApoE:DMPC induced increases of intraplatelet cGMP and cAMP levels correlate with the concomitant inhibition of aggregation.

PRP ($2-3 \times 10^8$ cells/ml) was pre-incubated with 0, 20 or 50 μg protein/ml of apoE:DMPC for 10 min at 20°C. Aggregation was initiated by addition of "threshold" concentration of ADP (1-2 μM) at 37°C and allowed to proceed for 3 min at which point the platelets were immediately processed for cGMP (**panel A**) and cAMP (**panel B**) measurements. Individual points were obtained from three separate experiments.

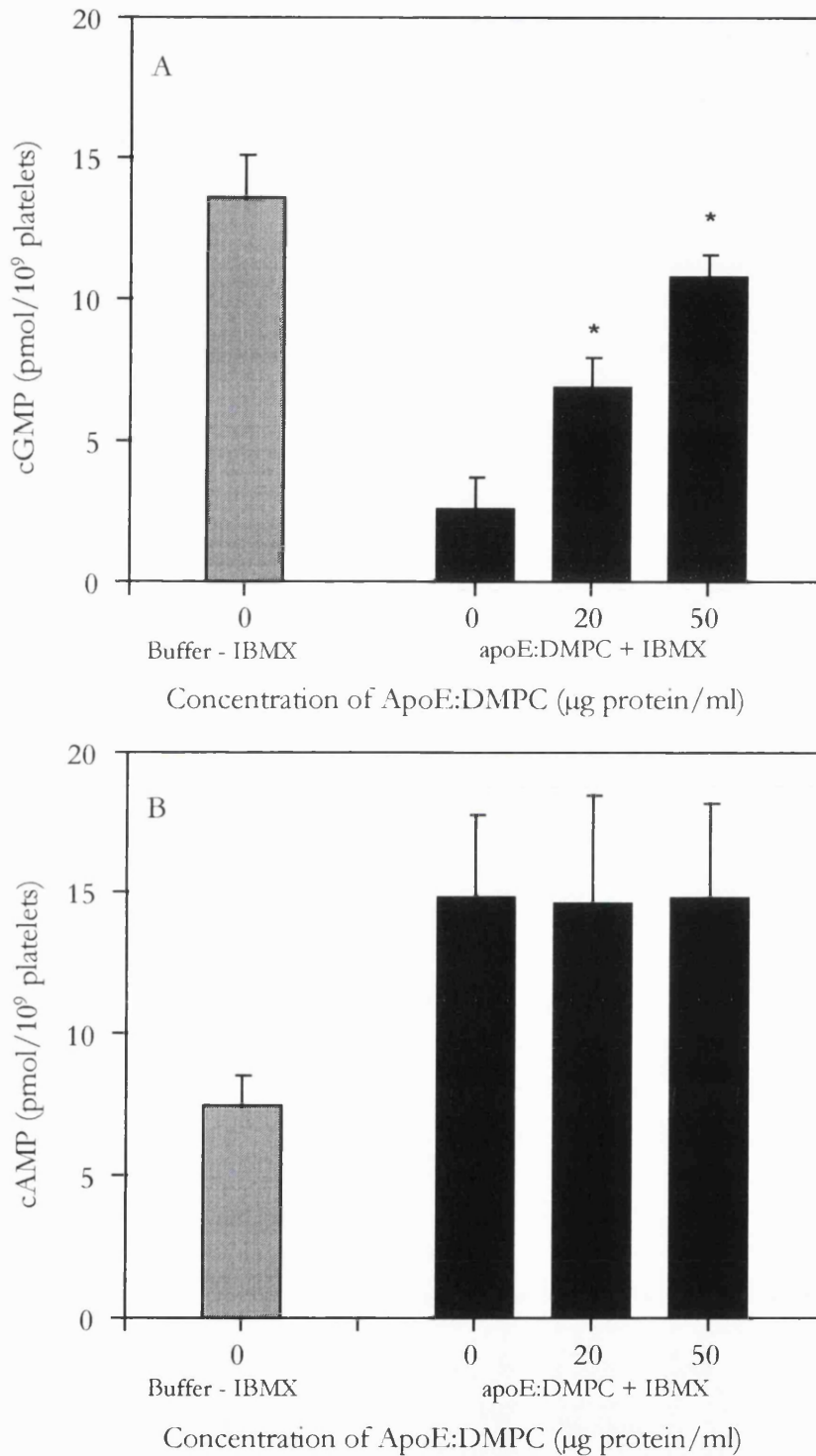


Figure 4.3-4 In the presence of IBMX, apoE:DMPC vesicles still elicited a dose-dependent rise in cGMP but not cAMP.

PRP ($2-3 \times 10^8$ cells/ml) was pre-incubated in the absence or presence of IBMX (1 mM) for 10 min and then incubated with 20 or 50 μg protein/ml of apoE:DMPC for 10 min at 20 °C. Aggregation was initiated by addition of "threshold" concentration of ADP (1-2 μM) at 37 °C and allowed to proceed for 3 min at which point the platelets were immediately processed for cGMP (**panel A**) and cAMP (**panel B**) measurements. Results are expressed as mean \pm SEM of three separate experiments. The difference between the means (\pm apoE) assessed by Student's *t*-test. *** $P < 0.001$. * $P < 0.05$.

4.3.4 EFFECTS OF THE NO DONOR, S-NITROSO-L-GLUTATHIONE, ON ADP INDUCED PLATELET AGGREGATION.

NO, S-nitrosothiols, and other NO donors activate intraplatelet SGC [287, 288]. This results in increased cGMP concentrations and inhibition of platelet aggregation [287, 289]. S-Nitroso-L-Glutathione (GSNO), an S-nitrosothiol, has been shown to be an extremely potent inhibitor of collagen-induced platelet aggregation [288]. However, no data exists on the *in vitro* effects of GSNO on ADP-stimulated aggregation. When washed platelets were pre-incubated for 30 s with GSNO, ADP stimulated aggregation was inhibited in a dose dependent manner (Figure 4.3-5). Indeed, ADP-induced aggregation was as sensitive to GSNO (IC_{50} value of 128 ± 28 nM) as that reported for collagen (IC_{50} value of 120 ± 4 nM) [288]. This implies that both collagen- and ADP-induced platelet aggregation are exquisitely sensitive to extracellular NO generation and thus intracellular cGMP production.

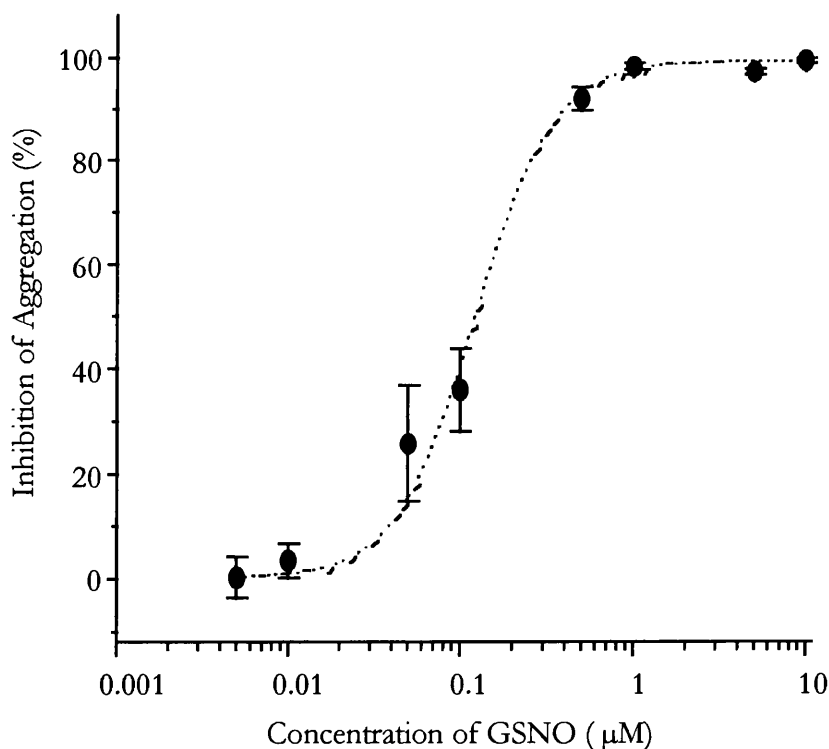


Figure 4.3-5 GSNO inhibits platelet aggregation in a dose dependent manner.

Aliquots of washed platelets ($3 \times 10^8/ml$) were pre-incubated with various concentrations of GSNO for 1 min at 37 °C. The extent of aggregation was measured 3 min after addition of a pre-determined threshold concentration of ADP (5-7 μ M) and expressed as a percentage of controls with buffer alone. Results are expressed as mean \pm SEM of three separate experiments. The IC_{50} was calculated using Microcal Origin software.

4.3.5 EFFECTS OF SOLUBLE GUANYLATE CYCLASE INHIBITORS ON APOE:DMPC TREATED PLATELETS.

Further support for cGMP having a pre-eminent role was obtained by use of SGC inhibitors. Methylene blue has been used as a selective inhibitor of SGC for a number of years [290] and indeed this reagent effectively reversed the anti-platelet effect of 20 µg protein/ml apoE:DMPC vesicles (Figure 4.3-6, *panel A*). However, this compound has been reported to inhibit PGI₂ production [291], generate superoxide anions [292], and directly inhibit NOS [293]. Recently, a more potent and specific inhibitor of SGC has been described; 1*H*-[1,2,4]oxadiazolo[4,3-*a*]quinoxalin-1-one (ODQ) [283, 294]. This reagent not only impaired the anti-platelet action of the NO donor, GSNO, but also efficiently blocked the anti-aggregatory effect of 50 µg protein/ml apoE:DMPC vesicles (7.5 ± 8.9 versus 68.7 ± 4.4 % inhibition; $P < 0.001$, $n = 3$; Figure 4.3-6, *panel B*). This agent also blocked the apoE:DMPC- and GSNO-induced rise in intraplatelet cGMP levels (Figure 4.3-7).

4.3.6 EFFECTS OF NOS INHIBITORS ON THE AGGREGATION OF APOE:DMPC TREATED PLATELETS

One important cellular mechanism for up-regulation of cGMP is through stimulation of NOS [295, 296]. This enzyme acts on L-arginine to produce NO, which then activates heme-containing SGC, its physiological target [67, 297]. When I pre-incubated platelets with L-NMMA or L-NAME, the chemical analogues of L-arginine and competitive inhibitors of NOS [295, 296], the anti-platelet action of apoE:DMPC vesicles was found to be essentially blocked (Figure 4.3-8, *panel A*). These inhibitory reactions were enantiomer-specific since D-NMMA was ineffective. Moreover, two additional inhibitors of NOS, Ethyl-ITU [298, 299] and DPI [300], also reversed the anti-platelet effect of apoE (Figure 4.3-8, *panel B*) while having no discernible effect on platelet aggregation themselves. Finally, haemoglobin, a competitor for NO binding to guanylate cyclase [301], also suppressed the anti-aggregatory effect of apoE:DMPC (Figure 4.3-8, *panel A*).

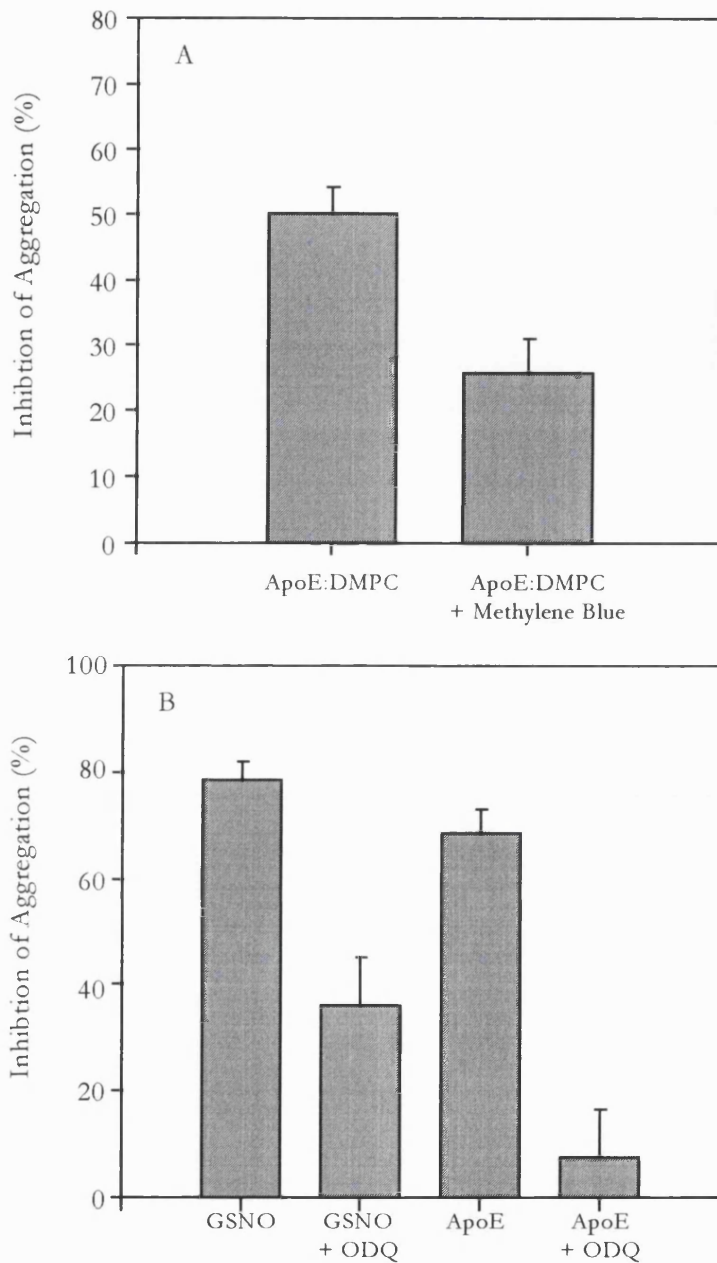


Figure 4.3-6 SGC inhibitors prevent the anti-aggregatory action of apoE:DMPC complexes.

Panel A, aliquots of PRP ($2-3 \times 10^8$ cells/ml) were pre-incubated with $10 \mu\text{M}$ methylene blue for 10 min at 20°C and then for a further 10 min with $20 \mu\text{g}$ protein/ml apoE:DMPC. The extent of aggregation was measured 3 min after addition of a pre-determined threshold concentration of ADP ($1-2 \mu\text{M}$) and expressed as a percentage of controls with buffer alone. Results are expressed as mean \pm SEM of three separate experiments. **Panel B**, aliquots of washed platelets (3×10^8 /ml) were pre-incubated with 100 nM ODQ for 30 min at 20°C and then for a further 1 min at 37°C with either buffer, apoE:DMPC ($50 \mu\text{g}$ protein/ml) or, as a positive control, the NO donor, GSNO (200 nM). The extent of aggregation was measured 3 min after addition of a pre-determined threshold concentration of ADP ($5-7 \mu\text{M}$) and expressed as a percentage of controls with buffer alone. Results are expressed as mean \pm SEM of three separate experiments.

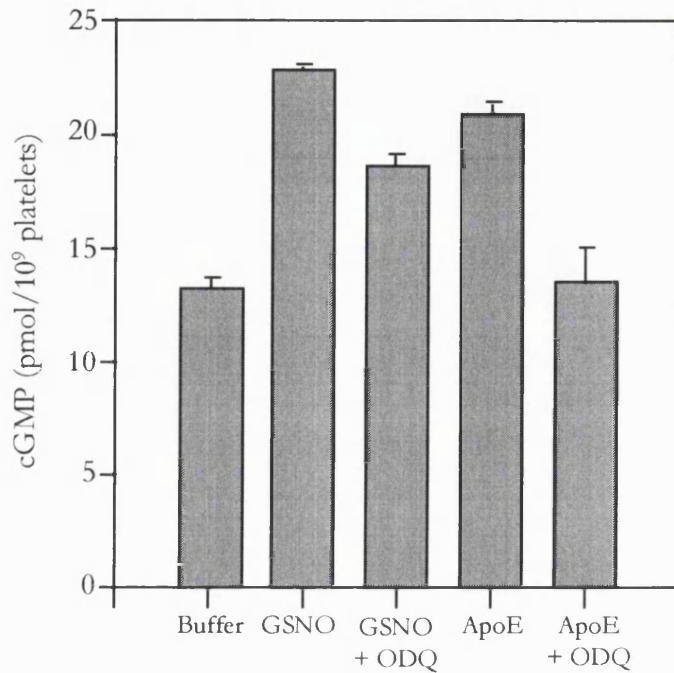


Figure 4.3-7 SGC inhibitors prevent cGMP increases induced by apoE:DMPC complexes.

Aliquots of washed platelets (3×10^8 cells/ml) were pre-incubated with 100 nM ODQ for 30 min at 20 °C. Then for a further 1 min at 37 °C with either buffer, apoE:DMPC (50 µg protein/ml) or, as a positive control, the NO donor, GSNO (200nM). Aggregation was initiated by addition of “threshold” concentration of ADP (5-7 µM) at 37 °C and allowed to proceed for 3 min at which point the platelets were immediately processed for cGMP measurements. Results are expressed as mean \pm SEM of three separate experiments.

4.3.7 STIMULATION OF PLATELET NOS ACTIVITY BY APOE:DMPC VESICLES.

4.3.7.1 Haemoglobin Assay

Incubation of freshly prepared HbO₂ with washed platelets (3×10^8 platelets/ml) and GNSO produced the theoretical molar response curve (Figure 4.3-9, *panel A*). However, when the HbO₂ (3.6 µM) was pre-incubated with unstimulated, ADP-stimulated or apoE:DMPC (50 µg/ml) treated platelets no significant differences in HbO₂ consumption were noted (Figure 4.3-9, *panel B*). Greater than 35 % of the HbO₂ was consumed in all the preparations tested. However, this was regarded as being non-specific to NOS activity since addition of L-NMMA (1 mM) had no effect.

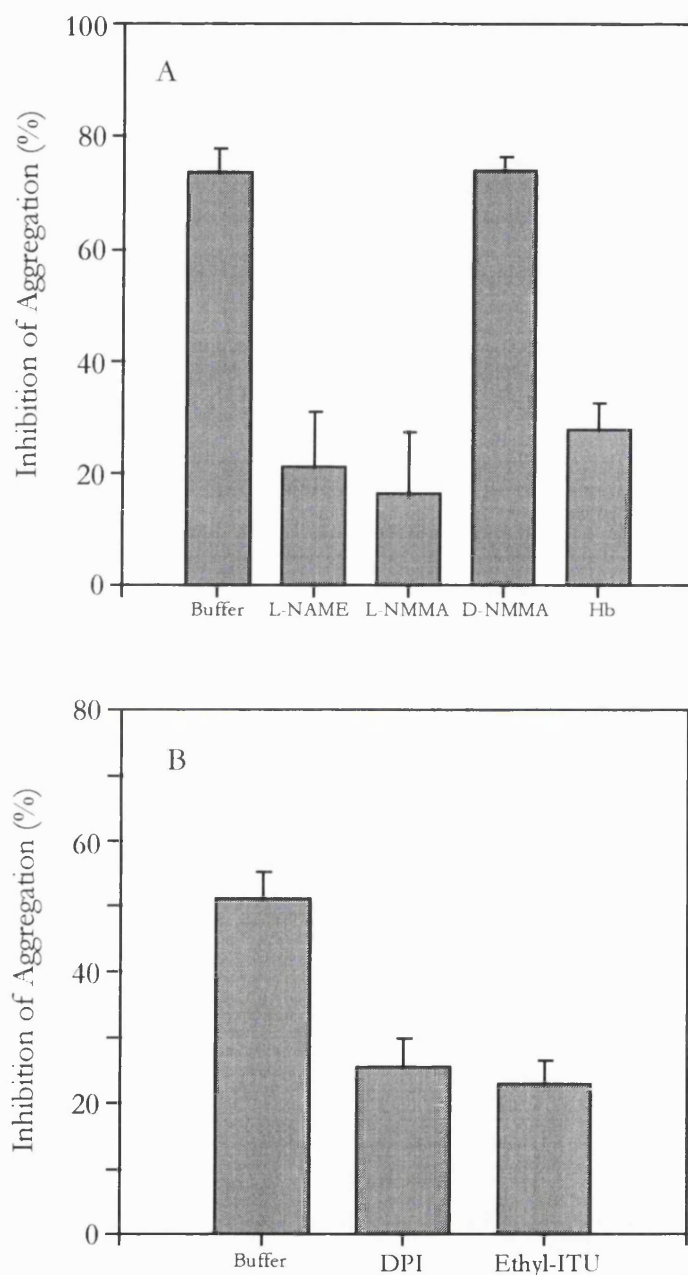


Figure 4.3-8 NOS inhibitors prevent the anti-aggregatory action of apoE:DMPC complexes.

Panel A, aliquots of PRP ($2-3 \times 10^8$ cells/ml) were pre-incubated with 300 μ M L-NAME, L-NMMA, D-NMMA or 100 nM haemoglobin (Hb) for 10 min at 20 °C and then for a further 10 min with 10 μ g protein/ml apoE:DMPC. The extent of aggregation was measured 3 min after addition of a pre-determined threshold concentration of ADP (1-2 μ M) and expressed as a percentage of controls with buffer alone. Results are expressed as mean \pm SEM of three separate experiments. **Panel B**, aliquots of PRP ($2-3 \times 10^8$ cells/ml) were pre-incubated with 20 μ g protein/ml apoE:DMPC for 9 min at 20 °C and then for a further 1 min at 37 °C with 100 nM DPI or 3 μ M Ethyl-ITU. Aggregation measurements were carried out as before and results are expressed as the mean \pm SEM of three independent experiments.

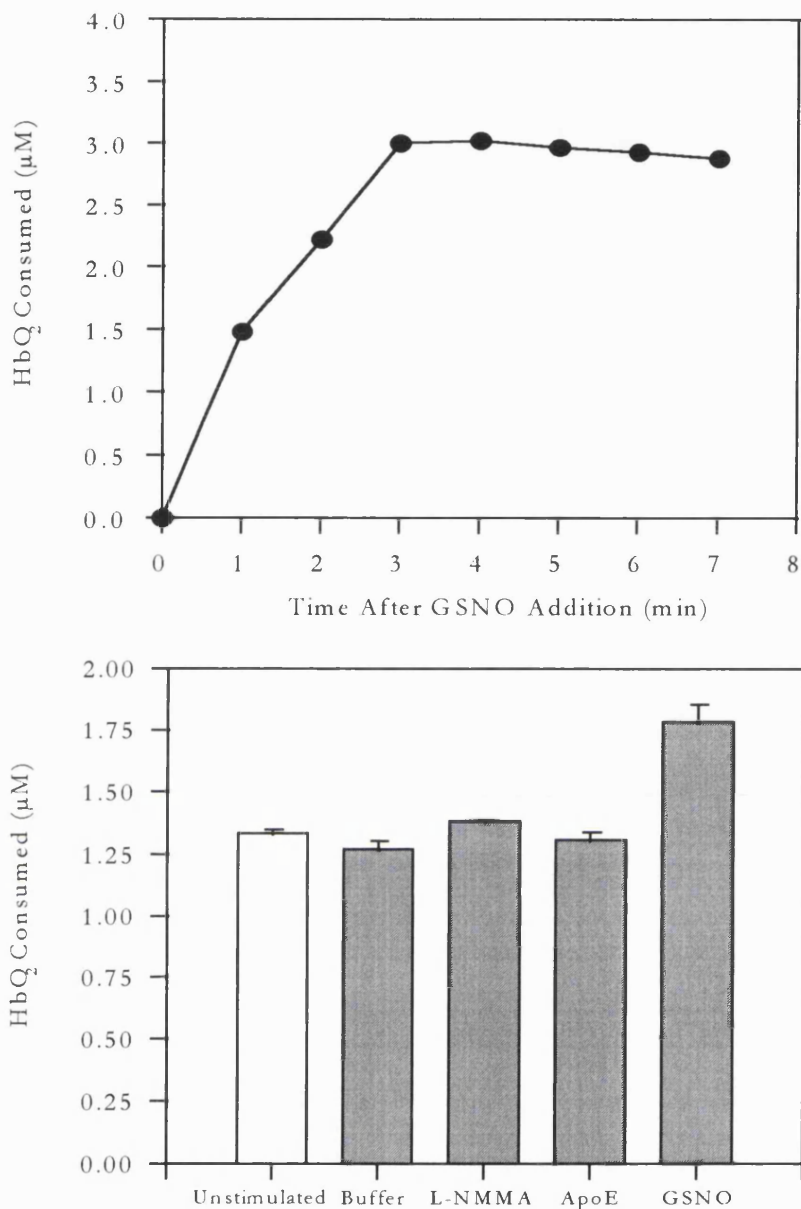


Figure 4.3-9 Consumption of HbO₂ by platelets.

Panel A, Aliquots of “washed” platelet suspensions ($600\ \mu\text{l}$, 3×10^8 cells/ml) were incubated in the aggregometer with $3.6\ \mu\text{M}$ HbO₂ and $5\ \mu\text{M}$ GSNO at $37\ ^\circ\text{C}$. At defined time intervals up to 10 min, a portion ($100\ \mu\text{l}$) was removed, rapidly centrifuged ($12000\ \text{g}$ for 30 s) and the amount of HbO₂ consumed calculated. **Panel B**, Aliquots of platelet suspensions ($100\ \mu\text{l}$, 3×10^8 cells/ml) were incubated at $20\ ^\circ\text{C}$ with $3.6\ \mu\text{M}$ HbO₂ and either buffer, apoE:DMPC ($50\ \mu\text{g}$ protein/ml), L-NMMA ($1\ \text{mM}$) or GSNO ($2.5\ \mu\text{M}$) for 10 min. The samples were transferred to an aggregometer ($37\ ^\circ\text{C}$, $900\ \text{rpm}$) where “threshold” quantities of ADP were added ($5\text{--}7\ \mu\text{M}$). After a further 3 min incubation, aggregation was terminated by a rapid centrifugation ($12000\ \text{g}$ for 10 s) and the amount of HbO₂ consumed was calculated. Also, additional control tubes in which ADP was omitted were prepared.

4.3.7.2 Nitrite/Nitrate Assay.

When PRP (2×10^8 platelets/ml) was pre-incubated for 10 min with increasing quantities of apoE:DMPC, no significant increase in the $\text{NO}_2^-/\text{NO}_3^-$ content of PRP was noted (Figure 4.3-10). Additionally, no significant differences were noted between the $\text{NO}_2^-/\text{NO}_3^-$ PPP content and that of the aggregating PRP in the absence of apoE:DMPC ($2.79 \pm 0.03 \mu\text{M}$ versus $3.49 \pm 0.75 \mu\text{M}$ respectively, $P > 0.05$).

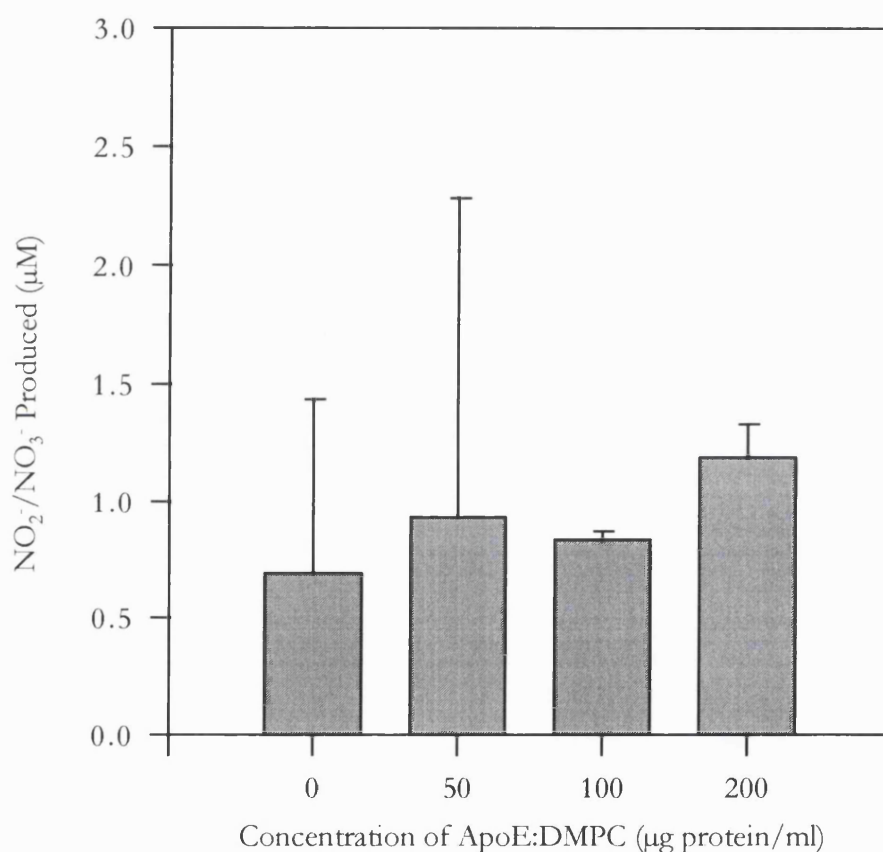


Figure 4.3-10 Production of $\text{NO}_2^-/\text{NO}_3^-$ by platelets.

The $\text{NO}_2^-/\text{NO}_3^-$ produced by platelets was measured in PRP ± 10 min pre-incubation with apoE:DMPC ($20 \mu\text{g} - 200 \mu\text{g}$ protein/ml, 20°C). Aggregation was initiated with "threshold" quantities of ADP ($1-2 \mu\text{M}$). After 3 min, aggregation was terminated by a rapid centrifugation (12000 g for 10 s). Eighty μl of the platelet supernatant was removed and total NO_2^- and NO_3^- levels were measured using a commercial $\text{NO}_2^-/\text{NO}_3^-$ assay kit. Results are expressed as the mean \pm SEM of three independent experiments. All samples were corrected for the $\text{NO}_2^-/\text{NO}_3^-$ content of PPP.

4.3.7.3 The Citrulline Assay.

Intact Platelet Preparation.

No significant increase in enzyme activity could be detected in unstimulated, ADP-stimulated or apoE:DMPC (50 µg protein/ml) treated platelets (Table 4.3-2).

Platelet Treatment	L-[³ H]arginine Conversion (%)
Unstimulated	1.79 ± 0.04
ADP Stimulated	1.68 ± 0.04
ApoE:DMPC + ADP	1.73 ± 0.06
L-NAME + ADP	1.65 ± 0.03

Table 4.3-2 Conversion of L-[³H]arginine to L-[³H]citrulline in intact platelet preparations.

L-[³H]arginine-labelled washed platelets (3×10^8 cells/ml) were incubated for 10 min with buffer, apoE:DMPC liposomes (50 µg protein/ml) or L-NAME (1 mM). The samples were transferred to an aggregometer (37 °C, 900 rpm). Buffer or "threshold" quantities of ADP (5-7 µM) were added and after a further 3 min incubation, the samples were processed for L-[³H]citrulline measurements as outlined in section 4.2.7.3. Results are expressed as the mean ± SEM of three independent experiments.

Lysed Platelet Preparations.

The basal rate of L-[³H]citrulline formation in platelet lysates, in the presence of all essential co-factors was 0.18 ± 0.03 pmol/h/ 10^9 platelets. In the absence of Ca^{2+} the formation of L-[³H]citrulline was not detectable. When platelets were incubated with apoE:DMPC vesicles for 10 min, the activity of NOS was markedly increased as judged by the 4-fold increase in conversion of L-[³H]arginine to L-[³H]citrulline (0.71 ± 0.17 pmol/h/ 10^9 apoE:DMPC-treated platelets; $P < 0.05$, $n=4$). Addition of L-NAME (1 mM) negated any such increase (Figure 4.3-11).

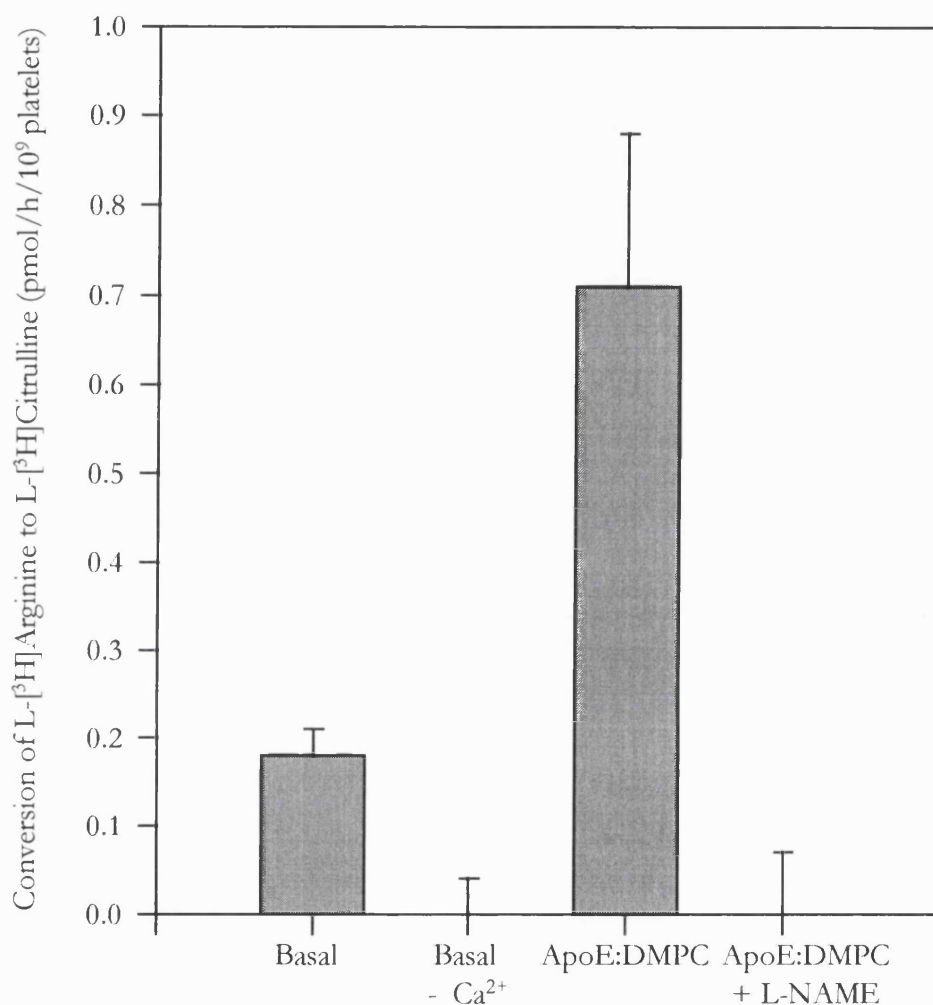


Figure 4.3-11 ApoE:DMPC complexes increase intraplatelet NO synthase activity in lysed platelet preparations.

Washed platelets (10^9 cells) were incubated with or without apoE-DMPC vesicles ($50 \mu\text{g}$ protein/ 3×10^8 cells) for 10 min at 37°C in a final volume of 1 ml and cell lysates were prepared as described in section 4.2.7.3. NOS activity was assessed by measuring the conversion of L-[³H]arginine to L-[³H]citruilline in the absence and presence of the specific inhibitor L-NAME (1 mM) and CaCl_2 (1.2 mM) using the NOSdetect assay kit. Results are expressed as picomoles of L-[³H]citruilline produced per h per 10^9 platelets and are corrected for non-enzymatic production of L-[³H]citruilline; values are the means \pm SEM of at least three independent experiments.

4.4 Discussion

4.4.1 CHOLESTEROL REMOVAL STUDIES.

Recently, Higashihara and colleagues reported that apoE:DMPC complexes inhibit collagen- or thrombin-induced aggregation, apparently by avidly sequestering cholesterol from platelet plasma membranes [271]. Cholesterol-deficient platelets are known to respond poorly to agonists, in part because phospholipase-mediated release of arachidonate from membrane phospholipids, and its conversion to pro-aggregatory thromboxane A₂, is impaired [281, 302, 303]. However, several reasons suggest that sequestration of platelet cholesterol is an unlikely explanation for our findings with ADP as agonist. Thus, our pre-incubations with apoE:DMPC were much shorter (30 s *versus* 30 min) and the small amount of cholesterol released (<1 % *versus* 10 %) would seem insufficient to cause the concomitant marked inhibition of aggregation observed (typically 60 - 70 %). Indeed, ADP-induced aggregation is relatively unaffected by membrane cholesterol depletion; platelets with 20 % less cholesterol retain a normal sensitivity to ADP [281]. Moreover, Desai et al. [235] and I (*Chapter 3, Figure 3.3-1*) have previously shown that HDL-E from cirrhotic plasma is a highly potent inhibitor of platelet aggregation; such HDL is enriched in free cholesterol [273] and would tend to donate rather than remove cholesterol from the platelet plasma membrane [273, 304, 305]. Finally, I provided direct evidence that cholesterol removal was implausible by use of chemically modified apoE; CHD-apoE:DMPC was unable to suppress platelet aggregation but still removed the same amount of platelet cholesterol as inhibitory apoE:DMPC. Interestingly, and in contrast to the report of Higashihara et al. [271], I found human apoE:DMPC complexes to be ineffective inhibitors of thrombin induced platelet aggregation during the 30 s time scale studied (*Chapter 3, Figure 3.3-3*). However, these discrepant results could be explained by the original hypothesis of Higashihara et al. Their prolonged pre-incubation period with apoE:DMPC (30 min), removed 10 % of the platelet membrane cholesterol. Since the thrombin receptor in the platelet surface membrane is known to be sensitive to cholesterol depletion and decreased membrane microviscosity [306], this may explain why apoE was able to inhibit thrombin-induced aggregation in their study.

4.4.2 APOE:DMPC STIMULATES INTRAPLATELET cGMP PRODUCTION.

As outlined in *section 1.2.5*, calcium is central to the control of platelet reactivity, interacting with diverse second messengers through a myriad of complex, but tightly regulated, signalling pathways. Two important control elements involved in the suppression of Ca²⁺ mobilisation and hence, platelet activation are the cyclic nucleotides, cAMP and cGMP. I found that apoE induced increases in both cGMP and cAMP. Nevertheless, additional

experiments implicated a stimulation of guanylate cyclase activity and a rise in cGMP as prerequisites for the anti-platelet action of apoE. Thus, inhibitors of SGC; methylene blue and more importantly ODQ, which has greater selectivity [283, 294], were able to reverse the anti-aggregatory action of apoE. Inhibition by ODQ also blocked the apoE:DMPC-induced rise in cGMP. Similarly, studies with the general PDE inhibitor, IBMX supported a primary role for cGMP, since this reagent abolished the apoE:DMPC induced rise in cAMP but not the dose-dependent increase in cGMP. Interestingly, these findings were consistent with second messenger “cross-talk” [32], namely that the increase in cGMP invoked by apoE in the absence of IBMX had inhibited cAMP PDE III [86, 307, 308], permitting cAMP levels to rise.

4.4.3 INDIRECT EVIDENCE FOR AN APOE:DMPC STIMULATION OF PLATELET NOS.

The involvement of platelet NOS in mediating the anti-aggregatory action of apoE was suggested by several lines of indirect experimental evidence. Thus, NOS inhibitors of distinct structural and functional types, the amino acid analogues of L-arginine, L-NMMA and L-NAME, a non-amino acid analogue, Ethyl-ITU and the flavoprotein inhibitor, DPI, all reversed the anti-platelet action of apoE. These chemicals inhibit cellular production of NO by binding to NOS to displace either L-arginine or, in the case of DPI, essential cofactors [300]. Because all these reagents were used at concentrations close to their quoted IC₅₀ values for specific NOS inhibition, it seems unlikely that they will be acting via diverse NO-independent mechanisms to block the apoE:DMPC effects. Furthermore, haemoglobin, which strongly inhibits the actions of NO on guanylate cyclase by forming a haemoglobin-NO adduct, was found to suppress the anti-platelet action of apoE. As haemoglobin does not penetrate platelets [309], this implies that apoE generated sufficient NO for secretion to occur. Presumably, this secreted NO functions in a paracrine manner thus, sustaining the dampening influence on platelet activation. Indeed, it has recently been demonstrated that endogenously produced platelet NO is a potent inhibitor of platelet recruitment as well as aggregation [310].

4.4.4 DIRECT EVIDENCE FOR AN APOE:DMPC STIMULATION OF PLATELET NOS.

4.4.4.1 Background.

Evidence of a direct involvement of platelet NOS was more difficult to obtain since platelet NOS activity is known to be low compared with other cell types [311]. Indeed, before any effects of apoE:DMPC could be evaluated, an accurate and sensitive assay of platelet NOS activity had to be developed.

To date, there have been at least 13 reports of intraplatelet NOS activity measurements in humans [296, 310, 312-322]. Activity was evaluated by a variety of techniques including: highly specialised (non-commercial) porphyrinic microsensors [310, 312, 313], the haemoglobin assay [314, 296], the nitrite/nitrate assay [315, 316] and the citrulline assay [315, 317-322]. However, many discrepant results were reported concerning: whether NO is released spontaneously by unstimulated platelets; the absolute amounts of NO produced by stimulated platelets (estimates range from fmol to nmol NO/ 10^8 platelets); and the number of platelets required for reliable detection (ranging from 1×10^7 to 2×10^{11} platelets/assay tube).

These discrepancies may not only reflect differences in methodology, but also in the platelet populations studied. Platelets are formed by fragmentation of the cytoplasm of megakaryocytes [8, 11, 12, 323, 324]. Recently, megakaryocytes have been identified as containing at least two forms of NOS [325-329]. One is the Ca^{2+} -dependent, constitutive, low activity, endothelial enzyme, eNOS. The other is the Ca^{2+} independent, cytokine-inducible, high activity enzyme, iNOS, which requires *de-novo* protein synthesis for expression (see *section 1.2.6.2*). In human platelets some authors report the presence both eNOS and iNOS [318, 329, 330] others, however, find only eNOS [296, 320, 331]. Indeed, of the 13 reports, five describe high basal activity without agonist stimulation (indicative of iNOS activity) [314-316, 318, 322], while five report a strict dependency on agonist stimulation and a relatively low activity (classical markers of eNOS activity) [296, 312, 313, 317, 320]. Three reports do not comment on NOS characteristics [321, 310, 319]. Platelets are anucleated and thus have only a limited residual capacity for synthesizing proteins [8, 11, 12, 323, 324]. It is likely, therefore, that both platelet NO synthases are synthesized at the level of the megakaryocyte and are acquired by platelets during their formation. This raises the possibility that platelets prepared from volunteers with endotoxemia or other cytokine-related conditions [328], would contain both iNOS and eNOS isoforms and hence have a relatively high basal enzyme activity. In the studies outlined in this thesis most platelets preparations were obtained from young (age 19 - 32 years), healthy individuals. From the current literature, it was difficult to predict the level of NOS activity in my platelet population. Accordingly, I examined platelet NOS activity using three distinct assays each offering a differing degree of sensitivity: the haemoglobin assay, the nitrite/nitrate assay and the citrulline assay.

4.4.4.2 NOS Assays.

HbO₂ avidly binds NO to form metHb and this reaction can be monitored spectrophotometrically by following the consumption of HbO₂. The technique was readily established and incubation of freshly prepared HbO₂ with platelets and the NO donor, GNSO, produced the theoretical molar response curve. However, even with a reported sensitivity of 2 nM [314, 332], no changes in absorbance were seen when HbO₂ was added to my platelet system with and without apoE. This indicated that insufficient NO was secreted for detection by this assay. Similarly, attempts to measure the amount of NO₂⁻ and NO₃⁻, the solution decomposition products of NO, were unsuccessful because insufficient NO was formed. Using this method, the sensitivity of this assay is reported to have a detection limit of 2.5 μM [333], well beyond the range of NO detection reported for platelet eNOS activity [296, 312, 313, 317, 320]. Modifications of the Griess reaction, using fluorescent probes [2,3-diaminonaphthalene (DAN) assay] [334] and free radical scavenger molecules (carboxy PTIO) [335] can increase the sensitivity of this assay to 10 nM. However, results from the HbO₂ experiments suggest that even this level of sensitivity would be insufficient to produce meaningful NOS observations in my platelet preparations.

In principle, the third technique to quantify platelet NOS activity, the conversion of L-[³H]arginine to L-[³H]citrulline plus NO, should not lack sensitivity because the radioactive substrate is available with high specific activity and several μCi can be added per assay [336]. However, NOS measurements using this method on intact platelets proved unsuccessful. This was probably due to a combination of insufficient platelets for a strong signal (1 x 10⁸ platelets/assay tube), a low level of L-[³H]arginine uptake into the platelet and a subsequent dilution of label by intracellular stores of arginine.

Indeed, I was only able to demonstrate involvement of the L-arginine: NO pathway in mediating the anti-platelet effects of apoE:DMPC by utilising a lysed platelet citrulline assay. Measurement of platelet NOS activity used very large numbers of lysed platelets (10⁹ cells per assay tube), with the cofactors required for optimal activity added into the assay “cocktail”. Under these conditions, lysates from platelets pre-treated with apoE:DMPC had a 4-fold increased ability to convert L-[³H]arginine to L-[³H]citrulline, which could be abolished in the presence of L-NAME. In addition, the formation of L-[³H]citrulline was entirely dependent on the presence of Ca²⁺. It is therefore likely that my platelet populations contain only eNOS. Indeed, this is in good agreement with my intraplatelet cGMP data; platelets had a very low cGMP content that was only up regulated in the presence of agonist. Platelet eNOS requires Ca²⁺-calmodulin for activation and presumably, an agonist

is needed to supply the initial burst of Ca^{2+} needed for such up-regulation [296]. Intriguingly, this may explain the paradoxical results obtained using IBMX to inhibit platelet PDEs. Basal cAMP levels were increased two-fold because of inhibition of platelet cAMP PDE. However, control levels of cGMP were diminished. Presumably, this was because the rise in cAMP restricted Ca^{2+} mobilisation. Since platelet eNOS, requires activation by Ca^{2+} , the reductions in Ca^{2+} flux would limit NO release and hence production of cGMP [32, 295, 296].

Although, only relatively low levels of NO could be detected in my system (fmol/h/ 10^9 platelets), this observation is not contradictory to a pre-eminent role of eNOS in apoE:DMPC-induced inhibition. Thus, I have shown that platelets are exquisitely sensitive to NO with even a very small increase in the extracellular supply of NO having dramatic effects (only 40 pmol GSNO per 10^8 platelets inhibits platelet aggregation by 50 %). Presumably intracellular NO production would be even more potent.

After my preliminary experiments implicating the L-arginine:NO pathway as the anti-platelet mechanism of apoE:DMPC were underway, a report was published indicating that total HDL decreases platelet function by the same pathway [316]. Although these results provide compelling support for my observations using apoE:DMPC, there are a number of important differences between our reports. Firstly, the authors showed an impressive basal production of platelet NO without agonist stimulation. This activity could be detected by both the citrulline and nitrite/nitrate assay indicating the presence of iNOS activity. Indeed, the same authors have recently published two reports identifying both iNOS and eNOS in their platelet population [318, 330]. This basal iNOS activity could be upregulated in the presence of HDL. Secondly, the authors used thrombin as their agonist of choice during the entire study. However, it is thought that eNOS is not activated during platelet aggregation induced by this agonist [295, 313]. Indeed, although the reasons for this effect are obscure, my observation that apoE:DMPC does not inhibit thrombin-stimulated aggregation are in agreement with this finding. Interestingly, these authors report that control levels of NOS activity are not stimulated by thrombin. However, NOS activity in the presence of thrombin and HDL is greatly enhanced. These studies indicate that HDL in conjunction with thrombin could possibly modify platelet iNOS activity by some unknown mechanism. Since my platelet population did not contain iNOS, the effects of apoE:DMPC on iNOS activity could not be evaluated. However, human macrophages have recently been demonstrated to over-produce NO in response to apoE [337]. Since these cells express an abundance of iNOS, an apoE-iNOS link is highly probable. However, these authors did

not investigate the mechanism of action of apoE on iNOS activity, therefore it is unclear whether the effect was due to an increase in gene expression or by post translational modification/phosphorylation.

4.4.5 CONCLUSIONS.

In summary, as indicated in Figure 4.4-1, I believe that my findings provide clear evidence for the L-arginine:NO signal transduction pathway as the mechanism by which apoE exerts its anti-platelet effect. Less clear, however, are the initial steps to activate this pathway. The ability of HDL-E [7] and apoE:DMPC [271] complexes to be bound by platelets in a saturable manner suggests that a distinctive apoE receptor may be present in the platelet surface membrane, a proposal consistent with the benign action of CHD-apoE:DMPC. Platelet eNOS activity could be up regulated, in lysed isolated platelets supplemented with its essential cofactors. This indicates that apoE does not increase arginine uptake into the platelet [338, 339] since there is no extracellular arginine in washed platelet suspensions. It also implies that apoE activates the enzyme by a mechanism independent of the availability of cofactors. Furthermore, apoE:DMPC failed to stimulate cGMP production in the absence of an agonist. This indicates that apoE:DMPC cannot directly activate platelet eNOS. This raises the intriguing possibility that occupation of specific receptors by apoE may “prime” platelets to help attenuate eNOS activation when challenged by agonists or other agents. However, the mechanisms that control NO production in platelets are unclear. Indeed, very little is known about the nature of the enzyme itself. While both eNOS and iNOS mRNAs have been identified in human platelets [318, 329, 330], the low levels of expressed protein have hindered their characterisation. Indeed, as well as the “native” 135 kDa eNOS protein [320, 326], a novel 80 kDa isoform of eNOS has been identified by 2 groups [329, 331]. Platelet eNOS was also reported to be membrane-bound [320, 326], this leads to the appealing prospect that translocation from the membrane to the cytosol could affect platelet NOS activity, possibly by an apoE receptor stimulated phosphorylation of the enzyme. Alternatively, location of eNOS at the plasma membrane could play a direct role in apoE induced signal transduction; either by directly coupling the enzyme’s activation to occupancy of the apoE surface receptor or potentially via an indirect apoE receptor-mediated signalling cascade. Both these events could be localised in caveolae-like domains at the platelet surface, which are known to be rich in signalling receptors and signalling intermediates [68, 340]. Obviously, identifying and characterising the apoE receptor on the platelet surface membrane is of extreme importance in further elucidating the anti-platelet role of apoE:DMPC.

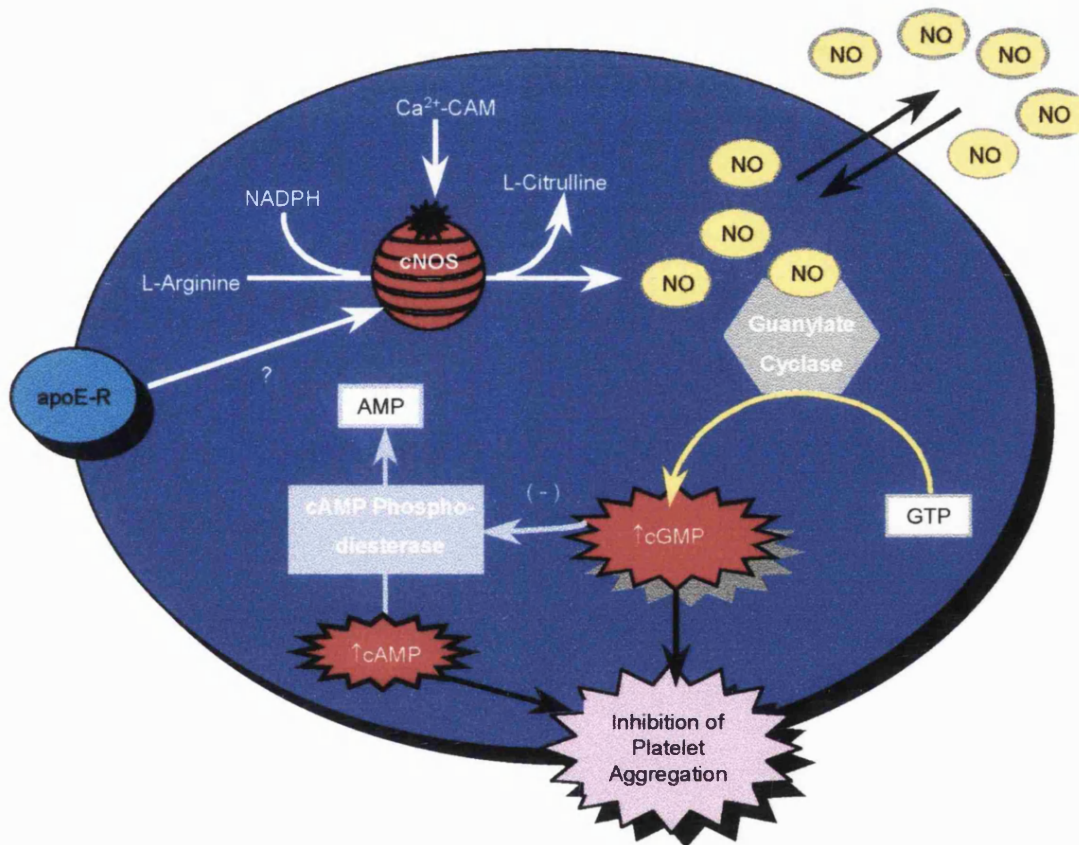


Figure 4.4-1 Proposed mechanism for apoE-mediated inhibition of agonist-induced platelet aggregation

Occupation of putative cell-surface receptors (apoE-R) by apoE causes upregulation of the constitutive enzyme eNOS when an agonist-induced burst of Ca²⁺-calmodulin occurs (Ca²⁺-CAM). Some of the NO generated acts on SGC to produce inhibitory cGMP, the concomitant rise in cAMP occurring by second messenger 'cross-talk'. The remainder of the NO produced rapidly diffuses out of the cell and, since extracellular haemoglobin restricts the apoE inhibitory effect, appears to function in a paracrine manner to sustain the dampening influence on platelet activation. Whether this apoE-generated diffusible NO can also act on other cell types remains to be established.

Chapter 5

5. MOLECULAR CHARACTERISATION OF A HUMAN PLATELET RECEPTOR THAT BINDS APOLIPOPROTEIN E

5.1 Introduction.

Since the molecular characterisation of the LDL-R, an ever-increasing number of related apoE-binding proteins have been discovered. As outlined in *section 1.3.7*, the known mammalian members of the LRSF comprise LDL-R itself, the VLDL-R, the newly characterised brain receptor, apoER2 (also termed LR7/8B), the giant (~600 kDa) multifunctional α 2-macroglobulin receptor/LRP and gp330/megalin (reviewed in [141-144, 168]). In addition, several related receptors have been discovered in chicken [174, 341]. The LRSF members are type 1 receptors with short cytoplasmic tails containing one or a few FxNPxY internalisation motifs. The extracellular domains contain: **i)** clusters of the ~40 residue LDL-R class A repeats that bind ligands, including apoE, RAP and in some cases lactoferrin, **ii)** clusters of “spacer” regions containing the consensus peptide YWTD, and **iii)** single elements or pairs of EGF repeats. In addition to the LRSF members, other proteins with LDL-R class A repeats include: perlecan, a large multidomain basement membrane HSPG composed of four LDL-R class A domains and four growth factor-like domains [342] and GRL101, a hybrid receptor described in the mollusc *Lymnea stagnalis* composed of an amino-terminal cluster of LDL-R class A repeats and a carboxyl-terminal domain similar to regions in guanine nucleotide binding protein-coupled receptors [343]. To date, however, the exact nature of the apoE receptor on platelets is unknown; cells of the megakaryocytic lineage do not contain the classical LDL-R [226, 227] and the presence of other LRSF members has yet to be established.-

The aim of the study outlined in the following chapter was to search for a platelet receptor capable of binding apoE. Identification and molecular characterisation of candidate receptors was achieved using two separate strategies. Initially, the structural/functional sites on the apoE polypeptide capable of invoking an anti-platelet response were identified using a variety of tools including apoE variants, thrombolytic fragments, synthetic peptides and receptor antagonists. Then, using the insights gleaned from these analyses, molecular biology strategies were employed to identify the presence of residual platelet mRNA with homology to known apoE receptors.

5.2 Specialised Materials and Methods.

5.2.1 MATERIALS.

ApoE-2 was purified from plasma obtained from type III hyperlipidaemic patients as described previously (*section 2.4.3*). Purified recombinant human apoE-4, apoE-3 and the 22 kDa apoE thrombolytic fragment were provided as a kind gift from Dr. K. Weisgraber (San Francisco, USA). Three synthetic peptides E₁₄₁₋₁₅₅, E_{(141-155)₂}, and E₂₆₃₋₂₈₆ corresponding to areas of the apoE polypeptide were supplied by Dr. J. Harmony (Ohio, USA). The additional apoE peptide, E₁₃₃₋₁₄₅, was synthesized by Genosys (Cambridge, UK). Recombinant human RAP, purified human placental LRP and monoclonal anti-human LRP antibody (α 2MR2) were supplied as a kind gift from Dr. J. Gliemann (Aarhus, Denmark). The megakaryoblastoid cell lines, HEL and Meg-01 cells were provided as kind gifts from Dr. A. Goodall (RFHSM, London, UK) and Dr. J. Martin (University College London, London, UK), respectively. Foetal liver RNA was kindly provided by Dr A. Walker (RFHSM). CHO cell extracts from cells over-expressing either full length apoER2 without cytoplasmic insert, apoER2 Δ 4-6 with insert or VLDL-R were supplied by Dr. X. Sun (Hammersmith Hospital, London, UK). All other chemicals were supplied by Sigma Chemical Co. unless otherwise stated.

5.2.2 APOE:DMPC COMPLEXES.

All apoE isoforms, fragments and peptides were incorporated into small, unilamellar vesicles of DMPC as outlined in *section 2.4.4* and were extensively dialysed against Tyrode's buffer before use.

5.2.3 PLATELET AGGREGATION.

Washed platelets (80 μ l) were pre-incubated for 30 s with Tyrode's buffer (20 μ l) and aggregation was initiated by addition of increasing concentrations of ADP at 37 °C in a Payton dual-channel aggregometer fitted with 0.1 ml cuvettes. The "threshold" concentration of ADP was determined and was used in subsequent experiments in which the Tyrode's buffer was replaced by the 22 kDa apoE thrombolytic fragment, apoE peptides, lactoferrin, apoE-2:DMPC, apoE-3:DMPC or apoE-4:DMPC. For receptor competition experiments, washed platelets were co-incubated for 10 min at 37 °C with 1.47 μ M RAP and 1.47 μ M (~50 μ g protein/ml) apoE:DMPC.

5.2.4 HEPATOCARCINOMA CELL CULTURE.

HepG2 cells were grown in Dulbecco's Modified Eagle's Medium (Life Technologies) supplemented with 2 mM glutamine, 10 % heat inactivated foetal bovine

serum (FBS), 100 µg/ml streptomycin and 100 U/ml penicillin. The cells were cultured as a monolayer in 75 cm² tissue culture flasks at 37 °C in a humidified atmosphere of 5 % CO₂ and 95 % air. The cells were passaged every 7 days by trypsinization and passing through a 19 G needle to produce a single cell suspension. The cells were then reseeded at 1 x 10⁵ cells/ml. For receptor studies, the cells were harvested from the flasks by scraping and centrifuged at 450 g for 10 min at 4 °C. The cell pellet was washed by dispersion in PBS (pH 7.4) and recentrifugation.

5.2.5 MEGAKARYOBLASTIC CELL CULTURE.

HEL and Meg-01 cells were cultured in RPMI 1640 (Life Technologies) media supplemented with 2 mM glutamine, 10 % heat inactivated FBS, 100 µg/ml streptomycin and 100 U/ml penicillin. The cells, grown in suspension culture, were incubated at 37 °C in a humidified atmosphere of 5 % CO₂ and 95 % air. The cells were passaged every 3 to 5 days and reseeded at 2 x 10⁵ cells/ml. For mRNA extraction and membrane preparations, HEL and Meg-01 cells were harvested by centrifugation at 450 g for 10 min at 4 °C and washed in PBS.

5.2.6 PREPARATION OF PURIFIED CELL MEMBRANES.

Membrane vesicles were prepared from extensively washed HepG2 cells (1 x 10⁶), HEL cells (1 x 10⁶) or PGI₂-treated platelets (1 x 10⁹). The cells in 1 ml of lysis buffer (50 mM HEPES, 150 mM NaCl, 1 mM CaCl₂, pH 7.4 containing the protease inhibitors: 1 mM PMSF, 0.02 mg/ml leupeptin, and 10 mM benzamidine) were disrupted by controlled ultrasonication of 9 x 10 s bursts, allowing a cooling time of 10 s between each burst (Sanyo Soniprep 150, small probe, set on an amplitude of 8 microns). Lysates were centrifuged at 19000 g for 30 min to eliminate intact cells, mitochondria and granules. The supernatant was centrifuged at 100000 g for 1 h to pellet the membrane fraction. This pellet was resolubilised in membrane buffer (50 mM HEPES, 150 mM NaCl, 1 mM CaCl₂, 0.05 % Tween 20, 20 mM CHAPS and protease inhibitors). Protein concentrations were determined by the BCA method (Pierce & Warriner, Chester, UK) using BSA as a standard. Membrane preparations were used either immediately for Western blotting or were stored at -70 °C for up to 2 weeks.

5.2.7 WESTERN BLOTTING OF THE LRP.

HepG2, HEL and platelet membrane fractions (all 200 µg/lane), and purified placental LRP (2 µg/lane), were subjected to 3 - 8 % gradient SDS-PAGE under non-reducing conditions and electrophoretically transferred to Hybond ECL nitrocellulose membranes (Amersham International plc). Following transfer, the membrane was

removed and immunoblotted essentially as outlined in *section 2.3.3.* using: a 1/10 dilution of monoclonal anti-LRP (α 2MR2), a 1/1000 dilution of anti-primary antibody-horse radish peroxidase conjugate and the blot was visualised using an enhanced chemiluminescence (ECL) substrate (Amersham International plc). Briefly, the ECL detection reagent was prepared by mixing equal volumes of the two ECL ingredients (5 ml per mini-gel blot). The nitrocellulose blot was incubated in a clean trough with the ECL reagent for 1 min at room temperature. The excess detection reagent was drained from the blot by touching each side against filter paper before the blot was carefully wrapped in cling film. The blot was transferred to a film cassette, secured with tape and briefly exposed (usually 30 s – 5 min) to X-ray film (Hyperfilm ECL, Amersham International plc).

5.2.8 PREPARATION OF WASHED PLATELETS, MONOCYTES, LYMPHOCYTES AND NEUTROPHILS FOR RNA EXTRACTION.

Washed platelets were isolated from 200 ml freshly drawn blood as outlined in *section 2.5.5.* Care was taken to avoid contaminating PRP with nucleated cells when removing it from the buffy coat and red blood cell fractions. The final platelet preparations were free of other cell types as determined by phase contrast microscopy.

Mononuclear cells and polymorphonuclear leukocytes were isolated from 40 ml of fresh blood. The blood was collected into 4 ml of 2.7 % EDTA, pH 7.0, and erythrocytes were sedimented by incubation with 3.3 ml of 2 % methyl cellulose for 30 - 40 min at 37 °C. The supernatant containing leukocytes and platelets was removed and centrifuged at 250 *g* for 10 min at 4 °C. The subsequent supernatant containing platelets was discarded and the leukocyte pellet resuspended in a total of 50 ml of ice-cold erythrocyte lysis buffer (0.82 % NH₄Cl containing 5 mM KCl brought to pH 7.4 with 4.4 % NaHCO₃). This procedure lysed any remaining erythrocytes during 10 min incubation on ice and the leukocytes were collected by centrifugation (10 min, 250 *g*). The cell pellet was fractionated further by resuspension in 20 ml of PBS and centrifugation (450 *g* for 30 min) through Ficoll-Paque (10 ml). Blood neutrophils sedimented through the Ficoll-Paque layer to form a pellet, whereas a mixed suspension of monocytes and lymphocytes remained at the interface. The two cell populations were removed and washed in 50 ml of cold PBS.

5.2.9 ASSESSMENT OF RNA INTEGRITY.

RNA was extracted from platelets, HEL cells, Meg-01 cells, monocytes/lymphocytes, neutrophils and human liver tissue as outlined before (*section 2.6.2*). The quality of this RNA was assessed by RT-PCR for U1A RNA [344]. U1A is a

“housekeeping” RNA species which forms part of the U1A spliceosome complex [345] and is required by all living cells. Briefly, 500 ng aliquots of the reverse transcription reaction mixture (*section 2.6.3*) were subjected to PCR (*section 2.6.4*) with 5 μ M U1A1 primer (GGC CCG GCA TGT GGT GCA TAA) and 5 μ M U1A2 primer (CAG TAT GCC AAG ACC GAC TCA GA) in a total volume of 50 μ l. After heating at 95 °C for 5 min, amplification proceeded for 35 cycles, with denaturation for 30 s at 95 °C, annealing of primers for 30 s at 56 °C and extension for 30 s at 72 °C. Finally, the reaction was completed by an extension step at 72 °C for 10 min. Reaction products were visualised and photographed under UV light after electrophoresis of 10 μ l of the product in a 2 % agarose gel containing 0.3 μ g/ml ethidium bromide. A successful RNA preparation gave a clean PCR product of 230 bp in length (see Figure 5.3-8, *panel B*).

5.2.10 INITIAL RT-PCR AMPLIFICATION OF LRSF MEMBERS FROM HEL CELL cDNA.

Sequences of oligonucleotide primers used for PCR amplification were based on alignment of published cDNA sequences corresponding to the highly conserved cysteine-rich LDL-R class A binding domains from human LRSF members. Sufficient degeneracy was incorporated into the primers to encompass divergence among the various receptors. Two different degenerate sense primers were designed. LDLA1 was designed against the LDL-R, VLDL-R and apoER2, while LDLA2 was designed against the LRP and gp330. The anti-sense degenerate primer, LDLA3, was designed against all the human LRSF members. Additionally, all the sequences were designed to incorporate restriction sites for easy cloning of the PCR products. The sense primers (LDLA1: 5'-GAT CGG ATC CTG (C/T)(C/G)(A/C) (G/T)GA TGG (C/T)TC (T/C/A)GA TGA-3' and LDLA2: 5'-GAT CGG ATC CTC TGG GGA (C/T)(G/A)(G/A) CAG TGA (C/T)GA-3') contained a BamHI site (underlined) while the antisense primer (LDLA3: 5'-GAT CGA ATT C(C/T)C (G/A/C)CC (A/G)TC (A/G)CA (G/T)(C/A)(G/T) CCA-3') contained an EcoRI site (doubly underlined).

RNA was extracted from HEL cells and human liver tissue as outlined before (*section 2.6.2*). Five μ l (~ 500 ng) aliquots of the reverse transcription reaction mixture (*section 2.6.3*) were subjected to “hot-start” PCR (*section 2.6.4*) with 10 μ M sense primer (LDLA1 or LDLA2) and 10 μ M anti-sense primer (LDLA3) in a total volume of 50 μ l. After heating at 95 °C for 10 min, amplification proceeded for 40 cycles, with denaturation for 30 s at 95 °C, annealing of primers for 1 min at 53 °C, and extension for 1 min at 72 °C.

After 20 cycles, additional Taq polymerase was added to each tube. Finally, the reaction was completed by an extension step at 72 °C for 10 min. One tenth (5 µl) of the products of the initial amplification reaction were then subjected to a subsequent round of PCR amplification thereby greatly increasing detection of rare transcripts. Reaction products were visualised and photographed under UV light after electrophoresis of 10 µl of the product in a 2 % agarose gel containing 0.3 µg/ml ethidium bromide. DNA bands of interest were extracted from the agarose gel using the QIAquick gel extraction kit (*section 2.6.6*) and digested with EcoRI and BamHI. These digested PCR products were again separated on a 2 % agarose gel, purified, cloned into pUC18 and sequenced (*section 2.6.8*).

5.2.11 PLATELET, HEL AND MEG-01 CELL RT-PCR AMPLIFICATION.

To specifically amplify the O-linked sugar domain, the transmembrane region and a unique cytoplasmic insertion sequence of apoER2, “hot-start” PCR was carried out on platelet, HEL, Meg-01, monocyte/lymphocyte and neutrophil cDNA. Briefly, 5 µl aliquots (~ 500 ng cDNA) of each reverse transcription reaction mixture were subjected to RT-PCR with 40 cycles and primer annealing at 65 °C in a total volume of 50 µl (sense primer: 1 µM of oligonucleotide 2092: 5'-GGA GG(C/A) TGT GAA TAC CT(G/A) TGC-3' and antisense primer: 1 µM of oligonucleotide 2696: 5'-CGA TCA AAG CTG CTG ATT GC-3'). Again, after 20 cycles additional Taq was added to each tube. The reaction products were cloned into pTAG (R&D Systems Europe Ltd, Abingdon, UK) according to the manufacturer's instructions and sequenced as before. To amplify the region corresponding to the ligand binding domain, PCR was carried out using conditions and primers (oligonucleotide 24: 5'-TCT CCG GCT TCT GGC GCT-3' and oligonucleotide 1114: 5'-TCT GGT CCA GGA GCT GGA A-3') as described elsewhere [173]. Since multiple products of unexpected length were obtained due to mis-priming, the ligand binding domain PCR products were subjected to Southern blotting [346]. Briefly, after denaturation, the PCR products were blotted onto a Hybond-N nylon membrane (Amersham International plc) and crosslinked under UV light for 5 min. Membranes were probed with an internal oligo probe (oligonucleotide 71: TGC GGC TCC AGC ATC TTG) which had been 5' ³²P-labelled using polynucleotide kinase (Promega). Membranes were pre-hybridized at 50 °C for 2 h in a buffer containing 5 x saline sodium citrate (SSC), 7% SDS, 20 mM NaPO₄, 10 x Denhardt's solution before the addition of 10 fmol/ml of labelled probe. Hybridization was performed at 50 °C for 16 h and the membrane subsequently washed in a solution containing 3 x SSC, and 1% SDS at 50 °C. Membranes

were autoradiographed overnight at -70 °C using Kodak XOMAT-AR film in cassettes fitted with Dupont Lightening Plus intensifying screens.

5.2.12 LONG RT-PCR.

To amplify the full length open reading frame of apoER2, the Expand Long Template PCR system (Boehringer Mannheim) was used. Briefly, 2 µl (~ 200 ng cDNA) of HEL cDNA was subjected to “long” PCR using the “system 1” protocol described by the manufacturers. The primer annealing temperature was 64 °C in a total volume of 50 µl (sense primer: oligonucleotide 24 and antisense primer: oligonucleotide 2918: 5'-GAG GCA CGA AGG GGG TGA T-3', both at 300 nM). Reaction products were analysed by electrophoresis of 10 µl of the product in a 1 % agarose gel containing 0.3 µg/ml ethidium bromide. The reaction products were cloned into pCRII (Invitrogen, Leek, Netherlands) according to the manufacturer's instructions and restriction mapped by Dr. D. Vinogradov, using the following enzymes: BspI, EcoRI, BstYI, HindIII, SmaI, AvaII, SacI, HincII, PstI, BbsI and XhoI (New England Biolabs, Hitchin, UK). Various restriction fragments were sub-cloned into pUC18 and sequenced.

5.2.13 PREPARATION OF ANTI-APOER2 ANTIBODIES.

An anti-peptide antiserum directed against human apoER2 was commissioned (Genosys) using the deduced polypeptide sequence from the published cDNA. The peptide chosen corresponded to 17 amino acids (865-881: CLGETREPEDPAPALKE) within the unique cytoplasmic insert of apoER2.

Western blotting was employed to assess the quality the anti-peptide antiserum, which was designated α ER2Ins. CHO cell extracts from cells over-expressing either full length apoER2 (without cytoplasmic insert), apoER2 Δ 4-6 (with insert) or, as a negative control, VLDL-R were all subjected to 8 % SDS-PAGE under non-reducing and reducing conditions. Separated proteins were electrophoretically transferred to Hybond ECL nitrocellulose membranes and any binding sites blocked for 30 min at room temperature or overnight at 4 °C in PBS containing 5 % milk powder, 0.1 % Tween-20 and 0.2 % 2-chloracetamide. The α ER2Ins was diluted 1/3000 in blocking buffer and incubated with the blot for 1 h. The blot was washed 6 x 5 min in wash buffer (PBS containing 0.1 % Tween-20 and 0.2 % 2-chloracetamide) and then incubated for 30 min in a 1/10000 dilution of anti-rabbit IgG coupled to horseradish peroxidase. Finally, after washing, the blot was visualised using the ECL chemiluminescence substrate.

5.2.14 IMMUNOPRECIPITATION OF PLATELET APOER2.

One ml of platelets (1×10^9 cells) were cell surface labelled using the ECL protein biotinylation module (Amersham International plc). The subsequent platelet pellet was washed in PBS and lysed at 4 °C in 250 μ l of lysis buffer (PBS containing 1 % CHAPS and Complete Mini protease inhibitor cocktail [Boehringer Mannheim]). The lysed sample was diluted to 0.25 % CHAPS using PBS containing protease inhibitors and incubated overnight on a rotating wheel with 10 μ l pre-immune serum at 4 °C. Protein A beads (50 μ l) were added for 3 h and the mixture was then centrifuged for 1 min at 13000 g. The supernatant was removed and divided into 2 x 450 μ l aliquots. One portion was incubated overnight with 10 μ l pre-immune sera, the other with 10 μ l α ER2Ins, and then for a further 3 h with 50 μ l Protein A beads. The beads were isolated as before, washed ten times with PBS containing 0.25 % CHAPS and protease inhibitors, and were boiled in SDS-PAGE buffer to elute the immunoprecipitated proteins. The samples were run on an 8 % gel, electroblotted onto nitrocellulose and the cell surface labelled immunoprecipitates detected using a streptavidin alkaline phosphatase conjugate and NBT/BCIP substrate as outlined in *section 2.3.3.3*.

5.2.15 ISOLATION OF CYTOSOLIC PLATELET PROTEINS WHICH BIND CYTOPLASMIC APOER2.

Cytosolic proteins were prepared by ultrasonic disruption of washed platelets suspended in 20 ml of ice-cold PBS, containing 2 mM sodium orthovanadate and the protease inhibitor cocktail, using a Sanyo Soniprep 150 (15 x 20 s bursts at 8 μ m amplitude with 20 s cooling intervals). Lysates were freed of intact cells, mitochondria and granules by centrifugation at 19000 g for 30 min at 4 °C and then recentrifuged at 100000 g for 1 h to pellet the membranes, leaving cytosolic proteins in the supernatant. Ten mg of the peptide used for α ER2Ins production was coupled to a 1 ml NHS-Sepharose HiTrap column (Pharmacia) as described by the manufacturers. The platelet cytosol was pre-cleared by passage through a Sepharose 4-B column (10 ml) equilibrated in sonication buffer and then recirculated through the peptide-Sepharose matrix overnight at 4 °C. The column was washed with 10 vol. of buffer and bound proteins eluted with PBS containing 0.5 M NaCl. The eluate was concentrated and desalted using a Vivaspin 15 ml concentrator (10000 MWCO; Vivascience Ltd., Binbrook, UK) and the proteins separated by SDS-PAGE. Gels were either silver stained or immunoblotted for phosphotyrosine (P-Tyr Western Blotting Kit; Calbiochem).

5.3 Results and Discussion.

5.3.1 IDENTIFICATION OF THE ANTI-PLATELET DOMAIN WITHIN THE APOE MOLECULE.

A step towards understanding the mechanism(s) by which apoE inhibits platelet aggregation, is identification of functionally important domains within this apolipoprotein. Indeed, if an anti-platelet domain is defined, it could be used to identify the nature of the cellular interactions that lead to changes in intracellular NO signalling. To this end, I sought to identify a fragment or synthetic peptide of apoE that would mimic the inhibitory activity of the native apolipoprotein.

5.3.1.1 The Inhibitory Activity of ApoE is Located in its Amino Terminus.

Thrombin cleaves apoE at residues 191 and 215 (reviewed in [89]), generating a 22 kDa amino-terminal fragment (1-191) and a 10 kDa carboxyl-terminal fragment (215-299) that closely approximate the two functional domains of apoE (*section 1.3.6*). Preliminary experiments indicated that the anti-platelet activity of apoE was localised in the amino-terminal domain of the protein, since the 22 kDa thrombolytic fraction of apoE was equally as potent as “native” apoE when tested at 0.57 μM (Figure 5.3-1).

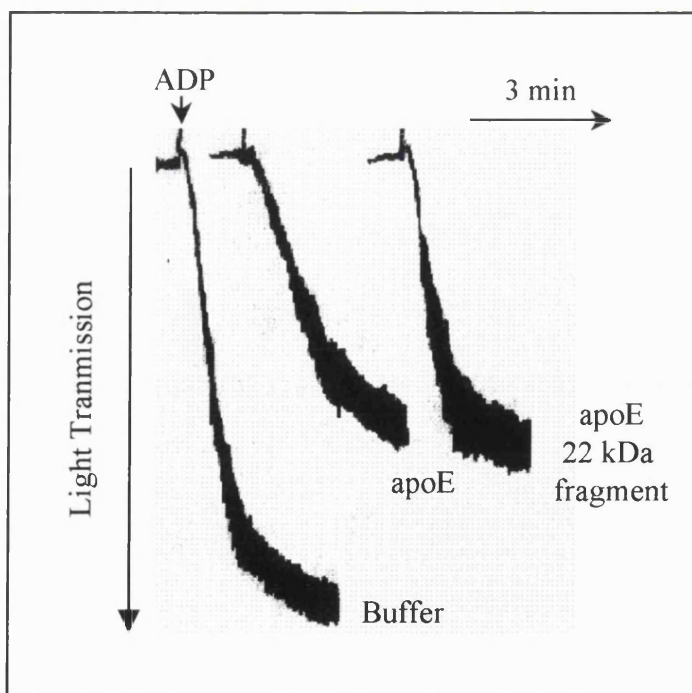


Figure 5.3-1 The inhibitory activity of apoE is located in its amino terminus.

Washed platelets ($3 \times 10^8 / \text{ml}$) were pre-incubated with 0.57 μM of either apoE:DMPC or the apoE 22 kDa fragment for 30 s at 37 °C and then threshold concentrations of ADP added (5-7 μM).

5.3.1.2 Effects of ApoE Synthetic Peptides and Lactoferrin on Platelet Aggregation.

A number of approaches, including the use of monoclonal antibodies, natural mutants, site-specific mutants generated *in vitro* and synthetic peptides have indicated that residues 130-160 of apoE are important for its physiological function (reviewed in [89]). Indeed, this region of apoE facilitates its binding to both HSPG and LRSF members [89]. Since the 22 kDa thrombolytic fragment of apoE contains residues 130-160, several peptides corresponding to sequences within this region (Table 5.3-1) were tested for their ability to inhibit platelet aggregation. This included a tandem peptide, E₍₁₄₁₋₁₅₅₎₂, which is reported to have a higher affinity for LRSF members than its monomeric equivalent (E₁₄₁₋₁₅₅), probably due to its ability to form an α -helical structure similar to “native” apoE [347]. A peptide sequence within the carboxyl 10 kDa apoE fragment (E₂₆₃₋₂₈₆) served as a control.

Activity was localised to the region encompassed by residues 133-155 since peptides: E₁₃₃₋₁₄₅, E₁₄₁₋₁₅₅ and E₍₁₄₁₋₁₅₅₎₂ all inhibited platelet aggregation to a similar degree, ~ 30 % as effective as “native” apoE when tested at 3.0 μ M (Table 5.3-2). In contrast, a peptide corresponding to the carboxyl-terminal 10 kDa apoE fragment (E₂₆₃₋₂₈₆) had no significant anti-platelet activity. The essential feature of the inhibitory activity appeared to be the presence of a lysine and arginine rich area; amino acids 142-145 (RKLR). Indeed, the importance of arginine residues for the anti-platelet effect of apoE was demonstrated directly in *Chapters 3 & 4*. Thus, neutralisation of the arginine residues of apoE blocked not only the anti-aggregatory effect (*section 3.3.7*) but also the increase in intra-platelet levels of cGMP (*section 4.3.2*). Taken together, these data support the idea that the positively-charged motif encompassed by residues 142-145 of apoE is particularly important in facilitating inhibition of platelet aggregation.

Peptide	Amino acid sequence
E ₁₄₁₋₁₅₅	LR K LR K RLLRDADDL
Tandem E ₍₁₄₁₋₁₅₅₎₂	LR K LR K RLLRDADDL-LR K LR K RLLRDADDL
E ₁₃₃₋₁₄₅	LRVRLASHLR K LR
E ₂₆₃₋₂₈₆	SWFEPLVEDMQRQWAGLVEKVQAA
Lactoferrin ₂₄₋₃₅	QRNMR K VRGPPV

Table 5.3-1 Amino acid sequences of apoE and lactoferrin peptides.

Arginine (R) and lysine (K) residues implicated in receptor binding are highlighted in bold.

Polypeptide	Inhibition of Aggregation (% of control)
“native” apoE	70.05 ± 7.3 %, <i>P</i> <0.001
E ₁₄₁₋₁₅₅	26.5 ± 3.0 %, <i>P</i> <0.001
Tandem E ₍₁₄₁₋₁₅₅₎₂	26.3 ± 5.9 %, <i>P</i> <0.05
E ₁₃₃₋₁₄₅	21.9 ± 3.5 %, <i>P</i> <0.02
E ₂₆₃₋₂₈₆	4.2 ± 3.1 %, <i>P</i> =NS

Table 5.3-2 Synthetic peptides inhibit ADP-induced platelet aggregation.

PRP ($1-2 \times 10^8$ cells/ml) was pre-incubated with peptide or apoE:DMPC (all 3.0 μ M) for 10 min at 37 °C. The extent of aggregation was measured 3 min after addition of a pre-determined threshold concentration of ADP (5-7 μ M) and is expressed as a percentage of controls with buffer alone. Points are the mean percentage inhibition of aggregation (\pm SEM) for three separate platelet suspensions. The difference between the means (\pm apoE) assessed by Student's *t*-test.

It is intriguing that the putative anti-platelet sequence (142-145) is located within the LRSF-binding region, since I have previously shown that aqueous solutions of apoE, which bind poorly to LDL-R [275], are ineffective inhibitors of platelet aggregation (section 3.3.4). Indeed, additional support for the involvement of a LRSF member was provided by the observation that lactoferrin, though less potent than apoE, also exhibited anti-platelet properties (25.0 ± 13.4 % versus 88.9 ± 3.3 % inhibition at 3.0 μ M, *P*<0.05, *n*=3, Figure 5.3-2, panels A & B and [348, 349]). This 76 kDa glycoprotein contains a RKvR motif in its amino-terminal domain (residues 28-31, Table 5.3-1), which binds to platelets and inhibits aggregation [350, 351]. Interestingly, lactoferrin also binds to LRSF members: LRP, gp330 and VLDL-R [159, 352]. However, this must be viewed with some caution as human lactoferrin has been shown to possess both high-affinity and low-affinity binding sites on platelets [348]. The high-affinity site has recently been shown to be a specific lactoferrin receptor that is distinct from the LRSF members [353]. Nevertheless, the identification of the low-affinity site is still unknown but might be a receptor that shares affinity for both lactoferrin and apoE. Interestingly, however, the VLDL-R may be discounted at this stage, since the putative anti-platelet sequence of apoE (RKxR:142-145) does not mediate binding to VLDL-R [354].

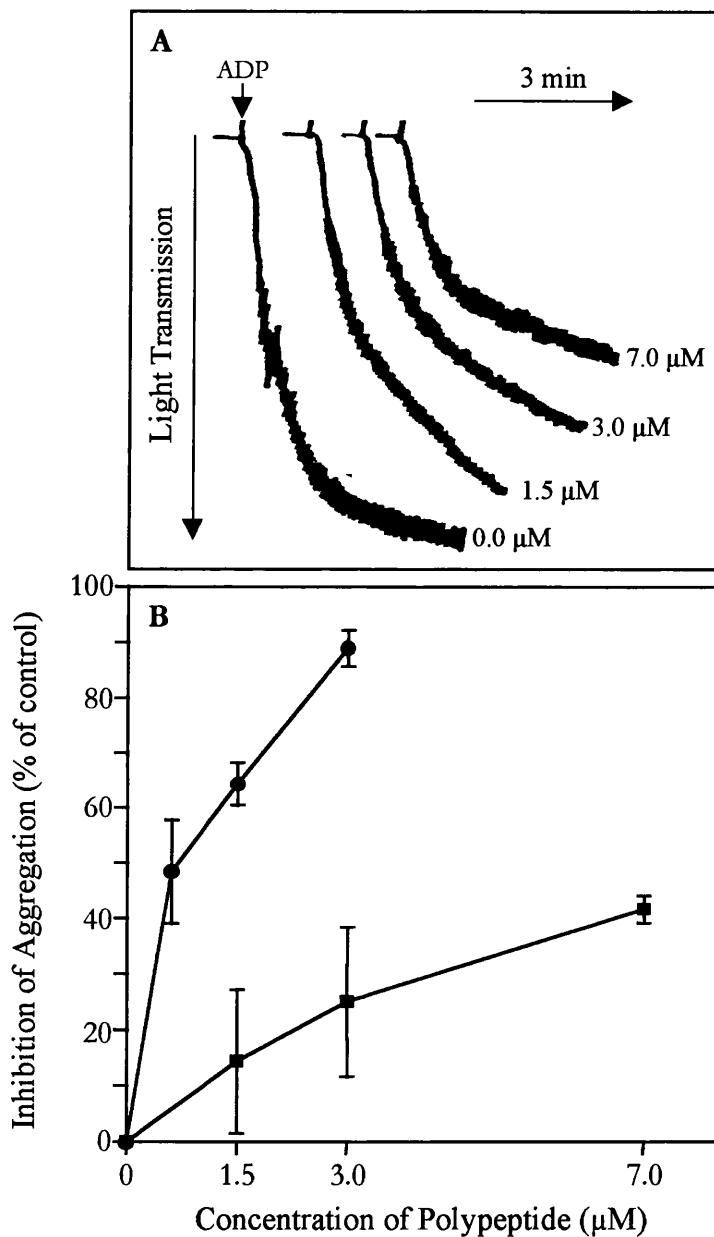


Figure 5.3-2 Lactoferrin inhibits ADP-induced platelet aggregation.

Panel A, Washed platelets (3×10^8 cells/ml) were pre-incubated with increasing quantities of lactoferrin for 30 s at 37°C and then threshold concentrations of ADP ($5\text{--}7 \mu\text{M}$) added. **Panel B**, Washed platelets (3×10^8 cells/ml) were pre-incubated with lactoferrin (●) or apoE-3:DMPC (◼) as before. The extent of aggregation was measured 3 min after addition of a pre-determined threshold concentration of ADP ($5\text{--}7 \mu\text{M}$) and is expressed as a percentage of controls with buffer alone. Points are the mean percentage inhibition of aggregation (\pm SEM) for three separate platelet suspensions.

5.3.2 CHARACTERISTICS OF THE PLATELET APOE RECEPTOR.

The circumstantial evidence cited so far suggests that the anti-platelet effects of apoE are mediated via an interaction with a LRSF member. In order to further test this hypothesis, a LRSF antagonist, which would compete with apoE for binding to these receptors, was sought.

5.3.2.1 Effect of RAP on ApoE-Induced Inhibition of Platelet Aggregation.

The LRSF antagonists most commonly used in the literature include: specific anti-LRSF blocking antibodies [355-359], lactoferrin [159, 352, 360] and the 39 kDa endoplasmic reticulum/Golgi receptor-associated protein (RAP) [178-180]. Unfortunately, anti-LRSF blocking antibodies are not generally available and problems may occur if the antibody binds to the platelet Fc receptor; an interaction that can lead to unpredictable effects on platelet aggregation [361, 362]. Similarly, although lactoferrin could be used, its effects on newly-characterised LRSF members are still to be elucidated and its ability to inhibit platelet aggregation would confuse the interpretation of any results obtained. RAP, on the other hand, is well characterised; it binds to all the known mammalian LRSF members, and *in vitro* experiments show that it inhibits binding of apoE to these receptors [178-180]. When RAP and apoE:DMPC were co-incubated with platelets, the anti-platelet action of apoE:DMPC was found to be significantly reduced (30.6 ± 6.6 versus 62.5 ± 2.9 % inhibition; $P < 0.001$, $n=3$, Figure 5.3-3, *panels A and B*). In contrast, no significant effect on platelet aggregation was observed with RAP treatment alone when compared to untreated controls (9.8 ± 6.6 versus 0.0 ± 2.8 % inhibition; $P > 0.05$, $n=3$, Figure 5.3-3, *panel A*). Thus, these data provide compelling evidence that the anti-platelet effects of apoE are mediated via an interaction with a LRSF member.

5.3.2.2 HEL Cells and Platelets Do Not Contain the LRP.

Since apoE, lactoferrin and RAP are all recognised by the well characterised LRP [159], it is a candidate cell surface protein for mediating the anti-platelet effects of apoE. Recently, a monoclonal antibody has been raised against LRP, which has been used to investigate the expression of LRP on a variety of cell types [156]. This antibody, designated $\alpha 2MR2$, was used to probe membrane extracts from both platelets and HEL cells for the presence of LRP. Membrane extracts of the hepatocarcinoma cell line, HepG2, and purified placental LRP served as controls. As shown in Figure 5.3-4, both HepG2 extracts and purified LRP readily stained a 500 kDa species, however, HEL and platelet extracts were devoid of staining. Since this study was performed using the highly sensitive ECL detection system, it is unlikely that cells of the megakaryocytic lineage express the LRP.

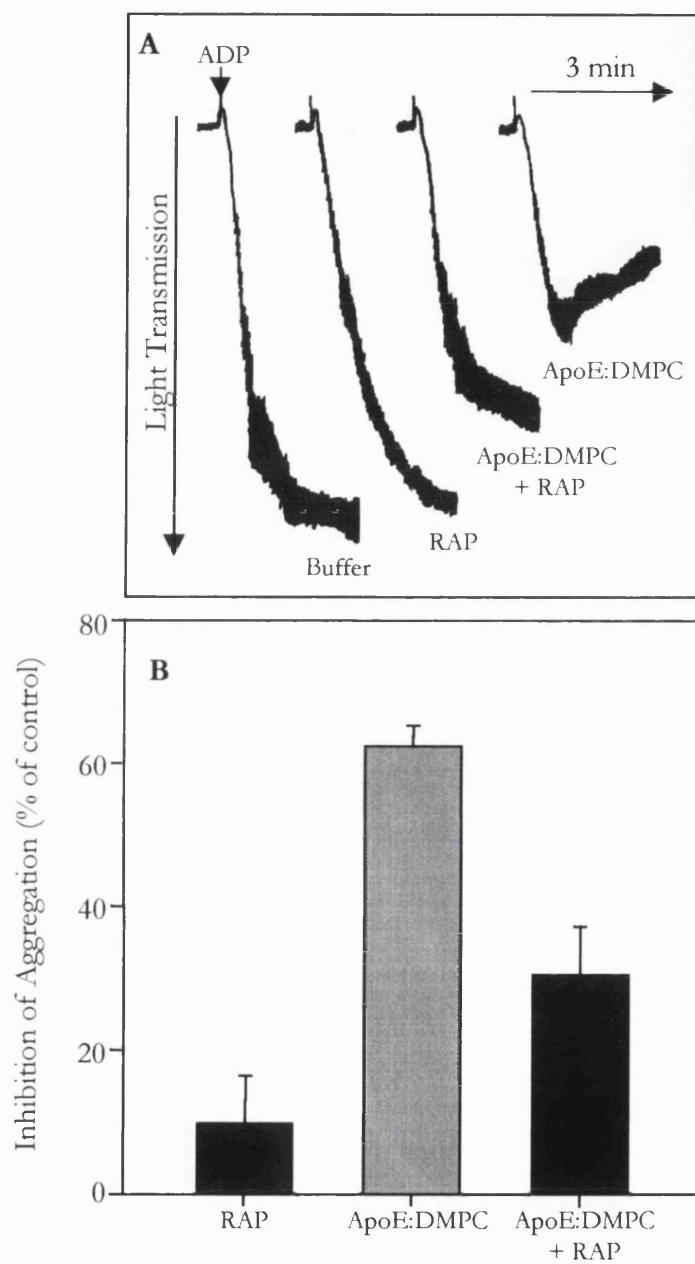


Figure 5.3-3 RAP blocks the anti-aggregatory effect of apoE:DMPC.

Panel A, Aliquots of PRP ($1-2 \times 10^8$ cells/ml) were pre-incubated with either $1.47 \mu\text{M}$ apoE:DMPC ($50 \mu\text{g protein/ml}$), $1.47 \mu\text{M}$ RAP or both apoE:DMPC and RAP for 10 min at 20°C then threshold concentrations of ADP ($1-2 \mu\text{M}$) were added. The aggregation traces shown are from one experiment but were reproduced in two independent assays. **Panel B,** The extent of aggregation was measured 3 min after addition of a pre-determined threshold concentration of ADP ($5-7 \mu\text{M}$) and is expressed as a percentage of controls with buffer alone. Points are the mean percentage inhibition of aggregation (\pm SEM) for three separate platelet suspensions.

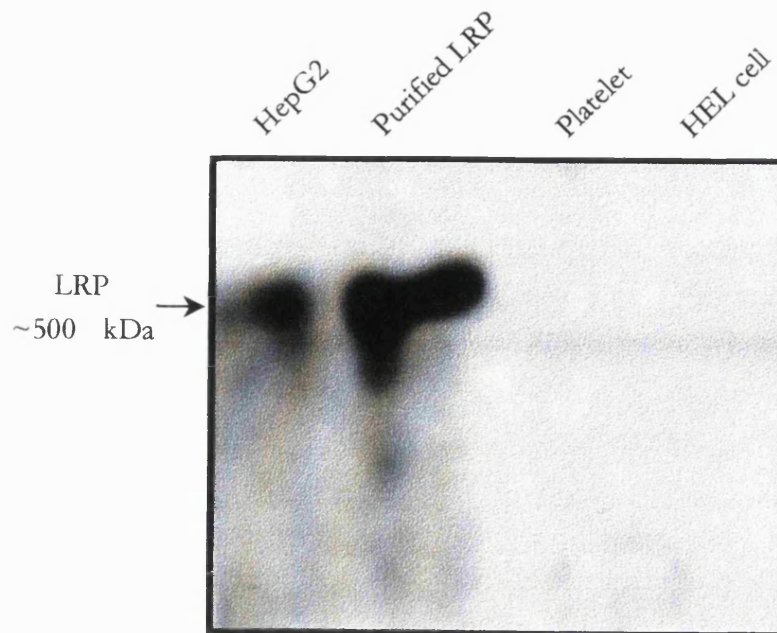


Figure 5.3-4 Immunoblot analysis of LRP in platelet membranes.

Cell membranes were isolated as described in section 5.2.6. Membrane extracts (200 μg) and purified LRP (2.5 μg) were run on a 3 - 8 % SDS-PAGE gel under non-reducing conditions prior to Western blotting using $\alpha 2\text{MR2}$. The LRP bands were visualised using the Amersham ECL substrate.

5.3.2.3 Inhibition of Platelet Aggregation by ApoE Isoforms.

Human apoE exists in three common polymorphic forms (section 1.3.5): apoE-2 (Arg158Cys), apoE-3 (wild type) and apoE-4 (Cys112Arg), which have been shown to possess differing affinities towards the various LRSF members. ApoE-3 and apoE-4 both exhibit high affinity binding to all LRSF members studied to date [89]. ApoE-2, on the other hand, binds poorly to both the LDL-R and LRP (only 1 % [278, 363] and 40 % [154] of apoE-3 binding activity, respectively) but binds normally to the VLDL-R [354, 364]. In an attempt to further clarify the ligand specificity of the platelet apoE receptor, the inhibitory potency of the three apoE isoforms was determined. ApoE-3, apoE-2 and apoE-4 (all 20 μg protein/ml) inhibited ADP-induced aggregation to a similar degree (Figure 5.3-5, *panel A*). Repeated experiments could not distinguish the ability of apoE-2, apoE-3 and apoE-4 to inhibit washed platelet aggregation (E-2; 70.0 ± 8.3 % *versus* E-3; 81.8 ± 8.4 % *versus* E-4; 74.9 ± 7.7 % inhibition at 50 μg protein/ml [1.47 μM] apoE:DMPC, $P > 0.05$, $n=3$, Figure 5.3-5, *panel B*). These data indicate that the anti-platelet effects of apoE are mediated via an interaction with a LRSF member that has a relaxed specificity towards the apoE isoforms, probably reflecting a ligand binding domain structure similar to that of the VLDL-R.

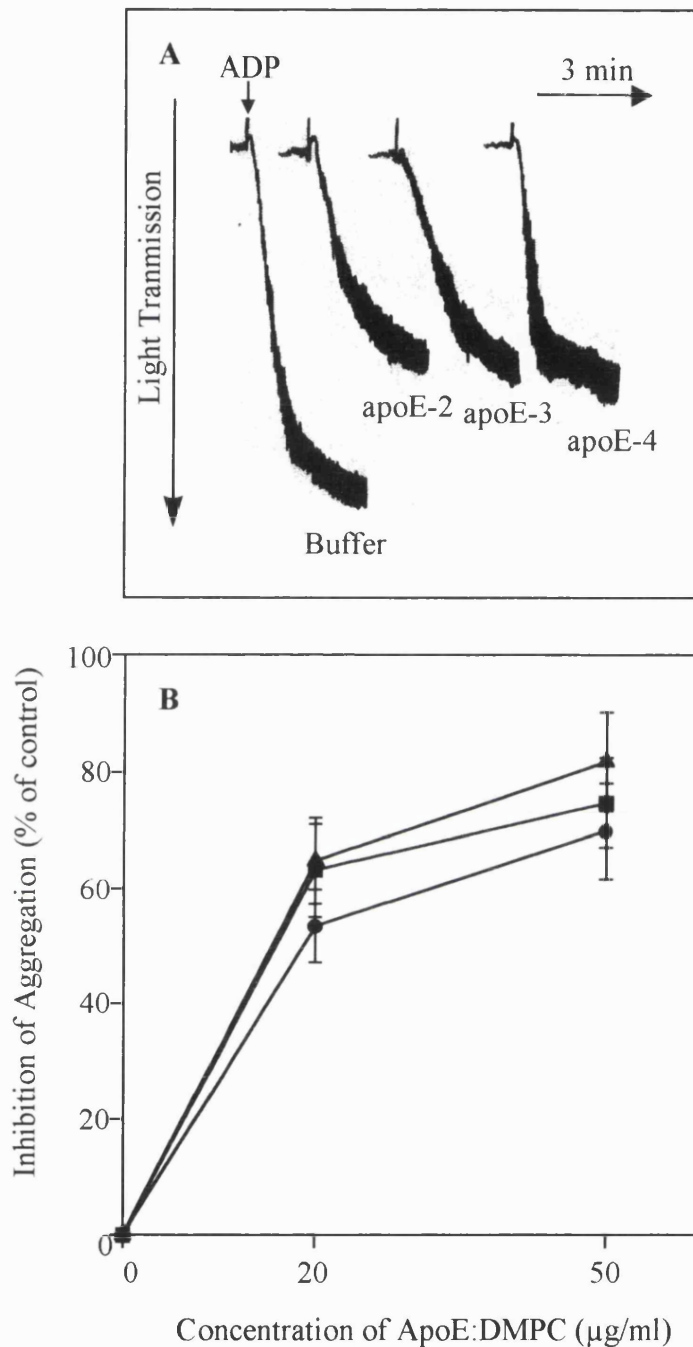


Figure 5.3-5 ApoE-2, apoE-3 and apoE-4 all inhibit ADP-induced platelet aggregation.

Panel A, Washed platelets (3×10^8 cells/ml) were pre-incubated with 20 μg protein/ml apoE-2:DMPC, apoE-3:DMPC or apoE-4:DMPC for 30 s at 37 °C and then threshold concentrations of ADP (5-7 μM) added. **Panel B,** Washed platelets (3×10^8 cells/ml) were pre-incubated with apoE-2:DMPC (●), apoE-3:DMPC (▲) or apoE-4:DMPC (◐) as before. The extent of aggregation was measured 3 min after addition of a pre-determined threshold concentration of ADP (5-7 μM) and is expressed as a percentage of controls with buffer alone. Points are the mean percentage inhibition of aggregation (\pm SEM) for three independent experiments.

5.3.3 CHARACTERISTICS OF THE PLATELET APOE RECEPTOR - CONCLUSIONS.

The evidence cited so far strongly suggests that the trigger for NO release, and hence for inhibition of aggregation, is an interaction of apoE with a LRSF member. However, it is highly unlikely that the well characterised receptors, LDL-R, LRP or VLDL-R, mediate the apoE-induced inhibition of platelet aggregation. Thus, it has previously been reported that platelets and megakaryocytes do not contain "classical" LDL receptors [226, 227]. Likewise, in the present study, I have demonstrated by an extremely sensitive Western blotting procedure that cells of the megakaryocytic lineage are devoid of LRP. In agreement with these observations, I found that the monomeric apoE peptide, E₁₄₁₋₁₅₅, was just as effective an anti-platelet agent as the tandem peptide E_{(141-155)₂}, however, due to its low α -helical content [347], E₁₄₁₋₁₅₅ has a low binding affinity for both the LDL-R [365] and LRP [366]. Additionally, apoE-2, which is defective in binding to both the LDL-R and LRP, inhibited platelet aggregation to the same extent as wild type apoE-3. Since both *in vitro* [354] and *in vivo* [364] experiments have demonstrated that the VLDL-R binds to apoE-2 with the same affinity as apoE-3 and apoE-4, it would seem a likely candidate for mediating the anti-platelet effects of apoE. However, the putative anti-platelet sequence of apoE (RKxR: 142-145) is not involved in mediating its binding to the VLDL-R. This conclusion is born from the observation that 1D7, an anti-apoE monoclonal antibody, binds to an epitope in the immediate vicinity of residues 143-145 [138] but fails to compete with apoE for binding to the VLDL-R [354]. This implies that the anti-platelet effects of apoE are mediated by one of the newly characterised apoE receptors, gp330 or apoER2. Alternatively, platelets might contain a completely novel receptor.

5.3.4 HOMOLGY CLONING OF THE PLATELET RECEPTOR.

In order to identify the platelet receptor, a homology cloning approach was instigated. Sets of degenerate primers were used in RT-PCR to amplify the cysteine-rich class A, apoE binding repeats of the LRSF members. This domain was chosen because class A repeats are highly conserved not only between the individual LRSF members but also within each individual receptor. This greatly increases the chance of detecting proteins that contain multiple class A repeats, since the oligonucleotide primers can anneal to many different sites along the cDNA transcript. In addition, this domain has been identified in a number of related proteins/receptors, which are not regarded as LRSF members. Of particular interest is a newly identified gene in *L. stagnalis*, which has homology with both class A repeats and G-protein activating domains [343]. If

mammalian cells express similar hybrid receptors, these proteins might well mediate apoE-induced intra-platelet NO production. Therefore, the oligonucleotide primers were designed to incorporate sufficient degeneracy to amplify unknown proteins/receptors as well as known LRSF members. However, based on the cDNA sequences of known human class A repeats, the level of degeneracy required for the sense primer was deemed excessively high. Therefore, two degenerate sense primers were designed, one to amplify human “LRP-like” class A repeats, the other to amplify “LDL-R-like” repeats. Additionally, since human peripheral blood platelets are anucleate fragments of precursor megakaryocytes and as such contain only small amounts of residual intact mRNA, two well characterised human leukaemia megakaryoblastic cell lines HEL [258, 259] and Meg-01 [258, 260] were also used in the RT-PCR.

5.3.4.1 RT-PCR Using Degenerate Primers Designed Against “LRP-like” Class A Repeats.

Initial RT-PCR experiments using HEL mRNA and the LDLA2/LDLA3 primer pair (designed against the LRP and gp330) gave a specific 130 bp product (Figure 5.3-6, *panel A*) which is consistent with the distances between each class A repeat (~40 amino acids). However, sequence analysis of this product revealed 100 % identity with the human basement membrane HSPG, perlecan. Neither LRP nor gp330 were found, thus confirming the earlier LRP Western blotting data (*section 5.3.2.2*). In contrast, two specific PCR products (~130 bp and ~275 bp) were successfully amplified from foetal liver mRNA (Figure 5.3-6, *panel B*). Upon sequencing, both products were identified as LRP transcripts; the 130 bp product representing one complete class A repeat and the 275 bp product representing two repeats, thus demonstrating the ability of these oligonucleotides to identify LRSF member transcripts.

Perlecan HSPG contains four class A repeats [367], binds apoE *in vitro* and *in vivo* and has been previously characterised as an endocytotic receptor for apoE-containing lipoproteins (reviewed in [342]). Nevertheless, previous experiments characterising the nature of the platelet receptor precluded a prominent role for perlecan in mediating the anti-platelet effects of apoE. Thus, RAP does not block apoE binding by perlecan [158, 159, 368-370] and apoE-2 is bound with much lower affinity than apoE-3 [125]. Moreover, perlecan is regarded as a passive endocytotic receptor, since ligand binding does not appear to trigger intra-cellular events [342].

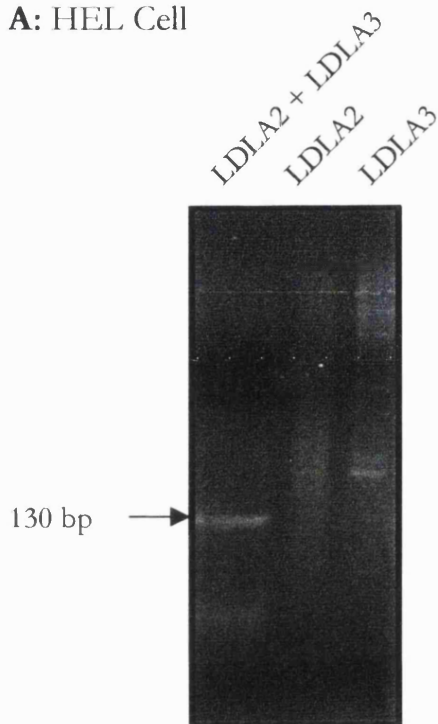
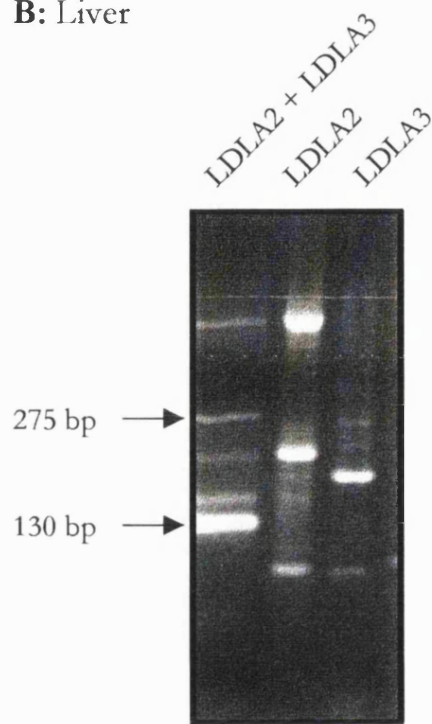
A: HEL Cell**B: Liver**

Figure 5.3-6 RT-PCR using degenerate primers designed against the LRP and gp330.

Five μ l aliquots of HEL (**panel A**) or foetal liver (**panel B**) cDNA were subjected to “hot-start” PCR (section 5.2.10) in a total volume of 50 μ l, with either 10 μ M sense primer (LDLA2) alone, 10 μ M anti-sense primer (LDLA3) alone or both LDLA2 and LDLA3 together. After heating at 95 °C for 10 min, amplification proceeded for 40 cycles, with denaturation for 30 s at 95 °C, annealing for 1 min at 53 °C and extension for 1 min at 72 °C. Finally, the reaction was completed by an extension step at 72 °C for 10 min. One tenth (5 μ l) of the products of the initial amplification reaction were then subjected to a subsequent round of PCR amplification. Reaction products were visualised and photographed under UV light after electrophoresis of 10 μ l of the product in a 2 % agarose gel containing 0.3 μ g/ml ethidium bromide. PCR products that were unique to the LDLA2/LDLA3 primer pair were excised from the gel, cloned and sequenced as outlined in sections 2.6.6-2.6.8.

5.3.4.2 RT-PCR Using Degenerate Primers Designed Against “LDL-R-like” Class A Repeats.

Experiments using HEL mRNA and primers designed against the LDL-R, VLDL-R and apoER-2 (LDLA1/LDLA3) produced more promising results. Sequence analysis of a specific 120 bp product (Figure 5.3-7, *panel A*) revealed 100 % identity with the newly described human apoER2. Neither the VLDL-R nor any other LRSF member was detected in HEL cells. Control experiments using the same primer pair and human foetal liver mRNA gave a specific 130 bp product (Figure 5.3-7, *panel B*) that had 100 % identity to human LRP.

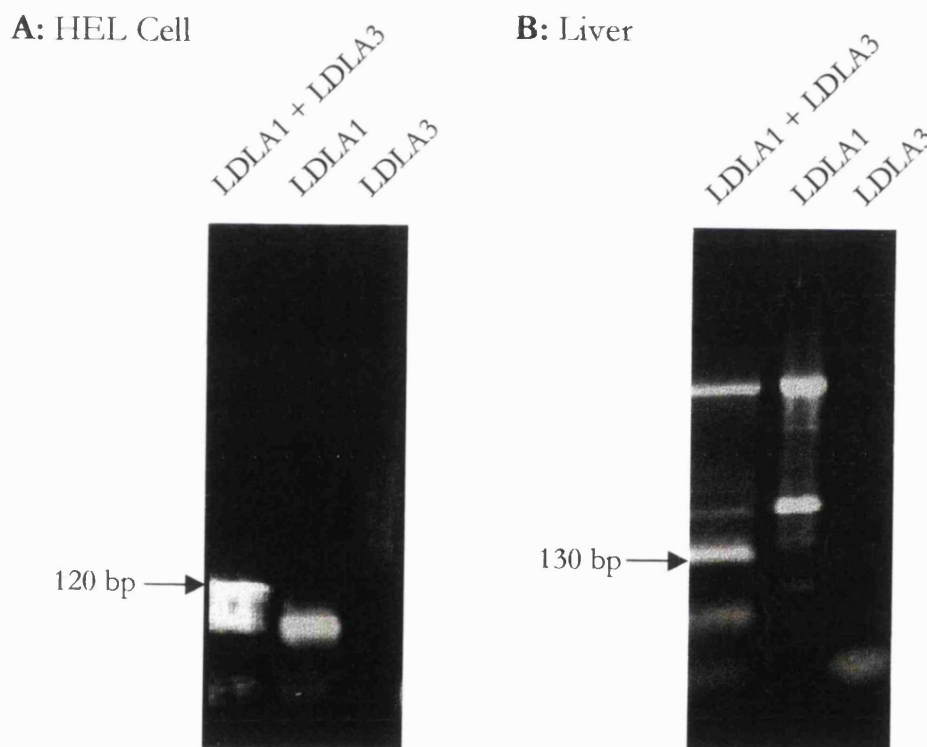


Figure 5.3-7 RT-PCR using degenerate primers designed against the LDL-R, VLDL-R and apoER2

Five μ l aliquots of HEL (panel A) or foetal liver (panel B) cDNA subjected to “hot-start” PCR (section 5.2.10) in a total volume of 50 μ l, with either 10 μ M sense primer (LDLA1) alone, 10 μ M anti-sense primer (LDLA3) alone, or both LDLA1 and LDLA3 together. PCR was performed as outlined in Figure 5.3-6. PCR products that were unique to the LDLA2/LDLA3 primer pair were excised from the gel, cloned and sequenced as outlined in sections 2.6.6-2.6.8.

As outlined in *section 1.3.7.5*, apoER2 is expressed predominantly in the mammalian brain and placenta and consists of five domains that resemble those of the LDL-R and the VLDL-R [172]. An important structural difference among these three receptors is the number of class A repeat sequences in their ligand-binding domains; apoER2 and LDL-R contain seven, whereas the VLDL-R has eight. Although apoER2 and LDL-R contain the same number of repeats, the ligand-binding domain structure of apoER2 is more closely related to that of VLDL-R. This is reflected not only in the amino acid homology between the proteins (ranging from 45 - 63 % identity per class A repeat) but also in the ligand binding domain architecture [172]. Moreover, the high degree of homology between apoER2 and VLDL-R make it an ideal candidate for mediating the anti-platelet effects of apoE. Thus, the ligand specificity of apoER2 resembles that of a “VLDL-R-like” platelet protein; apoER2 binds to both RAP [174] and apoE-containing lipoproteins [172, 173] with high affinity. Indeed, apoE-2 binds to apoER2 with the same affinity as apoE-3 and apoE-4 (personal communication, T. Yamamoto). Intriguingly, the major difference between apoER2 and the VLDL-R is an insertion sequence of 59 amino acids in the cytoplasmic tail of apoER2 (Figure 5.3-8, *panel A*), which is stated to represent a unique sequence not found in any published protein [172, 175]. Can this insertion sequence mediate apoE-induced NO production? Clearly, further characterisation of platelet apoER2 is required.

5.3.5 CHARACTERISATION OF PLATELET APOER2.

5.3.5.1 RT-PCR Using Specific Primers Designed Against ApoER2.

To confirm the presence of apoER2 in cells of the megakaryocytic lineage, RT-PCR was carried out using mRNA from HEL cells, Meg-01 cells and platelets with a specific primer pair. These primers, encompass the O-linked sugar domain, the transmembrane region and the unique cytoplasmic insertion sequence of apoER2 and are predicted to amplify a 604 bp product (Figure 5.3-8, *panel A*). Accordingly, a product of ~600 bp was amplified from HEL, Meg-01 and platelet mRNA but not from blood monocytes, lymphocytes or neutrophils (Figure 5.3-8, *panel B*).

Analysis of the published cDNA sequence for apoER2 indicated that the 604 bp PCR product should contain one restriction site for SmaI and two for PstI. The expected sizes of the restriction fragments are indicated in Figure 5.3-9, *panel A* and were indeed obtained on both SmaI and PstI digestion (Figure 5.3-9, *panel B*). Further confirmation that the 604 bp product was apoER2 was obtained by direct sequencing (results not shown).

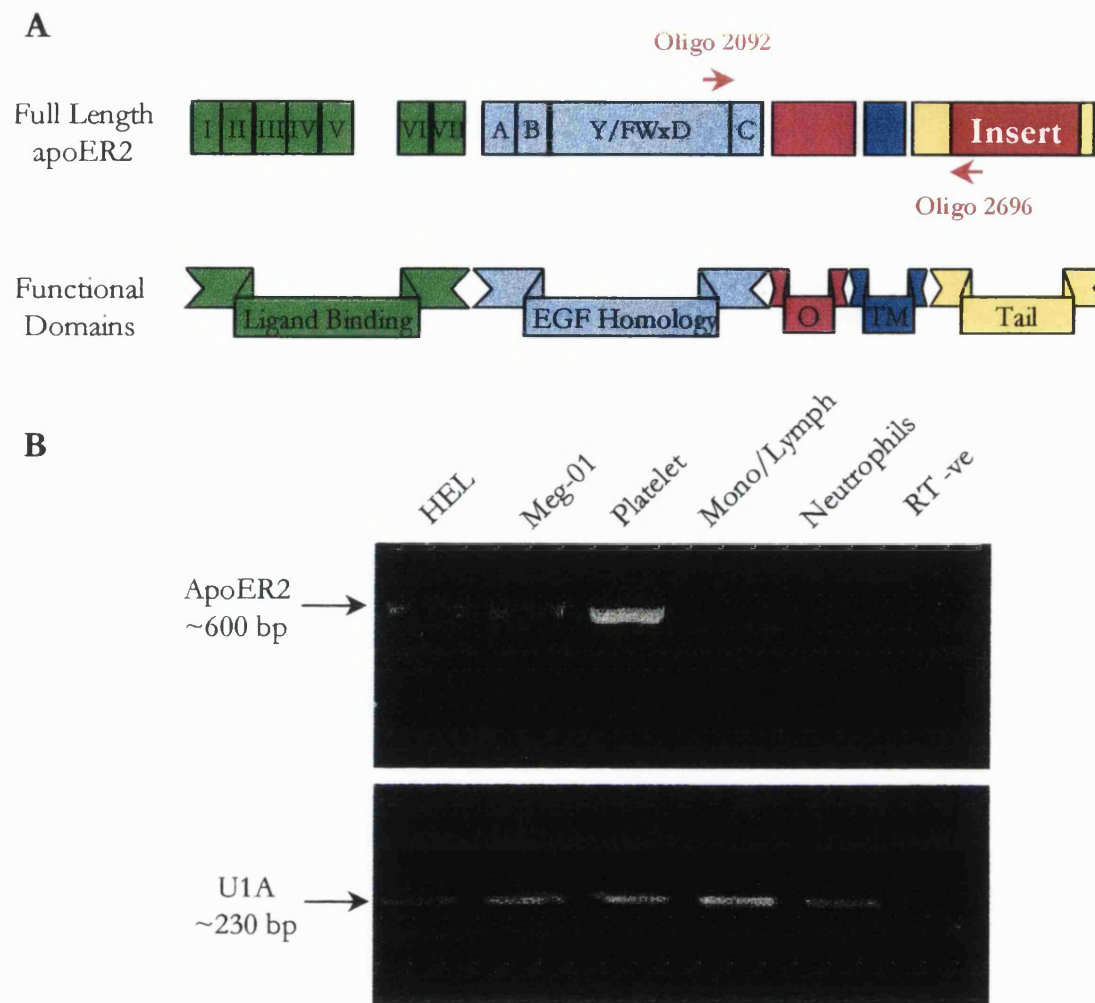


Figure 5.3-8 Specific primers directed towards apoER2 amplify a 604 bp product in platelets.

Panel A, The relevant structural features of apoER2. The LDL-R class A repeats (I - VII), epidermal growth factor (EGF) homology repeats (A,B & C), Y/FWxD repeats, O-linked sugar domain (O), transmembrane region (TM) and cytoplasmic tail containing a unique 59 amino acid insert (Insert) are indicated. **Panel B**, mRNA from platelets, HEL cells, Meg-01 cells, monocytes/lymphocytes and neutrophils were used for cDNA synthesis with reverse transcriptase. The integrity of the cDNA produced was confirmed by a U1A RT-PCR (section 5.2.9). The resulting viable cDNAs were used for apoER2 PCR amplification with the indicated primer combinations (red arrows, Panel A). Amplified products were separated on 2 % agarose gels. The results shown were from one experiment but were reproduced in two independent reactions.

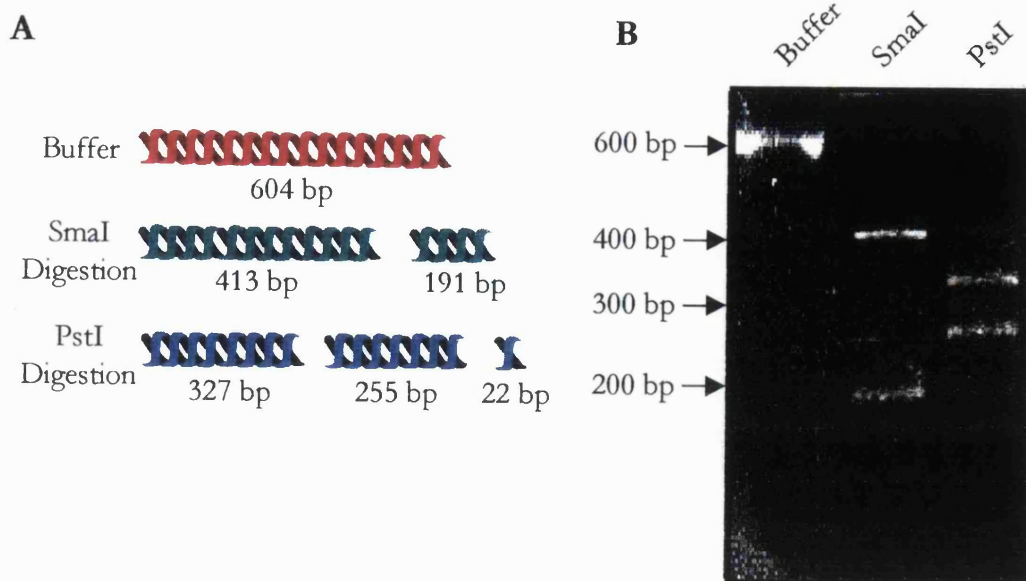


Figure 5.3-9 Restriction mapping of the platelet 604 bp PCR product.

Panel A, The predicted product sizes after digestion of the 604 bp apoER2 PCR product with the restriction enzymes, SmaI and PstI. **Panel B**, The 604 bp PCR product was incubated for 1 h with either buffer alone, SmaI or PstI using the reaction conditions outlined in Table 2.6-2. Digested products were separated on a 2 % agarose gel.

5.3.5.2 Alternative Splicing of Platelet ApoER2.

Recent studies at the cDNA and genomic level have revealed that several splice variants of apoER2 are produced in the brain [173, 175]. These include variants of apoER2 either lacking repeats 4-6 (apoER2 Δ 4-6) or 4-7 (apoER2 Δ 4-7) in the ligand binding domain. In order to determine whether any of these variants are expressed in cells of the megakaryocytic lineage, RT-PCR was carried out using mRNA from HEL cells, Meg-01 cells and platelets with published primers that flank the ligand-binding domain of apoER2 [173] (Figure 5.3-10, *panel A*). As previously reported, multiple products of unexpected length were obtained probably due to mis-priming. However, Southern hybridisation using an internal probe radiolabelled with ^{32}P gave a major band of ~ 700 bp (Figure 5.3-10, *panel B*). This is the expected length for the PCR product corresponding to apoER2 Δ 4-6 (704 bp).

To determine whether any additional variants are expressed, long RT-PCR was carried out using mRNA isolated from HEL cells with a pair of primers that flank the open reading frame of apoER2 (Figure 5.3-11, *panel A*). A major PCR product of about 2500 nucleotides (~95 % of total) and a minor product of about 2300 nucleotides (~5 % of total) were obtained (Figure 5.3-11, *panel B*). Both products are substantially shorter than the 2894 bp expected for full-length apoER2. Cloning, restriction mapping and partial sequencing of the long RT-PCR products confirmed the absence of repeats 4-6 of the ligand-binding domain in both transcripts (experiments performed by Dr. D. Vinogradov, results not shown). Additionally, the minor band at 2300 bp corresponded to a variant of apoER2 Δ 4-6 lacking the 59 amino acid insertion sequence in the cytoplasmic domain (apoER2 Δ 4-6 Δ Insert; Figure 5.3-11, *panel C*).

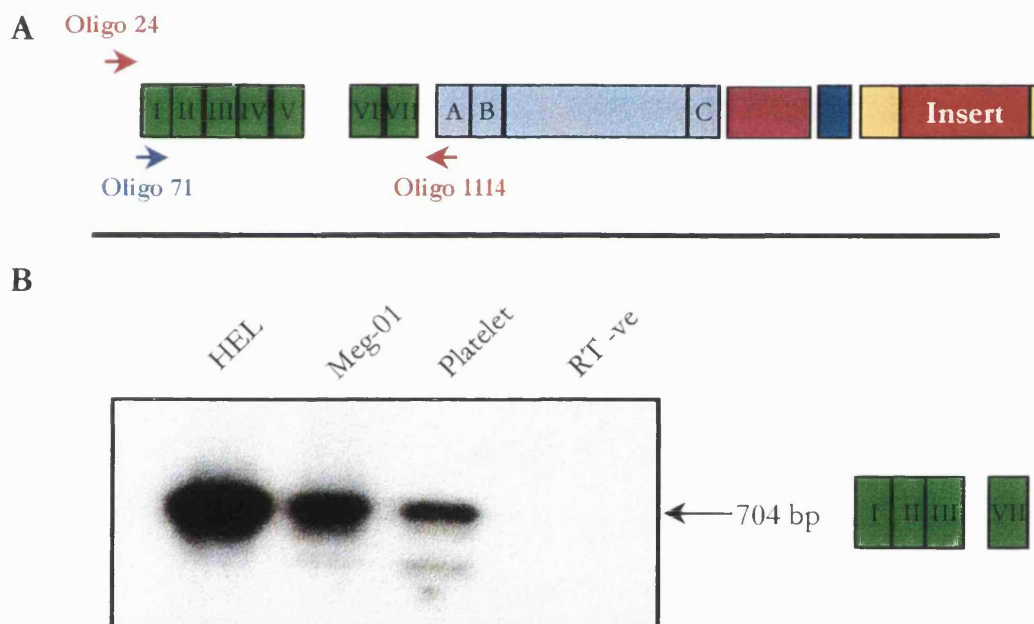


Figure 5.3-10 Expression of apoER2 Δ 4-6 in human platelets.

cDNA from platelets, HEL cells and Meg-01 cells were used for PCR with the indicated primer combinations (red arrows). PCR products were subsequently subjected to Southern blotting using an internal oligonucleotide probe (oligo 71, blue arrow) as outlined in section 5.2.11. The results shown were from one experiment but were reproduced in two independent reactions.

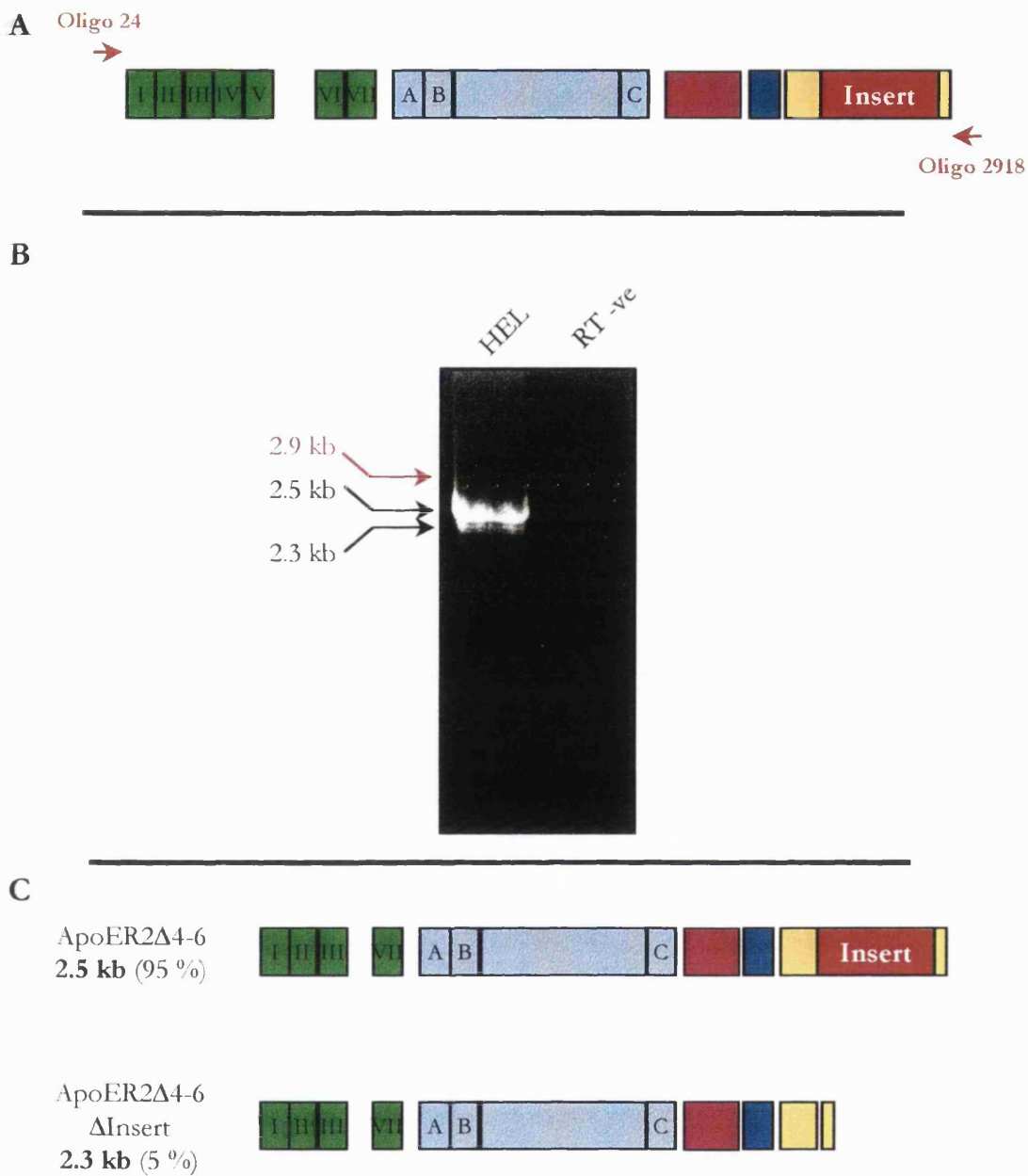


Figure 5.3-11 Long PCR of HEL cell apoER2.

Panels A & B, cDNA from HEL cells was used for long PCR with the indicated primer combinations (red arrows). Amplified products were separated on 1 % agarose gels. Panel C, Structural features of apoER2 in HEL cells with the functional domains indicated as described in Figure 5.3-8.

5.3.6 PRODUCTION OF AN ANTI-PEPTIDE ANTISERUM TO APOER2.

Due to the extreme sensitivity of RT-PCR, the identification of mRNA transcripts in platelets by this procedure does not necessarily imply that the protein is expressed. Moreover, the instability of residual platelet mRNA makes Northern blot analysis difficult. I therefore decided to produce an anti-peptide antiserum against apoER2 and use this to detect any expressed protein in platelets.

In order to identify an immunogenic region of the apoER2 polypeptide, three main criteria were assessed: the hydrophilicity of the region (using the Hopp and Woods scale [371]), the presence of β -turns and the presence of charged residues [372, 373]. Using these criteria, the most antigenic region of apoER2 was estimated to be a stretch of 17 amino acids (865-881: CLGETREPEDPAPALKE) within the unique cytoplasmic insert of the receptor. Therefore, a rabbit anti-peptide antiserum (α ER2Ins) directed against this peptide was commissioned (Genosys, Cambridge, UK). However, although anti-peptide antisera invariably react strongly with the synthetic antigenic peptide, the ability of this antisera to react with “native” protein is not guaranteed. Thus, Western blotting of solubilized lysates from recombinant CHO cells over-expressing apoER2 was employed to assess the specificity and titre of α ER2Ins. As shown in Figure 5.3-12, α ER2Ins readily stained a non-reduced \sim 130 kDa species and a reduced 160 kDa species in extracts of CHO cells over-expressing apoER2 Δ 4-6 with cytoplasmic insert. This shift in molecular mass between reduced and non-reduced apoER2 Δ 4-6 is characteristic of all LRSF members [374]. In contrast, α ER2Ins failed to detect any proteins in the extracts of CHO cells over-expressing the VLDL-R or apoER2 without cytoplasmic insert (apoER2 Δ Insert). Additionally, the pre-immune sera did not produce any signals in any of the CHO cell extracts tested (results not shown). Thus, these results indicate that α ER2Ins is a sensitive and specific antiserum for the detection of apoER2. However, because this antiserum was commissioned before alternative splicing of apoER2 was recognised, it is only useful for the detection of apoER2 variants containing the cytoplasmic insert.

5.3.7 IMMUNOPRECIPITATION OF PLATELET APOER2.

Western blotting of platelet extracts with α ER2Ins, under identical conditions as described above, produced multiple bands of unexpected sizes due to the secondary antibody cross-reacting with numerous cellular platelet proteins (results not shown). To circumvent this problem, an immunoprecipitation protocol employing cell surface labelled

platelets was adopted. Using this procedure, α ER2Ins recognised a specific platelet cell surface protein with a reduced molecular mass of 132 kDa (Figure 5.3-13). The apparent differences in molecular mass between CHO cells over-expressing apoER2 Δ 4-6 and platelet apoER2 Δ 4-6 (~160 kDa *vs.* 132 kDa) may be explained by differences in the glycosylation. Indeed, it has been recently shown that differences in the ability of cells to glycosylate the VLDL-R can lead to molecular mass shifts of ~17 kDa in SDS-PAGE analysis [375]. Since apoER2 has almost double the potential O-linked glycosylation sites in its O-linked sugar domain as compared to the VLDL-R, it is reasonable to assume that an even greater molecular mass shift of the apoER2 can occur between different cell types.

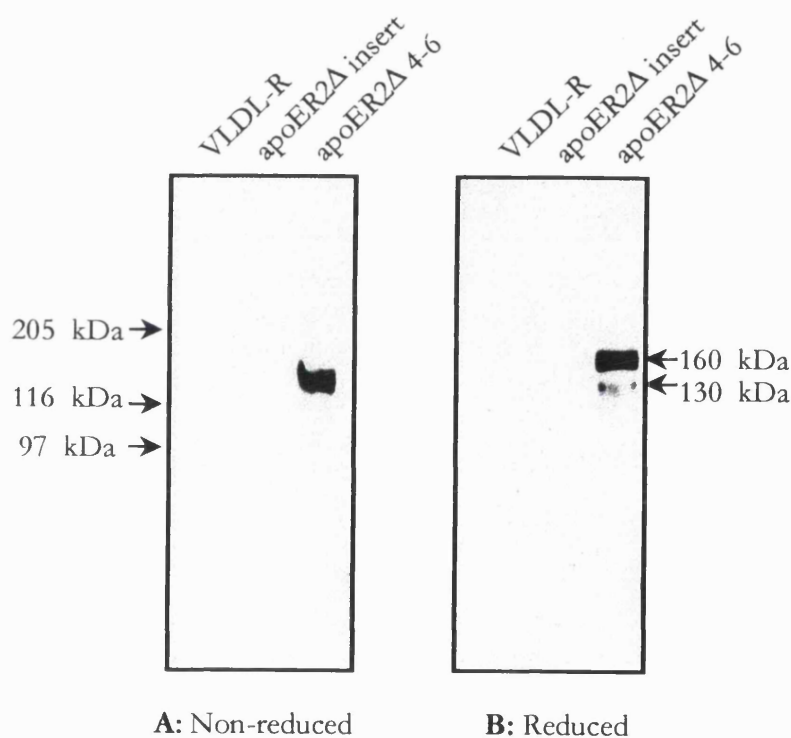


Figure 5.3-12 Western blotting of apoER2 using the anti-peptide antiserum α ER2Ins.

CHO cell extracts over-expressing either apoER2 Δ Insert, apoER2 Δ 4-6 (with insert) or VLDL-R were subjected to 8 % SDS-PAGE under non-reducing (panel A) and reducing (panel B) conditions, prior to Western blotting using α ER2Ins. ApoER2 bands were visualised using the ECL substrate (Amersham International plc).

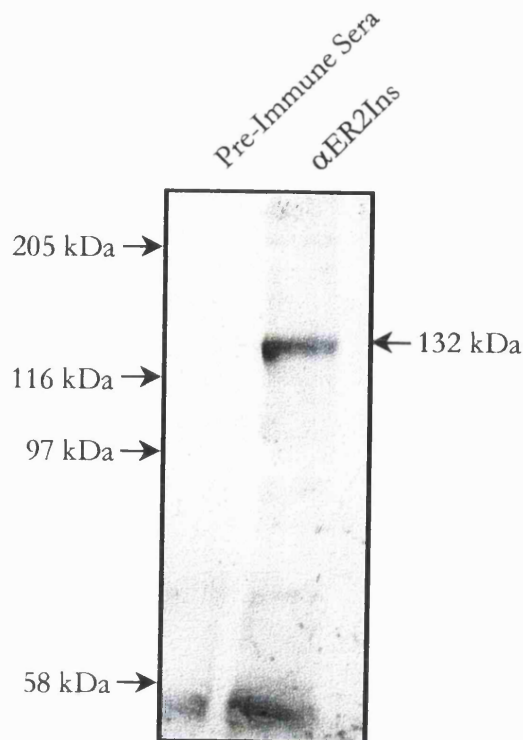


Figure 5.3-13 Immunoprecipitation of platelet apoER2.

Intact platelets were biotinylated, lysed and subjected to immunoprecipitation. Precipitated cell surface proteins were reduced and separated by electrophoresis on an 8 % gel, transferred onto nitrocellulose and detected with streptavidin-alkaline phosphatase. The results shown were from one experiment but were reproduced in two independent immunoprecipitations.

5.3.8 THE ROLE OF APOER2 VARIANTS IN PLATELETS AND MEGAKARYOCYTES.

A striking feature of platelet apoER2 expression is the deletion of ligand binding repeats 4-6 (apoER2 Δ 4-6). This presumably reflects the skipping of exon 5 during RNA processing of the apoER2 gene in the parent megakaryocyte. Intriguingly, Kim and colleagues in Japan have demonstrated that deletion of binding repeats 4, 5, 6 and 7 of apoER2 have no effect on apoE binding to this receptor [173] indicating that only repeats 1-3 of apoER2 are required for apoE recognition. One could therefore speculate that the gross structural reorganisation of the binding domain of platelet apoER2 Δ 4-6, compared to the LDL-R and VLDL-R, might explain its apparent relaxed specificity towards apoE isoforms and peptides (Table 5.3-3). However, it should be noted that the precise molecular interactions occurring between apoE and its receptors are still subject to debate.

Indeed, until very recently the binding reaction seemed to be based on ionic interactions between the positively charged helices of apoE (residues 130-160), and negative residues in the binding repeats of the LRSF members [89]. However, a recent crystallographic analysis of repeat 5 in the LDL-R has revealed that most of the negatively charged residues are co-ordinated with Ca^{2+} and are, therefore, unavailable to bind apoE [148]. Clearly, for a definitive explanation of the apparent differences in ligand specificity between the LRSF members, we need to know the crystal structure of each of the apoE/LRSF complexes [147].

Ligand Specificity	Platelet Receptor (apoER2 Δ 4-6)	VLDL-R	LDL-R
ApoE RKxR motif	✓	✗ [354]	✓ [89]
Monomeric RKxR peptide	✓	?	✗ [347]
ApoE-2	✓	✓ [354]	✗ [278]
Lactoferrin	✓ (?)	✓ (?) [352]	?
RAP	✓	✓ [178]	✓ [180]

Table 5.3-3 Comparison of the ligand specificities of the LDL-R, VLDL-R and the platelet apoE receptor.

Another feature of platelet apoER2 mRNA analysis was the apparent expression of two different splice variants (apoER2 Δ 4-6 and apoER2 Δ 4-6 Δ insert) within the one cell type. Note, however, that definitive evidence for apoER2 Δ 4-6 Δ insert protein expression must await the production of an antibody that can immunoprecipitate both variants. Placing this aside, it has been known for some time that the VLDL-R and its chicken homologue, LR8, are expressed as splice variants with and without the O-linked sugar domain [169, 376-378]. However, these variants appear to be expressed in a mutually exclusive fashion in different cell types [377, 378]. This implies that the two platelet receptors have different functions to perform in the megakaryocyte and platelet. Thus, since apoER2 can endocytose and degrade apoE-containing lipoproteins [172, 173] and hence supply extracellular lipids, it is conceivable that apoER2 Δ 4-6 Δ insert could act as a classical “LDL-R-type” receptor and provide a lipid source to the growing megakaryocyte. Indeed, as apoER2 is the only LRSF member characterised in megakaryocytic cells so far, such a role for this receptor is expected. On the other hand, since it is unlikely that the

mature circulating platelets contain the conventional endocytotic pathways required for lipoprotein utilisation, it is feasible to assume that apoER2 Δ 4-6 with cytoplasmic insert is packaged into the platelet to perform a cell signalling function. Obviously, additional studies are required to clarify the functional roles of apoER2 splice variants in platelets and megakaryocytes.

5.3.9 IS APOER2 A SIGNAL TRANSDUCTANT?

5.3.9.1 Src Homology 3 (SH3) Recognition Motifs.

In summary, I believe that my findings provide clear evidence that platelets contain the newly described LRSF member, apoER2. Since it is the only characterised LRSF member expressed in cells of the megakaryocytic lineage, this implies that it mediates the anti-platelet effects of apoE. Indeed, the amino acid sequence of the cytoplasmic domain of apoER2 suggests a cell-signalling role for this receptor. In particular, platelet apoER2 contains a 59 amino acid insert that is missing from all other LRSF members. This insert has a high degree of conservation between human and mouse apoER2, implying a functional significance [175]. However, Brandes et al., state that it represents a unique sequence not found in any published protein [175]. I disagree. By searching protein domain databases [379] (Internet address: <http://www.ncbi.nlm.nih.gov/BLAST>), I have identified three proline-rich motifs, designated *P1*, *P2* and *P3* (Figure 5.3-14) which fulfil minimal consensus sequences for Src Homology 3 (SH3) domain recognition, namely PxxP with each proline usually preceded by an aliphatic residue. In particular, the arginine and additional proline in sequence *P1* (REPEDPAP) almost certainly confer high affinity binding [380-382].

SH3 domains were first defined in the human proto-oncogene product Src and have now been identified in a large number of proteins, many of which participate in tyrosine kinase-mediated signal transduction. Tyrosine kinase signalling pathways proceed through a series of modular protein-protein recognition domains. These domains recognise small specific sequence motifs in target proteins, thereby non-covalently tethering proteins so that they can act together, or upon one another. They include Src-homology-2 (SH2) and phosphotyrosine-binding domain (PTB), which both bind specific phosphotyrosine (pTyr)-containing peptide motifs, as well as SH3 domains that bind to PxxP motifs (reviewed in [380-384]). In response to binding, SH3 domain containing signalling molecules often undergo tyrosine (de)phosphorylation, which may evoke positive or negative regulation of specific intracellular signalling cascades (cf. platelets [46]). Recent structural and mutagenic analysis of PxxP peptide-SH3 complexes show that peptides

associated with SH3 domains adopt a left-handed polyproline type II helix [385]. Intriguingly, when the amino acid sequence of the apoER2 cytoplasmic insert was submitted to the Fischer and Eisenberg's Fold Recognition algorithm [386] (Internet address: <http://www.doe-mbi.ucla.edu/>), which predicts three-dimensional structure from primary sequences, the P1 motif of apoER2 was predicted to have a 3D structure resembling the SH3 recognition motif present in human protein tyrosine phosphatase 1B [387] (results not shown). Although supporting the concept that apoER2-P1 is a SH3 recognition motif, it should be noted that this method of prediction is, at the present time, unreliable.

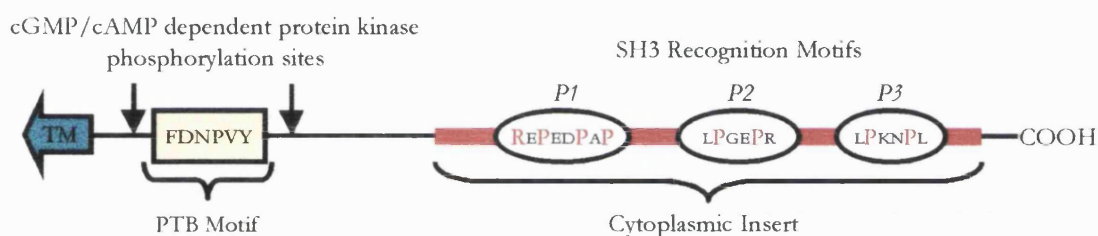


Figure 5.3-14 The cytoplasmic tail of apoER2 contains PTB recognition motifs, SH3 recognition motifs and cGMP/cAMP dependent protein kinase phosphorylation sites.

The cytoplasmic domain of platelet apoER2 consists of 115 amino acids with the amino-terminal 25 residues containing the internalisation (PTB-binding) motif common to all LRSF members. Flanking this region are two cGMP/cAMP dependent protein kinase phosphorylation sites. The unique 59 amino acid insert of apoER2 contains three proline-rich motifs (P1-P3) which fulfil the PxxP consensus sequence for SH3 domain recognition.

5.3.9.2 Cytoplasmic ApoER2 Binds a 40 kDa Tyrosine Phosphorylated Protein in Platelet Cytosol.

Fortuitously, the 17-mer peptide we selected for antibody production encompasses P1, the proline-rich motif most likely to undergo high affinity binding by SH3 domains. To assess whether this motif could interact with platelet proteins, the peptide was linked to Sepharose and equilibrated with platelet cytosol. A 40 kDa protein was bound and this was tyrosine phosphorylated, as determined by Western blotting using a monoclonal anti-phosphotyrosine antibody (Figure 5.3-15). This implies that this putative SH3 motif is indeed functional.

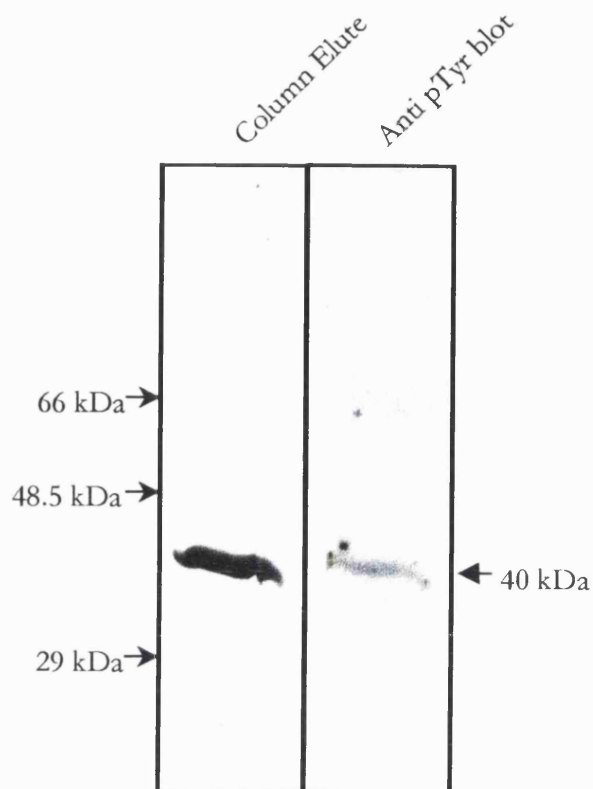


Figure 5.3-15 Cytoplasmic apoER2 binds a 40 kDa tyrosine-phosphorylated protein in platelet cytosol.

A 17-residue peptide sequence encompassing a potential SH3 recognition motif within cytoplasmic apoER2 was coupled to NHS-Sepharose and equilibrated with platelet cytosol. Bound proteins were eluted with 0.5 M NaCl, separated by SDS-PAGE and detected by silver staining or by Western blotting using the monoclonal anti-phosphotyrosine antibody, PY20.

5.3.9.3 The Phosphotyrosine-Binding Motif.

Interestingly, the so-called internalisation motif ($\Psi_x\text{NP}_x\text{Y}$, where Ψ is hydrophobic, Figure 5.3-14), common to all LRSF members, is also implicated in tyrosine kinase signal transduction [388]. This motif can be recognised by PTB domains present in numerous signalling molecules, including X11 neuronal protein or when tyrosine phosphorylated the docking molecules Shc and IRS-1 [389]. Indeed, these $\Psi_x\text{NP}_x\text{Y}$ motifs are responsible for propagating the outside-in signalling of the insulin receptor and TrkA nerve growth factor receptor (reviewed in [384]) to name just a few. Intriguingly, two observations suggest that this PTB recognition motif in platelet apoER2 is functional. Firstly, platelet GPIIb-IIIa also has the $\Psi_x\text{NP}_x\text{Y}$ sequence and this undergoes phosphorylation to bind Shc [390]. Secondly, although phosphorylation of the conserved LDL-R sequence, FDNPVY, is not required for endocytosis [391], tyrosine-phosphorylation is implicated in regulating receptor degradation [392].

5.3.10 PLATELET APOER2 AND eNOS ACTIVATION.

The principle factor determining the formation of tyrosine kinase signalling complexes is the presence of many different signalling motifs covalently linked within the same polypeptide chain (reviewed in [380-384]). This allows for the formation of a protein-protein network that disseminates signalling information to diverse cellular processes. Since the cytoplasmic domain of apoER2 contains both PTB ($\Psi_x\text{NP}_x\text{Y}$) and SH3 (P_{xxx}P) recognition motifs, it is extremely likely that activation of apoER2 triggers the formation of a tyrosine phosphorylation signalling cascade which ultimately leads to increases in platelet NOS activity. This hypothesis is strengthened by the observation that insulin also inhibits platelet aggregation by activating eNOS in a mechanism analogous to that of apoE [286, 393]. Moreover, platelets express an insulin receptor [394], which contains a $\Psi_x\text{NP}_x\text{Y}$ motif in its cytoplasmic domain [395] and has the potential to stimulate tyrosine kinase signalling pathways (reviewed in [396]). Indeed, the ability of insulin to activate platelet eNOS is blunted when platelets are incubated with the general tyrosine kinase inhibitor, genistein [286]. Less clear, however, is how an apoER2 (or indeed, insulin) mediated tyrosine kinase signalling cascade could ultimately influence platelet eNOS activity.

All NOS isoforms undergo reversible phosphorylation by a variety of protein kinases, implying that cross-talk may occur between NO and other signalling pathways. However, the nature and consequences of NOS phosphorylation are poorly understood [68, 397, 398]. Indeed, although regulation of eNOS activity by phosphorylation at multiple sites, including tyrosine [397], has been suggested [68, 399], the activation of different kinases and/or phosphatases appears stimulus-dependent so that either down- or upregulation of eNOS can occur [397, 399]. Obviously, the confusion expressed in the current literature make it difficult to predict the precise nature of any downstream signalling cascades from apoER2, particularly since I have yet to identify any signalling molecules that bind to apoER2 recognition motifs. However, this dilemma is not unique [400-402]. The concept of conserved protein domains that act as key regulatory participants in different, often interconnecting, pathways is still relatively new and there remain many gaps in our current understanding. Obviously, a key step forward will be characterisation of the cytosolic 40 kDa protein recognised by the putative SH3 motif in cytoplasmic apoER2. This has been amino-terminal sequenced (results not shown) and, as this has no match in databanks, future efforts will be directed at cloning its gene. Nevertheless, I believe that there is strong circumstantial evidence to support my hypothesis. Namely, that the cytoplasmic tail of apoER2 is activated by apoE allowing

SH3/PTB domain-mediated binding of either a protein tyrosine kinase, phosphatase or adaptor molecule; and that any of these events constitutes the initial module of a protein-protein signal transduction network that upregulates eNOS to produce NO (Figure 5.3-16). Finally, the Thr₈₁₅ (RKNT) and Thr₈₂₉ (RKTT) residues flanking the PTB motif of apoER2 are potential targets for cGMP- or cAMP-dependent protein kinases [403, 404]. Because the biochemical consequence of apoE-induced release of platelet NO is a rise in intracellular cGMP and cAMP, it is tempting to speculate that this constitutes a feedback loop to inactivate apoER2 and restore the cell to a functional state.

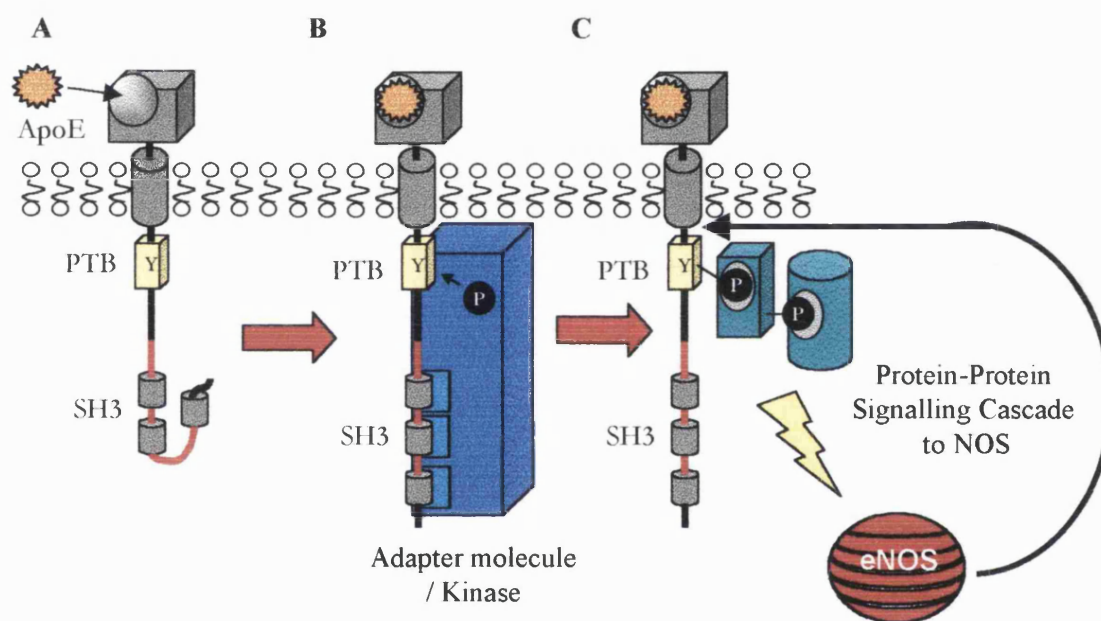


Figure 5.3-16 Hypothesis - a novel cell signalling role for apoER2 in platelets.

I propose herein, a unique cell signalling role for apoE and its newly discovered receptor - apoER2. ApoER2 is activated by apoE (A) to bind a 40 kDa cytosolic adaptor molecule or tyrosine kinase, via its SH3 motifs (B). This binding causes a tyrosine phosphorylation of either the PTB motif (shown) or the adaptor molecule/kinase itself, which in turn binds other adaptor molecules or tyrosine kinases which ultimately triggers additional (de)phosphorylation events to upregulate eNOS (C). The subsequent cGMP and cAMP produced activates the cGMP/cAMP dependent protein kinases that feed back to apoER2.

Chapter 6

6. GENERAL DISSUSSION

6.1 The ApoE/ApoER2/NO Link: Implications for Vascular Disease.

As outlined in *section 1.3.8*, atherosclerosis is an arterial disease that is recognised as a principal cause of death in the western world [193]. Intensive epidemiological, genetic and biochemical studies have indicated that atherosclerosis is a multifactorial disorder to which hyperlipidaemia, increased oxidative stress, hypertension and increased platelet reactivity may contribute (reviewed in [194, 195]). Indeed, blood platelets are intimately involved in the atherosclerotic process. They play a central protagonistic role both in early lesion development and in forming the platelet-rich thrombi characteristic of the final arterial thromboembolism [405]. Moreover, recent evidence also indicates that platelets can directly initiate an inflammatory response of the vessel wall by expressing CD40 ligand (CD40L) within seconds of activation [406]. CD40L on platelets induces endothelial cells to secrete chemokines and express cell adhesion molecules [406], thereby generating signals for the recruitment and extravasation of leukocytes at the site of injury. Such mechanisms promote the formation of atherosclerotic lesions [194, 195].

Obviously, establishing apoE as an important regulatory mechanism for the control of platelet homeostasis, by augmenting platelet eNOS activity, has profound consequences for atherosclerosis biomedical research. Not simply because large surveys confirm that platelet reactivity increases prevalence [279] and incidence [280] of coronary heart disease, or that low or dysfunctional apoE and HDL-E are important risk factors for coronary heart disease [407-412], but because my work constitutes the first link between apoE and NO. Thus, in the cardiovascular system perturbed NO synthesis or action has been implicated in almost all diseases associated with increased vascular tone, vasospasm or enhanced adhesion of platelets or leukocytes to the arterial wall [413]. Such studies suggest that the ability of apoE to stimulate platelet production of NO, some of which may be secreted and hence potentially available to function in a paracrine manner, can have wider implications. Indeed, in addition to their fundamental role in homeostasis, platelets are also regarded as a good model system for the study of signal transduction pathways [3-5]. Therefore, one could postulate that the newly assigned cell signalling function of apoE and apoER2 presented in this thesis may have a physiological significance beyond its role in inhibiting platelet aggregation.

Intriguingly, there is also evidence from our laboratory that an apoE/NO link also occurs in endothelium. Using human umbilical vein endothelial cells (HUVECs), we initially confirmed that upregulation of VCAM-1 by inflammatory cytokines could be inhibited by co-incubation with NO donors [414]. Similar inhibitions were achieved by transfecting HUVECs with pCMV.apoE3 and the secreted apoE correlated closely with VCAM-1 downregulation ($r=-0.93$, $P<0.001$) [415]. We also found an increase in L-[^3H]arginine \rightarrow L-[^3H]citrulline, implying that high local levels of apoE act in a paracrine fashion to stimulate NO production and suppress VCAM-1 [unpublished observation]. As vascular endothelium overlying atherosclerotic lesions is also exposed to an abundance of apoE secreted by resident macrophages, we have proposed that this will limit endothelial activation and stem further monocyte recruitment. Significantly, HUVECs also express apoER2 containing the cytoplasmic insert [unpublished observation and 416] and we currently hypothesize that its activation by apoE suppresses VCAM-1 expression via NO production. Interestingly, there is further circumstantial evidence in the literature to suggest an apoE/NO link in endothelium. Thus, apoE inhibits endothelial cell proliferation [417], an effect that can be mirrored by NO donors [418, 419]. Clearly, a more detailed investigation of eNOS activation by apoE in platelets and endothelial cells is imperative for understanding the role of apoE in the atherosclerotic process.

6.2 The apoE/apoER2/NO Link: Implications for Neurological Diseases.

Until 10 years ago, apoE was best known for its central role in plasma lipoprotein metabolism and cholesterol transport [89, 90]. Although less widely appreciated, apoE also serves a lipid transport role in the nervous system [90, 113, 121, 420, 421], where it plays an important role in neuronal growth and regeneration. In 1993, the view of apoE was significantly changed when investigators at Duke University made the unexpected discovery that one of the three common apoE alleles, apoE-4, was associated with Alzheimer's disease (AD) [207, 208]. This landmark observation stimulated much interest, and attention is now focusing on the underlying mechanisms of how apoE might contribute to the aetiology of AD.

Although the exact biochemical mechanism connecting the presence of apoE-4 with neuronal dysfunction in AD patients has yet to be resolved, one may speculate that apoE-induced NO over-production contributes to the pathophysiology of the disease. Indeed, over-production of NO by activated microglia has been implicated in the pathogenesis of numerous neurological disorders, including AD [422, 423]. Microglia are a brain-specific

form of monocyte-derived macrophages. Intriguingly, human macrophages have recently been demonstrated to over-produce NO in response to apoE [337]. Moreover, in a recent collaborative study with Dr. P. Cullen of Münster University, Germany, we have found that activated macrophages also express high levels of apoER2 (unpublished observation), although inactivated monocytes do not (*section 5.3.5*). Importantly, these macrophages also increased NO production in response to apoE.

Intriguingly, there is also indirect evidence to suggest that apoE can act directly on neuronal cells to elicit production of NO. Thus, apoE influences neurite out-growth in cultured neurones [421, 424], while broadly analogous findings are found for NO inasmuch as activation of NOS causes growth arrest and differentiation of cultured neuronal cells [425]. This is of particular interest since platelets show many similarities with neurones [426, 427] and can exhibit functional abnormalities in a number of neurological disorders, including Alzheimer's disease [428, 429]. The reasons for the similarities between these two physiologically distinct cell types are unclear but may be due to a common embryonic origin [427]. This could possibly explain why platelets contain apoER2, a receptor that is predominantly expressed in the brain.

If apoER2-mediated over-production of NO in neuronal cells and microglia is implicated in the pathogenesis of AD, this in itself would not explain the over-representation of apoE-4 in AD cases, since apoE-4 binds normally to apoER2 (*section 5.3.4.2*). However, it should be noted that the characterisation of apoE-containing lipoproteins in the brain is ongoing [430] and is still relatively unknown, mainly due to the technical difficulties of isolating lipoproteins from human brain tissue. In human plasma apoE-3 and apoE-4 have differing preferences in their lipoprotein associations; apoE-3 associates with HDL, while apoE-4 prefers VLDL. Since, the lipid environment of apoE affects its ability to bind to its receptors [89], the possibility arises that "native" brain apoE-4-containing lipoproteins might have a greater affinity for apoER2. Clearly, further basic experiments are required to establish whether an apoER2/NO link is present in neuronal cells and to define the interactions between apoER2 and "native" brain lipoproteins.

6.3 Conclusions.

The primary aim of my thesis was to characterise the anti-platelet properties of apoE and to investigate the molecular mechanisms involved. These data were expected to give valuable insights to a possible cell signalling function for apoE. Therefore, using the platelet as a

convenient model system for identifying and characterising signalling pathways [3-5], I sought to delineate the molecular influences that apoE might exert.

I initially verified that apoE purified from plasma was a highly potent inhibitor of platelet aggregation, and somewhat to my surprise, found that apoE could directly influence the activity of platelet NOS. Further studies implied that the trigger for NO release was an interaction between apoE and a LRSF member. Therefore, based on the conserved cysteine-rich binding region of this super family, I used sets of degenerate primers and RT-PCR to identify the platelet receptor. Again surprising results were obtained; platelets contained splice variants of apoER2, a newly described receptor reported to be confined mainly to the brain. Finally, I focused my attention on the cytoplasmic tail of apoER2 since this is the area where “outside-in” signalling from apoE would be propagated. Thus, and in contradiction to published observations, I discovered a number of interesting sequence motifs that implicated apoER2 in tyrosine kinase signalling.

Therefore, in many regards the aims of this thesis have been satisfied, since the results presented here have begun to characterise a unique role for apoE and its receptors. Indeed, to quote the title of the St Clair & Beisiegel editorial in October 1997's *Current Opinions in Lipidology* - “What do all the apoE receptors do?” [431]. Although, many open questions are still posed, I believe that my present hypothesis provides a key answer regarding apoER2, namely that apoE-activated cytoplasmic apoER2 contains recognition motifs, which generate a signal transduction network through modular protein-protein interactions that ultimately triggers additional (de)phosphorylation events to upregulate eNOS. Note, however, it is also conceivable that apoER2 will not only link to NO production, but may signal to a variety of different pathways via its PTB and SH3 recognition motifs. The very fact that modular protein-protein interactions exist to disseminate signalling stimuli to a variety of often interconnecting pathways makes this a distinct possibility.

Obviously, a more detailed molecular description of eNOS activation by apoE is required. Presently, the role of apoER2-mediated tyrosine kinase phosphorylation pathways in the regulation of eNOS is far from clear (*section 5.3.10*). However, a detailed molecular dissection of the downstream signalling from apoER2 is now an achievable goal. Indeed, the identification of signalling motifs within cytoplasmic apoER2 has provided the necessary impetus to further characterise apoE-mediated signalling cascades. Hopefully, this will one day allow insights into the physiological regulation and actions of not only apoER2 but also eNOS, and may aid the design of specifically-targeted therapeutic drugs [432] for both atherosclerosis and Alzheimer's disease.

BIBLIOGRAPHY

1. Savi P and Herbert JM (1996). ADP receptors on platelets and ADP-selective antiaggregating agents. *Med. Res. Rev.* **16**: 159-179.
2. Puri RN and Colman RW (1997). ADP-induced platelet activation. *Crit. Rev. Biochem. Mol. Biol.* **32**: 437-502.
3. Watson SP and Authi KS eds. (1996). *Platelets: A Practical Approach*. Oxford University Press, New York.
4. Ashby B (1994). Interactions among prostaglandin receptors. *Receptor* **4**: 31-42.
5. Sargeant P and Sage SO (1994). Calcium signalling in platelets and other nonexcitable cells. *Pharmacol. Ther.* **64**: 395-443.
6. Siest G, Pillot T, Régis-Bailly A, Leininger-Muller B, Steinmetz J, Galteau MM and Visvikis S (1995). Apolipoprotein E: an important gene and protein to follow in laboratory medicine. *Clin. Chem.* **41**: 1068-1086.
7. Desai K, Bruckdorfer KR, Hutton RA and Owen JS (1989). Binding of apoE-rich high density lipoprotein particles by saturable sites on human blood platelets inhibits agonist-induced platelet aggregation. *J. Lipid Res.* **30**: 831-840.
8. Schrör K, Tschöpe D and Rösen P (1994). Megakaryocytes and platelets in cardiovascular diseases. *Euro. J. Clin. Invest.* **24 Suppl 1**: 1.
9. Warkentin TE and Kelton JG (1995). The Platelet Life Cycle. *Blood: Principles and Practice of Hematology* (Handin RI, Lux SE and Stossel TP eds.) JB Lippincott Company, Philadelphia, pp 973-976.
10. Hoffbrand AV (1993). Platelets, Blood Coagulation and Haemostasis. *Essential Haematology* Blackwell Science Ltd, pp 299-302.
11. Isenberg WM and Bainton DF (1991). Megakaryocyte and Platelet Structure. *Hematology: Basic Principles and Practice* (Hoffman R ed.) Churchill Livingstone Inc., pp 1157-1165.
12. Brown AS and Martin JF (1994). The megakaryocyte platelet system and vascular disease. *Eur. J. Clin. Invest.* **24 Suppl 1**: 9-15.
13. Clemetson KJ and Clemetson JM (1994). Molecular abnormalities in Glanzmann's thrombasthenia, Bernard-Soulier syndrome, and platelet-type von Willebrand's disease. *Curr. Opin. Hematol.* **1**: 388-393.
14. Perutelli P and Mori PG (1992). The human platelet membrane glycoprotein IIb/IIIa complex: a multi functional adhesion receptor. *Haematologica* **77**: 162-168.
15. Gerrard JM, White JG and Peterson DA (1978). The platelet dense tubular system: its relationship to prostaglandin synthesis and calcium flux. *Thromb. Haemost.* **40**: 224-231.
16. Holmsen H (1994). Significance of testing platelet functions in vitro. *Eur. J. Clin. Invest.* **24 Suppl 1**: 3-8.
17. Steen VM, Holmsen H and Aarbakke G (1993). The platelet-stimulating effect of adrenaline through alpha 2-adrenergic receptors requires simultaneous activation by a true stimulatory platelet agonist. Evidence that adrenaline per se does not induce human platelet activation in vitro. *Thromb. Haemost.* **70**: 506-513.

18. Caen JP and Rosa JP (1995). Platelet-vessel wall interaction: from the bedside to molecules. *Thromb. Haemost.* **74**: 18-24.
19. Andrews RK, López JA and Berndt MC (1997). Molecular mechanisms of platelet adhesion and activation. *Int. J. Biochem. Cell Biol.* **29**: 91-105.
20. Moroi M and Jung SM (1997). Platelet receptors for collagen. *Thromb. Haemost.* **78**: 439-444.
21. Gear AR (1984). Rapid platelet morphological changes visualized by scanning-electron microscopy: kinetics derived from a quenched-flow approach. *Br. J. Haematol.* **56**: 387-398.
22. White JG (1968). Fine structural alterations induced in platelets by adenosine diphosphate. *Blood* **31**: 604-622.
23. Kroll MH and Schafer AI (1989). Biochemical mechanisms of platelet activation. *Blood* **74**: 1181-1195.
24. Siess W (1989). Molecular mechanisms of platelet activation. *Physiol. Rev.* **69**: 58-178.
25. Wagner WR and Hubbell JA (1992). ADP receptor antagonists and converting enzyme systems reduce platelet deposition onto collagen. *Thromb. Haemost.* **67**: 461-467.
26. Cattaneo M, Canciani MT, Lecchi A, Kinlough-Rathbone RL, Packham MA, Mannucci PM and Mustard JF (1990). Released adenosine diphosphate stabilizes thrombin-induced human platelet aggregates. *Blood* **75**: 1081-1086.
27. Mustard JF and Packham MA (1970). Factors influencing platelet function: adhesion, release, and aggregation. *Pharmacol. Rev.* **22**: 97-187.
28. Born GVR (1962). Aggregation of blood platelets by adenosine diphosphate and its reversal. *Nature* **194**: 927-929.
29. Zawilska KM, Born GV and Begent NA (1982). Effect of ADP-utilizing enzymes on the arterial bleeding time in rats and rabbits. *Br. J. Haematol.* **50**: 317-325.
30. Maffrand JP, Bernat A, Delebassée D, Defreyn G, Cazenave JP and Gordon JL (1988). ADP plays a key role in thrombogenesis in rats. *Thromb. Haemost.* **59**: 225-230.
31. Heemskerk JWM and Sage SO (1994). Calcium signalling in platelets and other cells. *Platelets* **5**: 295-316.
32. Haynes DH (1993). Effects of cyclic nucleotides and protein kinases on platelet calcium homeostasis and mobilization. *Platelets* **4**: 231-242.
33. Brass LF (1991). The biochemistry of platelet activation. *Hematology: Basic Principles and Practice* (Hoffman R ed.). Churchill Livingstone Inc., pp 1177-1193.
34. Hourani SM, Hall DA (1994). Receptors for ADP on human blood platelets. *Trends Pharmacol. Sci.* **15**: 103-108.
35. Mills DC, Robb IA and Roberts GC (1968). The release of nucleotides, 5-hydroxytryptamine and enzymes from human blood platelets during aggregation. *J. Physiol. (Lond)*. **195**: 715-729.
36. Hallam TJ and Rink TJ (1985). Responses to adenosine diphosphate in human platelets loaded with the fluorescent calcium indicator quin2. *J. Physiol. (Lond)*. **368**: 131-146.

37. Sage SO and Rink TJ (1986). Kinetic differences between thrombin-induced and ADP-induced calcium influx and release from internal stores in fura-2-loaded human platelets. *Biochem. Biophys. Res. Commun.* **136**: 1124-1129.
38. MacKenzie AB, Mahaut-Smith MP and Sage SO (1996). Activation of receptor-operated cation channels via P2X1 not P2T purinoceptors in human platelets. *J. Biol. Chem.* **271**: 2879-2881.
39. Mills DC and Smith JB (1972). The control of platelet responsiveness by agents that influence cyclic AMP metabolism. *Ann. N. Y. Acad. Sci.* **201**: 391-399.
40. Daniel JL, Dangelmaier C, Jin J, Ashby B, Smith JB and Kunapuli SP (1998). Molecular basis for ADP-induced platelet activation. I. Evidence for three distinct ADP receptors on human platelets. *J. Biol. Chem.* **273**: 2024-2029.
41. Jin J, Daniel JL and Kunapuli SP (1998). Molecular basis for ADP-induced platelet activation. II. The P2Y1 receptor mediates ADP-induced intracellular calcium mobilization and shape change in platelets. *J. Biol. Chem.* **273**: 2030-2034.
42. Gerrard JM, Carroll RC, Israels SJ and Beattie LL (1987). Protein Phosphorylation. *Platelets in Biology and Pathology III* (MacIntyre DE and Gordon JL eds.) Elsevier, Amsterdam, pp 317-351.
43. Daniel JL, Molish IR, Rigmaiden M and Stewart G (1984). Evidence for a role of myosin phosphorylation in the initiation of the platelet shape change response. *J. Biol. Chem.* **259**: 9826-9831.
44. Haslam RJ, Koide HB and Hemmings BA (1993). Pleckstrin domain homology *Nature* **363**: 309-310.
45. Carty DJ, Freas DL and Gear AR (1987). ADP causes subsecond changes in protein phosphorylation of platelets. *Blood* **70**: 511-515.
46. Jackson SP, Schoenwaelder SM, Yuan Y, Salem HH and Cooray P (1996). Non-receptor protein tyrosine kinases and phosphatases in human platelets. *Thromb. Haemostas.* **76**: 640-650.
47. Jennings LK, Fox JE, Edwards HH and Phillips DR (1981). Changes in the cytoskeletal structure of human platelets following thrombin activation. *J. Biol. Chem.* **256**: 6927-6932.
48. Lindberg U and Markey F (1987). Platelet microfilaments and motility. *Platelets in Biology and Pathology III* (MacIntyre DE and Gordon JL eds.). Elsevier, Amsterdam, pp 317-351.
49. Fox JE and Berndt MC (1989). Cyclic AMP-dependent phosphorylation of glycoprotein Ib inhibits collagen-induced polymerization of actin in platelets. *J. Biol. Chem.* **264**: 9520-9526.
50. Oda A, Daley JF, Cabral C, Kang JH, Smith M and Salzman EW (1992). Heterogeneity in filamentous actin content among individual human blood platelets. *Blood* **79**: 920-927.
51. Heptinstall S, Glenn J and Spangenberg P (1992). Changes in G-actin after platelet activation in platelet rich plasma. *Thromb. Haemost.* **68**: 727-730.
52. Vane JR (1994). Towards a better aspirin. *Nature* **367**: 215-216.
53. Glusa E (1991). Hirudin and platelets. *Semin. Thromb. Hemost.* **17**: 122-125.
54. Walsh PN, Mills DC and White JG (1977). Metabolism and function of human platelets washed by albumin density gradient separation. *Br. J. Haematol.* **36**: 287-296.

55. Vane JR, Anggard EE and Botting RM (1990). Regulatory functions of the vascular endothelium. *N. Engl. J. Med.* **323**: 27-36.
56. Eigenthaler M, Nolte C, Halbrügge M and Walter U (1992). Concentration and regulation of cyclic nucleotides, cyclic nucleotide-dependent protein kinases and one of their major substrates in human platelets. Estimating the rate of cAMP-regulated and cGMP-regulated protein phosphorylation in intact cells. *Eur. J. Biochem.* **205**: 471-481.
57. Brass LF, Hoxie JA and Manning DR (1993). Signaling through G proteins and G protein-coupled receptors during platelet activation. *Thromb. Haemost.* **70**: 217-223.
58. Tateson JE, Moncada S and Vane JR (1977). Effects of prostacyclin on cyclic AMP concentrations in human platelets. *Prostaglandins* **13**: 389-397.
59. Haslam RJ and Rosson GM (1975). Effects of adenosine on levels of adenosine cyclic 3',5'-monophosphate in human blood platelets in relation to adenosine incorporation and platelet aggregation. *Mol. Pharmacol.* **11**: 528-544.
60. Zavoico GB and Feinstein MB (1984). Cytoplasmic Ca²⁺ in platelets is controlled by cyclic AMP: antagonism between stimulators and inhibitors of adenylate cyclase. *Biochem. Biophys. Res. Commun.* **120**: 579-585.
61. O'Rourke F, Zavoico GB and Feinstein MB (1989). Release of Ca²⁺ by inositol 1,4,5-trisphosphate in platelet membrane vesicles is not dependent on cyclic AMP-dependent protein kinase. *Biochem. J.* **257**: 715-721.
62. Lapetina EG, Lacal JC, Reep BR, Molina Y and Vedia L (1989). A ras-related protein is phosphorylated and translocated by agonists that increase cAMP levels in human platelets. *Proc. Natl. Acad. Sci. USA* **86**: 3131-3134.
63. Berry S, Dawicki DD and Steiner M (1989). Time resolved analysis of tubulin phosphorylation during platelet activation. *Biochem. Biophys. Res. Commun.* **159**: 170-176.
64. van Willigen G and Akkerman JW (1991). Protein kinase C and cyclic AMP regulate reversible exposure of binding sites for fibrinogen on the glycoprotein IIB-IIIa complex of human platelets. *Biochem. J.* **273**: 115-120.
65. Lincoln J, Hoyle CHV and Burnstock G eds. (1997). *Nitric Oxide in Health and Disease*. Cambridge University Press, Cambridge.
66. Schmidt HH and Walter U (1994). NO at work. *Cell* **78**: 919-925.
67. Anggard E (1994). Nitric oxide: mediator, murderer, and medicine. *Lancet* **343**: 1199-1206.
68. Sase, K, and Michel, T (1997). Expression and regulation of endothelial nitric oxide synthase. *Trends Cardiovasc. Res.* **7**: 28-37.
69. Radomski MW and Moncada S (1993). The biological and pharmacological role of nitric oxide in platelet function. *Mechanisms of Platelet Activation and Control* (Authi KS, Watson SP and Kakkar VV eds). Plenum Press, New York, pp 251-264.
70. Mayer B and Hemmens B (1997). Biosynthesis and action of nitric oxide in mammalian cells. *Trends Biochem. Sci.* **22**: 477-481.

71. Buechler WA, Ivanova K, Wolfram G, Drummer C, Heim JM and Gerzer R (1994). Soluble guanylyl cyclase and platelet function. *Ann. N. Y. Acad. Sci.* **714**: 151-157.
72. Tremblay J, Gerzer R and Hamet P (1988). Cyclic GMP in cell function. *Adv Second Messenger Phosphoprotein Res.* **22**: 319-383.
73. Garbers DL (1992). Guanylyl cyclase receptors and their endocrine, paracrine, and autocrine ligands. *Cell* **71**: 1-4.
74. Chhajlani V, Axelsson KL, Ahlner J and Wikberg JE (1989). Purification of soluble guanylate cyclase enzyme from human platelets. *Biochem. Int.* **19**: 1039-1044.
75. Nguyen BL, Saitoh M and Ware JA (1991). Interaction of nitric oxide and cGMP with signal transduction in activated platelets. *Am. J. Physiol.* **261**: H1043-H1052.
76. Brüne B and Lapetina EG (1989). Activation of a cytosolic ADP-ribosyltransferase by nitric oxide-generating agents. *J. Biol. Chem.* **264**: 8455-8458.
77. Radomski MW, Palmer RM and Moncada S (1987). Endogenous nitric oxide inhibits human platelet adhesion to vascular endothelium. *Lancet* **2:8567** 1057-1058.
78. Vaandrager AB and de Jonge HR (1996). Signalling by cGMP-dependent protein kinases. *Mol. Cell. Biochem.* **157**: 23-30
79. Walter U (1993). The biological and pharmacological role of nitric oxide in platelet function. *Mechanisms of Platelet Activation and Control* (Authi KS, Watson SP and Kakkar VV eds). Plenum Press, New York, pp 251-264.
80. Walter U (1989). Physiological role of cGMP and cGMP-dependent protein kinase in the cardiovascular system. *Rev. Physiol. Biochem. Pharmacol.* **113**: 41-88.
81. Walter U, Eigenthaler M, Geiger J and Reinhard M (1993). Role of cyclic nucleotide-dependent protein kinases and their common substrate VASP in the regulation of human platelets. *Adv. Exp. Med. Biol.* **344**: 237-249.
82. Grünberg B, Kruse HJ, Negrescu EV and Siess W (1995). Platelet rap1B phosphorylation is a sensitive marker for the action of cyclic AMP- and cyclic GMP-increasing platelet inhibitors and vasodilators. *J. Cardiovasc. Pharmacol.* **25**: 545-551.
83. Hidaka H and Asano T (1976). Human blood platelet 3', 5'-cyclic nucleotide phosphodiesterase. Isolation of low-K_m and high-K_m phosphodiesterase. *Biochim. Biophys. Acta.* **429**: 485-497.
84. Grant PG, Mannarino AF and Colman RW (1990). Purification and characterization of a cyclic GMP-stimulated cyclic nucleotide phosphodiesterase from the cytosol of human platelets. *Thromb. Res.* **59**: 105-119.
85. Grant PG and Colman RW (1984). Purification and characterization of a human platelet cyclic nucleotide phosphodiesterase. *Biochemistry* **23**: 1801-1807.
86. Manganiello VC, Taira M, Degerman E and Belfrage P (1995). Type III cGMP-inhibited cyclic nucleotide phosphodiesterases (PDE3 gene family). *Cell Signal.* **7**: 445-455.
87. Gotto AM, Pownall HJ and Havel RJ (1986). Introduction to plasma lipoproteins. *Methods Enzymol.* **128**: 3-41.

88. Driscoll DM and Getz GS (1986). Molecular and cell biology of lipoprotein biosynthesis. *Methods Enzymol.* **128**: 42-70.
89. Weisgraber KH (1994). Apolipoprotein E: structure-function relationships. *Adv. Protein. Chem.* **45**: 249-302.
90. Mahley RW (1988). Apolipoprotein E: cholesterol transport protein with expanding role in cell biology. *Science* **240**: 622-630.
91. Shore VG and Shore B (1973). Heterogeneity of human plasma very low density lipoproteins. Separation of species differing in protein components. *Biochemistry* **12**: 502-507.
92. Utermann G (1975). Isolation and partial characterization of an arginine-rich apolipoprotein from human plasma very-low-density lipoproteins: apolipoprotein E. *Hoppe Seylers Z. Physiol. Chem.* **356**: 1113-1121.
93. Weisgraber KH and Mahley RW (1986). Characterisation of apolipoprotein E-containing lipoproteins. *Methods Enzymol.* **129**: 145-166.
94. Mahley RW (1985). Atherogenic lipoproteins and coronary artery disease: concepts derived from recent advances in cellular and molecular biology. *Circulation* **72**: 943-948.
95. Gibson JC, Rubinstein A, Bukberg PR and Brown WV (1983). Apolipoprotein E-enriched lipoprotein subclasses in normolipidemic subjects. *J. Lipid Res.* **24**: 886-898.
96. Rall SC Jr, Weisgraber KH and Mahley RW (1982). Human apolipoprotein E. The complete amino acid sequence. *J. Biol. Chem.* **257**: 4171-4178.
97. McLean JW, Elshourbagy NA, Chang DJ, Mahley RW and Taylor JM (1984). Human apolipoprotein E mRNA. cDNA cloning and nucleotide sequencing of a new variant. *J. Biol. Chem.* **259**: 6498-6504.
98. Olaisen B, Teisberg P, Gedde-Dahl T Jr (1982). The locus for apolipoprotein E (apoE) is linked to the complement component C3 (C3) locus on chromosome 19 in man. *Hum. Genet.* **62**: 233-236.
99. Das HK, McPherson J, Bruns GA, Karathanasis SK and Breslow JL (1985). Isolation, characterization, and mapping to chromosome 19 of the human apolipoprotein E gene. *J. Biol. Chem.* **260**: 6240-6247.
100. Paik YK, Chang DJ, Reardon CA, Davies GE, Mahley RW, Taylor JM (1985). Nucleotide sequence and structure of the human apolipoprotein E gene. *Proc. Natl. Acad. Sci. USA* **82**: 3445-3449.
101. Lauer SJ, Walker D, Elshourbagy NA, Reardon CA, Levy-Wilson B, Taylor JM (1988). Two copies of the human apolipoprotein C-I gene are linked closely to the apolipoprotein E gene. *J. Biol. Chem.* **263**: 7277-7286.
102. Francke U, Brown MS, Goldstein J (1984). Assignment of the human gene for the low density lipoprotein receptor to chromosome 19: synteny of a receptor, a ligand, and a genetic disease. *Proc. Natl. Acad. Sci. USA* **81**: 2826-2830.
103. Humphries SE, Berg K, Gill L, Cumming AM, Robertson FW, Stalenhoef AF, Williamson R and Borresen AL (1984). The gene for apolipoprotein C-II is closely linked to the gene for apolipoprotein E on chromosome 19. *Clin. Genet.* **26**: 389-396.
104. Surguchov AP (1990). The apolipoprotein gene family: organization of upstream elements and regulation of gene expression. *Biomed. Sci.* **1**: 344-353.

105. Wernette-Hammond ME, Lauer SJ, Corsini A, Walker D, Taylor JM, Rall SC Jr (1989). Glycosylation of human apolipoprotein E. The carbohydrate attachment site is threonine 194. *J. Biol. Chem.* **264**: 9094-9101.
106. Lin CT, Xu YF, Wu JY and Chan L (1986). Immunoreactive apolipoprotein E is a widely distributed cellular protein. Immunohistochemical localization of apolipoprotein E in baboon tissues. *J. Clin. Invest.* **78**: 947-958.
107. Huang Y, von Eckardstein A, Wu S, Maeda N and Assmann G (1994). A plasma lipoprotein containing only apolipoprotein E and with gamma mobility on electrophoresis releases cholesterol from cells. *Proc. Natl. Acad. Sci. USA* **91**: 1834-1838.
108. Elshourbagy NA, Liao WS, Mahley RW and Taylor JM (1985). Apolipoprotein E mRNA is abundant in the brain and adrenals, as well as in the liver, and is present in other peripheral tissues of rats and marmosets. *Proc. Natl. Acad. Sci. USA* **82**: 203-207.
109. Pitas RE, Boyles JK, Lee SH, Foss D and Mahley RW (1987). Astrocytes synthesize apolipoprotein E and metabolize apolipoprotein E-containing lipoproteins. *Biochim. Biophys. Acta.* **917**: 148-161.
110. Boyles JK, Pitas RE, Wilson E, Mahley RW and Taylor JM (1985). Apolipoprotein E associated with astrocytic glia of the central nervous system and with nonmyelinating glia of the peripheral nervous system. *J. Clin. Invest.* **76**: 1501-1513.
111. Messmer-Joudrier S, Sagot Y, Mattenberger L, James RW and Kato AC (1996). Injury-induced synthesis and release of apolipoprotein E and clusterin from rat neural cells. *Eur. J. Neurosci.* **8**: 2652-2661.
112. Pitas RE, Boyles JK, Lee SH, Hui D and Weisgraber KH (1987). Lipoproteins and their receptors in the central nervous system. Characterization of the lipoproteins in cerebrospinal fluid and identification of apolipoprotein B, E (LDL) receptors in the brain. *J. Biol. Chem.* **262**: 14352-14360.
113. Boyles JK, Zoellner CD, Anderson LJ, Kosik LM, Pitas RE, Weisgraber KH, Hui DY, Mahley RW, Gebicke-Haerter PJ, Ignatius MJ et al. (1989). A role for apolipoprotein E, apolipoprotein A-I, and low density lipoprotein receptors in cholesterol transport during regeneration and remyelination of the rat sciatic nerve. *J. Clin. Invest.* **83**: 1015-1031.
114. de Chaves EI, Rusinol AE, Vance DE, Campenot RB and Vance JE (1997). Role of lipoproteins in the delivery of lipids to axons during axonal regeneration. *J. Biol. Chem.* **272**: 30766-30773.
115. Murakami M, Ushio Y, Morino Y, Ohta T and Matsukado Y (1988). Immunohistochemical localization of apolipoprotein E in human glial neoplasms. *J. Clin. Invest.* **82**: 177-188.
116. Mazzone T (1996). Apolipoprotein E secretion by macrophages: its potential physiological functions. *Curr. Opin. Lipidol.* **7**: 303-307.
117. Utermann G, Hees M and Steinmetz A (1977). Polymorphism of apolipoprotein E and occurrence of dysbetalipoproteinaemia in man. *Nature* **269**: 604-607.
118. Zannis VI and Breslow JL (1981). Human very low density lipoprotein apolipoprotein E isoprotein polymorphism is explained by genetic variation and posttranslational modification. *Biochemistry* **20**: 1033-1041.

119. Utermann G, Jaeschke M and Menzel J (1975). Familial hyperlipoproteinemia type III: deficiency of a specific apolipoprotein (apo E-III) in the very-low-density lipoproteins. *FEBS. Lett.* **56**: 352-355.
120. van Bockxmeer FM, Mamotte CD, Gibbons FR and Taylor RR (1994). Apolipoprotein epsilon 4 homozygosity- a determinant of restenosis after coronary angioplasty. *Atherosclerosis* **110**: 195-202.
121. Weisgraber KH and Mahley RW (1996). Human apolipoprotein E: the Alzheimer's disease connection. *FASEB. J.* **10**: 1485-494.
122. Weisgraber KH, Rall SC Jr and Mahley RW (1981). Human E apoprotein heterogeneity. Cysteine-arginine interchanges in the amino acid sequence of the apo-E isoforms. *J. Biol. Chem.* **256**: 9077-9083.
123. Steinmetz A, Jakobs C, Motzny S and Kaffarnik H (1989). Differential distribution of apolipoprotein E isoforms in human plasma lipoproteins. *Arteriosclerosis* **9**: 405-411.
124. Rall SC Jr and Mahley RW (1992). The role of apolipoprotein E genetic variants in lipoprotein disorders. *J. Intern. Med.* **231**: 653-659.
125. Mann WA, Meyer N, Weber W, Meyer S, Greten H and Beisiegel U (1995). Apolipoprotein E isoforms and rare mutations: parallel reduction in binding to cells and to heparin reflects severity of associated type III hyperlipoproteinemia. *J. Lipid Res.* **36**: 517-525.
126. Wetterau JR, Aggerbeck LP, Rall SC Jr and Weisgraber KH (1988). Human apolipoprotein E3 in aqueous solution. I. Evidence for two structural domains. *J. Biol. Chem.* **263**: 6240-6248.
127. Aggerbeck LP, Wetterau JR, Weisgraber KH, Wu CS and Lindgren FT (1988). Human apolipoprotein E3 in aqueous solution. II. Properties of the amino- and carboxyl-terminal domains. *J. Biol. Chem.* **263**: 6249-6258.
128. Aggerbeck LP, Wetterau JR, Weisgraber KH, Mahley RW and Agard DA (1988). Crystallization and preliminary X-ray diffraction studies on the amino-terminal (receptor-binding) domain of human apolipoprotein E3 from serum very low density lipoproteins. *J. Mol. Biol.* **202**: 179-181.
129. Wilson C, Wardell MR, Weisgraber KH, Mahley RW and Agard DA (1991). Three-dimensional structure of the LDL receptor-binding domain of human apolipoprotein E. *Science* **252**: 1817-1822.
130. Westerlund JA and Weisgraber KH (1993). Discrete carboxyl-terminal segments of apolipoprotein E mediate lipoprotein association and protein oligomerization. *J. Biol. Chem.* **268**: 15745-15750.
131. Sparrow JT, Sparrow DA, Fernando G, Culwell AR, Kovar M and Gotto AM Jr (1992). Apolipoprotein E: phospholipid binding studies with synthetic peptides from the carboxyl terminus. *Biochemistry* **31**: 1065-1068.
132. Yokoyama S, Kawai Y, Tajima S and Yamamoto A (1985). Behavior of human apolipoprotein E in aqueous solutions and at interfaces. *J. Biol. Chem.* **260**: 16375-16382.
133. Myant NB (1990). *Cholesterol Metabolism, LDL and the LDL receptor*. Academic press, San Diego.
134. Weisgraber KH, Innerarity TL and Mahley RW (1978). Role of lysine residues of plasma lipoproteins in high affinity binding to cell surface receptors on human fibroblasts. *J. Biol. Chem.* **253**: 9053-9062.
135. Mahley RW, Innerarity TL, Pitas RE, Weisgraber KH, Brown JH and Gross E (1977). Inhibition of lipoprotein binding to cell surface receptors of fibroblasts following selective modification of arginyl residues in arginine-rich and B apoproteins. *J. Biol. Chem.* **252**: 7279-7287.

136. Mahley RW, Innerarity TL and Weisgraber KH (1980). Alterations in metabolic activity of plasma lipoproteins following selective chemical modification of the apoproteins. *Ann. N. Y. Acad. Sci.* **348**: 265-280.
137. Innerarity TL, Friedlander EJ, Rall SC Jr, Weisgraber KH and Mahley RW (1983). The receptor-binding domain of human apolipoprotein E. Binding of apolipoprotein E fragments. *J. Biol. Chem.* **258**: 12341-12347.
138. Raffai R, Maurice R, Weisgraber K, Innerarity T, Wang X, MacKenzie R, Hiramata T, Watson D, Rassart E and Milne R (1995). Molecular characterization of two monoclonal antibodies specific for the LDL receptor-binding site of human apolipoprotein E. *J. Lipid Res.* **36**: 1905-1918.
139. Weisgraber KH, Innerarity TL, Harder KJ, Mahley RW, Milne RW, Marcel YL and Sparrow JT (1983). The receptor-binding domain of human apolipoprotein E. Monoclonal antibody inhibition of binding. *J. Biol. Chem.* **258**: 12348-12354.
140. Lalazar A, Weisgraber KH, Rall SC Jr, Giladi H, Innerarity TL, Levanon AZ, Boyles JK, Amit B, Gorecki M, Mahley RW, et al (1988). Site-specific mutagenesis of human apolipoprotein E. Receptor binding activity of variants with single amino acid substitutions. *J. Biol. Chem.* **263**: 3542-3545.
141. Yamamoto T and Bujo H (1996). Close encounters with apolipoprotein E receptors. *Curr. Opin. Lipidol.* **7**: 298-302.
142. Herz J and Willnow TE (1995). Lipoprotein and receptor interactions in vivo. *Curr. Opin. Lipidol.* **6**: 97-103.
143. Innerarity TL (1991). The low-density lipoprotein receptor. *Curr. Opin. Lipidol.* **2**: 156-162.
144. Schneider WJ, Nimpf J and Bujo H (1997). Novel members of the low density lipoprotein receptor superfamily and their potential roles in lipid metabolism. *Curr. Opin. Lipidol.* **8**: 315-319.
145. Mehta KD, Chang R and Norman J (1996). *Chiloscyllium plagiosum* low-density lipoprotein receptor: evolutionary conservation of five different functional domains. *J. Mol. Evol.* **42**: 264-272.
146. Bieri S, Djordjevic JT, Daly NL, Smith R and Kroon PA (1995). Disulfide bridges of a cysteine-rich repeat of the LDL receptor ligand-binding domain. *Biochemistry* **34**: 13059-13065.
147. Brown MS, Herz J and Goldstein JL (1997). LDL-receptor structure. Calcium cages, acid baths and recycling receptors. *Nature* **388**: 629-630.
148. Fass D, Blacklow S, Kim PS and Berger JM (1997). Molecular basis of familial hypercholesterolaemia from structure of LDL receptor module. *Nature* **388**: 691-693.
149. Herz J, Hamann U, Rogne S, Myklebost O, Gausepohl H and Stanley KK (1988). Surface location and high affinity for calcium of a 500-kd liver membrane protein closely related to the LDL-receptor suggest a physiological role as lipoprotein receptor. *EMBO. J.* **7**: 4119-4127.
150. Brown MS, Herz J, Kowal RC and Goldstein JL (1991). The low-density lipoprotein receptor-related protein: double agent or decoy? *Curr. Opin. Lipidol.* **2**: 65-72.
151. Herz J, Kowal RC, Goldstein JL, Brown MS (1990). Proteolytic processing of the 600 kd low density lipoprotein receptor-related protein (LRP) occurs in a trans-Golgi compartment. *EMBO. J.* **9**: 1769-1776.

152. Beisiegel U, Weber W, Ihrke G, Herz J, Stanley KK (1989). The LDL-receptor-related protein, LRP, is an apolipoprotein E-binding protein. *Nature* **341**: 162-164.
153. Kowal RC, Herz J, Goldstein JL, Esser V and Brown MS (1989). Low density lipoprotein receptor-related protein mediates uptake of cholesteryl esters derived from apoprotein E-enriched lipoproteins. *Proc. Natl. Acad. Sci. USA.* **86**: 5810-5814.
154. Kowal RC, Herz J, Weisgraber KH, Mahley RW, Brown MS and Goldstein JL (1990). Opposing effects of apolipoproteins E and C on lipoprotein binding to low density lipoprotein receptor-related protein. *J. Biol. Chem.* **265**: 10771-10779.
155. Mahley RW and Innerarity TL (1983). Lipoprotein receptors and cholesterol homeostasis. *Biochim. Biophys. Acta.* **737**: 197-222.
156. Moestrup SK, Gliemann J and Pallesen G (1992). Distribution of the alpha 2-macroglobulin receptor/low density lipoprotein receptor-related protein in human tissues. *Cell. Tissue. Res.* **269**: 375-382.
157. Herz J, Kowal RC, Ho YK, Brown MS and Goldstein JL (1990). Low density lipoprotein receptor-related protein mediates endocytosis of monoclonal antibodies in cultured cells and rabbit liver. *J. Biol. Chem.* **265**: 21355-21362.
158. Nykjaer A, Bengtsson-Olivecrona G, Lookene A, Moestrup SK, Petersen CM, Weber W, Beisiegel U and Gliemann J (1993). The alpha 2-macroglobulin receptor/low density lipoprotein receptor-related protein binds lipoprotein lipase and beta-migrating very low density lipoprotein associated with the lipase. *J. Biol. Chem.* **268**: 15048-15055.
159. Willnow TE, Goldstein JL, Orth K, Brown MS and Herz J (1992). Low density lipoprotein receptor-related protein and gp330 bind similar ligands, including plasminogen activator-inhibitor complexes and lactoferrin, an inhibitor of chylomicron remnant clearance. *J. Biol. Chem.* **267**: 26172-26180.
160. Kristensen T, Moestrup SK, Gliemann J, Bendtsen L, Sand O, Sottrup-Jensen L (1990). Evidence that the newly cloned low-density-lipoprotein receptor related protein (LRP) is the alpha 2-macroglobulin receptor. *FEBS. Lett.* **276**: 151-155.
161. Sottrup-Jensen L (1989). Alpha-macroglobulins: structure, shape, and mechanism of proteinase complex formation. *J. Biol. Chem.* **264**: 11539-11542.
162. Orth K, Madison EL, Gething MJ, Sambrook JF and Herz J (1992). Complexes of tissue-type plasminogen activator and its serpin inhibitor plasminogen-activator inhibitor type 1 are internalized by means of the low density lipoprotein receptor-related protein/alpha 2-macroglobulin receptor. *Proc. Natl. Acad. Sci. USA.* **89**: 7422-7426.
163. Nykjaer A, Petersen CM, Moller B, Jensen PH, Moestrup SK, Holtet TL, Etzerodt M, Thogersen HC, Munch M, Andreasen PA, et al (1992). Purified alpha 2-macroglobulin receptor/LDL receptor-related protein binds urokinase.plasminogen activator inhibitor type-1 complex. Evidence that the alpha 2-macroglobulin receptor mediates cellular degradation of urokinase receptor-bound complexes. *J. Biol. Chem.* **267**: 14543-14546.
164. Kerjaschki D and Farquhar MG (1983). Immunocytochemical localization of the Heymann nephritis antigen (GP330) in glomerular epithelial cells of normal Lewis rats. *J. Exp. Med.* **157**: 667-686.

165. Chatelet F, Brianti E, Ronco P, Roland J and Verroust P (1986). Ultrastructural localization by monoclonal antibodies of brush border antigens expressed by glomeruli. II. Extrarenal distribution. *Am. J. Pathol.* **122**: 512-519.
166. Saito A, Pietromonaco S, Loo AK and Farquhar MG (1994). Complete cloning and sequencing of rat gp330/"megalin," a distinctive member of the low density lipoprotein receptor gene family. *Proc. Natl. Acad. Sci. USA.* **91**: 9725-9729.
167. Takahashi S, Kawarabayasi Y, Nakai T, Sakai J and Yamamoto T (1992). Rabbit very low density lipoprotein receptor: a low density lipoprotein receptor-like protein with distinct ligand specificity. *Proc. Natl. Acad. Sci. USA.* **89**: 9252-9256.
168. Jingami H and Yamamoto T (1995). The VLDL receptor: wayward brother of the LDL receptor. *Curr. Opin. Lipidol.* **6**: 104-108.
169. Webb JC, Patel DD, Jones MD, Knight BL and Soutar AK (1994). Characterization and tissue-specific expression of the human "very low density lipoprotein (VLDL) receptor" mRNA. *Hum. Mol. Genet.* **3**: 531-537.
170. Yamamoto T, Takahashi S, Sakai J and Kawarabayasi Y (1993). The VLDLR: a second lipoprotein receptor that may mediate uptake of fatty acids into muscle and fat cells. *Trends Cardiovas. Med.* **3**: 144-148.
171. Frykman PK, Brown MS, Yamamoto T, Goldstein JL and Herz J (1995). Normal plasma lipoproteins and fertility in gene-targeted mice homozygous for a disruption in the gene encoding very low density lipoprotein receptor. *Proc. Natl. Acad. Sci. USA.* **92**: 8453-8457.
172. Kim DH, Iijima H, Goto K et al (1996). Human apolipoprotein E receptor 2. A novel lipoprotein receptor of the low density lipoprotein receptor family predominantly expressed in brain. *J. Biol. Chem.* **271**: 8373-8380.
173. Kim DH, Magoori K, Inoue TR et al (1997). Exon/intron organisation, chromosome localization, alternative slicing, and transcriptional units of the human apolipoprotein E receptor 2 gene. *J. Biol. Chem.* **272**: 8498-8504.
174. Novak S, Hiesberger T, Schneider WJ and Nimpf J (1996). A new low density lipoprotein receptor homologue with 8 ligand binding repeats in brain of chicken and mouse. *J. Biol. Chem.* **271**: 11732-11736.
175. Brandes C, Novak S, Stockinger W, Herz J, Schneider WJ and Nimpf J (1997). Avian and murine LR8B and human apolipoprotein E receptor 2: differentially spliced products from corresponding genes. *Genomics* **42**: 185-191.
176. Bu G, Geuze HJ, Strous GJ and Schwartz AL (1995). 39 kDa receptor-associated protein is an ER resident protein and molecular chaperone for LDL receptor-related protein. *EMBO. J.* **14**: 2269-2280.
177. Bu G and Rennke S (1996). Receptor-associated protein is a folding chaperone for low density lipoprotein receptor-related protein. *J. Biol. Chem.* **271**: 22218-22224.
178. Battey FD, Gafvels ME, FitzGerald DJ, Argraves WS, Chappell DA, Strauss JF 3rd, Strickland DK (1994). The 39-kDa receptor-associated protein regulates ligand binding by the very low density lipoprotein receptor. *J. Biol. Chem.* **269**: 23268-23273.

179. Kounnas MZ, Argraves WS and Strickland DK (1992). The 39-kDa receptor-associated protein interacts with two members of the low density lipoprotein receptor family, alpha 2-macroglobulin receptor and glycoprotein 330. *J. Biol. Chem.* **267**: 21162-21166.
180. Medh JD, Fry GL, Bowen SL, Pladet MW, Strickland DK and Chappell DA (1995). The 39-kDa receptor-associated protein modulates lipoprotein catabolism by binding to LDL receptors. *J. Biol. Chem.* **270**: 536-540.
181. Willnow TE, Armstrong SA, Hammer RE and Herz J (1995). Functional expression of low density lipoprotein receptor-related protein is controlled by receptor-associated protein in vivo. *Proc. Natl. Acad. Sci. USA.* **92**: 4537-4541.
182. Havel RJ and Kane JP (1989). *The Metabolic Basis of Inherited Disease* (Scriver CR et al. eds.) McGraw-Hill, New York, Vol 1 pp 1129-1138.
183. Choi SY, Fong LG, Kirven MJ and Cooper AD (1991). Use of an anti-low density lipoprotein receptor antibody to quantify the role of the LDL receptor in the removal of chylomicron remnants in the mouse in vivo. *J. Clin. Invest.* **88**: 1173-1181.
184. Bradley WA, Hwang SL, Karlin JB, Lin AH, Prasad SC, Gotto AM Jr and Gianturco SH (1984). Low-density lipoprotein receptor binding determinants switch from apolipoprotein E to apolipoprotein B during conversion of hypertriglyceridemic very-low-density lipoprotein to low-density lipoproteins. *J. Biol. Chem.* **259**: 14728-14735.
185. Thuren T, Sisson P and Waite M (1991). Activation of hepatic lipase catalyzed phosphatidylcholine hydrolysis by apolipoprotein E. *Biochim. Biophys. Acta.* **1083**: 217-220.
186. Thuren T, Weisgraber KH, Sisson P and Waite M (1992). Role of apolipoprotein E in hepatic lipase catalyzed hydrolysis of phospholipid in high-density lipoproteins. *Biochemistry* **31**: 2332-2338.
187. Rensen PCN and van Berkel TJC (1996). Apolipoprotein E effectively inhibits lipoprotein lipase-mediated lipolysis of chylomicron-like triglyceride-rich lipid emulsions in vitro and in vivo. *J. Biol. Chem.* **271**: 14791-14799.
188. De Pauw M, Vanloo B, Weisgraber K and Rosseneu M (1995). Comparison of lipid-binding and lecithin:cholesterol acyltransferase activation of the amino- and carboxyl-terminal domains of human apolipoprotein E3. *Biochemistry* **34**: 10953-10966.
189. Huang Y, Zhu Y, Langer C, Raabe M, Wu S, Wiesenhutter B, Seedorf U, Maeda N, Assmann G and von Eckardstein A (1997). Effects of genotype and diet on cholesterol efflux into plasma and lipoproteins of normal, apolipoprotein A-I-, and apolipoprotein E- deficient mice. *Arterioscler. Thromb. Vasc. Biol.* **17**: 2010-2019.
190. Von Eckardstein A (1996). Cholesterol efflux from macrophages and other cells *Curr. Opin. Lipidol.* **7**: 308-319.
191. Plump AS and Breslow JL (1995). Apolipoprotein E and the apolipoprotein E-deficient mouse. *Annu. Rev. Nutr.* **15**: 495-518.
192. Plump AS, Smith JD, Hayek T, Aalto-Setälä K, Walsh A, Verstuyft JG, Rubin EM and Breslow JL (1992). Severe hypercholesterolemia and atherosclerosis in apolipoprotein E-deficient mice created by homologous recombination in ES cells. *Cell* **71**: 343-353.

193. World Health Organisation (1985). Classification of atherosclerotic lesions. *WHO. Tech. Rep. Serv.* **143**: 1-20.
194. Ross R (1995). Cell biology of atherosclerosis. *Annu. Rev. Physiol.* **57**: 791-804.
195. Ross R (1993). The pathogenesis of atherosclerosis: a perspective for the 1990s. *Nature* **362**: 801-809.
196. Schaefer EJ, Gregg RE, Ghiselli G, Forte TM, Ordovas JM, Zech LA and Brewer HB Jr (1986). Familial apolipoprotein E deficiency. *J. Clin. Invest.* **78**: 1206-1219.
197. Scheer WD, Boudreau DA, Malcom GT and Middaugh JP (1995). Apolipoprotein E and atherosclerosis in Alaska Natives. *Atherosclerosis* **114**: 197-202.
198. O'Brien KD, Deeb SS, Ferguson M, McDonald TO, Allen MD, Alpers CE and Chait A (1994). Apolipoprotein E localization in human coronary atherosclerotic plaques by in situ hybridization and immunohistochemistry and comparison with lipoprotein lipase. *Am. J. Pathol.* **144**: 538-548.
199. Rosenfeld ME, Butler S, Ord VA, Lipton BA, Dyer CA, Curtiss LK, Palinski W and Witztum JL (1993). Abundant expression of apoprotein E by macrophages in human and rabbit atherosclerotic lesions. *Arterioscler. Thromb.* **13**: 1382-1389.
200. Linton MF, Atkinson JB and Fazio S (1995). Prevention of atherosclerosis in apolipoprotein E-deficient mice by bone marrow transplantation. *Science* **267**: 1034-1037.
201. Boisvert WA, Spangenberg J and Curtiss LK (1995). Treatment of severe hypercholesterolemia in apolipoprotein E-deficient mice by bone marrow transplantation. *J. Clin. Invest.* **96**: 1118-1124.
202. Shimano H, Ohsuga J, Shimada M, Namba Y, Gotoda T, Harada K, Katsuki M, Yazaki Y and Yamada N (1995). Inhibition of diet-induced atheroma formation in transgenic mice expressing apolipoprotein E in the arterial wall. *J. Clin. Invest.* **95**: 469-476.
203. Bellosta S, Mahley RW, Sanan DA, Murata J, Newland DL, Taylor JM and Pitas RE (1995). Macrophage-specific expression of human apolipoprotein E reduces atherosclerosis in hypercholesterolemic apolipoprotein E-null mice. *J. Clin. Invest.* **96**: 2170-2179.
204. Jonasson L, Holm J, Skalli O, Bondjers G and Hansson GK (1986). Regional accumulations of T cells, macrophages, and smooth muscle cells in the human atherosclerotic plaque. *Arteriosclerosis* **6**: 131-138.
205. Kelly ME, Clay MA, Mistry MJ, Hsieh-Li HM and Harmony JA (1994). Apolipoprotein E inhibition of proliferation of mitogen-activated T lymphocytes: production of interleukin 2 with reduced biological activity. *Cell. Immunol.* **159**: 124-139.
206. Clay MA, Anantharamaiah GM, Mistry MJ, Balasubramaniam A and Harmony JA (1995). Localization of a domain in apolipoprotein E with both cytostatic and cytotoxic activity. *Biochemistry* **34**: 11142-11151.
207. Corder EH, Saunders AM, Strittmatter WJ, Schmechel DE, Gaskell PC, Small GW, Roses AD, Haines JL and Pericak-Vance MA (1993). Gene dose of apolipoprotein E type 4 allele and the risk of Alzheimer's disease in late onset families. *Science* **261**: 921-923.
208. Strittmatter WJ, Saunders AM, Schmechel D, Pericak-Vance M, Enghild J, Salvesen GS and Roses AD (1993). Apolipoprotein E: high-avidity binding to beta-amyloid and increased frequency of type 4 allele in late-onset familial Alzheimer disease. *Proc. Natl. Acad. Sci. USA.* **90**: 1977-1981.

209. Kawanishi C, Suzuki K, Odawara T, Iseki E, Onishi H, Miyakawa T, Yamada Y, Kosaka K, Kondo N and Yamamoto T (1996). Neuropathological evaluation and apolipoprotein E gene polymorphism analysis in diffuse Lewy body disease. *J. Neurol. Sci.* **136**: 140-142.
210. Namba Y, Tomonaga M, Kawasaki H, Otomo E and Ikeda K (1991). Apolipoprotein E immunoreactivity in cerebral amyloid deposits and neurofibrillary tangles in Alzheimer's disease and kuru plaque amyloid in Creutzfeldt-Jakob disease. *Brain Res.* **541**: 163-166.
211. Seubert P, Vigo-Pelfrey C, Esch F, Lee M, Dovey H, Davis D, Sinha S, Schlossmacher M, Whaley J, Swindlehurst C, et al. (1992). Isolation and quantification of soluble Alzheimer's beta-peptide from biological fluids. *Nature* **359**: 325-327.
212. Haass C and Selkoe DJ (1993). Cellular processing of beta-amyloid precursor protein and the genesis of amyloid beta-peptide. *Cell* **75**: 1039-1042.
213. Strittmatter WJ, Weisgraber KH, Huang DY, Dong LM, Salvesen GS, Pericak-Vance M, Schmechel D, Saunders AM, Goldgaber D and Roses AD (1993). Binding of human apolipoprotein E to synthetic amyloid beta peptide: isoform-specific effects and implications for late-onset Alzheimer disease. *Proc. Natl. Acad. Sci. USA.* **90**: 8098-8102.
214. Crowther RA (1993). Tau protein and paired helical filaments of Alzheimers disease. *Curr. Opin. Struct. Biol.* **3**: 202-206.
215. Billingsley ML and Kincaid RL (1997). Regulated phosphorylation and dephosphorylation of tau protein: effects on microtubule interaction, intracellular trafficking and neurodegeneration. *Biochem. J.* **323**: 577-591.
216. Strittmatter WJ, Weisgraber KH, Goedert M, Saunders AM, Huang D, Corder EH, Dong LM, Jakes R, Alberts MJ, Gilbert JR, et al (1994). Hypothesis: microtubule instability and paired helical filament formation in the Alzheimer disease brain are related to apolipoprotein E genotype. *Exp. Neurol.* **125**: 163-171.
217. Genis I, Gordon I, Sehayek E and Michaelson DM (1995). Phosphorylation of tau in apolipoprotein E-deficient mice. *Neurosci. Lett.* **199**: 5-8.
218. Masliah E, Mallory M, Ge N, Alford M, Veinbergs I and Roses AD (1995). Neurodegeneration in the central nervous system of apoE-deficient mice. *Exp. Neurol.* **136**: 107-122.
219. Surya II and Akkerman JW (1993). The influence of lipoproteins on blood platelets *Am. Heart. J.* **125**: 272-275.
220. Malle E and Sattler W (1994). Platelets and Lipoproteins: Native, modified and platelet modified lipoproteins. *Platelets* **5**: 70-83.
221. Hassall DG, Forrest LA, Bruckdorfer KR, Marenah CB, Turner P, Cortese C, Miller NE and Lewis B (1983). Influence of plasma lipoproteins on platelet aggregation in a normal male population. *Arteriosclerosis* **3**: 332-338.
222. Farbiszewski R, Skrzydlewski Z and Worowski K (1969). The effect of lipoprotein fractions on adhesiveness and aggregation of blood platelets. *Thromb. Diath. Haemorrh.* **21**: 89-92.
223. Hassall DG, Owen JS and Bruckdorfer KR (1983). The aggregation of isolated human platelets in the presence of lipoproteins and prostacyclin. *Biochem. J.* **216**: 43-49.
224. Zhao B, Dierichs R, Liu B and Holling-Rauss M (1994). Functional morphological alterations of human blood platelets induced by oxidized low density lipoprotein. *Thromb. Res.* **74**: 293-301.

225. Naseem KM, Goodall AH and Bruckdorfer KR (1993). The effects of native and oxidised low density lipoproteins on platelet activation. *Biochem. Soc. Trans.* **21**: 140S
226. Bochkov VN, Kuz'menko ES, Rezink T and Tkachuk VA (1994). "Classical" apo B, E-receptor does not mediate the activating effect of low density lipoproteins on the second messenger system in human platelets and vascular smooth muscle cells. *Biokhimiia* **59**: 1330-1339.
227. Pedreno J, de Castellarnau C, Cullaré C, Sánchez J, Gómez-Gerique J, Ordóñez-Llanos J and González-Sastre F (1992). LDL binding sites on platelets differ from the "classical" receptor of nucleated cells. *Arterioscler. Thromb.* **12**: 1353-1362.
228. Koller E and Koller F (1992). Binding characteristics of homologous plasma lipoproteins to human platelets. *Methods Enzymol.* **215**: 383-398.
229. Koller E, Koller F and Binder BR (1989). Purification and identification of the lipoprotein-binding proteins from human blood platelet membrane. *J. Biol. Chem.* **264**: 12412-12418.
230. Pedreno J, Camejo EH, Wiklund O and Masana L (1997). CD36 is a specific platelet receptor for native and modified low-density lipoproteins. *Atherosclerosis* **134**: 185.
231. Nordoy A, Refsum N, Thelle D and Jaeger S (1979). Platelet function and serum high density lipoproteins. *Thromb. Haemost.* **42**: 1181-1186.
232. Aviram M and Brook JG (1983). Characterization of the effect of plasma lipoproteins on platelet function in vitro. *Haemostasis* **13**: 344-350.
233. Silverman DI, Ginsburg GS and Pasternak RC (1993). High-density lipoprotein subfractions. *Am. J. Med.* **94**: 636-645.
234. Schmitz G and Assmann G (1982). Isolation of human serum HDL1 by zonal ultracentrifugation. *J. Lipid Res.* **23**: 903-910.
235. Desai K, Mistry P, Bagget C, Burroughs AK, Bellamy MF and Owen JS (1989). Inhibition of platelet aggregation by abnormal high density lipoprotein particles in plasma from patients with hepatic cirrhosis. *Lancet* **1**: 693-695.
236. Mackness MI and Durrington PN (1992). Lipoprotein separation and analysis for clinical studies. *Lipoprotein Analysis: A Practical Approach* (Converse CA and Skinner ER eds). Oxford university press, New York, pp 1-42.
237. Milne RW, Weech PK and Marcel YL (1992). Immunological methods for studying and quantifying lipoproteins and apolipoproteins *Lipoprotein Analysis: A Practical Approach* (Converse CA and Skinner ER eds). Oxford University press, New York, pp 80-81.
238. Gries A, Nimpf J, Nimpf M, Wurm H and Kostner GM (1987). Free and apoB-associated Lpa-specific protein in human serum. *Clin. Chim. Acta.* **164**: 93-100.
239. Schumaker VN and Puppione DL (1986). Sequential floatation ultracentrifugation. *Methods Enzymol.* **128**: 155-170.
240. Edelstein C and Scanu AM (1986). Precautionary measures for collecting blood destined for lipoprotein isolation. *Methods Enzymol.* **128**: 151-155.

241. Bradford MM (1976). A rapid and sensitive method for the quantitation of microgram quantities of protein utilizing the principle of protein-dye binding. *Anal. Biochem.* **72**: 248-254.
242. Spector T (1978). Refinement of the coomassie blue method of protein quantitation. A simple and linear spectrophotometric assay for less than or equal to 0.5 to 50 microgram of protein. *Anal. Biochem.* **86**: 142-146.
243. Hames BD and Rickwood D (1983). *Gel Electrophoresis of Proteins: A Practical Approach*. IRL press Ltd, Oxford.
244. Hames BD (1983). An introduction to polyacrylamide gel electrophoresis. *Gel Electrophoresis of Proteins: A Practical Approach*. (Hames BD and Rickwood D eds). IRL press Ltd, Oxford, pp 1-92.
245. Harlow E and Lane D (1988). *Antibodies: A Laboratory Manual*. Cold Spring Harbor laboratory publications, New York.
246. Butler P, Riddell DR, Owen JS, Burroughs AK, McIntyre N and Mistry PK (1996) Apolipoprotein E allele frequencies in hyperlipidaemia of primary biliary cirrhosis. *Hepatology*, **24**: 313A.
247. Mezdour H, Nomura S, Yamamura T and Yamamoto A (1992). Concentration and distribution of apolipoproteins A-I and E in normolipidemic, WHHL and diet-induced hyperlipidemic rabbit sera. *Biochim. Biophys. Acta.* **1127**: 116-123.
248. Lee BR, Miller JM, Yang CY, Ramdas L, Yang ML, Morrisett JD and Mims MP (1991). Amino acid sequence of rabbit apolipoprotein E. *J. Lipid Res.* **32**: 165-171.
249. An der Lan B and Chrambach (1983). Analytical and preparative gel electrofocusing. *Gel Electrophoresis of Proteins: A Practical Approach*. (Hames BD and Rickwood D eds). IRL press Ltd, Oxford, pp 157-188.
250. Osborne JC (1986). Delipidation of plasma lipoproteins. *Methods Enzymol.* **128**: 213-222.
251. Rall SC, Weisgraber KH and Mahley RW (1986). Isolation and characterization of apolipoprotein E. *Methods Enzymol.* **128**: 273-287.
252. Innerarity TL, Pitas RE and Mahley RW (1986). Lipoprotein-receptor interactions. *Methods Enzymol.* **129**: 542-548.
253. Forte TM and Nordhausen RW (1986). Electron microscopy of negatively stained lipoproteins. *Methods Enzymol.* **128**: 442-457.
254. Basu SK, Ho YK, Brown MS, Bilheimer DW, Anderson RG and Goldstein JL (1982). Biochemical and genetic studies of the apoprotein E secreted by mouse macrophages and human monocytes. *J. Biol. Chem.* **257**: 9788-9795.
255. Zucker MB (1989). Platelet aggregation measured by the photometric method. *Methods Enzymol.* **169**: 117-133.
256. McNicol A (1996). Platelet preparation and estimation of functional responses. *Platelets: A Practical Approach* (Watson SP and Authi KS eds). Oxford University press, New York, pp 1-26.
257. McGregor JL, Gaynet O, Mercier N, McGregor L and Chignier E (1996). Use of PCR to identify glycoproteins involved in platelet adhesion *Platelets: a practical approach* (Watson SP and Authi KS eds). Oxford University press, New York, pp 146-152.
258. Vittet D, Mathieu MN, Launay JM and Chevillard C (1992). Platelet receptor expression on three human megakaryoblast-like cell lines. *Exp. Hematol.* **20**: 1129-1134.

259. Tabilio A, Rosa JP, Testa U, Kieffer N, Nurden AT, Del Canizo MC, Breton-Gorius J and Vainchenker W (1984). Expression of platelet membrane glycoproteins and alpha-granule proteins by a human erythroleukemia cell line (HEL). *EMBO J.* **3**: 453-459.
260. Ogura M, Morishima Y, Ohno R, Kato Y, Hirabayashi N, Nagura H and Saito H (1985). Establishment of a novel human megakaryoblastic leukemia cell line, MEG-01, with positive Philadelphia chromosome. *Blood* **66**: 1384-1392.
261. Sambrook J, Fritsch EF and Maniatis T (1989). In vitro amplification of DNA by the polymerase chain reaction. *Molecular Cloning: A Laboratory Manual*. Cold Spring Harbor Publications, New York, pp 14.1-14-22.
262. Chomczynski P and Sacchi N (1987). Single-step method of RNA isolation by acid guanidinium thiocyanate-phenol-chloroform extraction. *Anal. Biochem.* **162**: 156-159.
263. Sambrook J, Fritsch EF and Maniatis T (1989). Gel Electrophoresis of DNA. *Molecular Cloning: A Laboratory Manual*. Cold Spring Harbor Publications, New York, pp 6.1-6.62.
264. Sambrook J, Fritsch EF and Maniatis T (1989). Enzymes used in molecular cloning. *Molecular Cloning: A Laboratory Manual*. Cold Spring Harbor Publications, New York, pp 5.3-5.32.
265. Sambrook J, Fritsch EF and Maniatis T (1989). Plasmid Vectors. *Molecular Cloning: A Laboratory Manual*. Cold Spring Harbor Publications, New York, pp 1.1-1.110.
266. Kunitake ST and Kane JP (1982). Factors affecting the integrity of high density lipoproteins in the ultracentrifuge. *J. Lipid Res.* **23**: 936-940.
267. Fainaru M, Havel RJ and Imaizumi K (1977). Apoprotein content of plasma lipoproteins of the rat separated by gel chromatography or ultracentrifugation. *Biochem. Med.* **17**: 347-355.
268. Murdoch SJ and Breckenridge WC (1994). Development of a density gradient ultracentrifugation technique for the resolution of plasma lipoproteins which avoids apoE dissociation. *Analyt. Biochem.* **222**: 427-434.
269. Cheung MC (1986). Characterization of apolipoprotein A-containing lipoproteins. *Methods Enzymol.* **129**: 130-145.
270. James RW, Proudfoot A and Pometta D (1989). Immunoaffinity fractionation of high-density lipoprotein subclasses 2 and 3 using anti-apolipoprotein A-I and A-II immunosorbent gels. *Biochim. Biophys. Acta.* **1002**: 292-301.
271. Higashihara M, Kinoshita M, Teramoto T, Kume S and Kurokawa K (1991). The role of apoE in inhibitory effects of apoE-rich HDL on platelet function. *FEBS Lett.* **282**: 82-86.
272. Owen JS, Brown DJ, Harry DS, McIntyre N, Beaven GH, Isenberg H and Gratzner WB (1985). Erythrocyte echinocytosis in liver disease. Role of abnormal plasma high density lipoproteins. *J. Clin. Invest.* **76**: 2275-2285.
273. Owen JS, Goodall H, Mistry P, Harry DS, Day RC and McIntyre N (1984). Abnormal high density lipoproteins from patients with liver disease regulate cholesterol metabolism in cultured human skin fibroblasts. *J. Lipid Res.* **25**: 919-931.

274. Teramoto T, Kato H, Hashimoto Y, Kinoshita M, Toda G and Oka H (1985). Abnormal high density lipoprotein of primary biliary cirrhosis analyzed by high performance liquid chromatography. *Clin. Chim. Acta.* **149**: 135-148.
275. Innerarity TL, Pitas RE, and Mahley RW (1979). Binding of arginine-rich (E) apoprotein after recombination with phospholipid vesicles to the low density lipoprotein receptors of fibroblasts. *J. Biol. Chem.* **254**: 4186-4190.
276. Gianturco SH, Gotto AM Jr, Hwang SL, Karlin JB, Lin AH, Prasad SC and Bradley WA (1983). Apolipoprotein E mediates uptake of Sf 100-400 hypertriglyceridemic very low density lipoproteins by the low density lipoprotein receptor pathway in normal human fibroblasts. *J. Biol. Chem.* **258**: 4526-4533.
277. Hussain MM, Mahley RW, Boyles JK, Fainaru M, Brecht WJ and Lindquist PA (1989). Chylomicron-chylomicron remnant clearance by liver and bone marrow in rabbits. Factors that modify tissue-specific uptake. *J. Biol. Chem.* **264**: 9571-9582.
278. Mahley RW, Innerarity TL, Rall SC and Weisgraber KH (1984). Plasma lipoproteins: apolipoprotein structure and function. *J. Lipid Res.* **25**: 1277-1294.
279. Elwood PC, Renaud S, Sharp DS, Beswick AD, O'Brien JR and Yarnell JW (1991). Ischemic heart disease and platelet aggregation. The Caerphilly Collaborative Heart Disease Study. *Circulation* **83**: 38-44.
280. Thaulow E, Erikssen J, Sandvik L, Stormorken H and Cohn PF (1991). Blood platelet count and function are related to total and cardiovascular death in apparently healthy men. *Circulation* **84**: 613-617.
281. Shattil SJ, Anaya-Galindo R, Bennett J, Colman RW and Cooper RA (1975). Platelet hypersensitivity induced by cholesterol incorporation. *J. Clin. Invest.* **55**: 636-643.
282. Huang Y, von Eckardstein A, Wu S and Assmann G (1995). Effects of the apolipoprotein E polymorphism on uptake and transfer of cell-derived cholesterol in plasma. *J. Clin. Invest.* **96**: 2693-2701.
283. Moro MA, Russel RJ, Celtek S, Lizasoain I, Su Y, Darley-Usmar VM, Radomski MW and Moncada S (1996). cGMP mediates the vascular and platelet actions of nitric oxide: confirmation using an inhibitor of the soluble guanylyl cyclase. *Proc. Natl. Acad. Sci. USA.* **93**: 1480-1485.
284. Mellion BT, Ignarro LJ, Ohlstein EH, Pontecorvo EG, Hyman AL and Kadowitz PJ (1981). Evidence for the inhibitory role of guanosine 3', 5'-monophosphate in ADP-induced human platelet aggregation in the presence of nitric oxide and related vasodilators. *Blood* **57**: 946-955.
285. Ignarro LJ (1991). Signal transduction mechanisms involving nitric oxide. *Biochem. Pharmacol.* **41**: 485-490.
286. Trovati M, Massucco P, Mattiello L, Mularoni E, Cavalot F and Anfossi G (1994). Insulin increases guanosine-3',5'-cyclic monophosphate in human platelets. A mechanism involved in the insulin anti-aggregating effect. *Diabetes* **43**: 1015-1019.
287. Mellion BT, Ignarro LJ, Myers CB, Ohlstein EH, Ballot BA, Hyman AL and Kadowitz PJ (1983). Inhibition of human platelet aggregation by S-nitrosothiols. Heme-dependent activation of soluble guanylate cyclase and stimulation of cyclic GMP accumulation. *Mol. Pharmacol.* **23**: 653-664.

288. Radomski MW, Rees DD, Dutra A and Moncada S (1992). S-nitroso-glutathione inhibits platelet activation in vitro and in vivo. *Br. J. Pharmacol.* **107**: 745-9
289. Lieberman EH, O'Neill S and Mendelsohn ME (1991). S-nitrosocysteine inhibition of human platelet secretion is correlated with increases in platelet cGMP levels. *Circ. Res.* **68**: 1722-1728.
290. Gruetter CA, Kadowitz PJ and Ignarro LJ (1981). Methylene blue inhibits coronary arterial relaxation and guanylate cyclase activation by nitroglycerin, sodium nitrite, and amyl nitrite. *Can. J. Physiol. Pharmacol.* **59**: 150-156.
291. Okamura T, Yoshida K and Toda N (1990). Suppression by methylene blue of prostaglandin I₂ synthesis in isolated dog renal arteries. *J. Pharmacol. Exp. Ther.* **254**: 198-203.
292. Marshall JJ, Wei EP and Kontos HA (1988). Independent blockade of cerebral vasodilation from acetylcholine and nitric oxide. *Am. J. Physiol.* **255**: H847-854.
293. Mayer B, Brunner F and Schmidt K (1993). Inhibition of nitric oxide synthesis by methylene blue. *Biochem. Pharmacol.* **45**: 367-374.
294. Garthwaite J, Southam E, Boulton CL, Nielsen EB, Schmidt K and Mayer B (1995). Potent and selective inhibition of nitric oxide-sensitive guanylyl cyclase by 1H-[1,2,4]oxadiazolo[4,3-a]quinoxalin-1-one. *Mol. Pharmacol.* **48**: 184-188.
295. Radomski MW, Palmer RM and Moncada S (1990). Characterization of the L-arginine:nitric oxide pathway in human platelets. *Br. J. Pharmacol.* **101**: 325-328.
296. Radomski MW, Palmer RM and Moncada S (1990). An L-arginine/nitric oxide pathway present in human platelets regulates aggregation. *Proc. Natl. Acad. Sci. USA.* **87**: 5193-5197.
297. Moncada S (1991). The 1991 Ulf von Euler Lecture. The L-arginine: nitric oxide pathway. *Acta. Physiol. Scand.* **145**: 201-127.
298. Southan GJ, Szabó C and Thiemermann C (1995). Isothioureas: potent inhibitors of nitric oxide synthases with variable isoform selectivity. *Br. J. Pharmacol.* **114**: 510-516.
299. Garvey EP, Oplinger JA, Tanoury GJ, Sherman PA, Fowler M, Marshall S, Harmon MF, Paith JE and Furfine ES (1994). Potent and selective inhibition of human nitric oxide synthases. Inhibition by non-amino acid isothioureas. *J. Biol. Chem.* **269**: 26669-26676.
300. Stuehr DJ, Fasehun OA, Kwon NS, Gross SS, Gonzalez JA, Levi R and Nathan CF (1991). Inhibition of macrophage and endothelial cell nitric oxide synthase by diphenyleneiodonium and its analogs. *FASEB. J.* **5**: 98-103.
301. Salvemini D, Radziszewski W, Korbut R and Vane J (1990). The use of oxyhaemoglobin to explore the events underlying inhibition of platelet aggregation induced by NO or NO-donors. *Br. J. Pharmacol.* **101**: 991-995.
302. Stuart MJ, Gerrard JM and White JG (1980). Effect of cholesterol on production of thromboxane B₂ by platelets in vitro. *N. Engl. J. Med.* **302**: 6-10.
303. Worner P and Patscheke H. (1980). Hyperreactivity by an enhancement of the arachidonate pathway of platelets treated with cholesterol-rich phospholipid-dispersions. *Thromb. Res.* **18**: 439-451.

304. Owen JS, Rafique S, Osman E and Burroughs AK (1992). Ability of S-adenosyl-L-methionine to ameliorate lipoprotein-induced membrane lipid abnormalities and cellular dysfunctions in human liver disease. *Drug Invest.* **4(suppl. 4)**: 22-40.
305. Rothblat GH, Arbogast LY and Ray EK (1978). Stimulation of esterified cholesterol accumulation in tissue culture cells exposed to high density lipoproteins enriched in free cholesterol. *J. Lipid Res.* **19**: 350-358.
306. Tandon N, Harmon JT, Rodbard D and Jamieson GA (1983). Thrombin receptors define responsiveness of cholesterol-modified platelets. *J. Biol. Chem.* **258**: 11840-11845.
307. Fisch A, Michael-Hepp J, Meyer J and Darius H (1995). Synergistic interaction of adenylate cyclase activators and nitric oxide donor SIN-1 on platelet cyclic AMP. *Eur. J. Pharmacol.* **289**: 455-461.
308. Maurice DH and Haslam RJ (1990). Nitroprusside enhances isoprenaline-induced increases in cAMP in rat aortic smooth muscle. *Eur. J. Pharmacol.* **191**: 471-475.
309. Gruetter CA, Barry BK, McNamara DB, Gruetter DY, Kadowitz PJ and Ignarro L (1979). Relaxation of bovine coronary artery and activation of coronary arterial guanylate cyclase by nitric oxide, nitroprusside and a carcinogenic nitrosoamine. *J. Cyclic Nucleotide Res.* **5**: 211-224.
310. Freedman JE, Loscalzo J, Barnard MR, Alpert C, Keaney JF and Michelson AD (1997). Nitric oxide released from activated platelets inhibits platelet recruitment. *J. Clin. Invest.* **100**: 350-356.
311. Lincoln J, Hoyle CHV and Burnstock G eds. (1997). *Nitric Oxide in Health and Disease*. Cambridge University Press, Cambridge, pp 39.
312. Lantoin F, Brunet A, Bedioui F, Devynck J and Devynck MA (1995). Direct measurement of nitric oxide production in platelets: relationship with cytosolic Ca²⁺ concentration. *Biochem. Biophys. Res. Commun.* **215**: 842-848
313. Malinski T, Radomski MW, Taha Z and Moncada S (1993). Direct electrochemical measurement of nitric oxide released from human platelets. *Biochem. Biophys. Res. Commun.* **194**: 960-965.
314. Zhou Q, Hellermann GR and Solomonson LP (1995). Nitric oxide release from resting human platelets. *Thromb. Res.* **77**: 87-96.
315. Chen LY and Mehta JL (1997). Downregulation of nitric oxide synthase activity in human platelets by nitroglycerin and authentic nitric oxide. *J. Investig. Med.* **45**: 69-74.
316. Chen LY and Mehta JL (1994). Inhibitory effect of high-density lipoprotein on platelet function is mediated by increase in nitric oxide synthase activity in platelets. *Life Sci.* **55**: 1815-1821.
317. Martina V, Bruno GA, Trucco F, Zumpano E, Tagliabue M, Di Bisceglie C and Pescarmona G (1998). Platelet cNOS activity is reduced in patients with IDDM and NIDDM. *Thromb. Haemost.* **79**: 520-522.
318. Mehta JL, Chen LY, Kone BC, Mehta P and Turner P (1995). Identification of constitutive and inducible forms of nitric oxide synthase in human platelets. *J. Lab. Clin. Med.* **125**: 370-377.
319. Delacrétaiz E, de Quay N, Waeber B, Vial Y, Schulz PE, Burnier M, Brunner HR, Bossart H and Schaad NC (1995). Differential nitric oxide synthase activity in human platelets during normal pregnancy and pre-eclampsia. *Clin. Sci.* **88**: 607-610.

320. Sase K and Michel T (1995). Expression of constitutive endothelial nitric oxide synthase in human blood platelets. *Life Sci.* **57**: 2049-2055.
321. Das I, Khan NS, Puri BK, Sooranna SR, de Bellerocche J and Hirsch SR (1995). Elevated platelet calcium mobilization and nitric oxide synthase activity may reflect abnormalities in schizophrenic brain. *Biochem. Biophys. Res. Commun.* **212**: 375-380.
322. Noris M, Benigni A, Boccardo P, Aiello S, Gaspari F, Todeschini M, Figliuzzi M and Remuzzi G (1993). Enhanced nitric oxide synthesis in uremia: implications for platelet dysfunction and dialysis hypotension. *Kidney Int.* **44**: 445-450.
323. Lelchuk R, Carrier M, Hancock V and Martin JF (1990). The relationship between megakaryocyte nuclear DNA content and gene expression. *Int. J. Cell. Cloning.* **8**: 277-282.
324. Hancock V, Martin JF and Lelchuk R (1993). The relationship between human megakaryocyte nuclear DNA content and gene expression. *Br. J. Haematol.* **85**: 692-697.
325. Berkels R, Stockklauser K, Rösen P and Rösen R (1997). Current status of platelet NO synthases. *Thromb. Res.* **87**: 51-55.
326. Wallerath T, Gath I, Aulitzky WE, Pollock JS, Kleinert H and Forstermann U (1997). Identification of the NO synthase isoforms expressed in human neutrophil granulocytes, megakaryocytes and platelets. *Thromb. Haemost.* **77**: 163-167.
327. Lelchuk R, Radomski MW, Martin JF and Moncada S (1992). Constitutive and inducible nitric oxide synthases in human megakaryoblastic cells. *J. Pharmacol. Exp. Ther.* **262**: 1220-1224.
328. de Belder A, Radomski M, Hancock V, Brown A, Moncada S and Martin J (1995). Megakaryocytes from patients with coronary atherosclerosis express the inducible nitric oxide synthase. *Arterioscler. Thromb. Vasc. Biol.* **15**: 637-641.
329. Piggazi A, Fabian A, Johnston J, Upchurch GR and Loscalzo J (1995). Identification of nitric oxide synthases in human megakaryocytes and platelets. *Circulation* **92:Suppl. I** I-365.
330. Chen LY and Mehta JL (1996). Further evidence of the presence of constitutive and inducible nitric oxide synthase isoforms in human platelets. *J. Cardiovasc. Pharmacol.* **27**: 154-158.
331. Muruganandam A and Mutus B (1994). Isolation of nitric oxide synthase from human platelets. *Biochim. Biophys. Acta.* **1200**: 1-6.
332. Kelm M, Feelisch M, Spahr R, Piper HM, Noack E and Schrader J (1988). Quantitative and kinetic characterization of nitric oxide and EDRF released from cultured endothelial cells. *Biochem. Biophys. Res. Commun.* **154**: 236-244.
333. Archer S (1993). Measurement of nitric oxide in biological models. *FASEB. J.* **7**: 349-360.
334. Misko TP, Schilling RJ, Salvemini D, Moore WM and Currie MG (1993). A fluorometric assay for the measurement of nitrite in biological samples. *Anal. Biochem.* **214**: 11-16.
335. Amano F and Noda T (1995). Improved detection of nitric oxide radical (NO) production in an activated macrophage culture with a radical scavenger, carboxy PTIO and Griess reagent. *FEBS Lett.* **368**: 425-428.

336. Lincoln J, Hoyle CHV and Burnstock G [eds] (1997). *Nitric Oxide in Health and Disease*. Cambridge University Press, Cambridge, pp 215-231.
337. Vitek MP, Snell J, Dawson H and Colton CA (1997). Modulation of nitric oxide production in human macrophages by apolipoprotein-E and amyloid-beta peptide. *Biochem. Biophys. Res. Commun.* **240**: 391-394.
338. Vasta V, Meacci E, Famararo M and Bruni P (1995). Identification of a specific transport system for L-arginine in human platelets. *Biochem. Biophys. Res. Commun.* **206**: 878-884.
339. Vasta V, Meacci E, Maurenzig L, Famararo M and Bruni P (1996). Agonist-regulated L-arginine uptake in human platelets. Evidence against intracellular utilization of the amino acid. *Biochem. Mol. Biol. Int.* **38**: 911-919.
340. Dorahy DJ, Lincz LF, Meldrum CJ and Burns GF (1996). Biochemical isolation of a membrane microdomain from resting platelets highly enriched in the plasma membrane glycoprotein CD36. *Biochem. J.* **319**: 67-72.
341. Morwald S, Yamazaki H, Bujo H, Kusunoki J, Kanaki T, Seimiya K, Morisaki N, Nimpf J, Schneider WJ and Saito Y (1997). A novel mosaic protein containing LDL receptor elements is highly conserved in humans and chickens. *Arterioscler. Thromb. Vasc. Biol.* **17**: 996-1002.
342. Williams JW and Fuki IV (1997). Cell-surface heparan sulfate proteoglycans: dynamic molecules mediating ligand catabolism. *Curr. Opin. Lipidol.* **8**: 253-262.
343. Tensen CP, Van Kesteren ER, Planta RJ, Cox KJA, Burke JF, Van Heerikhuizen H and Vreugdenhil E (1994). A G protein-coupled receptor with low density lipoprotein-binding motifs suggests a role for lipoproteins in G-linked signal transduction. *Proc. Natl. Acad. Sci. USA.* **91**: 4816-4820
344. Brink AA, Oudejans JJ, Jiwa M, Walboomers JM, Meijer CJ and van den Brule AJ (1997). Multiprimered cDNA synthesis followed by PCR is the most suitable method for Epstein-Barr virus transcript analysis in small lymphoma biopsies. *Mol. Cell. Probes.* **11**: 39-47.
345. Moras D and Poterszman A (1995). RNA-protein interactions. Diverse modes of recognition. *Curr. Biol.* **5**: 249-51.
346. Southern EM. (1975). Detection of specific sequences among DNA fragments separated by gel electrophoresis. *J. Mol. Biol.* **98**: 503-517.
347. Dyer CA, Cistola DP, Parry GC and Curtiss LK (1995). Structural features of synthetic peptides of apolipoprotein E that bind the LDL receptor. *J. Lipid Res.* **36**: 80-88.
348. Maneva A.I, Taleva BM, Manev VV and Sirakov L (1993). Lactoferrin binding to human platelets. *Int. J. Biochem.* **25**: 707-712.
349. Qian ZY, Jolles P, Migliore-Samour D and Fiat AM (1995). Isolation and characterization of sheep lactoferrin, an inhibitor of platelet aggregation and comparison with human lactoferrin. *Biochim. Biophys. Acta.* **1243**: 25-32.
350. Leveugle B, Mazurier J, Legrand O, Mazurier C, Montreuil J and Spik G (1993). Lactotransferrin binding to its platelet receptor inhibits platelet aggregation. *Eur. J. Biochem.* **213**: 1205-1211.

351. Mazurier J, Legrand D, Leveugle B, Rochard E, Montreuil J and Spik G (1994). Study on the binding of lactotransferrin (lactoferrin) to human PHA-activated lymphocytes and non-activated platelets. Localisation and description of the receptor-binding site. *Adv. Exp. Med. Biol.* **357**: 111-119.
352. Hiesberger T, Hermann M, Jacobsen L, Novak S, Hodits RA, Bujo H, Meilinger M, Huttinger M, Schneider WJ and Nimpf J (1995). The chicken oocyte receptor for yolk precursors as a model for studying the action of receptor-associated protein and lactoferrin. *J. Biol. Chem.* **270**: 18219-18226.
353. Nillesse N, Pierce A, Lecocq M, Benaissa M and Spik G (1994). Expression of the lactotransferrin receptor during the differentiation process of the megakaryocyte Dami cell line. *Biol. Cell.* **82**: 149-159.
354. Takahashi S, Oida K, Ookubo M, Suzuki J, Kohno M, Murase T, Yamamoto T and Nakai T (1996). Very low density lipoprotein receptor binds apolipoprotein E2/2 as well as apolipoprotein E3/3. *FEBS Lett.* **386**: 197-200.
355. Hodits RA, Nimpf J, Pfistermueller DM, Hiesberger T, Schneider WJ, Vaughan TJ, Johnson KS, Haumer M, Kuechler E, Winter G, et al (1995). An antibody fragment from a phage display library competes for ligand binding to the low density lipoprotein receptor family and inhibits rhinovirus infection. *J. Biol. Chem.* **270**: 24078-24085
356. Kounnas MZ, Henkin J, Argraves WS and Strickland DK (1993). Low density lipoprotein receptor-related protein/alpha 2-macroglobulin receptor mediates cellular uptake of pro-urokinase. *J. Biol. Chem.* **268**: 21862-21867.
357. Kounnas MZ, Moir RD, Rebeck GW, Bush AI, Argraves WS, Tanzi RE, Hyman BT and Strickland DK (1995). LDL receptor-related protein, a multifunctional ApoE receptor, binds secreted beta-amyloid precursor protein and mediates its degradation. *Cell* **82**: 331-340
358. Kounnas MZ, Chappell DA, Wong H, Argraves WS and Strickland DK (1995). The cellular internalization and degradation of hepatic lipase is mediated by low density lipoprotein receptor-related protein and requires cell surface proteoglycans. *J. Biol. Chem.* **270**: 9307-9312
359. Mikhailenko I, Kounnas MZ and Strickland DK (1995). Low density lipoprotein receptor-related protein/alpha 2-macroglobulin receptor mediates the cellular internalization and degradation of thrombospondin. A process facilitated by cell-surface proteoglycans. *J. Biol. Chem.* **270**: 9543-9549
360. Huettinger M, Retzek H, Hermann M and Goldenberg H. (1992). Lactoferrin specifically inhibits endocytosis of chylomicron remnants but not alpha-macroglobulin. *J. Biol. Chem.* **267**: 18551-18557.
361. Naik UP, Ehrlich YH and Kornecki E (1995). Mechanisms of platelet activation by a stimulatory antibody: cross-linking of a novel platelet receptor for monoclonal antibody F11 with the Fc gamma RII receptor. *Biochem. J.* **310**: 155-162
362. Perutelli P, Marchese P and Mori PG (1992). Monoclonal antibody-induced platelet aggregation does not require interaction between antibody and platelet Fc receptor. *Haematologica* **77**: 186-187
363. Mahley RW and Angelin B (1984). Type III hyperlipoproteinemia: recent insights into the genetic defect of familial dysbetalipoproteinemia. *Adv. Intern. Med.* **29**: 385-411

364. van Dijk KW, van Vlijmen BJ, van der Zee A, van't Hof B, van der Boom H, Kobayashi K, Chan L, Havekes LM and Hofker MH (1998). Reversal of hypercholesterolemia in apolipoprotein E2 and apolipoprotein E3-Leiden transgenic mice by adenovirus-mediated gene transfer of the VLDL receptor. *Arterioscler. Thromb. Vasc. Biol.* **18**: 7-12
365. Dyer CA and Curtiss LK (1991). A synthetic peptide mimic of plasma apolipoprotein E that binds the LDL receptor. *J. Biol. Chem.* **266**: 22803-22806.
366. Wang XS and Gruenstein E (1997). Rapid elevation of neuronal cytoplasmic calcium by apolipoprotein E peptide. *J. Cell. Physiol.* **173**: 73-83.
367. Iozzo RV, Cohen IR, Grassel S and Murdoch AD (1994). The biology of perlecan: the multifaceted heparan sulphate proteoglycan of basement membranes and pericellular matrices *Biochem. J.* **302**: 625-639.
368. Willnow TE, Sheng Z, Ishibashi S and Herz J (1994). Inhibition of hepatic chylomicron remnant uptake by gene transfer of a receptor antagonist. *Science* **264**:1471-1474.
369. Mokuno H, Brady S, Kotite L, Herz J and Havel RJ (1994). Effect of the 39-kDa receptor-associated protein on the hepatic uptake and endocytosis of chylomicron remnants and low density lipoproteins in the rat. *J. Biol. Chem.* **269**:13238-13243.
370. Vassiliou G and Stanley KK (1994). Exogenous receptor-associated protein binds to two distinct sites on human fibroblasts but does not bind to the glycosaminoglycan residues of heparan sulfate proteoglycans. *J. Biol. Chem.* **269**: 15172-15178.
371. Hopp TP and Woods KR (1981). Prediction of protein antigenic determinants from amino acid sequences. *Proc. Natl. Acad. Sci. USA.* **78**: 3824-3828
372. Stern PS (1991). Predicting antigenic sites on proteins. *Trends Biotechnol.* **9**: 163-169
373. Hopp TP (1989). Use of hydrophilicity plotting procedures to identify protein antigenic segments and other interaction sites. *Methods Enzymol.* **178**: 571-585
374. Patel DD, Forder RA, Soutar AK and Knight BL (1997). Synthesis and properties of the very-low-density-lipoprotein receptor and a comparison with the low-density-lipoprotein receptor. *Biochem. J.* **324**: 371-377.
375. Kobayashi K, Oka K, Forte T, Ishida B, Teng B, Ishimura-Oka K, Nakamuta M and Chan L (1996). Reversal of hypercholesterolemia in low density lipoprotein receptor knockout mice by adenovirus-mediated gene transfer of the very low density lipoprotein receptor. *J. Biol. Chem.* **271**: 6852-6860.
376. Martensen PM, Oka K, Christensen L, Rettenberger PM, Petersen HH, Christensen A, Chan L, Heegaard CW, and Andreasen PA (1997). Breast carcinoma epithelial cells express a very low-density lipoprotein receptor variant lacking the O-linked glycosylation domain encoded by exon 16, but with full binding activity for serine proteinase/serpin complexes and Mr-40000 receptor-associated protein. *Eur. J. Biochem.* **248**: 583-591
377. Lindstedt KA, Bujo H, Mahon MG, Nimpf J and Schneider WJ (1997). Germ cell-somatic cell dichotomy of a low-density lipoprotein receptor gene family member in testis. *DNA Cell. Biol.* **16**: 35-43.

378. Bujo H, Lindstedt KA, Hermann M, Dalmau LM, Nimpf J and Schneider WJ (1995). Chicken oocytes and somatic cells express different splice variants of a multifunctional receptor. *J. Biol. Chem.* **270**: 23546-23551.
379. Altschul SF, Gish W, Miller W, Myers EW and Lipman DJ (1990). Basic local alignment search tool. *J. Mol. Biol.* **215**: 403-410.
380. Pawson T (1995). Protein modules and signalling networks. *Nature* **373**: 573-580.
381. Cohen GB, Ren R and Baltimore S (1995). Modular binding domains in signal transduction. *Science* **80**: 238-248.
382. Lim WA (1996). Reading between the lines: SH3 recognition of an intact protein. *Structure* **4**: 657-659.
383. Denhardt DT (1996). Signal-transducing protein phosphorylation cascades mediated by Ras/Rho proteins in the mammalian cell: the potential for multiplex signalling. *Biochem. J.* **318**: 729-747.
384. Lin D and Pawson T (1997). *Trends Cell Biol.* **7**: August centre fold
385. Yu H, Chen JK, Feng S, Dalgarno DC, Brauer AW and Schreiber SL (1994). Structural basis for the binding of proline-rich peptides to SH3 domains. *Cell* **76**: 933-945.
386. Fischer D and Eisenberg D (1996). Protein fold recognition using sequence-derived predictions. *Protein Sci.* **5**: 947-955.
387. Barford D, Flint AJ and Tonks NK (1994). Crystal structure of human protein tyrosine phosphatase 1B. *Science* **263**: 1397-1404 .
388. Margolis B (1996). The PI/PTB domain: a new protein interaction domain involved in growth factor receptor signalling. *J. Lab. Clin. Med.* **128**: 235-241.
389. Gustafson TA, HE W, Craparo A, Schaub CD and O'Neill TJ (1995). Phosphotyrosine-dependant interaction of Shc and IRS-1 with the NPEY motif of the insulin receptor via a novel (non SH2) domain. *Mol. Cell. Biol.* **15**: 2500-2508.
390. Law DA, Nannizzi-Alaimo L and Phillips DR (1996). Outside-in integrin signal transduction *J. Biol. Chem.* **271**: 10811-10815.
391. Chen WJ, Goldstein JL and Brown MS (1990). NPXY, a sequence often found in cytoplasmic tails, is required for coated pit-mediated internalisation of the low density lipoprotein receptor. *J. Biol. Chem.* **265**: 3116-3123.
392. Fantus IG, Goerge R, Tang S, Chong P and Poznansky MJ (1996). The insulin-mimetic agent vanadate promotes receptor endocytosis and inhibits intracellular ligand-receptor degradation by a mechanism distinct from the lysosomotropic agents. *Diabetes* **45**: 1084-1093.
393. Trovati M, Anfossi G, Massucco P, Mattiello L, Costamagna C, Piretto V, Mularoni E, Cavalot F, Bosia A and Ghigo D (1997). Insulin stimulates nitric oxide synthesis in human platelets and, through nitric oxide, increases platelet concentrations of both guanosine-3', 5'-cyclic monophosphate and adenosine-3', 5'-cyclic monophosphate. *Diabetes* **46**: 742-749
394. Falcon C, Pfliegler G, Deckmyn H and Vermeylen J (1988). The platelet insulin receptor: detection, partial characterization, and search for a function. *Biochem. Biophys. Res. Commun.* **157**: 1190-1196.

395. Eck MJ, Dhe-Paganon S, Trub T, Nolte RT and Shoelson SE (1996). Structure of the IRS-1 PTB domain bound to the juxtamembrane region of the insulin receptor. *Cell* **85**: 695-705.
396. Myers MG Jr and White MF (1996). Insulin signal transduction and the IRS proteins. *Annu. Rev. Pharmacol. Toxicol.* **36**: 615-658.
397. Michel T, Li GK and Busconi L (1993). Phosphorylation and subcellular translocation of endothelial nitric oxide synthase. *Proc. Natl. Acad. Sci. USA.* **90**: 6252-6256.
398. Garcia-Cardena G, Fan R, Stern DF, Liu J and Sessa WC (1996). Endothelial nitric oxide synthase is regulated by tyrosine phosphorylation and interacts with caveolin-1. *J. Biol. Chem.* **271**: 27237-27240.
399. Corson MA, James NL, Latta SE, Nerem RM, Berk BC and Harrison DG (1996). Phosphorylation of endothelial nitric oxide synthase in response to fluid shear stress. *Circ. Res.* **79**: 984-991.
400. Dorahy FJ, Berndt MC and Burns GF (1995). Capture by chemical crosslinkers provides evidence that integrin α IIB β 3 forms a complex with protein tyrosine kinases in intact platelets *Biochem. J.* **309**: 481-490.
401. Cloutier JF and Veillette A (1996). Association of inhibitory tyrosine protein kinase p50csk with protein tyrosine phosphatase PEP in T cells and other hemopoietic cells. *EMBO J.* **15**: 4909-4918.
402. Robinson A, Gibbins J, Rodriguez-Linares B, Finan PM, Wilson L, Kellie S, Findell P and Watson SP. (1996). Characterisation of Grb2-binding proteins in human platelets activated by Fc γ RIIA cross-linking. *Blood* **88**: 522-530.
403. Glass DB and Smith SB (1983). Phosphorylation by cyclic GMP-dependent protein kinase of a synthetic peptide corresponding to the autophosphorylation site in the enzyme. *J. Biol. Chem.* **258**: 14797-14803.
404. Glass DB, el-Maghrabi MR and Pilgis SJ (1986). Synthetic peptides corresponding to the site phosphorylated in 6-phosphofructo-2-kinase/fructose-2,6 biphosphatase as substrates of cyclic nucleotide-dependent protein kinases. *J. Biol. Chem.* **261**: 2987-2993.
405. White JG (1994). Platelets and atherosclerosis. *Eur. J. Clin. Invest. Suppl* **1**: 25-29.
406. Henn V, Slupsky JR, Gräfe M, Anagnostopoulos I, Förster R, Müller-Berghaus G and Kroczeck RA (1998). CD40 ligand on activated platelets triggers an inflammatory reaction of endothelial cells. *Nature* **391**: 591-594.
407. Mahley RW, Innerarity TL, Rall SC, Weisgraber KH and Taylor JM (1990). Apolipoprotein E: genetic variants provide insights into its structure and function. *Curr. Opin. Lipidol.* **1**: 87-95.
408. Fazio S, Lee YL, Ji ZS and Rall SC Jr (1993). Type III hyperlipoproteinemic phenotype in transgenic mice expressing dysfunctional apolipoprotein E. *J. Clin. Invest.* **92**: 1497-1503.
409. Kashyap VS, Santamarina-Fojo S, Brown DR, Parrott CL, Applebaum-Bowden D, Meyn S, Talley G, Paigen B, Maeda N and Brewer HB Jr (1995). Apolipoprotein E deficiency in mice: gene replacement and prevention of atherosclerosis using adenovirus vectors. *J. Clin. Invest.* **96**: 1612-1620.
410. Couderc R, Mahieux F, Bailleul S, Fenelon G, Mary R and Fermanian J (1993). Prevalence of apolipoprotein E phenotypes in ischemic cerebrovascular disease. A case-control study *Stroke* **24**: 661-664.

411. Genest JJ Jr, Bard JM, Fruchart JC, Ordovas JM, Wilson PF and Schaefer EJ (1991). Plasma apolipoprotein A-I, A-II, B, E and C-III containing particles in men with premature coronary artery disease. *Atherosclerosis* **90**: 149-157.
412. Wilson HM, Patel JC, Russell D and Skinner ER (1993). Alterations in the concentration of an apolipoprotein E-containing subfraction of plasma high density lipoprotein in coronary heart disease. *Clin. Chim. Acta.* **220**: 175-187.
413. Vallance P and Moncada S (1994). Nitric oxide: from mediator to medicines. *J. R. Coll. Physicians Lond.* **28**: 209-219.
414. Stannard AK, Riddell DR, Bradley NJ, Hassall DG, Graham A and Owen JS (1998). Apolipoprotein E and regulation of cytokine-induced cell adhesion molecule expression in endothelial cells. *Atherosclerosis*, in press.
415. Stannard AK, Riddell DR, Bradley NJ, Hassall DG, Graham A and Owen JS (1997). Apolipoprotein E and regulation of cytokine-induced vascular cell adhesion molecule-1 (VCAM-1) expression by endothelial cells. *Atherosclerosis*, **134**: 380.
416. Korschineck I, Lang I, Gharehbaghi-Schnell E, Ziegler S, Kaun C, Ambros P and Binder BR (1997). Identification of novel alternatively spliced apolipoprotein E receptor 2 mRNAs with altered ligand binding sites. *Thromb. Haemostas.* **SS**: O1630
417. Vogel T, Guo N, Guy R, Drezlich N, Krutzsch HC, Blake DA, Panet A and Roberts DD (1994). Apolipoprotein E: a potent inhibitor of endothelial and tumor cell proliferation. *J. Cell. Biochem.* **54**: 299-388.
418. Gooch KJ, Dangler CA and Frangos JA (1997). Exogenous, basal, and flow-induced nitric oxide production and endothelial cell proliferation. *J. Cell. Physiol.* **171**: 252-258.
419. Sarkar R, Webb RC and Stanley JC (1995). Nitric oxide inhibition of endothelial cell mitogenesis and proliferation. *Surgery* **118**: 274-279.
420. Ignatius MJ, Shooter EM, Pitas RE and Mahley RW (1987). Lipoprotein uptake by neuronal growth cones in vitro. *Science* **236**: 959-962.
421. Mahley RW, Nathan BP, Bellosa S and Pitas RE (1995). Apolipoprotein E: impact of cytoskeletal stability in neurons and the relationship to Alzheimer's disease. *Curr. Opin. Lipidol.* **6**: 86-91.
422. Ii M, Sunamoto M, Ohnishi K and Ichimori Y (1996). Beta-amyloid protein-dependent nitric oxide production from microglial cells and neurotoxicity. *Brain Res.* **720**: 93-100
423. Barger SW and Harmon AD (1997). Microglial activation by Alzheimer amyloid precursor protein and modulation by apolipoprotein E. *Nature* **388**: 878-881.
424. Nathan BP, Bellosa S, Sanan DA, Weisgraber KH, Mahley RW and Pitas RE (1994). Differential effects of apolipoproteins E3 and E4 on neuronal growth in vitro. *Science* **264**: 850-852
425. Peunova N and Enikolopov G (1995). Nitric oxide triggers a switch to growth arrest during differentiation of neuronal cells. *Nature* **375**: 68-73.
426. Da Prada M, Cesura AM, Launay JM and Richards JG (1988). Platelets as a model for neurones? *Experientia* **44**: 115-126.
427. Dreux C and Launay JM (1985). Blood platelets: neuronal model in psychiatric disorders. *Encephale* **11**: 57-64.

428. Rosenberg RN, Baskin F, Fosmire JA, Risser R, Adams P, Svetlik D, Honig LS, Cullum CM and Weiner MF (1997). Altered amyloid protein processing in platelets of patients with Alzheimer disease. *Arch. Neurol.* **54**: 139-144.
429. Davies TA, Long HJ, Tibbles HE, Sgro KR, Wells JM, Rathbun WH, Seetoo KF, McMenemy ME, Smith SJ, Feldman RG, Levesque CA, Fine RE and Simons ER (1997). Moderate and advanced Alzheimer's patients exhibit platelet activation differences. *Neurobiol. Aging* **18**: 155-162.
430. Guyton JR, Miller SE, Martin ME, Khan WA, Roses AD and Strittmatter WJ (1998). Novel large apolipoprotein E-containing lipoproteins of density 1.006-1.060 g/ml in human cerebrospinal fluid. *J. Neurochem.* **70**: 1235-1240.
431. St Clair RW and Beisiegel U (1997). What do all the apolipoprotein E receptors do? *Curr. Opin. Lipidol.* **8**: 243-245.
432. Brugge JS (1993). New intracellular targets for therapeutic drug design. *Science* **260**: 918-919.

PUBLICATIONS

Original Articles

1. Riddell DR, Sheikh S, James RW and Owen JS (1995). Immunoaffinity-isolated apolipoprotein E containing high density lipoprotein particles inhibit platelet aggregation. *Biochem. Soc. Trans.* **24**: 454S.
2. Riddell DR and Owen JS (1995). Inhibition of ADP-induced platelet aggregation by apolipoprotein E is not mediated by membrane cholesterol depletion. *Thromb. Res.* **80**: 499-508.
3. Riddell DR, Graham A and Owen JS (1997). Apolipoprotein E inhibits platelet aggregation through the L-arginine:nitric oxide pathway - implications for vascular disease. *J. Biol. Chem.* **272**: 89-95.
4. Riddell DR, Siripurapu V, Vinogradov DV, Gliemann J and Owen JS (1998). Blood platelets do not contain the low-density receptor-related protein (LRP). *Biochem. Soc. Trans.* **26**: S244.
5. Stannard AK, Riddell DR, Bradley NJ, Hassall DG, Graham A and Owen JS (1998). Apolipoprotein E and regulation of cytokine-induced cell adhesion molecule expression in endothelial cells. *Atherosclerosis* in press.
6. Riddell DR, Vinogradov DV, Stannard AK, Chadwick N and Owen JS (1998). Identification of apolipoprotein E receptor 2 in human blood platelets: a signal transductant molecule to activate nitric oxide synthase. *J. Biol. Chem.* submitted.
7. Cullen P, Kempter I, Cignarella A, Brennhäusen B, Mohr S, Riddell DR, Owen JS and Assmann G (1998). Effect of apoE and β -VLDL on nitric oxide production in human macrophages. *J. Clin. Invest.* in preparation.

Published Abstracts

1. Riddell DR, Sheikh S, and Owen JS (1995). Inhibition of platelet reactivity by plasma apolipoprotein E. *Platelets* **6**: 111.
2. Riddell DR and Owen JS (1996). Apolipoprotein E inhibits platelet aggregation through the L-arginine:nitric oxide pathway. *Platelets* **7**: 99.
3. Butler P, Riddell DR, Owen JS, Burroughs AK, McIntyre N and Mistry PK (1996). Apolipoprotein E allele frequencies in hyperlipidaemia of primary billiary cirrhosis. *Hepatology* **24**: 313A.
4. Graham A, Riddell DR and Owen JS (1996). Pro-atherogenic and thrombotic effects of peroxynitrite modified HDL₃. *J. Vasc. Res.* **33 (suppl. 1)**: 30.
5. Riddell DR, Vinogradov DV, Chadwick N, Stannard AK and Owen JS (1997) ApoE inhibits platelet aggregation through the L-arginine:nitric oxide pathway – initial characterisation of the patelet receptor. *FASEB J.* **11**: A143.
6. Stannard AK, Riddell DR, Bradley NJ, Graham A and Owen JS (1997). Apolipoprotein E (apoE) and regulation of cytokine-induced cell adhesion molecules on endothelial cells. *Atherosclerosis*, **134**: 380.

National and International Presentations

Invited Oral Presentations

1. Riddell DR, Sheikh S and JS Owen. Inhibition of platelet reactivity by plasma apolipoprotein E. **5th Erfurt Conference on Platelets** - Erfurt, Germany, Sept. 1994.
2. Riddell DR and JS Owen. Inhibition of platelet reactivity by plasma apolipoprotein E: a possible role for intra-platelet nitric oxide synthase? **18th European Lipoprotein Club** - Munich, Germany, Sept. 1995.

3. Riddell DR and Owen JS. Apolipoprotein E inhibits platelet aggregation through the L-arginine:nitric oxide pathway - implications for vascular disease. **6th Erfurt Conference on Platelets** - Erfurt, Germany, May 1996.
4. Riddell DR, Graham A and Owen JS. Apolipoprotein E, its receptors and nitric oxide - outlook to the future. **Metabolic Signalling and Plasma Homeostasis Workshop** - University College London, England, Dec. 1996.
5. Riddell DR, Vinogradov DV, Chadwick N, Stannard AK and Owen JS. Is apoER2 a signalling receptor? **4th Annual Scandinavian Atherosclerosis Conference** - Copenhagen, Denmark, May 1997.
6. Riddell DR, Vinogradov DV, Chadwick NC, Stannard AK and Owen JS. ApoE inhibits platelet aggregation through the L-arginine:nitric oxide pathway – initial characterisation of the platelet receptor. **17th International Congress of Biochemistry and Molecular Biology Young Scientists' Program** - Asilomar, California, USA, Aug. 1997.

Poster Presentations

1. Riddell DR and Owen JS. Apolipoprotein E increases intra-platelet cyclic nucleotide levels. **2nd Annual Copenhagen Atherosclerosis Conference** - Copenhagen, Denmark, May 1995.
2. Riddell DR, Sheikh S, James RW and Owen JS. Immunoaffinity-isolated apolipoprotein E containing high density lipoprotein particles inhibit platelet aggregation. **658th Biochemical Society Meeting** - Liverpool, England, April 1996.
3. Riddell DR, Graham A and Owen JS. Apolipoprotein E inhibits platelet aggregation through the L-arginine:nitric oxide pathway. **658th Biochemical Society Meeting** - Liverpool, England, April 1996.
4. Riddell DR, Graham A and Owen JS. Apolipoprotein E, its receptors and nitric oxide - outlook to the future. **Centre for Cardiovascular Biology and Medicine 1996 Symposium** - University College London, England, Dec. 1996.

5. Riddell DR, Vinogradov DV, Chadwick N, Stannard AK and Owen JS. ApoE inhibits platelet aggregation through the L-arginine:nitric oxide pathway – initial characterisation of the platelet receptor. **17th International Congress of Biochemistry and Molecular Biology Young Scientists' Program** - Asilomar, California, USA, Aug. 1997.
6. Riddell DR, Vinogradov DV, Chadwick N, Stannard AK and Owen JS. ApoE inhibits platelet aggregation through the L-arginine:nitric oxide pathway – initial characterisation of the platelet receptor. **17th International Congress of Biochemistry and Molecular Biology** – San Francisco, California, USA, Aug. 1997.
7. Riddell DR, Vinogradov DV, Chadwick NC, Stannard AK and Owen JS. ApoE inhibits platelet aggregation through the L-arginine:nitric oxide pathway – a role for apoER2. **Satellite Symposium of the XIth International Symposium on Atherosclerosis; Lipoprotein Metabolism, Obesity and Atherosclerosis** – Saint Malo, France, Oct. 1997.
8. Riddell DR, Vinogradov DV, Stannard AK, Chadwick NC and Owen JS. Does apoE receptor 2 (apoER2) in platelets have functional phosphotyrosine binding (PTB), SH2 and SH3 motifs which activate nitric oxide synthase (NOS)? **664th Biochemical Society Meeting** - Reading, England, Dec 1997.
9. Riddell DR, Siripurapu V, Vinogradov DV, Gliemann J and Owen JS. blood platelets do not contain the low-density receptor-related protein (LRP) **665th Biochemical Society Meeting** - Southampton, England, Mar 1998.

MEDICAL LIBRARY
ROYAL FREE HOSPITAL
BUMPSTEAD